A study of M0R1/GEM1 and kinl-like kinesins arabidopsis

Timothy James Hawkins

A Study of MOR1/GEM1 and Kinl-like Kinesins in *Arabidopsis*

By Timothy James Hawkins

Submitted in accordance with the requirements for the degree of Doctor of Philosophy

University of Durham,
School of Biological and Biomedical Sciences

September 2004

Declaration

The material contained in this thesis has not been submitted for a degree in the university of Durham or any other university. All original research within this thesis is the candidates own, apart from some experiments described in chapter 4. Research of the *gem1-1* & *gem1-2* phenotypes and the establishment that *gem1* is allelic to *mor1* was carried out by David Twell and Soon Ki Park.

Statement of copyright

Acknowledgements

Thank you to Patrick for his supervision, advice and inspiration. Thank you Abi and her skills as an English teacher for proof reading grammar, spelling and punctuation. Thank you to Mike for proof reading of scientific content and help and advise on yeast two-hybrid experiments. Thank you to Andrei for guidance in all aspects of practical research throughout my time in the lab so far. Finally many thanks to all members of the PJH lab, past and present.

Abstract

Microtubules perform essential functions in eukaryotic cells and, with other cytoskeletal elements, are involved in diverse cellular processes. Plant cells construct four microtubule arrays; There are two cortical arrays, the interphase cortical array, and the preprophase band, the mitotic spindle and the cytokinetic phragmoplast. The control and rearrangement of these arrays through the cell cycle is coordinated by Microtubule Associated Proteins or MAPs. These proteins have diverse functions including anchoring & crosslinking microtubules or otherwise regulating microtubule formation and destruction within the cell.

MOR1/GEM1 is the *Arabidopsis* member of the conserved XMAP215/TOGp family of proteins which are microtubule stablising MAPs and promote microtubule polymerization *in vitro*. In many organisms such stabilization is opposed by Kinl catastrophic kinesins, which depolymerise and destabilize microtubules. In addition to the further characterization of MOR1/GEM1, here in this thesis, two putative Kinl kinesins are identified in the *Arabidopsis* genome, a subfamily of kinesins previously uncharacterized in plants, AtCMK1 & AtCMK2.

Immunolocalisation shows that MOR1/GEM1 associates with all plant microtubule arrays throughout the cell cycle and is found to concentrate at the plus end of microtubules in the spindle next to chromosomes and the midline of the phragmoplast where oppositely orientated microtubules overlap. Furthermore, consistent with this localization, we show that a C-terminal fragment of MOR1/GEM1 which is absent in the pollen cytokinesis mutant, *gem1* can bind microtubules and as such we propose that the defects in the phragmoplast in *gem1* mutant is a result of the reduction of the MOR1/GEM1 protein to bind microtubules. Further studies indicate that unlike its budding yeast homologue Stu2, MOR1/GEM1 does not for dimers.

Immunolocalisation shows that AtCMK2 associates with all the plant microtubule arrays throughout the cell cycle, particularly the metaphase spindle. However in our experiments, AtCMK1 does not, but rather locates to structures within the cytoplasm, such as golgi vesicles or organelles. Here we also show that AtCMK kinesins form homodimers and do not physically interact with MOR1/GEM1 suggesting that these factors may be genetic interactors instead. Over-expression of AtCMK2 as a GFP fusion protein results in the disruption of microtubules, leaving short microtubule fragments and tubulin oligomers or aggregates, suggesting that AtCMK2 is a true *Arabidopsis* catastrophic kinesin. In addition, GUS promoter fusions show that the expression patterns of these two kinesins are very different.

List of Abbreviations

aa	Amino acid
AAMPPNP	5'-Adenylimidodiphophate
Ab	Antibody
ABA	Abscisic acid
ABRC	*Arabidopsis* Biological Resource Centre
AD	Activation Domain
ADP	Adenosine-diphosphate
AGI	*Arabidopsis* Genome Initiative
Alp14	Altered polarity protein 14 protein, *Schizosaccharomyces pombe*
alp14	Altered polarity protein 14 protein, *Schizosaccharomyces pombe*
Amp	Ampicillin (Antibiotic)
APC	Adenomatous Polyposis Coil (*Homo sapiens*)
Arabidopsis	Species, *Arabidopsis thaliana*
Ase1	Anaphase spindle elongation factor 1
AtCMK1	*Arabidopsis thaliana* Cental Motor Kinesin 1
AtCMK2	*Arabidopsis thaliana* Cental Motor Kinesin 2

ATK1	Kinesin 1 (*Arabidopsis thaliana*) (Formally KATA)
AtKSS	Katanin-like protein Small Subunit (*Arabidopsis thaliana*)
ATP	Adenosine-triphosphate
BAC	Bacterial Artificial Chromosome
BD	Binding Domain
Bim1p	Binding Microtubules 1 protein
BLAST	Basic Alignment Search Tool
BLASTN	Basic Alignment Search Tool Nucleotide
BLASTP	Basic Alignment Search Tool Protein
Bot1	*Botero1* (*Arabidopsis thaliana*)
bp	Base Pair
BSA	Bovine Serum Albumen
BY2	Bright Yellow
Cam	Chloramphenicol (Antibiotic)
cDNA	Complementary deoxyribonucleicacid
CDK	Cyclin-Dependant Kinase
CDS	Coding Sequence
C. elegans	Species, *Caenorhabditis elegans*
CENP-E	Centromere Protein E
CLIP-170	Cytoplasmic Linker Protein
CPAM	Cell Plate Assembly Matricies

C-Terminal	Carboxy-Terminal
DcKRP120-1	Dc Kinesin Related Protein, 120 kDa
DdCP224	*Dictostelium discoideum* centromere protein, 224 KiloDaltons
Dictostelium	Species, *Dictostelium discoideum*
Dis1	Sister Chromatid disjoining 1 protein *Schizosaccharomyces pombe*
dis1	Sister Chromatid disjoining 1 mutant *Schizosaccharomyces pombe*
DMSO	Dimethylsulphoxide
DNA	Deoxyribonucleic acid
dNTP	Deoxynucleoide Triphosphate
Drosophila	Species, *Drosphila melanogaster*
DTT	Dithiotheritol
EB1	End Binding 1
ECL	Enhanced Chemiluminescence
E. coli	Species, *Escherichia coli*
EDTA	Ethylenediaminetetra Acetic Acid
EGTA	Ethyleneglycol-bis(b-aminoethylether)-N,N,N',N'-tetra Acetic Acid
ERH3	Ectopic Root Hair 3, (*Arabidopsis thaliana*)
EST	Expressed Sequence Tag
EtOH	Ethanol
FITC	Flourescein isothiocyanate
fra2	Fragile fibre 2 (*Arabidopsis thaliana*)

FtsA	Filament-Forming Temperature-Sensitive A
FtsZ	Filament-Forming Temperature-Sensitive Z
GAL4	Transcritional activator required for galactose metabolism 4
GARLIC	Gilroy *Arabidopsis* Reverse Lethal Insertion Collection
GB	Genbank
GDP	guanyldiphosphate
GEM1	Gemini Pollen One (*Arabidopsis thaliana*)
GEM1	Gemini Pollen One (*Arabidopsis thaliana*)
gem1	Gemini Pollen One (*Arabidopsis thaliana*)
Gen	Gentamycin (Antibiotic)
GFP	Green Fluorescent Protein
GTP	guanyltriphosphate
GUS	β-Glucuronidase
HIK	hinkel (*Arabidopsis thaliana*)
hik	hinkel (*Arabidopsis thaliana*)
IDA	ligand iminodiacetic acid
IgG	Immunoglobulin G
IMAC	Immoilised-metal affinity chromatography
IPTG	Isopropylthio-β-D-galactoside
LB	Luria-Bertani Media
LiAc	Lithium Acetate

Kan	Kanamycin (Antibiotic)
kb	Kilobase
KCBP	Kinesin-Like Calmodulin Binding Protein
kDa	KiloDalton
KHC	Kinesin Heavy Chain
KinI	Kinesin, Internal motor
KLP	Kinesin-Like Protein
KLP5	Kinesin-Like Protein Five
KLP6	Kinesin-Like Protein Six
MAP	Microtubule Associated Protein
MAP65	Microtubule Associated Protein, 65 kDa (*Arabidopsis thaliana*)
MCAK	Mitotic Centromere Associated Kinesin (*Homo sapiens*)
MAPK	Mitogen-activated Protein Kinase
MES	2-(N-morpholino)ethanesulfonic acid
MeOH	Methanol
MOPS	3-(N-morpholino)propanesulfonic acid
MOR1	Microtubule Organisation One (*Arabidopsis thaliana*)
MOR1	Microtubule Organisation One (*Arabidopsis thaliana*)
mor1	Microtubule Organisation One (*Arabidopsis thaliana*)
mRNA	Messenger Ribonucleic Acid
msps	Mini Spindles protein (*Drosphila melanogaster*)
msps	Mini Spindles mutant (*Drosphila melanogaster*)

MT	Microtubule
MTOC	Microtubule Organising Centre
MURF	Muscle Ring Finger Protein
MW	Molecular Weight
NAA	Naphtalene Acetic Acid
NACK1	NPK Activating Kinase-like Protein
Nal	Naladixic acid (Antibiotic)
NCBI	National Centre for Biotechnology Information
NLS	Nuclear Localisation Sequence
N-Terminal	Amino-Terminal
NtKRP125	Nt Kinesin Related Protein, 125 kDa
OD_{600}	Optical Density at a Wavelength of 600 Nanometres
O/N	Overnight
PAGE	Polyaccrylamide Gel Electrophoresis
PAUP	Phylogenic Analysis Using Parsimony
PBS	Phosphate Buffered Saline
PBST	Phosphate Buffered Saline + Tween 20
PCD	Plant Conserved Domain
PCR	Polymerase Chain Reaction
PEG	Polyethyleneglycol
PFS	Planer Fenestrated Sheet

PIPES	Piperazine-N,N'-bis(2-ethanesulfonic acid)
PKH	Pollen Kinesin Homologue
ple	*pleiade* (*Arabidopsis*)
PPB	Preprophase Band
PRC1	Protein Regulating Cytokinesis 1
PSD	Plant Specific Domain
Rif	Rifampicin (Antibiotic)
RNA	Ribonucleic Acid
rsw1	*radial swelling 1* (*Arabidopsis*)
RT-PCR	Reverse Transcriptase Polymerase Chain Reaction
S. *cerevisiae*	Species, *Saccharomyces cerevisiae*
SD	Synthetic Dropout
SDS	Sodium Dodecyl Sulphate
SDW,SDH_2O	Sterile Distilled Water
SMART	Simple Molecular Architecture Search Tool
S. *pombe*	Species, *Schizosaccharomyces pombe*
spr1	*spiral1* mutant (Arabidopsis)
SPR1	*SPIRAL* gene (Arabidopsis)
SPR1	SPRIAL1 Protein (Arabidopsis)
Stu2p	(*Saccharomyces cerevisiae*)
TAE	Tris Acetate + EDTA
Taq	*Thermus aquaticus* Thermostable DNA Polymerase

TBLASTN	Translated BLAST Nucleotide
TBST	Tris-buffered Saline + Tween 20
T-DNA	Transfer DNA
TE	Tris/EDTA
TEM	Transmission Electron Microscopy
TEMED	NNN'N'-Tetramethylethelenediamine
TKRP125	Tobacco Kinesin-Related Protein 125kDa
TMBP200	Tobacco Microtubule Bundling Protein 200kDa
TOGp	Tumour Overexpressing Gene, Protein of
TON2	Tonneau 2 (*Arabidopsis*)
TON2	Tonneau 2 (*Arabidopsis*)
ton2	Tonneau 2 (*Arabidopsis*)
Tris	Tris-(hydroxymethyl)-aminomethane
TRITC	Tetramethylrhodamine isothiocyanate
TVN	Tubular Vesicular Networks
UTR	Untranslated Region of mRNA
UV	Ultraviolet light
VTV	Vesicle-tubule vesicle
WVD2	Wave-Dampendend 2
WT	Wild type
X-Gal	5-bromo-4-chloro-3-indolyl-β-D-galactoside
X-Gluc	5-bromo-4-chloro-3-indolyl-β-D-glucuronic acid

XKCM1	Xenopus laveis Kinesin Central Motor 1
XKIF2	Xenopus laveis Kinesin superfamily protein 2
XMAP215	Xenopus laveis Microtubule Associated Protein, 215 KiloDaltons
Y2H	Yeast Two-Hybrid
YPDA	Yeast extract, Peptone, Dextrose, Adenine (Media)
Zyg-9	Zygote defective 9 mutant (*Caenorhabditis elegans*)
Zyg-9	Zygote defective 9 protein (*Caenorhabditis elegans*)

Table of Contents

List of Tables

Illustrative Material

CHAPTER 1

Introduction

1.1 Overview

Microtubules perform essential functions in eukaryotic cells and, with other cytoskeletal elements, are involved in diverse cellular processes such as: cell division, morphogenesis, intracellular transport, signal transduction and specifically for plants, cell wall formation. The possession of a cytoskeletal network was previously considered to be unique to eukaryotic cells; however recent studies have led to the discovery of functional homologues of tubulin and actin in bacteria (Errington 2003).

Plant cells construct four microtubule assemblies that direct key processes in plant cell morphogenesis. There are two cortical arrays, the interphase cortical array, which is necessary for the formation of the cell wall and the direction of cell expansion; and the preprophase band, which delineates the plane of cell division. The spindle separates daughter chromosomes and the phragmoplast array, which guides vesicles to the site where they fuse to form the new cell plate. The alternation of these arrays through the cell cycle must be co-ordinated and this is probably performed by accessory proteins. These accessory proteins must anchor or crosslink microtubules or otherwise regulate microtubule formation and destruction within the cells. (Hussey & Hawkins 2001, Lloyd & Hussey 2001)

1.2 Microtubules and tubulin

Microtubules are hollow 25nm cylindrical polymers, present in the cytoplasm of eukaryotic cells. Each 25nm cylinder consists of 13 protofilaments assembled from heterodimers of α- and β- tubulin (Mandelkow & Mandelkow 1993, Lodish *et al.* 2000). Assembly is a spontaneous process, which requires GTP and is promoted by elevated temperatures but reversed by cooling (Mandelkow & Mandelkow

1993). The microtubule polymer is polar with each end exhibiting different kinetics of tubulin addition and loss. Importantly, microtubules are very dynamic, a property termed dynamic instability (Mitchison and Kirschner, 1984), and co-exist in growing and shrinking populations, which inter-convert infrequently.

1.2.1 Tubulin:

Tubulin consists of around 450 amino acids, depending on the isoform, and has a molecular mass of approximately 50kDa. The majority of tubulin isoforms fall into three main classes: α-tubulin, β-tubulin and γ-tubulin (Sullivan 1988, Oakley & Oakley 1989). Although δ, ε, ζ & η tubulins do exist, none of these classifications are present in several genomes including yeast and plants (Dutcher 2001). α- and β-tubulin show ~50% identity and form the heterodimer from which microtubules are assembled, whilst γ-tubulin is a specialized form involved in microtubule nucleation (Burns 1991). Each monomer binds a single GTP molecule, non-exchangeably in α tubulin and exchangeably in β tubulin. The β tubulin bound GTP is required for microtubule assembly, and its hydrolysis follows addition of a dimer to the microtubule end, upon which it become non-exchangeable within the microtubule (Kirchner & Mandelkow 1985, Erickson & O'Brian 1992).

The 3D structure of the prokaryotic protein, FtsZ, shares a remarkable similarity with that of α and β tubulin, although they only share a low degree of sequence similarity (Lowe & Amos 1998). FtsZ is found in chloroplasts and bacteria where it locates to the division site to form a ring-like septum. Both tubulin and FtsZ form tubules consisting of protofilaments, although in microtubules these protofilaments are arranged longitudinally, whereas in FtsZ they are helical. In addition, like tubulin, FtsZ is also a GTPase and as such, tubulin is now believed to have evolved from FtsZ (Erickson 1997).

α/β tubulin isoforms are encoded by different genes, with organisms containing different numbers of isoforms. Yeast genomes contain two α-tubulin genes and a single β-tubulin gene. Vertebrate genomes contain six α-tubulin genes and six β-tubulin genes (Villasante *et al.* 1986, Monteiro & Cleveland 1988), whereas plant genomes contain seven α-tubulin (Kopczak *et al.* 1992) and nine β-tubulin genes (Snustad *et al.* 1992). In both vertebrates and plants several of these isoforms are restricted to a single cell type or their expression is regulated through development (Sullivan 1988, Chu *et al.* 1998). Translation of tubulin can be autoregulated by the pool of free tubulin. Following reduction of this pool by microtubule assembly, the first four residues of β-tubulin (MREI) interact with tubulin leading to the destruction of polyribosome bound mRNA (Cleveland, 1989).

Tubulins are postranslationally modified in several ways. β-tubulin may be phosphorylated at serine 444 (Luduena *et al.* 1988), whereas α-tubulin undergoes several modifications including: acetylation of Lysine 40 (LeDizet & Pierno 1987) and the reversible removal of the carboxy-terminal tyrosine residue by a tubulin carboxypeptidase and tubulin tyrosine ligase, which requires ATP (Khawaja *et al.* 1988). A further postranslational modification of α-tubulin and β-tubulin is glutamination of glutamine 445 (Edde *et al.* 1990, Alexander *et al.* 1991). It is reasonable to assume that such chemical modifications would influence microtubule structure, assembly or interactions with other proteins. However, as yet, no evidence has been found to support such an effect.

1.2.2 Building a Microtubule:

The building blocks of microtubules are heterodimers of α- and β-tubulin monomers. Each monomer is 4nm in length, giving the heterodimer a length of 8nm. Lateral and longitudinal interactions between the α/β heterodimer subunits are responsible for maintaining the tubular structure of the microtubule. Longitudinal interactions consist of those, which hold α/β tubulin in an extremely

stable heterodimeric complex and interactions between heterodimers (Lodish *et al.* 2000). α/β-tubulin heterodimers associate or polymerize, end to end, into protofilaments. These strings of alternating α and β tubulin are spaced 8nm apart, all with the same orientation (Wade & Chretein 1993). Lateral interactions enable these protofilaments to associate side by side to give sheets, which close to form cylinders (Arnal *et al.* 2000). The microtubule cylinder has a diameter of 25nm and consists of 13 protofilaments, each with a spacing of 5nm, and are shifted lengthwise by 0.9nm with respect to their neighbour, giving the appearance that tubulin dimers produce helices which run around the microtubule (Wade & Hyman 1997). However, microtubules with other protofilament arrangements and other protofilament structures also exist. Other protofilament structures include: Sheets or C-tubes, which are incomplete microtubule walls; vinblastine induced protofilament spirals or 36nm coils of protofilaments exhibited at low temperatures (Mandelkow & Mandelkow 1995) The organisation of α and β tubulin heterodimers in the microtubule is polarised, resulting in structural and kinetic differences at the two ends. The faster growing end (+ end) has the β-tubulin subunit exposed, whereas the slower growing end (- end) has the α-tubulin subunit exposed.

1.2.3 Microtubule Assembly, Treadmilling and Dynamic Instability:

Microtubule assembly proceeds in three phases: nucleation, elongation and steady state. During the nucleation phase, microtubule seeds are formed and microtubules only grow from these above a threshold referred to as the critical concentration. This critical concentration depends on experimental assembly conditions (Valiron *et al.* 2001). During elongation, tubulin dimers add to the end of the microtubule and at steady state a fixed proportion of tubulin is in the assembled form, and a second tubulin pool remains soluble (Valiron *et al.* 2001). Nucleation involves tubulin oligomers, suggested to consist of between 6 and 13 tubulin dimers (Carlier & Pantaloni 1978, Voter & Erickson 1984, Fygenson *et al.* 1995, Flyvbjerg *et al.* 1996), in the formation of microtubule nuclei. The rate of such

nucleation is dependent on the initial concentration of tubulin (Caudron *et al.* 2000). The rate of elongation from solutions of pure tubulin *in vitro* is limited by the probability of tubulin dimers binding to the microtubule, rather than the rate at which dimers diffuse to microtubule ends (Caudron *et al.* 2000). At steady state, microtubules remain out of equilibrium, which requires continuous GTP hydrolysis (Valiron *et al.* 2001).

Treadmilling occurs because during steady state, microtubule ends behave differently, with the + end continuously incorporating new tubulin dimers and the - end continuously losing them (Margolis & Wilson 1978). If the end of the microtubule is not tethered then the microtubule appears to move; whereas if one end of the microtubule is fixed then treadmilling produces flux of tubulin dimers through the polymer, in a + to – direction (Margolis & Wilson 1981, Valiron *et al.* 2001).

Although a population of microtubules may exhibit a net steady state, an individual microtubule continuously oscillates between periods of growth and shrinkage, a property called dynamic instability. Although the growth and shrinkage of microtubules may be promoted by other factors such as MAPs, the process of dynamic instability is believed to be a result of whether GTP or GDP is present at the binding site of β-tubulin at the (+) end of microtubules. The microtubule becomes unstable when the (+) is capped by GDP tubulin instead of GTP, usually as a result of rapid shrinkage or where growth is so slow that the GTP of exposed tubulin at the end of the microtubule is hydrolysed to GDP before new GTP-tubulin subunits have been added. The microtubule can be switched back to growth if GTP-tubulin adds to the (+) end before bound GTP is hydrolysed. A switch from growth to shrinkage is referred to as 'catastrophe', whereas the switch from shrinkage to growth is referred to as 'rescue'. In addition microtubules may sometimes pause during which their length remains constant (Desai & Mitchison

FIGURE 1.1: Microtubule Growth, Shrinkage and Dynamic Instability

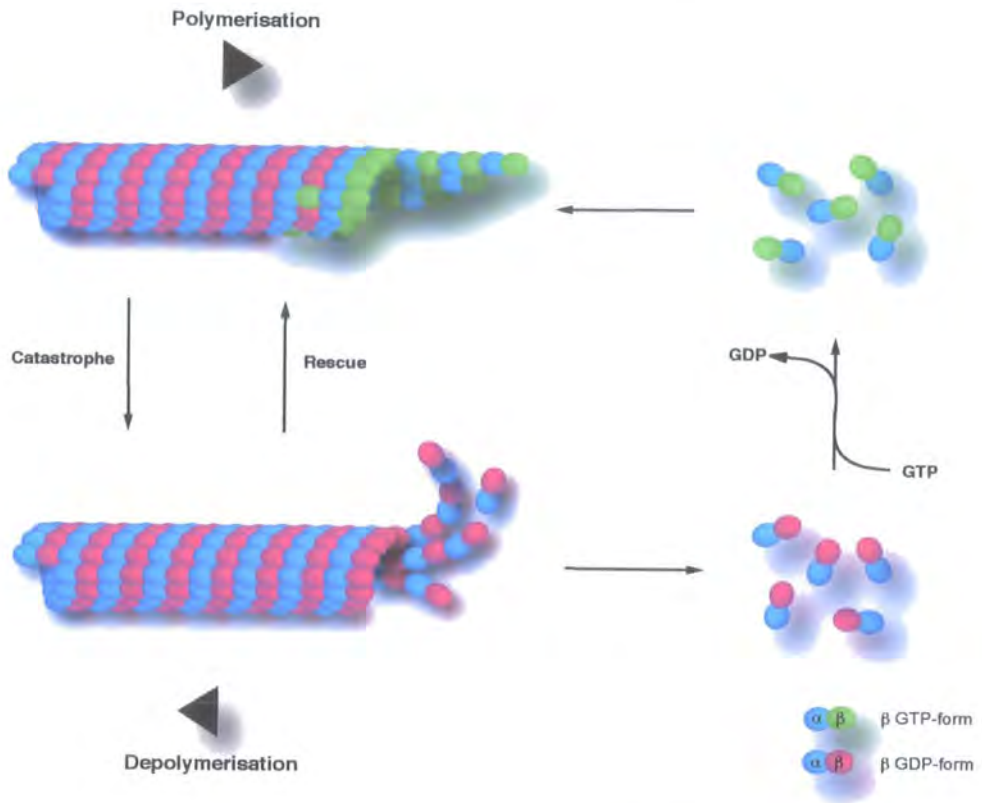

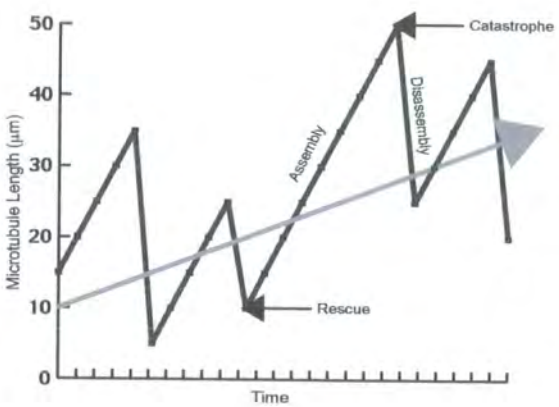

Microtubule growth and shrinkage.

Microtubules are hollow 25nm cylindrical polymers and consists of 13 protofilaments assembled from heterodimers of α and β tubulin which associate end to end giving the structure polarity. Upon contact with the exposed tubulin at the end of the polymer, the GTP in β-tubulin is hydrolysed to GDP. If GDP tubulin is at the end of the microtubule is becomes unstable and protofilaments splay out, to prevent this the end is coved by a tubulin GTP cap. If this cap is lost then the microtubule starts to depolymerse (Cayastrophe), If this cap is restored the the MT starts to grow again (Rescue). A microtubule may continually switch between these a property known as dynamic instability.

1997, Mitchison & Kirschner 1984a, Mitchison & Kirschner 1984b, Walker *et al.* 1988, Horio & Hotani 1986)(**FIGURE 1.1**)

1.2.4 Characteristics of Plant Tubulin

Although structurally plant microtubules are identical to their animal and yeast counterparts, plant microtubules are more dynamic (Hush *et al.* 1994, Yuan *et al.* 1994, Moore *et al.* 1997) and persist in the treadmilling state for longer (Shaw *et al.* 2003). Furthermore plant microtubules show different responses to anti-microtubule drugs than mammalian tubulin. Plant microtubules are more resistant to colchicine and are bound by the herbicides dinitroalinine and phosphorthioamidate (Anthony & Hussey 1999). Interestingly resistance to these drugs can be conferred by a single amino acid substitution, Thr239 to Ile239 or Met268 to Thr268 (Anthony & Hussey 1999). Another mutant of plant tubulin is *lefty*, plants of which show left hand twisting of various organs including roots (Furutani *et al.* 2000, Thitamadee *et al.* 2002, Hashimoto 2002). The mutation is an amino acid substitution in α-tubulin of Ser180 to Phe180, changing the shape of the tubulin dimer and as such the shape and orientation of the microtubule. In *lefty* mutants the microtubules are not transverse but rather are positioned at an angle leading to right handed helices. It has been suggested that as the cell wall maintains the shape of a cell and that this in turn is set up by the cortical microtubules (Giddings & Staehelin 1991), off-setting the angle of microtubules can offset the angle of cellulose microfibrils producing a twist which is propagated along a cell file (Hussey 2002, Lloyd *et al.* 2003).

1.3 The Microtubule Arrays

As previously mentioned microtubules create assemblies or arrays, which direct key processes in the cell. Plant cells construct four arrays only one of which, the spindle, which separates daughter chromosomes, do they share with other organisms such as fungi. There are two unique cortical arrays, the interphase

FIGURE 1.2: The Four Plant Microtubular Arrays

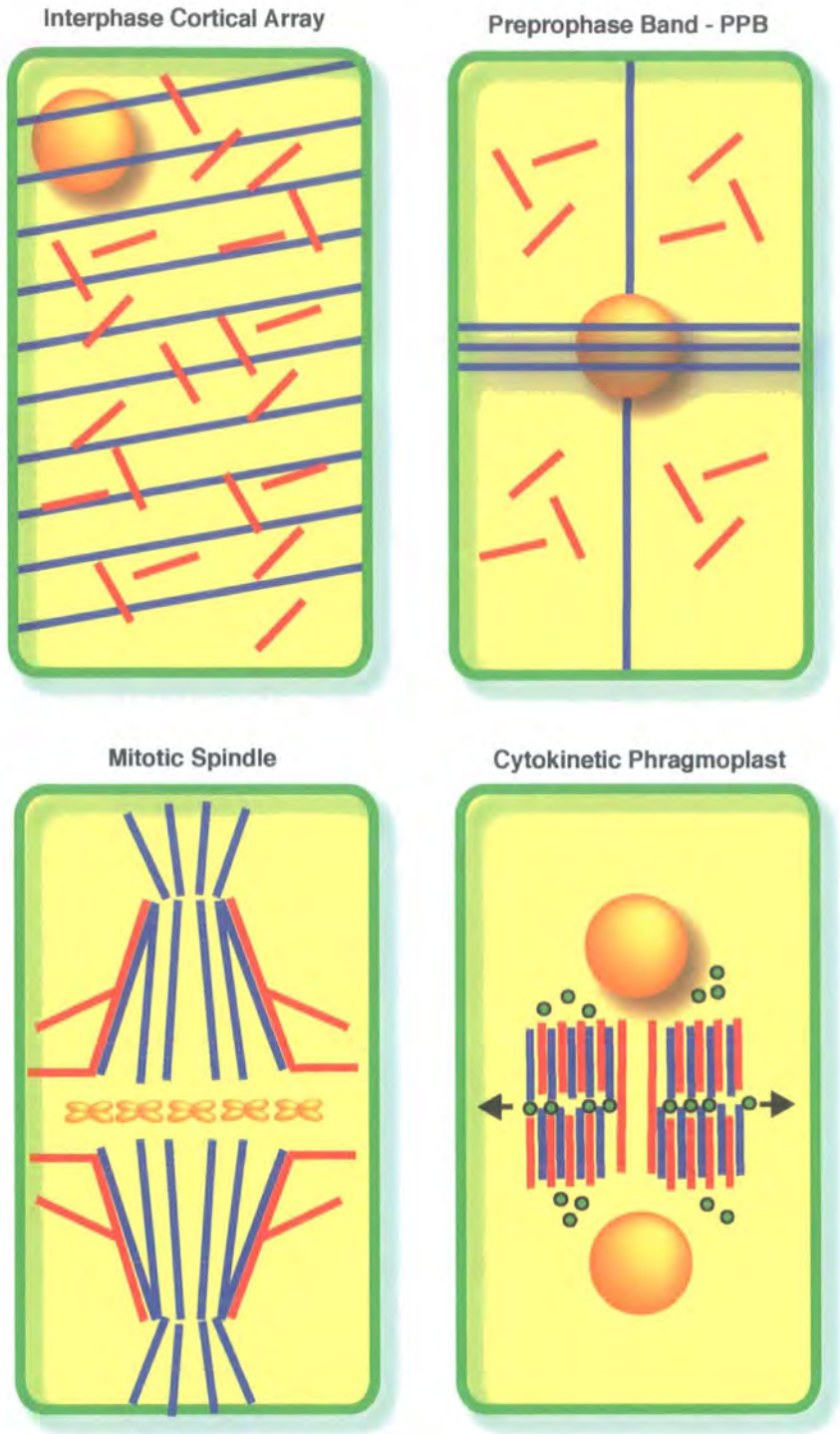

Figure 1.2: Plant cells construct four microtubule assemblies that direct key processes in plant cell morphogenesis. There are two cortical arrays, the interphase cortical array, which is necessary for the formation of the cell wall and the direction of cell expansion; and the preprophase band, which delineates the plane of cell division. The spindle separates daughter chromosomes and the phragmoplast array, which guides vesicles to the site where they fuse to form the new cell plate. MTs (Blue), Actin (Red), Nucleus/Chromosomes (Orange) & Vesicles/Cell wall (Green).

cortical array, which is necessary for the formation of the cell wall and the direction of cell expansion and the preprophase band, which delineates the plane of cell division. The third unique array is the cytokinetic phragmoplast (Hussey & Hawkins 2001) (**Figure 1.2**).

Cell division is a process, which has been conserved from bacteria to plants, animals and fungi (Nanninga 2001) and commonly involves microtubules and actin (FtsZ and FtsA in bacteria). Unlike plants, in animal and fungal cells cytokinesis involves a contractile ring. There are three stages: selection of the division site, assembly of protein complexes and finally constriction of the contractile ring and construction of the septum (Walther & Wendland 2003). However, because of the requirement of plant cells to produce a new cell wall at division, the cytokinetic apparatus is very different.

1.3.1 The Interphase Arrays: Cortical Microtubules and the Preprophase Band.

As described previously, the interphase cortical array is necessary for the formation of the cell wall and the direction of cell expansion. If cortical microtubules are depolymerised by the addition of anti-microtubule agents such as colchicine and dinitroaniline herbicides or are stabilised by taxol, cells expand and grow isotropically (Green 1962, Upadhyaya & Nooden 1977, Baskin *et al.*. 1994). In growing cells, the cortical microtubules and cellulose microfibrils of the cell wall are usually parallel to each other, orientated transversely to the direction of cell elongation. This co-alignment prompted the hypothesis that microtubules act as transmembranous guides for the deposition and alignment of cellulose microfibrils in the cell wall (Giddings and Staehelin 1991). The cortical microtubules are positioned beneath the plasma membrane, in parallel bundles with ordered regular spacing and could form guiding tracks for cellulose synthases (Giddings and Staehelin 1991). Although conversely, the organisation of microtubules also

appears to be reliant upon cortical microfibril orientation as disruption of microfibrils by the herbicide isoxaben results in disorganisation of cortical microtubular arrays (Fisher & Cyr 1998). Furthermore, ordered cortical microfibril deposition occurs in the absence of cortical microtubules, suggesting that there are also ordering mechanisms independent of cortical microtubules (Sugimoto *et al.* 2003).

To maintain these organised cortical microtubule arrays, factors such as microtubule associated proteins must tightly control their alignment, bundling and dynamicity. MAPs must cross-link microtubules to form these parallel arrays and could also link these structures to the plasma membrane. Several of these factors involved in microtubule organisation at the cortex have been identified by genetic approaches in *Arabidopsis*. These include: the *botero1/fra2* mutant, which displays incorrect orientation of interphase cortical microtubules and defects in anisotropic growth in root tip cells (Bichet *et al.* 2001); the temperature sensitive mutant *mor1* which causes cortical microtubule shortening and concomitant isotropic cell expansion with left-handed organ twisting (Whittington *et al.* 2001); the *zwichel* trichome-branching mutant (Oppenheimer *et al.* 1997) and finally, *spiral,* which exhibits right handed twisting of organs associated with defects in cell growth anisotropy and cortical microtubules form left-handed helices instead of transverse arrays (Furutani *et al.* 2000). All of these genes encode microtubule associated proteins and will be discussed further, later in the MAP section of this chapter.

The preprophase band, or PPB, is created prior to cell division and marks the future location of the cell plate. In addition, the PPB also influences cell polarity and the formation of the spindle. The PPB consists of an array of parallel cortical microtubules and actin, which encircle the cell at the cortex, producing a band around the nucleus, an image rather like the rings of Saturn. During the prophase transition, this band disappears, leaving an 'invisible' imprint, which is then followed by the cell plate (Verma 2001). Studies with MAP4-GFP have shown that PPB formation consists of four stages: PPB initiation, PPB narrowing, PPB maturation,

and PPB breakdown (Dhonukshe *et al.* 2003). During PPB formation microtubules form a broad ring, which covers two thirds the cells length, this structure then gradually narrows to form a ring structure with a width 2-5 μm. During maturation there is the flow of tubulin or microtubules from the cell cortex towards the region of PPB (Dhonukshe *et al.* 2003).

However, the PPB is absent in microsporogenesis (Hogan 1987), metasporogenesis (Webb & Gunning 1990, Wolniak & Larsen 1995) and the first asymmetrical mitosis of the embryo (Terasaka & Niitsu 1990). Endosperm cells do not have cortical microtubules, however the division site in such tissues has been found to be established by nuclear microtubules (Brown *et al.* 1999, Otegui & Staehelin 2000). The *Arabidopsis ton2* mutants have disorganised interphase microtubules and lack the preprophase band (Mayer *et al.* 1991, Torres-Ruiz & Jurgens 1994, Traas *et al.* 1995). The *TON2* gene is highly conserved in higher plants and encodes a protein whose C-terminal region is similar to B" regulatory subunits of type 2A protein phosphatases, PP2A (Camilleri *et al.* 2002). TON2 may be involved in the formation of a PP2A complex, which presumably controls the phosphorylation status of proteins important for the structure of the plant cortical cytoskeleton.

1.3.2 Mitosis and the Spindle:

The mitotic apparatus attaches and captures chromosomes at prophase, aligns these chromosomes at metaphase and then separates them at anaphase. This apparatus consists of the spindle and astral microtubules: the first is a spherical bundle of symmetrical microtubules, divided into opposing hemispheres with an equator where chromosomes align at metaphase. The second, the astral microtubules are a protrusion of microtubules focused at the spindle pole and extending in the opposite direction to the spindle microtubules (Lodish *et al.* 2000). The spindle consists of two sets of microtubules: the kinetochore microtubules,

which attach to chromosomes at the kinetochore; and polar microtubules, which do not attach to kinetochores but instead interdigitate with polar microtubules of the opposite hemisphere, the lateral interactions between which are responsible for holding the two hemispheres together (Lodish *et al.* 2000).

Kinetochores are large protein complexes that bind centromeres and by interacting with microtubules and motor proteins generate and regulate chromosomal movement. The kinetochore also functions in the spindle checkpoint; a surveillance mechanism that ensures that metaphase is complete before anaphase begins (Yu *et al.* 2000). The kinetochore is a plate-like structure, which lies within the centromere of the chromosome. Electron micrographs reveal that it consists of a stack of disks: the inner disk (40-60nm) is believed to be condensed chromatin, the outer disk (40-60nm) is a fibrous structure and is the point at which microtubules attach, and the middle disk (25-30nm) contains filamentous structures which are believed to hold the inner and outer disks together. For the kinetochore to be captured by the microtubule, proteins must exist which are capable of cross-linking microtubules and kinetochores (Lodish *et al.* 2000, Yu *et al.* 2000).

At metaphase, the chromosomes are aligned along the equator. Here the microtubules continue to have a flow of tubulin subunits through the microtubule towards the poles. The microtubules however, appear to be stationary as the loss of tubulin at the (-) is balanced by the addition of tubulin at the (+), a process referred to as 'treadmilling' (Valiron *et al.* 2001). At anaphase, the kinetochores on sister chromatids are pulled apart towards opposite poles. There are several possible mechanisms by which this may occur: a (-) directed motor at the kinetochore or a (+) end directed motor at the pole could generate forces to pull the chromosome towards the pole. Alternatively, the flow of tubulin through the microtubule, such as rapid depolymerisation at the (+), could move the kinetochore towards the pole (Lodish *et al.* 2000).

As described previously, the spindle is a bipolar apparatus with the slower growing minus ends anchored at the spindle poles and the faster growing plus ends are facing the spindle equator (Euteneur and McIntosh 1981). Often the spindle poles emanate from centrosomes, consisting of two centrioles and perinuclear material. However, all higher plant cells are acentrosomal and therefore microtubule nucleation and spindle assembly must occur in a different manner. Observations in other acentrosomal cells have lead to the hypothesis that acentrosomal spindle assembly involves the nucleation of microtubules around chromosomes and then self-organization into the bipolar spindle (Compton 2000, Wittmann *et al.* 2001). Although, this is less well understood in plant cells and the majority of microtubules here appear to be nucleated at the nuclear envelope (Lambert 1993, Stoppin *et al.* 1994, Azimzadeh *et al.* 2001). In plants these nuclear envelope microtubule converging centres are hypothesised to be the microtubule nucleation sites which then self-organise to form the spindle poles (Smirnova & Bajer 1994) One *Arabidopsis* protein that has been implicated in this acentrosomal mitotic spindle pole organisation is the kinesin, microtubule motor protein, ATK1 (formally KATA). Mutants of ATK1 lack microtubule focusing at the spindle pole during prophase and have abnormal bipolar spindles in prometaphase (Marcus *et al.* 2003). However, this is rectified by anaphase and chromosome segragation proceeds normally (Marcus *et al.* 2003). This suggests, therefore that mitotic plant cells contain an error-correcting mechanism.

1.3.3 Cytokinesis and the Phragmoplast:

Cytokinesis in plants is more complex than in animal cells as it requires the formation of a new cell plate, a process co-ordinated by a plant specific microtubule array, the phragmoplast.

Cytokinesis in the plant cell essentially involves the construction of and extracellular compartment in the cell; the large numbers of mutations which effect cytokinesis suggest that it is a process which is tightly controlled and involves

many different proteins. The phragmoplast is a loose cytoskeletal structure held together by two arrays of microtubule bundles and actin and is formed at anaphase by the reassembly of mitotic (spindle) microtubules (Gunning & Wick 1985, Verma & Gu 1996). The plate, a disk-like membrane bound structure, is built in the centre of the phragmoplast by fusion of Golgi derived vesicles (Kakimoto & Shibaoka 1988, Samuels *et al.* 1995, Staehelin & Driouich 1997, Staehelin & Hepler 1996). These vesicles are squeezed into 'dumbells', or vesicle-tubule vesicles (VTV), in order to prevent ballooning, by phragmoplastin, a dynamin-like protein (Gu & Verma 1996). The VTVs then fuse at their ends in a star-shaped body to give a 'honeycomb-like' structure between the positive ends of the phragmoplast microtubules. Once this initial cell plate structure is formed within the phragmoplast, it then extends centrifugally to the parental cell wall (Gu & Verma 1996, Samuels *et al.* 1995)

The phragmoplast is formed as the cell enters cytokinesis where microtubules from the spindle align perpendicular to the plane of the future cell plate with their plus ends pointing towards the equatorial region (Euteneuer *et al.* 1982). As the cell plate expands the microtubules depolymerise in the centre and repolymerise along the edge of the growing plate (Gu & Verma 1997, Gunning & Wick 1985). Subsequently, the microtubules in the expanding phragmoplast form two rings surrounding the growing edge of the cell plate (Grainger & Cyr 2000, Gu & Verma 1996, Mineyuki & Gunning 1990, Staehelin & Hepler 1996) providing support and guide vesicles to the forming cell plate.

Recently Segui-Simarro and colleagues have progressed the study of the phragmoplast using electron tomography with a three-dimentional resolution of approximately 7nm. Their data demonstrated that cytokinesis in *Arabidopsis* meristem cells may be divided into four phases: phragmoplast initials, solid phragmoplast, transitional phragmoplast, and ring shaped phragmoplast (Segui-Simarro *et al.* 2004).

At late anaphase phragmoplast initials are formed from groupings of polar microtubules and cell plate assembly points form at the equator, consisting of cell plate assembly matrix (CPAM) and Golgi derived vesicles. CPAM are only found surrounding growing cell plates and regulate cell plate growth. Phragmoplast microtubules terminate in the CPAM and hence vesicles are focused to the CPAM and the forming cell plate (Segui-Simarro *et al.* 2004).

The solid phragmoplast phase follows the fusion of vesicles and their expansion into dumbbell like shapes by dynamin as described previously. The solid phragmoplast is produced by the lateral expansion of the phragmoplast initials and the CPAM where vesicles fuse to the bulbous ends of the dumbbells to give the tubulovesicular membrane network or TVN (Segui-Simarro *et al.* 2004).

The transitional phragmoplast stage involves the disassembly of the CPAM and its associated microtubules which then reassemble to form the peripheral ring phragmoplast. The TVN becomes the planer fenestrated sheet or PFS by the removal of membrane via clathrin-coated vesicles and callose synthase. Individual holes or fenestrae are closed by the focusing of growth to these areas by small secondary complexes of CPAM and microtubules, which develop over the area to be closed. This produces a centrifugally expanding peripheral cell plate, which finally fuses with the cell wall (Segui-Simarro *et al.* 2004).

One example of a phragmoplast mutant is the *Arabidopsis hinkel* mutant which was identified as abnormal embryos, where the regular division patterns were severely perturbed with enlarged cells and incomplete cell walls (Strompen *et al.* 2002). Here, the phragmoplasts were seen to nearly span the diameter of the cell during cytokinesis, suggesting that lateral expansion of the phragmoplast was unaffected. However, the phragmoplasts in the *hik* mutants exhibited microtubules across the entire division plane (Strompen *et al.* 2002). In contrast wild-type cells

lack microtubules in the phragmoplast division plane, which suggests that the *HIK* gene product, a kinesin, is required for reorganisation of phragmoplast microtubules during cell plate formation (Strompen *et al.* 2002).

1.4 The Microtubular Cytoskeleton in Plant Development:

Positioning of the cell plate is of crucial importance for plant morphogenesis and is under cytoskeletal control. Dividing cells in developing plant organs put down their cell plate perpendicular to the organ surface. The cell then elongates perpendicularly to the cell plate, leading to the controlled elongation of plant organs. In contrast, during embryogenesis and meristem development, the cell plate is positioned parallel to the surface, creating new cell layers (Kost *et al.* 1999). In most situations a dividing plant cell produces two daughter cells of similar size. However, in some cell types an asymmetric cell division is required, here the cell plate is positioned non-medially. Such an asymmetric division leads to cells that differ in size, cytoplasmic content and cell fate determination. A good example of this is the asymmetric division of the microspore during pollen mitosis I, leading to the formation of a large vegetative cell and a smaller generative cell. Here the vegetative exits the cell cycle and stores metabolites required for the fast growth of the pollen tube, whereas the generative cell undergoes a further symmetrical mitotic division to form the two sperm cells (Twell *et al.* 1998).

Following cell division, most plant cells expand along one axis in a polarised manner (Kropf *et al.* 1998). The cellulose microfibrillar network of plant cell walls are arranged parallel to one another and resist radial expansion, leading to cell elongation perpendicular to the microfibril orientation (Green 1980). The enzyme responsible for cellulose production, cellulose synthase, is present in the plasma membrane and as mention previously, is thought to move along microtubules and use these as a template for the microfibril. Therefore, the orientation of cortical microtubules determines the direction of cell expansion. This was supported by the

observation that following the disruption of microtubules cell growth was depolarised (Green 1994, Akashi 1998, Baskin *et al.* 1994). Certain plant cell types, such as pollen tubes, root hairs and trichomes, undergo dramatic cell elongation during differentiation. The root hair is a protrusion from a specialised root epidermal cell, which elongates perpendicular to the root surface. During root hair morphogenesis, a bulge first appears on the surface of the epidermal cell; this is then followed by the elongation of this bulge to form the root hair (Schiefelbein & Somerville 1990). If microtubule dynamics are disturbed, multiple incorrectly located processes appear (Kost *et al.* 1999). In addition, the disruption or stabilisation of microtubules of existing elongating root hairs results in branching (Bibikova *et al.* 1999). Microtubules therefore ensure that root hairs are straight and orientated correctly relatively to the root surface (Kost *et al.* 1999). Trichomes are single cells, which consist of a stalk perpendicular to the epidermis, which usually branches into three branches whose orientation to the axis of the organ is controlled (Kost *et al.* 1999). During stalk outgrowth, disruption of the microtubule cytoskeleton leads to the production of balloon-like structures where the polarization of elongation is no longer controlled and later, the complete inhibition of branch formation (Kost *et al.* 1999).

1.5 MAPs: Microtubule Associated Proteins.

Purification of microtubules led to the initial definition of MAPs. Here, microtubules were isolated from cell extracts by multiple rounds of assembly, disassembly and differential centrifugation. These preparations contained approximately 80% tubulin and 20% associated proteins. Therefore, the first definition of a MAP was 'a protein that copurifies with tubulin during repeated cycles of assembly'. However, this focus on assembly would not include many other factors associated with microtubules, such as motor proteins like kinesins. Hence, an alternative definition was proposed by Solomon and colleagues: 'MAPs are proteins that are attached to microtubules *in vivo*' (Solomon *et al.* 1979) Most of the plant MAPs discovered so far have structural homologues in other eukaryotes, but not all animal or fungal

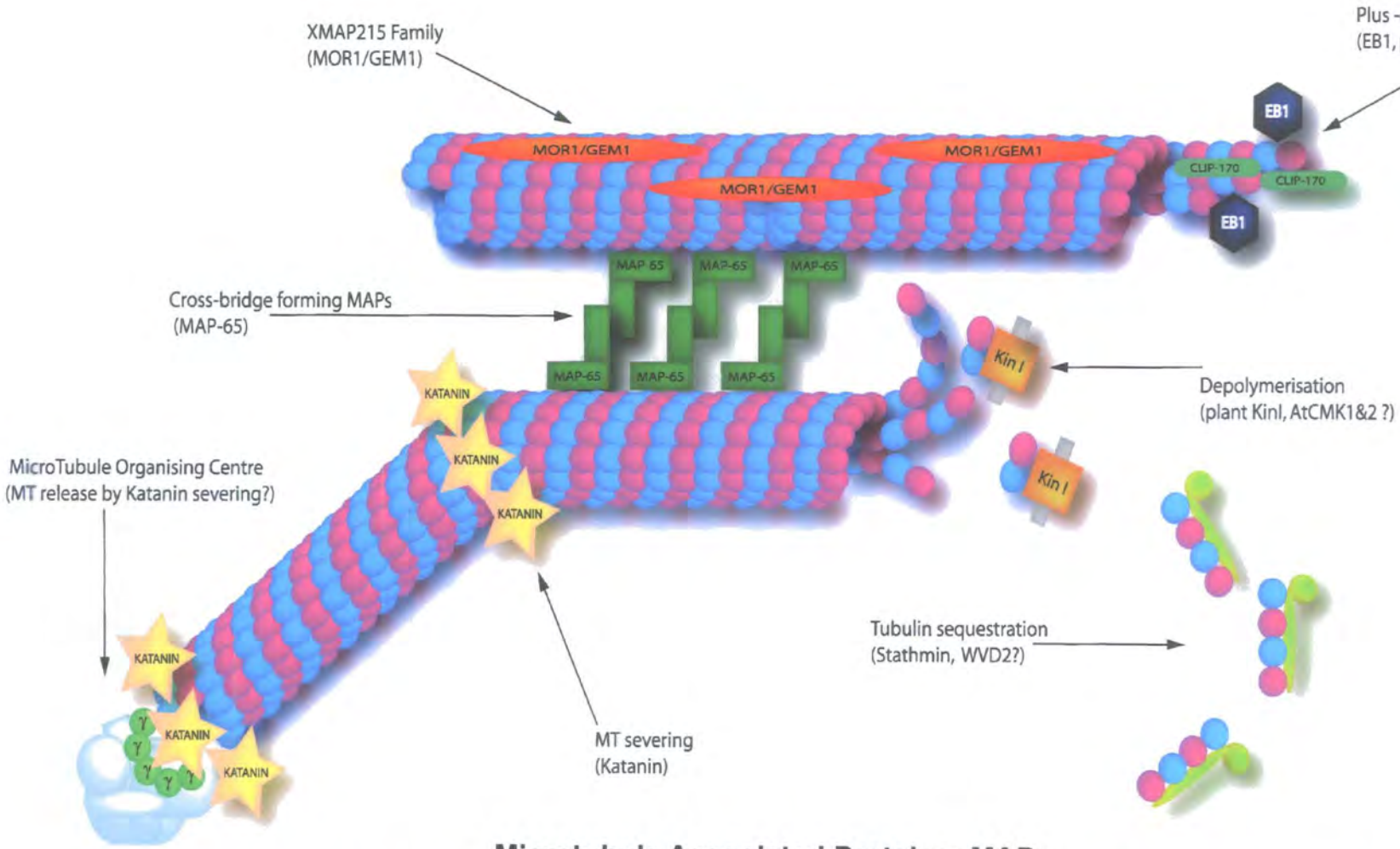

Microtubule Associated Proteins: MAPs

Different classes of MAPs: stabilising MAPs such as MOR1/GEM1; cross-bridging MAPs such as MAP65 which connect neighboring MTs; Plus-end binding MAPs such as EB1 which regulate plus end dynamics and possibly link with kinetochores; MT destabilising MAPs such as KinI-like kinesins which induce depolymerisation; Tubulin-sequestering proteins such as stathmin; and microtubule severing MAPs such as Katanin.

FIGURE 1.3: Types of Microtubules Associated Proteins

MAPs are present in plants (Gardiner & Marc 2003, Lloyd *et al.* 2004). An explanation for these differences may be that plant microtubules although structurally similar to their eukaryotic counterparts, differ in their organization and dynamics as discussed previously (**FIGURE 1.3**).

1.5.1 Classical MAPs.

There are many examples of microtubule associated proteins, some of which are specific to certain organisms; others which are conserved across organisms from humans to insects, yeast and plants. Several MAPs, specific to animals are particularly abundant and important in the brain, a tissue rich in microtubules. These types of MAPs include MAP4, MAP2, Tau, MAP1A and MAP1B (Cleveland 1993). They have been located to all of the microtubule arrays and function primarily to promote the polymerisation and stabilisation of microtubules (Ennulat *et al.* 1989, Hoshi *et al.* 1992, Joly *et al.* 1989, Kuznetsov *et al.* 1981). These proteins each have several isoforms which are all produced from a single gene and whose individual expression is closely linked to development (Himmler 1989, Lewis et al. 1986, Garner & Matus 1988). The microtubule binding capacity of these MAPs is located to stretches of amino acid repeats (Lewis *et al.* 1989, Lewis *et al.* 1988, West *et al.* 1991). Plant homologues of these classical mammalian MAPs have yet to be identified, a fact which may reflect fundamental differences in plant and animal microtubule arrays. However, other MAPs are members of protein families, which are conserved across phylogeny and homologues exist in many organisms, including plants.

1.5.2 A Plant Specific MAP; SPR1

The *Arabidopsis thaliana spiral1* (*spr1*) mutant shows right-handed helical growth in roots and etiolated hypocotyls (Furutani *et al.* 2000). The *SPR1* gene was identified by map-based cloning and found to encode a small protein (12kD) and genetic complementation with a SPR1:GFP fusion showed that SPR1 co-localises

with microtubules throughout the cell cycle and is highly expressed in those tissues undergoing rapid cell elongation (Sedbrook *et al.* 2004, Nakajima *et al.* 2004). SPR1:GFP concentrates at the growing ends of cortical microtubules but this fluorescence dissipates upon polymer shortening (Sedbrook *et al.* 2004). The SPR1 protein has a motif repeated at both ends separated by predicted a rod-like domain (Sedbrook *et al.* 2004). The Arabidopsis genome contains five SPR1 homologues, *SPIRAL1-LIKE* genes *SP1L1 –SP1L5* , which only show sequence similarity in the N- and C-terminal regions with a highly variable internal region (Nakajima *et al.* 2004) Furthermore the conserved N- and C- terminal regions of SPR1 are sufficient for microtubule localisation. It is suggested that SPR1 may act as an intermolecular linker which is involved in microtubule polymerization dynamics and guidance, which in turn influences touch-induced directional cell expansion and axial twisting (Sedbrook *et al.* 2004).

1.5.3 End-binding MAPs

An MT end undergoes conformational changes upon GTP hydrolysis of polymerising tubulin (Howard & Hyman 2003). The subunits that contain GTP with β-tubulin are thought to form straight protofilaments that align precisely along the wall of the adjacent protofilaments, thereby constructing two-dimensional sheets of protofilament at the ends of growing MTs. In contrast, GDP-tubulins form bent protofilaments that tend to splay out from the lattice; the ends of shrinking MT ends are typically frayed. These unique conformations at the growing or shrinking MT ends may be recognised and bound by specific proteins (Hashimoto 2003).

The EB1 family is a conserved group of MAPs that localise to spindle and cytoplasmic MTs, preferentially at their distal ends. EB1, EB for end binding, was originally identified as a binding partner of the tumour suppressor protein adenomatous polyposis coil protein, APC in humans (Su *et al.* 1995), an interaction believed to be implicated in the physical link between microtubules and kinetochores. Homologues have been identified in yeast Bim1p/Mal3 (Beinhauner

et al. 1997, Schwartz *et al.* 1997), Drosophila dEB1 (Lu *et al.* 2001), Dictyostelium DdEB1(Rehberg & Graf 2002) and *Arabidopsis*: AtEB1-1, AtEB1-2 and AtEB1-3 (Lloyd 2003). Mutations in several of these EB1 genes lead to spindle positioning defects (Schwartz *et al.* 1997, Beinhauner *et al.* 1997, Rogers *et al.* 2002b) and BIM1p has been shown to promote microtubule polymerization. EB1 functions as an 'antipause factor' at microtubule plus ends, regulating microtubule dynamics and promoting end-on attachment to different cellular sites. GFP-AtEB1-1 labels MT (distal) plus ends and small foci in the cell cortex. Consistent with studies in animal cells, AtEB1 was found at spindle poles of plant cells despite the absence of centrioles. Polar labeling was also observed during telophase, where AtEB1 surrounded the daughter nuclei. An interesting addition to the study of EB1 in plants is the existence of a possible APC homologue, the maize MAP TANGLED1 (Smith *et al.* 2001).

CLIP-170 is a mammalian MT -Membrane linker, which specifically associates with growing plus ends of microtubules (Galjart & Perex 2003). Several Clip170 homologues can be found in animals and fungi but no clear homologue has been found in plants. However, Gardiner & Marc have identified a possible candidate AAF02820 (Gardiner & Marc 2003) and experiments with YFP-CLIP170 expressing protoplasts show labeling of MT ends, suggesting that the plus ends of animal and plant MTs appear to be similar (Dhonukshe & Gadella 2003).

An additional role for CLIP170 and EB1 is to recruit other MAPs or cytoplasmic proteins to form MT plus end complexes. One protein, which forms these complexes with CLIP170 is the CLIP-Associated Protein1, CLASP1 (DmMAST/Orbit), an example of which exists in the *Arabidopsis* genome, NP_179609 (Gardiner & Marc 2003). CLASP1 is a component of the outer kinetochore, an area which binds MTs at their plus ends (Maiato *et al.* 2002).

1.5.4 Cross-bridge forming MAPs.

The MAP65 family of plant MAPs were first isolated from tobacco BY2 suspension cells and found to decorate all four plant microtubule arrays and to bundle microtubules *in vitro* (Jiang and Sonobe 1993). Biochemically purified 65kDa MAPs were found to induce bundling of neuronal microtubules (Chan *et al.* 1999) and form cross bridges in vitro which resemble the 25-30nm spacing between microtubules in plant cells (Lancelle 1986). Antibodies raised to bacterially expressed tobacco MAP65-1a, when used in immunohistochemical experiments, stain subsets of the cortical microtubule array and the preprophase band in interphase, the midzone of the spindle at late anaphase and the midzone of the phragmoplast (Smertenko 2000). The localisation to these midzone regions where microtubules overlap, suggests that it may play a role in the behaviour of anti-parallel microtubules at these sites. Furthermore in this study, bacterially expressed tobacco MAP65-1a was shown to bind microtubules and stimulate microtubule polymerisation *in vitro.* Subsequent screening of the tobacco expression library identified two further tobacco MAP65 family members, MAP65-1b and MAP65-1c (Hussey *et al.* 2002). The completion of the *Arabidopsis* genome allowed the identification of the complete MAP65 protein family from *Arabidopsis*. This family consists of nine members with molecular weights ranging from 54-80kDa. Members of this *Arabidopsis* family have been expressed in bacteria and shown to bind and bundle microtubules like other plant members of the family. (Hussey, unpublished data). Analysis of these sequences showed the presence of a 'destruction box', (R-XX-L-XXXX-N) a sequence present in all cell cycle regulated proteins (Glotzer *et al.* 1991, Hussey *et al.* 2002). This sequence targets the protein to the ubiquitin degradation pathway resulting in rapid degradation during cell cycle progression. There appear to be relatives of MAP65 in humans (PRC1) and yeast (Ase1p), although the primary sequence identity is very low. They do however, share the domain architecture of MAP65, consisting of two to three coiled coil regions and the destruction box. Interestingly, all of these MAPs have been located to the spindle midzone and therefore may share a common role here. The yeast example, Ase1p, has been shown to have similar

properties to the MAP65 family, including the binding and bundling of microtubules (Schuyler *et al.* 2003). Furthermore, the loss of Ase1p results in premature spindle disassembly and conversely, the overexpression of Ase1p is sufficient to trigger spindle elongation (Schuyler *et al.* 2003). It remains to be seen whether perturbation of MAP65 levels have similar results but is likely that the members of this extended family, MAP65/Ase1p/PRC1, all stabilise the spindle midzone through production of microtubule cross bridges and their levels are controlled in a cell cycle specific manner.

Cloning the *Arabidopsis PLEIADE* gene revealed that *PLE* is synonymous with *AtMAP65-3* (Müller *et al.* 2004; Hussey *et al.* 2002). *Ple* mutants were isolated in genetic screens for defects in root and embryo morphogenesis (Sorensen *et al.* 2002; Söllner *et al.* 2002; Müller *et al.* 2002). To date six *ple* alleles have been isolated and all are rerecessive and develop short irregular expanded roots with multinucleated cells and incomplete cell walls. AtMAP65-3/PLE localises in the midzone of overlapping microtubules during cell division and the mutations in *ple-1*, *ple-5* and *ple-6* cause C-terminal truncations of the AtMAP65-3/PLE protein (Müller *et al.* 2004). Therefore the *ple* phenotypes together with the subcellular localisation of MAP65-3/PLE support its essential role for the completion of cytokinesis.

The study of MAP65 proteins has been furthered recently by the functional dissection of a single *Arabidopsis* isoform, AtMAP65-1 by Smertenko and colleagues. (Smertenko *et al.* 2004) The expression programme of *AtMAP65-1* in various organs and tissues was determined by transforming *Arabidopsis* with an *AtMAP65-1* promoter::*GUS* reporter gene transcriptional fusion construct. *AtMAP65-1* is ubiquitously expressed in all organs and tissues apart from anthers and petals. Experiments designed to study the effect of AtMAP65-1 on the dynamics of microtubules revealed that recombinant AtMAP65-1 does not promote polymerization and does not stabilize microtubules against cold induced microtubule depolymerisation but rather induces microtubule bundling in vitro form

25nm cross-bridges (Smertenko *et al.* 2004). The C terminal half of the protein contains the microtubule binding activity and two alanine residues, 409 & 420 are essential for this interaction. Consistent with these findings A420 is mutated to valine in the AtMAP65-3/PLE gene in the cytokinesis–defective mutant, pleiade4 (Muller *et al.* 2002). Previously it was suggested that the 25-30 nm crossbridges between microtubules created using a carrot MAP65 enriched protein preparation were unlikely to be generated by monomeric MAP65 molecules (Chan *et al.* 1999). Therefore, Smertenko and colleagues assessed whether the recombinant AtMAP65-1 could form oligomers. Here it was demonstrated that AtMAP65-1 may form dimers and that the N terminal half of the protein contains a region responsible for this dimerisation.

1.5.5 A microtubule severing MAP.

Katanin, originally isolated from sea urchin eggs, is the only ATP dependant microtubule severing protein and is a heterodimer of 60 and 80kDa subunits. The p60 subunit is the catalytically active component and is sufficient to sever microtubules whereas p80 is a WD40 repeat protein, which targets the p60 to centrosomes. Although both the p60 and p80 homologues exist in the *Arabidopsis* genome, only p60 has been analysed by mutation and subcellular location in plants. There are several mutant alleles of the gene which encodes AtKSS: *FRAGILE FIBRE2, (FRA2)/BOTERO1, (BOT1)/ECTOPIC ROOT HAIR3 (ERH3)* (Bichet *et al.* 2001, Burk *et al.* 2001, Webb 2002). Phenotypes consist of problems with cortical microtubule orientation, anisotropic cell expansion, cell wall biosynthesis, cell elongation and cell specification in the *Arabidopsis* root epidermis. The reduced anisotropic growth was found to be correlated with random microtubule and cellulose microfilbril organisation. Therefore, the observed pleiotropic phenotypes are likely to be as a result of secondary effects on the organisation of the cell wall. Although here, cell shape and organ architecture are affected throughout the root and shoot, such genetic analysis has demonstrated a fundamental role for AtKSS, which appears to be limited to non-dividing cells.

However, examination of microtubule organisation in dividing cells of fra2 root tips showed a delay in the redistribution of microtubules associated with the nucleus to the cortex, following exit from the cell cycle (Burk *et al.* 2001). In addition, as AtKSS has been shown to localise to the nuclear membrane, these data lead to the suggestion that here, at the nuclear membrane, AtKSS microtubule severing activity may cut back microtubules, allowing them to recycle and redistribute into the cortical array.

1.5.6 Microtubule Stabilising MAPs.

Recently, a conserved family of microtubule associated proteins has been identified in several organisms, including yeast, insects, frogs, humans and plants. This family is currently the only family of MAPs (microtubule associated proteins) which is found to be common to animals and plants; and the abilities of the members of this family range from kinetochore function and spindle formation to cell morphogenesis.

All of the members of this family were independently discovered using several different techniques. The majority of these were identified by genetic screening, including Msps, in *Drosophila* (Cullen *et al.* 1999), Zyg-9 in *Caenorhabditis* (Hirsh & Vanderslice 1979), Dis1 and Alp14 in fission yeast (Ohkura *et al.* 1988, Garcia *et al.* 2001), Stu2 in budding yeast (Wang & Huffaker 1997) and MOR1 in *Arabidopsis*. Others made use of a variety of further approaches: DdCP224 in *Dictyostelium* was identified during immunoscreening of centrosomal proteins (Graf *et al.* 2000) and *Ch-TOG* in humans was cloned as a gene, which was found to be over expressed in human tumour cells (Charrasse *et al.* 1998). Also, XMAP215, the *Xenopus* member of the family, was purified as a 215kD protein factor which increased the elongation rate of microtubules in *Xenopus* egg extracts (Gard & Kirschner 1987).

Initially, Hirsh and Vanderslice (1976) isolated the *zyg-9*, zygote defective mutant. Here, this temperature sensitive mutant laid eggs that failed to hatch at the restrictive temperature. Later, Wood *et al.* (1980) and Kemphues *et al.* (1986) showed that this loss of Zyg-9 activity affected spindle formation in meiotic and the first mitotic division. Following these experiments, Gard and Kirschner (1987) purified XMAP215. XMAP215 is one of the most extensively studied proteins of the family. Tournebize (2000) immunodepleted XMAP215 and illustrated that it was a major microtubule stabilising factor in *Xenopus* egg extracts. The protein dramatically increases the growth rate of microtubules by seven to tenfold, and if depleted by 50-70%, this results in an increase in the catastrophe frequency and a reduction in microtubule length. Furthermore, this stabilisation was shown to be primarily due to the opposition of the activity of a microtubule destabilising factor, the kinesin, XKCM1. Importantly, the effects of XMAP215 depletion can be rescued by inhibition of XKCM1. Popov *et al.* (2001) analysed the function of different domains of the XMAP215 protein by expressing three GFP linked fragments: the N terminus, middle and the C terminus, FrN, FrM and FrC respectively. Here, FrN was found to co-localise with microtubules in egg extracts but not in cells; FrC co-localised with microtubules and centrosomes in extracts and cells; and FrM did not localise to microtubules or centrosomes. These findings lead to the proposal that the carboxy terminus of XMAP215 is responsible for the protein's ability to bind microtubules, and that the amino terminus is the site at which the protein's microtubule stabilisation and growth promotion is located.

In fission yeast, Ohkura *et al.* (1988) identified the *dis1* (defect in sister chromatid disjoining) cold sensitive mitotic mutant. However, it was found that Dis1 was not essential for cell division. More recently, Nakaseko *et al.* (2001) identified a second member of the family in fission yeast, Alp14. Again, although the *Alp14* mutant gave a phenotype, the Alp14 protein was found to be non-essential. However, *dis1 / alp14* double mutants were shown to be lethal. Wang and Huffaker (1997) identified the budding yeast equivalent, *STU2*, by screening for genes which

affected the function of tubulin. Severin *et al.* (2001) & Kosco *et al.* (2001) later demonstrated that STU2 was essential for cell division and was required for formation and orientation of the spindle.

Charrasse *et al.* (1998) showed that the human member of the Dis1/TOGp family, TOGp, the nearest homologue of MOR1, co-sedimented with taxol-stabilised microtubules in vitro, and that an enriched fraction could promote mirotubule assembly. Following these experiments, Dionne *et al.* (2000) showed that TOGp was required for microtubule aster assembly in an ATP dependent manner. Spittle *et al.* (1997, 1999, 2000) produced TOGp truncations to analyse the interaction of TOGp with the microtubule lattice. Here again, using co-pelleting assays, the microtubule binding domain was narrowed down to a region of 600 basic amino acids, located towards the amino terminus of the protein. The C-terminal section of the protein had a lower affinity for microtubules but did bind tubulin dimers.

Finally, the plant member of the family, MOR1 or AtMAP215, was identified in *Arabidopsis* by Whittington (2001), during a screen for microtubule organisation defects, and by ourselves during searches for an *Arabidopsis* XMAP215 homologue in the *Arabidopsis* genome sequence database. Whittington mutagenised seedlings and examined these with immunostaining of tubulin in first leaf epidermal cells. Using ecotype specific markers, *MOR1* was identified as a gene of approximately 14 kilobases, consisting of 53 exons. RT-PCR revealed a 6kb cDNA for MOR1, which encoded a protein with a predicted mass of 217kD. Two mutant alleles of *mor1* were identified. At the *Mor1-1* mutant allele, a base change of cytosine to thymine has caused the substitution of leucine with phenylalanine at the amino acid position of 174. However, the *mor1-2* mutant allele, has a guanine to adenine base change which has caused the substitution of glutamic acid with lysine, at amino acid position 195. In the *mor1-1* mutant protein, an amino acid with a hydrophobic side chain has been exchanged for one with an aromatic ring, possibly leading to steric hindrance; whereas in the *mor1-2* mutant

protein, an amino acid with a negative charge has been exchanged for one with a positive charge. These changes would lead to a change in the protein's structure, and in the case of *mor1-2*, such a change in charge in this area could abolish an electrostatic interaction with another protein or within the MOR1 protein itself. It is intriguing that both of these mutations result in an amino acid substitution in the same N-terminal HEAT repeat: a motif which is believed to be responsible for protein-protein interactions. In experiments with living cells, GFP-tubulin was expressed in the *mor1* mutant and microtubule organisation was examined. At the permissive temperature of 21°C, *mor1* microtubules appeared similar to those of wild type. However, on shifting to a restrictive temperature of 29°C, during a period of 90 minutes, cortical microtubules became progressively disorganised. Although eventually microtubules were short and misaligned, they were never completely disassembled. On returning to the permissive temperature of 21°C, within minutes, microtubules lengthened and organisation was restored. Examination of *mor1* plants at the restrictive temperature revealed several morphological defects, including: a left handed twist of organs, isotropic cell expansion and impaired root hair polarity. Furthermore, seeds germinated at the restrictive temperature are small and do not develop flowers. In addition, if plants are shifted to the restrictive temperature after flowers are produced, there is a loss of fertility.

1.5.7 Kinesins.

Kinesins constitute a superfamily of microtubule motor proteins that are found in eukaryotic organisms and in total nine subfamilies of kinesins have been identified (Kim & Endow 2000) (**FIGURE 1.4**). Members of the kinesin family perform many diverse cellular functions, such as transport of vesicles and organelles; spindle formation and elongation; chromosome segregation; microtubule dynamics and morhogenesis. Only a few kinesins have been characterised in plants, including *Arabidopsis*. Recently, a bioinformatic approach, using the complete *Arabidopsis* gemone, has revealed that it contains 61 kinesin genes and when compared with the other 4 completed eukaryotic genomes, the *Arabidopsis* gemone has the

Figure 1.4: A New Kinesin Tree

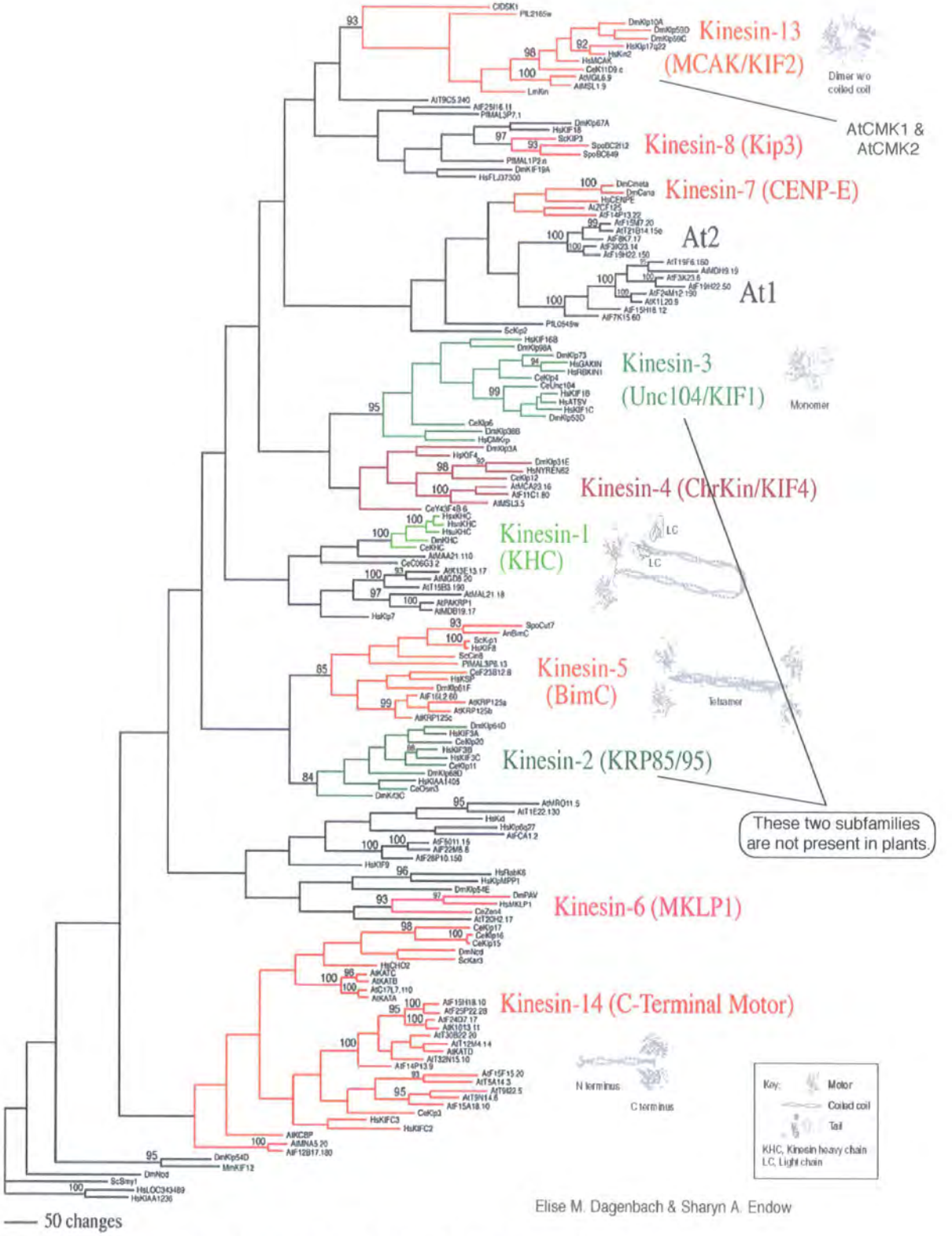

Reproduced from Dagenbach E.M. & Endow, S.A. (2004): A new kinesin tree. Journal of Cell Science 117, 3-7.

highest percentage of kinesin genes (Reddy & Day 2001). *Arabidopsis* has seven of the nine recognised subfamilies of kinesins, whereas some kinesins do not fall into any known family. These groups of kinesins, which are not present in yeast, *C. elegans* and *Drosphila* may represent new subfamilies specific to plants.

Members of the kinesin superfamily have a highly conserved motor domain. The first kinesin was identified in squid giant axons as a protein involved in transport of vesicles (Vale *et al.* 1985, Brady 1985). The conventional kinesin is a tetramer with two heavy chains and two light chains. The kinesin heavy chains (KHCs) contain the motor domain with ATPase activity, the central coiled-coil region and a tail that binds the light chains. Historically, proteins with homology to the KHC, but falling in different subfamilies, have been called kinesin-like proteins (KLPs). However, KHCs are now recognized as a subfamily of the kinesin superfamily and all members of the superfamily are referred to as kinesins. All kinesins have a domain with homology to the motor domain of KHC, but little sequence similarity outside of this domain. Kinesins bind microtubules and a variety of cargos (via the tail domain) and perform force generating tasks such as transport of vesicles and organelles, spindle formation and elongation, chromosome segregation and microtubule organization. The motor domain of KHC is in the N-terminal region but in other kinesins it can be located in the C-terminal or internally (Reddy & Day 2001).

The first plant kinesins to be identified were the *KAT* genes, which encode KATA, KATB, and KATC (Mitsui *et al.* 1993). KATA antibodies were found to stain microtubule bundles and the spindle, where by anaphase the staining was concentrated at the mid-zone which persisted in the phragmoplast (Liu & Palevitz 1996, Liu *et al.* 1996). More recently the ATK1 (formally known as KATA) mutant was found to have defective spindle organisation and meiotic chromosome segregation suggesting that ATK1/KATA has an important role in spindle morphogenesis (Chen *et al.* 2002). A forth member of the family, KATD is

structurally dissimilar and possess a centrally located motor domain (Tamura *et al.* 1999).

A second kinesin found in plants with a mitotic role was KCBP or kinesin-like calmodulin binding protein. KCBP localises to the PPB, the spindle and the phragmoplast (Bowser & Reddy 1997). Interestingly the kinesin's association with calmodulin appears to be involved in the regulation of is ability to bind microtubules as in the presence of calcium or calmodulin, the affinity of KCBP for microtubules is reduced (Deavours *et al.* 1998). Closer examination of the spindle revealed that during metaphase KCBP was associated with kinetochore fibres and during the transition to anaphase the kinesin redistributes to the spindle pole (Smirnova *et al.* 1998). KCBP is a minus end directed motor and considering the redistribution to the spindle pole it is suggested that KBCP draws microtubules together as it travels towards the pole (Lloyd and Hussey chapter). Furthermore, KBCP also appears to have a crucial role during interphase and cell expansion. The trichomes of zwi mutants are shorter and have fewer branches (Oppenheimer *et al.* 1997) and the ZWICHEL gene product was found to be KCBP.

TKRP125 is a novel kinesin isolated from tobacco BY2 cells and has been localised to all the plant microtubule arrays (Asada *et al.* 1997). In the PPB and phragmoplast it is distributed along microtubules but in the spindle it also accumulates at the equatorial plane or mid-line. It is likely that this kinesin facilitates the reorganisation of microtubules particularly during mitosis and the assembly of the phragmoplast as anti-TKRP125 antibodies inhibit translocation of microtubules within the phragmoplast. TKRP125 is a member of the bimC subfamily of kinesins and a bimC mutant phenotype consists of spindle poles which fail to separate, demonstrating its function in spindle bipolarity (Enos & Morris 1990). Therefore it has been suggested that the plant bimC, TKRP125 may have a similar role in separating the two halves of the cytokinetic phragmoplast (Lloyd & Hussey chapter). Anti-TKRP antibodies fail to label the line of overlap

between the two halfs of the phragmoplast, however a carrot homologue, DcKRP120 does label this zone.

A second kinesin, which is found at the mid-line of the phragmoplast, is *Arabidopsis* PAKRP1 (Phragmoplast associated Kinesin Related Protein). AtPAKRP1 is a member of the Xklp2 subfamily and starting at anaphase the protein becomes progressively concentrated at the plus end of phragmoplast microtubules (Lee and Liu 2000). Consist with this localisation, PAKRP1 is involved in maintenance of the phragmoplast as truncated fusion proteins cause the anti-parallel microtubules of the phragmoplast to become disorganized (Lee and Liu 2000). AtPAKRP2 shows a similar, yet punctate, localization to the phragmoplast mid-line and moves centrifugally with the growing cell plate. It is believed that AtPAKRP2 associates with golgi vesicles as this staining was altered by the golgi disruption drug brefeldin A (Lee *et al.* 2001).

A third type of plant kinesin, which associates with the phragmoplast are members of the CENP-E subfamily, NACK1/HIK and NACK2. NACK (NPK activating kinase-like protein) are kinesins, which bind to NPK1, a kinase kinase kinase, which is involved in the regulation of the phragmoplast (Nishihama *et al.* 2002). Studies with NACK1/HIK demonstrate that this kinesin is essential for the formation of the cell plate. Hinkel mutants were identified as abnormal Arabidopsis embryos where the regular division patterns were severely perturbed with enlarged cells and incomplete cell walls (Strompen *et al.* 2002). Here, the phragmoplasts were seen to nearly span the diameter of the cell during cytokinesis, suggesting that lateral expansion of the phragmoplast was unaffected. However, the phragmoplasts in the hik mutants did exhibit microtubules across the entire division plane (Strompen et al 2002). Wild-type cells lack microtubules in the phragmoplast division plane, suggesting that hik gene function is required for reorganisation of phragmoplast microtubules during cell plate formation.

1.5.8 Microtubule Destabalising MAPs.

Stathmin family

The small MT destabilizing phosphoprotein, oncoprotein 18 or stathmin, is located to spots within the interphase cytoplasm (Cassimeris 2002). Stathmin binds tubulin hetrodimers in a 1:2 ratio *in vitro* and destabilises microtubules by sequestering tubulin dimmers, reducing the concentration of free tubulin available for polymerization. In addition stathmin also increases catastrophe frequency at the plus end of microtubules, without affecting growth. Possible plant orthologues are the WAVE-DAMPENED2 (WVD2) group of small charged proteins, whose overexpression induces right-handed helical growth in roots (Yuen *et al.* 2003).

Catastrophic Kinesins.

Microtubule motor proteins such as kinesins can be described as mechanochemical enzymes which, conventionally, translate along microtubules by utilizing energy derived from the hydrolysis of ATP. This hydrolysis produces a conformational change within the protein which enables the kinesin to 'walk' along the microtubule. However, several kinesins are capable of utilizing this ATP dependant conformational change in a different manner.

XKCM1, the first of a new breed of kinesins

Initially, two studies indicated that kinesins were important in the regulation of microtubule assembly. Endow *et al.* (1994) showed that the minus end directed kinesin, Kar3p was capable of inducing minus-end depolymerisation of taxol stabilized microtubules in *in vitro* motility assays. In further studies, Lombillio *et al.* (1995) found that the rate of microtubule plus-end shortening induced by tubulin dilution was faster when the end was coupled to a bead via a kinesin. However, the most striking illustration of the involvement of kinesins in the regulation of

microtubule assembly came with the identification of the kinesin related protein XKCM1 by Walczak *et al.* (1996) from xenopus eggs. Here, it was shown that XKCM1 was essential for normal mitotic spindle formation and was capable of selectively promoting microtubule catastrophe.

Walczak *et al.* (1996) screened a xenopus ovary expression library with an antibody raised against a conserved region of the kinesin motor domain in order to identify those kinesins involved in cell division. Here, the most abundant clone encoded an 85 kDa kinesin, Xenopus Kinesin Central Motor, XKCM1. XKCM1 is a member of the Kinl kinesin subfamily, which also includes the mammalian KRP, MCAK (Mitotic centromere-associated kinesin) (Kim *et al.* 1997). Sequence analysis of the XKCM1 2402bp cDNA revealed that it encoded a 730 amino acid protein with a 250 amino acid amino terminal globular domain; a 130 Amino Acid carboxy terminal a helical domain and a centrally located 350 amino acid motor domain. This central positioning of the motor appears to be common to all Kinl kinesins, although this arrangement is not exclusive to the Kinl subfamily.

Antibodies raised against the amino terminus of XKCM1, used to determine its localization in cells, showed that during interphase, XKCM1 is diffuse throughout the cytoplasm and nucleus. At mitosis, although the diffuse pattern is observed, XKCM1 also becomes concentrated at the centromere and spindle poles. In addition, in *in vitro* experiments XKCM1 was again found at the centromeres and spindle poles but also along the spindle microtubules. This localisation to the spindle has also been observed for other kinl kinesins including MACK. During interphase, MCAK is diffusely distributed within the cytoplasm and the nucleus. At prophase, MCAK is recruited to mitotic centromeres and remains until telophase. (Wordeman & Mitchison 1995).

Depletion of endogenous XKCM1 from xenopus egg extracts by 25-99% results in the formation of aberrant spindles with long microtubule arrays radiating from the

centrally located chromatin, which were estimated to be 10x times the mass of normal bipolar spindles. In addition, it was observed that in these depleted extracts the frequency of microtubule catastrophes was reduced by four fold. Conversely, this spindle disorganisation was rescued by the addition of purified XKCM1.

Considering these data, Walcsak *et al.* (1996) proposed a model that implicated XKCM1 function in the regulation of microtubule dynamics at the kinetochore in addition to its role during spindle assembly. Here, XKCM1 acts to regulate oscillations observed at the kinetochore which are thought to be transitions due to switches between growth and shrinkage. XKCM1 would be positioned near the end of microtubules and walk towards the plus end, representing the plus end directed kinetochore motor detected in vitro by Hyman and Mitchison (1990). Upon reaching the plus end, XKCM1 would then trigger catastrophe. This would result in the movement of chromosomes back towards the pole in conjunction with microtubule depolymerisation. A proposed anchor for the chromosomes to these depolymerising microtubules was thought to be CENP-E.

How Do Kinl kinesins destabilize microtubules?

A possible mechanism for XKCM1 induced microtubule catastrophe was based on the GTP-cap model of dynamic instability. Growing microtubule ends are stabilised by a terminal cap of tubulin-GTP dimers. Following the incorporation into the microtubule, the β-tubulin bound GTP is hydrolysed to GDP. A catastrophe occurs due to the loss of this stabilizing tubulin-GTP cap. If the terminal β tubulin subunits of the (+) end of the microtubule are GDP-tubulin rather than GTP-tubulin, these subunits curl outwards and rapidly disassociate. XKCM1 would cause a conformational change in the terminal tubulin-GTP subunits, inducing the hydrolysis or release of GTP (Waters & Salmon 1996).

Early studies of XKCM1 showed that the protein bound microtubules in an ATP dependant manner, binding in the absence of ATP and its release in the presence

of ATP. Later studies (Desai *et al.* 1997) showed that both XKCM1 and XKIF2, a second xenopus KinI, were capable of catalytically destabilising microtubules and were targeted to microtubule ends where they induce a destabilising conformational change as proposed. Furthermore, Desai *et al.* (1997) demonstrated that ATP hydrolysis, a property of kinesins usually used for translocation, recycled XKCM1/KIF2, allowing multiple rounds of destabilisation by dissociating the XKCM1/XKIF2-tubulin dimer complex release upon microtubule depolymerisation. In these experiments, XKCM1 in the presence of ATP completely inhibited MT assembly and this XKCM1/KIF2 destabilising activity required ATP and was inhibited by the non-hydrolysable analogue, AAMPPNP.

Further to these findings, Moores *et al.* (2002) studied a member of the KinI family from Plasmodium falciparum (pKinI). Here, unlike MCAK, it was found that a fragment of pKinI consisting of only the motor core was capable of depolymerisation. Moores' experiments confirmed the ATP dependency of KinI activity, but also looked at the interaction of pKinI with microtubules through its ATPase cycle. These experiments studied the amount of pKinI bound to microtubules in the pellet fraction in the absence of nucleotide and in the presence of ADP.AlF (mimicking the ADP.Pi state) and ADP. In these assays all tubulin pelleted, indicating that microtubules are not depolymerised by pKinI in both these nucleotide states. In contrast, in the presence of the non-hydrolysable ATP analogue, AMPPNP, there was a clear increase in the amount of tubulin in the supernatant with increasing pKinI, which was not observed with the other nucleotides. This AMPPNP result suggests that the key step in KinI microtubule depolymerisation is coupled to ATP binding by the KinI motor core. In addition, where the concentration of pKinI was lower that that of polymerized tubulin the majority of pKinI was located in the pellet. At concentrations of pKinI higher than polymerised tubulin, pKinI was also present in the supernatant, thus suggesting that the binding ratio is one pKinI motor per tubulin dimer. EM results confirmed

these findings, showing that the motor protruded from the microtubule wall every 80 A, which is the same the length of a single tubulin dimer.

Moores presented a model for pKinI action based on these observations (**FIGURE 1.5**). pKinI binds the microtubule and exhibits microtubule-stimulated ADP release (Step 1). pKinI binding of ATP induces a conformational change in the kinesin and the underlying tubulin dimer, causing the dimer to bend outwards from the microtubule wall (Step 2). The ATP hydrolysis and phosphate release stages of the ATPase cycle detach the pKinI-tubulin dimer complex from the protofilament (Step 3) and then disassociate the pKinI-tubulin dimer complex, recycling the kinesin for a second round (Step 4). The crux of this mechanism is such that, whereas the conventional kinesin uses the energy of ATP hydrolysis to execute a powerstroke, KinI kinesins use it to bend protofilaments.

Niederstrasser *et al.* (2002) studied the interaction of XKCM1 with tubulin more closely. Experiments using zinc –induced tubulin polymers suggested that XKCM1 acts on a single protofilament. Tubulin polymers made of subtilisin-treated tubulin, which lacks its C-terminal tail (A region demonstrated to be important for the processivity of kinesins), are resistant to XKCM1-induced depolymerisation, indicating that the interaction between the acidic tail, and possibly basic residues in XKCM1, are required for its depolymerisation activity. However, in these experiments, XKCM1 was still found in the tubulin pellets, suggesting that the CT tail is required for depolymerisation but not necessarily binding.

Funtional analysis of KinI kinesin domains

Although the motor core of pKinI is sufficient for microtubule destabilisation, Maney *et al.* (2001) have shown, using molecular dissection, that the conserved motor domain of MCAK is necessary but not sufficient for microtubule depolymerisation.

FIGURE 1.5: The Catastrophic Mechanism of Kin I Kinesins

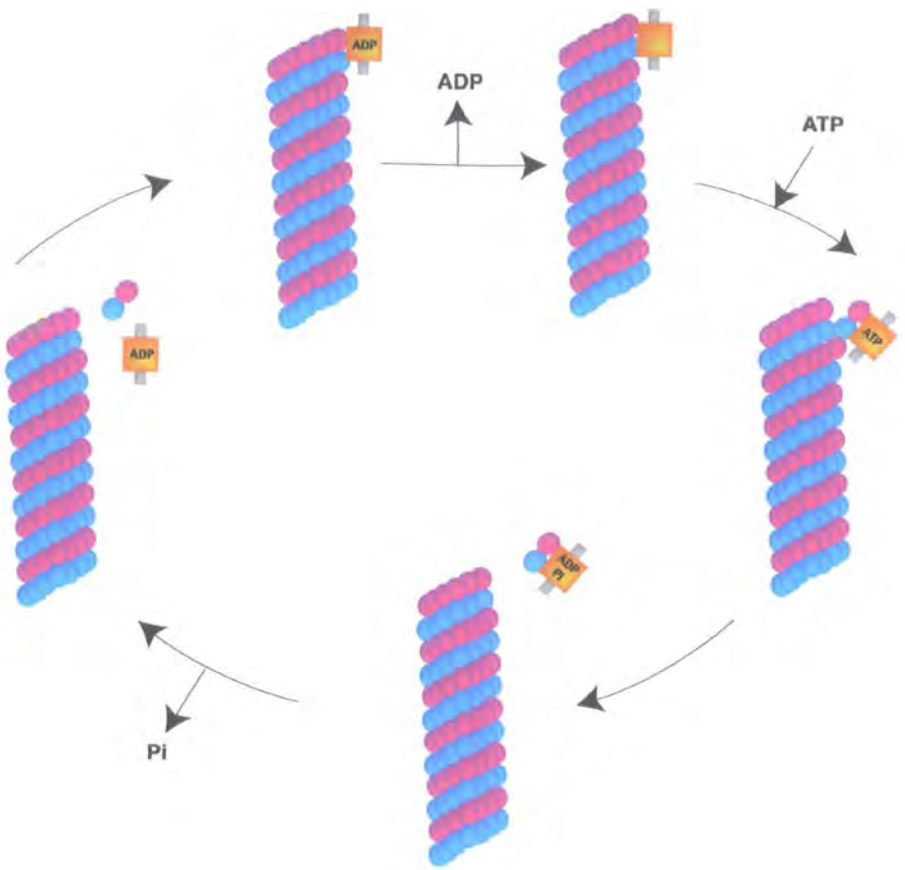

Model for the stages of KinI motor ATPase-coupled microtubule depolymerisation

Figure 1.4: This figure shows the Moores model for the microtubule depolymerisation activity of pKinI. The KinI motor binds to microtubule ends in a similar way to other kinesin motors, releasing bound ADP (1), when ATP binds (2) a conformational change in the tubulin dimer is induced. ATP hydrolysis and phosphate release stages of the ATPase cycle are required to separate the KinI-tubulin dimer complex from the protofilament (3) and then disassociate the motor from the tubulin dimer.(5) (Moores *et al.* 2002)

The addition of 30 amino acids to the amino terminal of the motor were required to restore the depolymerising activity of MCAK.

CHO cells were transfected with GFP-MCAK and a series of deletion constructs. The transfection of full length MCAK resulted in significant microtubule loss after 18hrs whereas the deletion of the entire C-terminal portion of MCAK up to the motor domain did not affect this activity. Two N-terminal deletions of residues 1-150 and 1-182 both showed the same activity as for full length MCAK. However, deletions of residues 1-201 and 1-232 resulted in reduced effectiveness to decrease polymer levels and almost total abolition of microtubule depolymerisation activity respectively. Although construct E232 is unable to depolymerise microtubules, in binding/extraction assays it was shown to still be capable of binding the polymer. Therefore residues 201-31 are required in addition to the motor domain to achieve significant depolymerisation, however, a further 19 residues, 182-20, are necessary to produce levels equal to or better than full length MCAK.

Kinl kinesins at the kinetochore

Recently, Garcia and colleagues (2002a, 2002b) identified two Kinl family proteins in fission yeast, KLP5 and KLP6. Both were found to localise to the mitotic kinetochores and the spindle midzone. During interphase, Klp5 localised to cytoplasmic microtubules in distinct dots and at mitosis, localises in a punctate pattern to the spindle. As the cell enters anaphase and the spindle elongates, the protein disassociates from the spindle microtubules but is retained at their central regions. Interestingly, it was found that, unlike MCAK where the kinesin forms homodimer complexes, they instead form a heterodimer with each other. Both these kinesins are required for accurate chromosome segregation and normal interphase microtubules. Single and double KLP5/6 deletion mutants were viable, although the cells did show a 20% increase in length with elongated microtubules, occasionally with oval morphology around the cell end. Mutants stayed longer in

mitosis and observations of the kinetochore and centrosome showed that sister centromeres move back and forth between the spindle poles with all strains showing severe chromosome segregation defects. Anti-tubulin staining in KLP over-expression cells showed that spindles are unevenly distributed within the cell, with chromosomes which are displaced from the centre, suggesting that the interaction between the spindle and the kinetochore has been compromised.

1.6 A proposed model for the effects of the *mor1* mutations on microtubule dynamics.

As mentioned previously the steady-state of length of microtubules appears to be determined by the relative activities of XMAP215 and XKCM1 in xenopus egg extracts (Tournebize *et al.* 2000). Also experiments using different fragments of the XMAP215 protein containing the N-terminus, middle and C-terminus showed that the N-terminus containing protein-protein interacting HEAT repeats (Andrade & Bork 1995) was responsible for the catastrophe-suppressing activity of XMAP215 and that the C-terminus was responsible for microtubule binding (Popov *et al.* 2001).

Considering these and other findings, it is possible to suggest two models to described the effect of the *mor1* mutations on microtubule dynamics (**SEE FIGURE 1.6**). At the permissive temperature a KinI-like kinesin can bind to MOR1 at the N-terminal HEAT repeat. At the restrictive temperature a conformational change in the protein caused by the *mor1* mutations releases the kinesin, which is now capable of depolymerising the microtubules (Model 1.). Alternatively, MOR1 decorates the microtubules at the permissive temperature, stabilising the long microtubules in the cortex. A shift to the restrictive temperature causes a loss of the N-terminus catastrophe-suppressing activity or microtubule –binding capability of MOR1, enabling a KinI-like kinesin to destabilize the long cortical microtubules (Model 2.).

1.7 Aim and Objectives.

Members of the XMAP215/TOGp family of proteins are regulators of microtubule dynamics and promote microtubule polymerization and stabilisation and are required for the correct formation of microtubule arrays. Examples of this type of microtubule associated protein have been identified in several organisms including humans, frogs, insects and yeast. Furthermore XMAP215/TOGp proteins participate in an antagonistic relationship with a type of microtubule destabilizing factor called catastrophic kinesins.

The aim of the project was to identify an *Arabidopsis* member of the XMAP215/TOGp family and using immunofluorescence microscopy study the proteins localization through the cell cycle. Further to this, to examine whether such an antagonistic relationship is evident in the plant cell, *Arabidopsis* examples of catastrophic kinesins were to be identified and these proteins characterized including their localization, function and expression pattern.

During the project a mutant of the *Arabidopsis* XMAP215-like protein, MOR1 (Microtubule Organisation) was published (Whittington *et al.* 2001)

FIGURE 1.6: Possible Antagonistic Relationship Between MOR1 and Arabidopsis Kinl-Like Kinesins

MOR1 vs Kinl-like kinesins

Model 1: a Kin-I-like kinesin binds to MOR1 via a protein-protein interaction at the N-terminal HEAT repeat resulting in the activity of the Kinl-like kinesin being reduced or abolished. At the restrictive temperature the mor1 mutation causes the association at the HEAT repeat to be lost, releasing the catatrophic kinesin allowing its destabilizing activity to predominate, which leads to short disorganized cortical microtubules.

Model 2: the mor1 mutation, at the restrictive temperature, cause the protein-protein interaction between the N-terminal HEAT repeat and microtubules to be lost. Release of the N-terminus of MOR1 might expose Kinl-like kinesin binding sites. The binding of Kinl-like kinesin allows it to destabilise the microtubules and produce short disorganised cortical microtubules.

CHAPTER 2

Materials and Methods

2.1 Materials

2.1.1 E. *coli* Strains

XL-1 Blue – *rec A1 end A1 gyrA96 thi-1 hsdR19 suoE44 relA1 lac[F' proAB lac^{q}ZDM15 Tn 10* (Tet ^{r})

DH5α – *supE44, σlacU169 (∅80 lacZσM15) hsdR17, recA1, endA1, gyrA96, thi-1, relA1.*

BL21 DE3 – *F- ampT hsdSB (r^B-m^B-) gal dcm (DE3)*

BL21 DE3 *

BL21 DE3 pLysS – *F- ampT hsdS_B (r^B-m^B-) gal dcm (DE3) pLysS (Cam^R)*

BL21 Tuner™ – *F- ampT hsdS_B (r^B-m^B-) gal dcm lacY1 (DE3)*

BL21 DE3 Rosetta™ – *F- ampT hsdS_B (r^B-m^B-) gal dcm (DE3) pRARE (Cam^R)*

BL21 DE3 Rosetta 2™ – *F- ampT hsdS_B (r^B-m^B-) gal dcm (DE3) pRARE2 (Cam^R)*

F-:	Strain does not contain the F episome.
F':	Strain contains an F plasmid, which harbors some bacterial chromosomal DNA.
RecA:	Abolishes homologous recombination.
EndA:	Endonuclease I activity absent; thought to improve quality of plasmid minipreps.
Gyr:	Mutation in DNA gyrase. Confers resistance to naladixic acid.
Thi:	Requires thiamine for growth in minimal medium.
HsdR:	Abolishes restriction but not methylation of certain sequences(r- m).
RelA:	"Relaxed" mutation permits RNA synthesis in the absence of protein synthesis.
ProAB:	Requires proline for growth on minimal medium.
Tn 10:	Contains the TetR transposable element, Tn 10.

AmpT: Lacks an outer membrane protease; improves recovery of intact recombinant proteins.

HsdS: Abolishes both restriction and methylation of DNA at certain sites (r-m-).

Gal: Unable to utilize galactose.

Dcm: No methylation of cytosines in the sequence CCWGG.

DE3: Contains a lambda prophage in which the gene for T7 RNA polymerase is under control of the lacUV5 promoter.

PLysS: Cam^R plasmid that carries the gene for T7 lysozyme.

LacY1: Abolishes *lac* permease.

PRARE: Cam^R plasmid that carries the tRNA genes for six codons rarely used in *E. coli.*

PRARE2: Cam^R plasmid that carries the tRNA genes for seven codons rarely used in *E. coli.*

Cam^R: Chloramphenicol resistance.

Tet^R: Tetracycline resistance.

2.1.2 *Agrobacterium* Strains

Details are as follows; strain, background, Chromosomal marker gene, Ti plasmid, plasmid marker gene, reference.

LBA4404 TiAch5, rif, pAL4404, spec & strep, Hoekema *et al.* 1983

C58C3 Industrial strain of the C58 background whose specific genotype is unknown. Resistance nal and strep

GV3101 C58, rif, pMP90 (pTiC58DT-DNA), gent, Koncz & Schell 1986

2.1.3 Yeast Strains

Y187

MATα, ura3- 52, his3- 200, ade 2- 101, trp 1- 901, leu 2- 3, 112, gal4Δ, met–,

gal80Δ, URA3 : : GAL1$_{UAS}$ -GAL1$_{TATA}$ -lacZ, MEL1

System - GAL4 2H-2, GAL4 2H-3, PT Libraries

Reporter - *lacZ, MEL1*

Markers - *trp1, leu2*

Harper *et al.* 1993

AH109

MATα, trp1-901, leu2-3, 112, ura3-52, his3-200, gal4Δ, gal80Δ, LYS2 : : GAL1$_{UAS}$-GAL1$_{TATA}$-HIS3, MEL1, GAL2$_{UAS}$-GAL2$_{TATA}$-ADE2, URA3::MEL1$_{UAS}$- MEL1$_{TATA}$-lacZ

System - GAL4 2H-3

Reporter – *HIS3, ADE2, lacZ, MEL1*

Markers – *trp1, leu1*

James *et al.* 1996

2.1.4 Arabidopsis Lines

Line name	Columbia
Source	LEHLE Seeds
Catalogue No.	WT-02-33-01
Ecotype	Columbia

2.2 Methods

MOLECULAR BIOLOGY

2.2.1 Nucleic Acids: general methods & cloning techniques

2.2.1.1. Restriction Digests

Digests were carried out in a total volume of 20μl, containing 2μl of plasmid miniprep DNA (>1μg), 2μl of 10x buffer and 2-4 units of the appropriate restriction endonuclease enzyme. Mixtures were made up to 20μl with sterile distilled water (sdH_2O). All reactions were incubated at the optimum temperature for two hours.

2.2.1.2 Agarose Gel Analysis

Agarose gel electrophoresis was used to separate PCR and restriction digest products. The appropriate amount of agarose was melted in a suitable volume of TAE buffer (0.04M Tris acetate, 1mM EDTA) in a microwave. Ethidium Bromide was added to the molten agarose to a final concentration of 0.5mg/ml prior to pouring into trays with various sized combs. The percentage of the gel was decided with regards to the size of DNA fragments to be separated. The set gels were transferred to an electrophoresis tank and submerged in TAE buffer. Samples were prepared by the addition of the required amount of 10 x loading dye and then loaded into the wells. Following electrophoresis, gels were visualized by UV illumination and photographed in a BioRad GelDoc. Ethidium Bromide contains a planar tricyclic phenanthride ring system that is able to intercalate between the stacked base pairs of double-stranded DNA. Following insertion into the helix, the drug lies perpendicular to the helical axis and makes van der waals contacts with base pairs above and below and its peripheral phenyl and ethyl groups project into the major groove of the DNA helix (Waring 1965). UV radiation at 302nm and 366nm is absorbed by the dye and this energy is re-emitted at 590nm in the red-orange region of the visible spectrum (Tuma *et al.* 1999).

2.2.1.3 DNA Recovery From Agarose Gels

Following electrophoresis as described above, DNA was recovered from gels using Ultrafree-DA centrifugal filter devices (Millipore) according to manufacturer's instructions.

2.2.1.4 Ligation of Vector and Insert DNA

PCR products were cloned using either TA cloning kits pGEM-T Easy (Promega) and TOPO 2.1 (Invitrogen) or via a Gateway™ (Invitrogen) BP reaction described in (**CHAPTER 2 SECTION 2.2.6**). The TA cloning kits utilize the fact that during

amplification, *Taq* polymerase has a nontemplate-dependant terminal transferase activity which produces single deoxyadenosine (A) overhangs to the 3' ends of all amplified fragments. Direct cloning is facilitated by the presence of a corresponding single deoxythymidine (T) overhang at the cloning site of the pGEM-T or TOPO2.1 vectors.

PGEMT reaction mixture

2X rapid ligation buffer, T4 DNA ligase	5ul	
pGEMT vector	1ul	50ng/ul
PCR product	Xul	
T4 DNA ligase	1ul	5 units
SdH2O	up to 1ul	

$$\frac{50\text{ng vector} \times \text{insert length in kb}}{3.0\text{ kb vector}} \times 3/1 = \text{Xng insert to use}$$

The insert and vector were used at a 3:1 molar ratio as established by gel analysis and calculated with the above formula, to promote efficient ligation. The mixture was then incubated for 1 hour at room temperature (22-23°C).

In addition to T/A overhangs, the TOPO2.1 vector has Topoisomerase I, covalently bound to the vector and is referred to as an activated vector. Topoisomerase I from *Vaccina* virus binds to duplex DNA at specific sites, cleaves the phosphodiester backbone and forms a covalent bond between tyrosine-274 of the topoisomerase and the 3' phosphate of the cleaved strand. The phospho-tyrosyl bond between the DNA and enzyme is then attacked by the 5' hydroxyl of the insert strand.

TOPO2.1 cloning mixture.

PCR product	0.5-4ul
Salt solution	1ul

SdH2O	up to 5ul
TOPO vector	1ul
	6ul

The reaction mixture is then incubated at room temperature (22-23C) for 5 minutes and then transferred to ice before being transformed into chemical competent XL1Blue or DH5α.

2.2.2 Transformations.

2.2.2.1 Preparation of Chemical Competent E. *coli*

1 ml of overnight culture was used to inoculate 100ml Psi broth (5g/l yeast extract, 20g/l Tryptone and 5g/l $MgSO_4$ pH 7.6) and incubated at 37°C with aeration until an A_{550} of 0.48 was obtained. This culture was then place on ice for 15 minutes and then cells were pelleted at 3-5000g for 5 minutes. The supernatant was discarded and 0.4 volumes of TfbI (30mM potassium acetate, 100mM RbCl, 10mM $CaCl_2$, 50mM manganese chloride and 15% v/v glycerol, pH5.8) were added. The cells were resuspened and again incubated on ice for 15 minutes. As before the cells were pelleted and following the removal of the supernatant were resuspened in 0.04 volumes of TfbII (10mM MOPS, 75mM CaCl2, 10mM RbCl and 15% v/v glycerol pH6.5). After incubation on ice of 15 minutes the cells were then separated into aliquots (typically 50-200μl) and quick frozen in liquid nitrogen and stored at –80.

2.2.2.2 Preparation of Electro-Competent *Agrobacterium.*

Agrobacterium tumifaciens strain C56C3 (Nickerson) was grown on LB agar plates (100mg/ml streptomycin, 25mg/ml Nalidixic Acid) incubated at 30°C. These colonies were then usede to inoculate a 5ml LB (100mg/ml streptomycin, 25mg/ml Nalidixic Acid) overnight culture incubated at 30°C. 100ml of this culture was then

used to inoculate a 50ml 2YT culture grown at 30°C until OD_{600nm} 0.45 was obtained. This was then chilled on ice and the the celles were pelleted by centrifugation at 4000g for 10 minutes. Cells were resuspended in 1 volume (50ml) of ice cold 10 % glycerol and pelleted as before. Resuspention and pelleting were repeated with reducing volumes of 10% glycerol, 0.5/0.02/0.02. The cells were finally resuspended in 0.01 volumes of 10 % glycerol and separated into 40ml aliquots, quick frozen in liquid nitrogen and stored at –80.

2.2.2.3 Transformation of *E. coli*; Heat Shock Method

An aliquot of RbCl chemical competent E. coli cells were thawed on ice to which was then added 10μl of ligation or BP reaction mixture. The cells were then incubated on ice for 30 minutes following which they were then 'heat shocked' at 42°C for 40 seconds and placed back on ice for a further 2 minutes. 500μl of LB (Luria-Bertani medium, 10g/l NaCl, 10g/l peptone, 5g/l yeast extract pH 7.0) was then added to the cells and they were allowed to recover at 37°C for one hour with shaking. Cells were the plated out on suitable selective LB agar plates.

2.2.2.4 Transformation of Electro-Competent *Agrobacterium*;

Electroporation cuvettes and SOC media were chilled on ice. 1-3μl of plasmid DNA was added to 40μl of thawed electro-competent cells and mixed gently on ice. Cells were then transferred to a chilled electroporation cuvette. The cells were then electroporated at 1440 volts (Eppendor Electroporator 2510). Immediately following electroporation, 200μl of chilled SOC was added to the cells in the cuvette (wash out) and then transferred to 760μl of chilled SOC. These cells were then incubated at 30°C with shaking (140rpm) for 3-4 hours and then plated out onto LB agar plates (100mg/ml streptomycin, 25mg/ml Nalidixic Acid, plus appropriate antibiotic selection for transformed plasmid).

2.2.3 Isolation of DNA from *E. Coli* and *Agrobacterium*

2.2.3.1 *E. coli*: Plasmid Mini,Midi and Maxi preps

Plasmid Mini,Midi and Maxi preps were carried out using the Qiaprep (Qiagen)/GeneElute(Sigma) plasmid miniprep kits, Qiagen tip-100 kit, and the Qiagen tip-500 kit respectively. DNA isolation was carried out according to manufacturer's instructions.

2.2.3.2 *Agrobacterium*: Plasmid Mini preps

Plasmid mini preps were carried out using the Wizard *Plus* SV miniprep kit (Promega) according to manufacturers instructions.

2.2.5 Polymerase Chain Reaction

2.2.5.1 General PCR Amplification of DNA Fragments

To produce DNA fragments for cloning PCR was carried out using a HYBAID *Omn-E* series thermocycler.

A typical PCR reaction mixture contained;
50 ng template DNA (genomic or cDNA), <1ng plasmid DNA
0.5mM Forward primer
0.5mM Reverse primer
10 x polymerase buffer (containing $MgCl_2$ in the case of Pfu)
2 or 3mM $MgCl_2$
0.2mM dNTPs (each)
x units of RedTaq (Helena Biosciences) or Pfu (Promega)
Reactions were then made up to 50µl with sdH_2O.

The thermocycler program was as follows; 94°C for 2 minutes, then 35 cycles of 94°C 1 minute, 55°C for 1 minute and 72°C for the appropriate time (RedTaq ~1kb/min or Pfu ~0.5kb/min) Following 35 cycles there was a final extension at 72°C for 10 minutes.

2.2.6 The GATEWAY™ Cloning System (Invitrogen)

GATEWAY™ is a system for cloning and subcloning DNA sequences and once in this system, DNA segments are transferred between vectors using site-specific recombination (**FIGURE 2.1**). It enables the transfer of one or more DNA sequences into multiple vectors in parallel reactions, while maintaining orientation and reading frame. The bases of the system, is that it uses phage lambda-based, site-specific recombination, instead of restriction endonucleases and ligase. The phage lambda recombination system *in vivo*, is used during the switch between the lytic and lysogenic pathways. Two reactions constitute the cloning pathway. The BP Reaction is a recombination reaction between an attB-flanked PCR product and a donor vector to create an entry clone. The LR Reaction is a recombination reaction between an entry clone and a destination vector, to create an expression clone. The BP and LR reactions are catalysed by the BP and LR clonase enzyme mixes respectively.

PCR primers were design to start with the required gateway sequences as below;

Forward primer:
GGGGACAAGTTTGTACAAAAAAGCAGGCTTC – 18-25 gene specific nucleotides

Reverse primer:
GGGACCACTTTGTACAAGAAAGCTGGGTC – 18-25 gene specific nucleotides

The primers above represent those for a protein fusion product, where the underlined nucleotides provide that the clone protein will be in frame with the N- or

C-terminal tags. If native expression is required additional sequences are included here such as a Kozak sequence for eukaryotic expression or a Shine-Dalgarno sequence for bacterial expression. In both cases unless a C-terminal fusion is required a stop codon must be included after the underlined nucleotides in the reverse primer.

This PCR product was then used in a BP reaction with a donor vector, typically pDONR207 in which the PCR product was recombined into the vector.

BP reaction mixture;

PCR product	1-10ml	4-100 fmoles
Donor vector	2ml	300ng
BP reaction buffer	4μl	
TE buffer	to a final volume of 16μl	
BP clonase mix	4μl	(Cat No. 11789-013)
	20μl	

This entry clone was then used in an LR reaction. Here the PCR fragment is recombined out of the entry vector and into the appropriate destination vector, such as His tag or GST fusion expression.

LR reaction mixture;

Entry vector	1-11ml	100-300ng
Destination vector	1-11ml	150ng
LR reaction buffer	4μl	
TE buffer	to a final volume of16 ml	
LR clonase mix	4μl	(Cat No. 11791-019)
	20μl	

Figure 2.1: The Gateway Cloning System

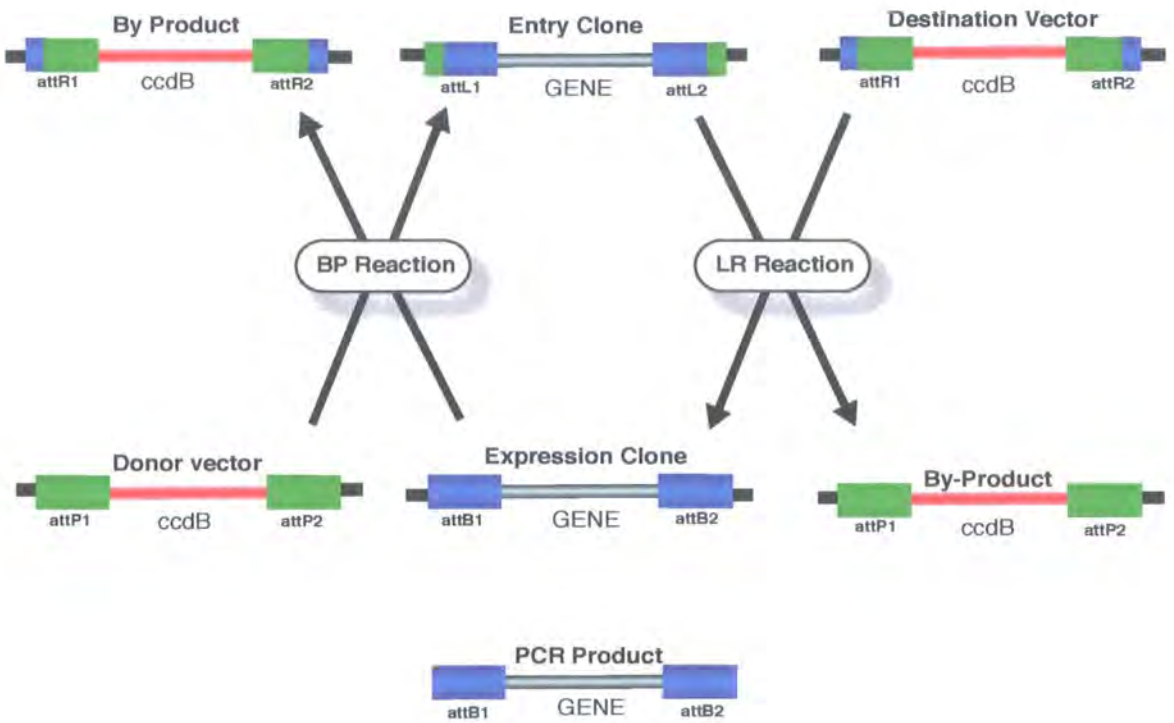

Figure 2.1: GATEWAY™ is a system for cloning and subcloning DNA sequences and once in this system, DNA segments are transferred between vectors using site-specific recombination. It enables the transfer of one or more DNA sequences into multiple vectors in parallel reactions, while maintaining orientation and reading frame. The bases of the system, is that it uses phage lambda-based, site-specific recombination, instead of restriction endonucleases and ligase. The phage lambda recombination system *in vivo*, is used during the switch between the lytic and lysogenic pathways. Two reactions constitute the cloning pathway. The BP Reaction is a recombination reaction between an attB-flanked PCR product and a donor vector to create an entry clone. The LR Reaction is a recombination reaction between an entry clone and a destination vector, to create an expression clone. The BP and LR reactions are catalysed by the BP and LR clonase enzyme mixes respectively

Following both reactions only E. *coli* with the correct recombinant vector grow due to the negative selection of the toxic cassette. This cassette is present in all donor and destination vectors and contains the ccdB gene, which is toxic to the E. *coli*. Strain DH5α. During the BP and LR reactions this cassette is recombined out.

For more information on the GATWAY system please consult the invitrogen technical manual.

CELL BIOLOGY

2.2.7.1 Fixation and microtubule staining in Arabidopsis tissue culture cells.

10ml of 3 day old (3 days since last subculture) Arabidopsis tissue culture cells were fixed for 30 minutes in freshly prepared parformaldehyde fixative(3.7% paraformaldehyde, 50 mM PIPES, pH 6.8, 5 mM EGTA, 2 mM $MgSO_4$, 0.4% Triton X-100) following the removal of all culture media. 50ml of the fixative was typically prepared as follows; 740 mg of Paraformadlehyde was added to10ml of cold distilled water. This was then incubated in a 65°C water bath for 5 minutes after which 100ml of 0.1M NaOH was added. The mixture remained at 65°C until the solution became clear, signifying that the paraformaldehyde had polymerized. The fixative was then removed from the water bath and the remaining constituents of the buffer were added. After fixation the cells were washed in PBS buffer (Na2HPO4 570mg/l Na2HPO4.12H2O 145mg/l KH2PO4 212mg/l NaCl 8g/l Tween 20 1ml/l) for a period of 5 minutes twice. The cells were then treated with an enzyme mixture () for 10 minutes to digest the cell wall. Following digestion the cells were washed in PBS as before.

The fixed cells were placed onto polylysine coated coverslips and allowed to attach for 10 minutes after which, unattached cells were poured off and the slides washed

in PBS. The slides were incubated in PBS buffer containing 2% BSA for 30 minutes to prevent unspecific binding of antibodies. Slides were the incubated for 1 hour with the primary antibody mixture. This mixture contained the serum raised to the protein of interest diluted typically 1:500 with PBS containing 2% BSA. The primary antibody mixture also contained commercial antibodies to tubulin diluted as directed by the manufactures. After incubation the slide was washed as before in PBS buffer. The slide was then incubated for 1 hour with the secondary antibody mixture. Here commercial antibodies to species specific IgGs conjugated to variety of fluorochromes were used (**TABLE 2.1**) these were again diluted in PBS + 2% BSA as directed by the manufactures. The slides were finally washed in PBS and mounted in VectaShield (Vector Laboratories).

2.2.7.2 Laser Scanning Confocal Microscopy (LSCM)

Tissue samples for immunofluorescence and GFP studies were viewed using a Zeiss Axioskop microscope (Carl Zeiss Ltd., Welwyn Garden City, Herts, UK) fitted with a Bio-Rad Radiance 2000 laser scanning system or a Zeiss Axiovert 200M microscope fitted with a Zeiss LSM 510 laser scanning system. Red and green channels were acquired sequentially using a green HeNe laser for the red channel and an Argon laser for the green channel. Fluorochromes used were FITC (Flourescein isothiocyanate) and TRITC (Tetramethylrhodamine isothiocyanate). FITC is exited at 494nm and emits at 520 and TRITC is exited at 554 and emits at 576.

TABLE 2.1

Antibody	**Species raised in**	**Conjugate**
Primary Antibodies		
Anti-AtMOR1	Mouse	-
Anti-AtCMK1	Mouse	-
Anti-AtCMK2	Mouse	-
Anti-tubulin	Rat	-

Anti-tubulin	Sheep	-
Secondary Antibodies		
Anti-Mouse IgG	Rabbit	TRITC
Anti-Sheep IgG		FITC
Anti-Rat IgG		FITC

Biochemistry

2.2.8 Dimentional SDS-PAGE (Polyacrylamide Gel Electrophoresis) analysis.

Glass plates were cleaned thoroughly with detergent, distilled water and 70% ethanol and assembled. The appropriate percentage resolving gel mixture, to give the optimal separation of proteins was prepared by adding the required amount of acrylamide to resolving buffer (0.75M TrisHCl, pH8.8, 10% Ammonium persulphate,10% SDS). The polymerization catalyst, TEMED, was added and the mixture was poured into the assembled plates and allowed to polymerize. Ethanol was layered on top of the gel mix to give a flat surface and to prevent drying out. The stacking gel was prepared again by the addition of the appropriate amount of acrylamide to stacking gel buffer (0.25M TrisHCl, pH6.8, 10% Ammonium persulphate, 10% SDS). The overlaying ethanol was removed from the resolving gel and a comb inserted above. TEMED was added to the stacking gel mix which was then poured into the gel assemble around the comb and allowed to polymerize. Following polymerization the comb was removed and the wells washed with distilled water. The gel assembly was disassembled and the gel was submerged vertically in a tank of gel running buffer (Tris 2.5mM,Glycine 19mM, SDS 0.01%). Protein samples were mixed 1:1 with 2 x sample buffer (0.25 M TrisHCl, pH 6.8, 4% SDS, 20% glycerol, 10% Mercaptoethanol) and loaded into

wells. A potential difference of 200 Volts was applied across the gel and proteins were allowed to migrate until the loading dye reached the base of the gel.

Gels were stained for 20 minutes in gel staining solution (50% MeOH, 10% Acetic acid, 1.25% Coomassie Brilliant Blue R-250) and then de-stained in de-stain solution (10% MeOH and 10% Acetic acid). Gels were stored in gel drying/storage buffer (25% EtOH, 2% Glycerol)

2.2.9 Electroblotting and Western Blotting

Protein was transferred from SDS-PAGE gels to Nitrocellulose membranes. The gel was placed next to a nitrocellulose membrane, with care to remove all air bubbles, in a transfer assembly. This was then submerged vertically in a tank of transfer buffer (Tris 2.5mM,Glycine 19mM, SDS $2x10^{-3}$%). The gel/membrane are orientated so that the membrane is nearest the + electrode as due to the effects of SDS on proteins they carry a – charge and hence migrate to the + pole, from gel to membrane. A potential difference of 20V was applied across the gel/membrane sandwich and proteins were allowed to migrate overnight. The membrane was washed in distilled water and the quality of transfer was assessed by staining with Amidoblack (0.5 g of Amidoblack in 50 ml of 5% acetic acid)

The membrane was washed with distilled water until all amidoblack stain was removed, and then incubated in milk buffer, 5% dried milk powder in TBST(10mM Tris of pH 7.4, 150mM NaCl, 0.5 ml/l), for 30 minutes, to block unspecific protein binding. Following blocking the membrane was incubated for one hour with the primary antibody to the protein of interest. The antibody was typically diluted 1:1000 in milk buffer. After incubation the membrane was washed in 2 x TBST buffer for a series of 3, 5 minute steps. Next the membrane was incubated as before for one hour with the secondary antibody. The secondary antibody was anti-mouse IgG conjugated to horseradish peroxidase (Amersham Pharmacia). This antibody was routinely used at a dilution of 1:3000 in milk buffer. Again following

this incubation the membrane was washed as before with 2 x TBST. To visualise the presence of the probed protein the membrane was finally incubated with 1 ml of ECL reaction solution (Amersham Pharmacia). Here the horseradish peroxidase, located to the protein of interest, catalyses a reaction between the ECL constituents, Luminol, 4-iodo-phenol and H_2O_2. Oxidised Luminol emits blue light that is captured on X-ray film. Luminesence generated by intense bands may appear within a few seconds, whereas faint bands need at least 30 minutes to develop (Schneppenheim & Rautenburg 1987).

2.2.10 Bacterial Expression of His-tagged Proteins

Following cloning of the required protein or protein fragment into the appropriate expression vector, pET28/pGAT4 (Novagen) for 6xHis fusions, these plasmids were transformed into E.*coli* BL21 expression cells. The choice of BL21 strain, was decided on the bases of their relative levels of expression of each protein. Cells were grown in 20ml overnight cultures with selection. These were then used to inoculate 2 litre expression cultures again with selection and incubated at 37°C with shaking. Once the culture had reached an OD_{600nm} of 0.45, expression was induced by the addition of IPTG to a final concentration of 1mM (The expression of the tagged protein in the pET system is controlled by the lac operon). The culture was then incubated at the optimal temperature with shaking at 250rpm for a minimum of 2 hours.

2.2.10.1 Purification of His Tagged Proteins

Nikel Column Purification of His-tagged Proteins

Immoilised-metal affinity chromatography (IMAC) was first used to purify proteins in 1975 (Porath et al. 1975) using the chelating ligand iminodiacetic acid (IDA). IDA was charged with metal ions such as Zn^{2+}, Cu^{2+} or Ni^{2+} and then used to purify a variety of different proteins (Sulkowski 1985). Metal chelate affinity chromatography separates proteins and peptides on the basis of their affinity for

metal ions that have been immobilized by chelation. Certain amino acids (e.g. histidine and cysteine) form complexes with the chelated metals around neutral pH (pH 6–8). It is primarily the histidine content of a protein that is responsible for its binding to a chelated metal, which makes the technique an excellent method for purifying recombinant proteins such as poly-histidine fusions, as well as many natural proteins. The metal chelate-forming ligand iminodiacetic acid (IDA) is coupled to sepharose beads by stable ether bonds via a seven or nine-atom spacer arm (**FIGURE 2.2**). The two chelating resins used in this thesis were Qiagen Ni-NTA and Amersaham HiTrap Chelating HP. The difference between these systems is that Ni-NTA uses nitrilotriacetic acid instead of IDA which has a third acetic acid group and therefore occupies four rather than three of the six ligand binding sites.

FIGURE 2.2

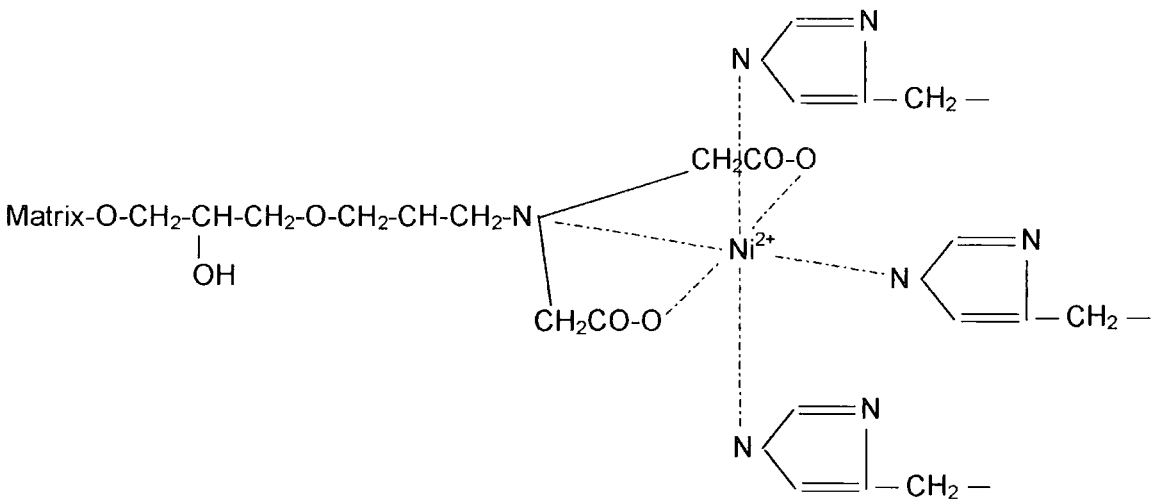

His-tag purification is based on the principle that the two or three remaining ligand binding sites in the coordination sphere of the nickel ion are bound by the nitrogen atoms in the imidazole ring of the R groups of the histadine residues of the His-tag. Binding background of contaminants is reduced by low concentrations of free imidazole in the binding and wash buffers. The recombinant His-tagged protein is

finally eluted from the column by washing with a high concentration of free imidazole (typically 500mM), which competes with the tag for the Ni ligand binding sites.

FIGURE 2.3

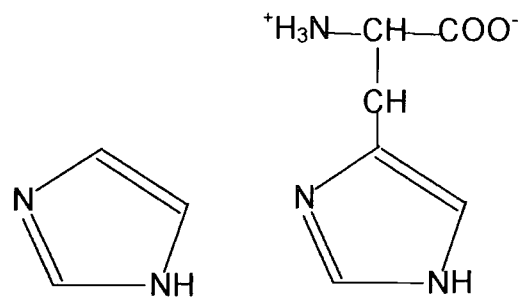

Imidazole Histidine

Expression cultures were centrifuged at 7000g for a period of 5 minutes to pellet the cells (Beckman J2-HC with JLA-10.500 fixed angle rotor). The supernatant was removed and pellets were re-suspended in ice cold. protein extraction buffer (50mM NaH_2PO_4, pH 8.0, 300mM NaCl, 5mM mercaptoethanol) containing protease inhibitors (1mM PMSF, 10 ng/ml leupeptine, 1 ng/ml pepstatine A). The cells were then sonicated in order to disrupt the cell membranes and release the expressed protein. This lysate was then centrifuged at 48,000g for 10 minutes to sediment all cell debris (Beckman J2-HC with JA-20 fixed angle rotor). The supernatant was passed through a 0.2mm filter and loaded onto a column containing 2ml of Ni-NTA (Qiagen). The supernatant and Ni-NTA were gently mixed on ice for 20 minutes to allow sufficient binding of His tagged protein to the Ni-NTA. Following the removal of lysate the Ni-NTA beads were washed with buffer (1M NaH_2PO_4 pH 8.0, 5M NaCl) containing increasing concentrations of imidazole in a stepwise gradient. Two washes of 2ml 20mM imidazole, one wash of 2ml 40mM imidazole (incubated for 5 minutes), two washes of 60mM imidazole and finally one wash of 80mM imidazole. The expressed His tagged protein was then eluted in a volume of 3ml of elution buffer(50mM NaH_2PO_4 pH 8.0, 300mM

NaCl, 250mM Imidazole). The yield and purity of protein was assessed by SDS PAGE analysis.

2.2.11 Production of polyclonal antibodies

The purified protein was concentrated to a final concentration of approximately 1 mg/ml. 100ml of this was then mixed 1:1 with Freuds incomplete adjuvant and agitated until a homogeneous emulsion was reached. 50ml of the emulsion was injected into the right and left sides of the peritoneal cavity of each of 3, 6 week old mice. These injections were repeated twice more at 14 day intervals. Ten days after the third immunization a tail bleed was taken from each mouse and the serum used in a western blot to check the antibodies specificity. If this was satisfactory the mouse was killed immediately and a cardiac bleed completed. The serum of this bleed was used for all following western blot and immunohistochemistry experiments.

2.2.12 Co-sedimentation, microtubule binding experiments.

The expressed protein to be studied was dialysed or with use of a PD10 desalting column was transferred into Cosed or MTSB buffer (50mM PIPES, 2mM EGTA 2mM MgSO4, 3mM, 100mM NaCl, 5 % Glycerol, 0.2% NP-40). Tubulin was isolated from porcine brain by two assembly/disassembly cycles followed by phophocellulose chromatography as described in Shelanski *et al.* (1973). Tubulin, and recombinant proteins were centrifuged at 150,000g for 15 min at 32°C remove any aggregates. For the assays with non-stabilised microtubules, tubulin at a concentration of 20μM was mixed with the specified concentration of recombinant protein, incubated at 32°C for 15 min and centrifuged at 100,000g for 15 min (Beckman TLX ultracentrifuge, rotor TLA120.1) The supernatant was collected and pellet was washed and resuspended in SDS-PAGE sample buffer.

2.2.13 Microtubule polymerization assay.

Pig brain tubulin was used at a final concentration of 20μm in all assays. Tubulin solution was stored at –80C. Before each assay, tubulin was rapidly thawed at 37°C, incubated on ice for 5 min and centrifuged at 200,00g for 10 min to pellet polymerized microtubule and tubulin aggregates. The supernatant was diluted to a 30μm tubulin stock with MTSB buffer (0.1M PIPES, pH6.8, 2 mM EGTA, 2 mM MgSO4, 2 mM DTT, 50mM NaCl and 10% glycerol). The blank was set up with the cuvette containing 100μl of 30μm in MTSB. Then GTP was added up to a final concentration of 1mM followed by recombinant protein. The final reaction volume was adjusted to 150μl with MTSB and the turbidity of the reaction was monitored at 350nm and 32°C using a Helios beta spectrophotometer equipped with Unicam Peltier temperature control unit (Thermospectronic, UK). Each experiment was repeated three times a represenative example is presented.

Silver Staining of Proteins on Nitrocellulose Membranes

Membrane with proteins was washed in TBST until traces of other stains such as amidoblack were removed. The membrane was then washed 3 times in distilled water. Membrane was incubated in the Erlenmeyer flack (2% Na_3-citrate, 0.8% $FeSO_4.7H_2O$) + 0.2% $AgNO_3$ for 2-5 minutes. Following appearance of bands, membrane was washed in distilled water and air-dried. In addition membrane can be fixed with photo fixer.

Yeast

2.2.15 Yeast Two-Hybrid

2.2.15.1 Small Scale yeast cell transformation

AH109 and Y187 yeast glycerol stocks were streaked out on to fresh YPAD (20g/l tryptone, 10g/l yeast extract, 20g/l agar, 30mg/l adenine hemisulphate, 2% glucose, pH 5.8) plates. A single colony from each plate was used to inoculate

10ml YPAD liquid cultures and grown overnight. 100ml YPAD was inoculated with the overnight culture to an OD_{600} of ~ 0.2 and incubated at 30°C for a further 4-4.5 hours. The cells were then pelleted at 3000rpm for 5 minutes and re-suspended in 50ml SDW. The cells were pelleted as before and re-suspended in 1.5 ml Li/TE (10mM Tris.Cl, 1mM EDTA, 10.2mg/ml LiAc pH 7.5) and transferred to an eppendorf. The cells were then pelleted at 1000rpm and re-suspended in 500µl Li/TE. 1µg of the required plasmid DNA was added to a fresh eppendorf tube along with 160µg of carrier DNA. To this 100µl of the appropriate yeast cells, 10µl DMSO and 600µl PEG/Li/TE (10mM Tris.Cl, 1mM EDTA, 10.2mg/ml LiAc, 400mg/ml PEG pH 7.5) were added and mixed gently. This mixture was then incubated at 30°C for 30 minutes and then transferred to 42°C for a further 15 minutes. The cells were then pelleted at 1000g (Jouan CR422 with Jouan M4 swing bucket rotor) and re-suspended in 1ml SDW. 100µl was then plated out onto selective media. SD media (6.7 g/l yeast nitrogen base, 20g/l agar, 2% glucose pH5.8) with the appropriate 10x dropout solution: - L (lysine) for cells transformed with pAS2 and –W (tryptophan) for cells transformed with pACT2.

The bait construct (pAS2) was transformed into Y187, whilst the activator construct (pACT2) was transformed in AH109. In addition the bait construct (pAS2) was also transformed into AH109 for autoactivation controls.

2.2.15.2 Yeast mating and diploid selection

Three colonies from AH109(pACT2)plates were each resuspended in 30ml SDW and spotted onto a YPAD plate in triplicate. Three Y187(pAS2) colonies were resuspended and spotted as before, but on top of the previously spotted AH109 colonies. The YPAD plate was then left on the bench (28°C) for two days allowing the yeast to mate. These colonies were then streaked out into – W –L SD media and incubated at 30°C overnight, to select for diploids.

2.2.15.3 β-galactosidase filter assay for the lacZ reporter gene.

A filter was placed onto the surface of the appropriate SD plate and allowed to wet. The plate with filter was incubated for 2 days at 30°C allowing the colonies to adhere to the surface of the filter. Following transfer the filter was removed and placed immediately into liquid N2 for ~ 5 seconds. The filter was then placed on to a second filter soaked with 1.8ml assay buffer (3ml/ml b-mercaptoethanol, 333mg/l X-Gal, 11.1g/l $Na_2HPO_4.2H_2O$, 5.5 g/l $NaH_2PO_4.H_2O$, 0.75 g/l KCL, 0.25 g/l $MgSO_4.7H_2O$ pH 7.0) in a petri dish, covered and incubated at room temperature. A blue colour developed between 30 minutes – 30h. Those Colonies that produced a blue colour and the time at which the colour was observed were recorded.

10x Dropout Solution.

300 mg/l L-isoleucine

1500 mg/l L-valine

200 mg/l L-adenine hemisulphate

200 mg/l L-arginine HCL

200 mg/l L-histidine HCL monohydrate

1000 mg/l L-leucine

300 mg/l L-lysine

200 mg/l L-methionine

500 mg/l L-phenylalanine

2000 mg/l L-theronine

200 mg/l L-tryptophan

300 mg/l L-tyrosine

200 mg/l L-uracil

2.2.16 Gus Staining

Plant tissue was submerged in GUS staining solution (50mM NaHPO4 pH 7,2, 0.5% Triton X-100, 0.5mM KfeCN (potassium ferrocyanide), 1mM X-Gluc). The

tissue was vacuum infiltrated using a desiccation device attached to an electric pump for approximately 5 minutes. The sample were then left for 48 hours at 37°C. Chlorophyll was removed from sample tissue post-staining with 70% ethanol. Samples were then placed in 30% glycerol for 20 minutes and mounted onto microscope slides.

2.2.17.1 *Arabidopsis* seed sterilization

Arabidopsis seeds were incubated in 10% Bleach for 10 minutes and then washed with sd water 3 times.

2.2.18 *Arabidopsis* & BY2 tissue culture media

Arabidopsis cell suspension culture media

A. thaliana suspension culture was maintained at 27°C in Murashige and Skoog medium (MSMO, MS salts with minimal organics) pH 5.7, containing 30 g/l sucrose and supplemented with 0.5 mg/l naphthalene acetic acid (NAA) and 0.05 mg/l kinetin.

BY2 cell suspension culture media

Tobacco BY-2 (Bright Yellow) suspension culture was maintained at 27°C in Murashige and Skoog medium pH 5.8, containing 4.31g/l MS salts, 30 g/l sucrose and supplemented with 0.2 mg/l 2.4D, 200mg/l KH_2PO_4, 100 mg/l Myo-inositol, 1mg/l Vitamin B2.

2.2.19 Production of Protoplasts

Filter sterilized enzyme solution () was added to *Arabidopsis* tissue culture cells in a petri dish under sterile conditions. The cells were the incubated at 25°C for approximately 24 hours for digestion of the cell wall to occur. Then the cells were filtered through 50mm gauss to remove aggregates. W5 media (18.4g/l CaCl2, 9g/l

NaCl, 800mg/l KCl, 1g/l glucose pH5.7) was the layered onto the filtrate and centrifuged at 100g for 5 minutes. The intact protoplasts visible as a band at the interface of the two solutions, were removed and added to a volume of W5 media and centrifuged at 100g for 5 minutes to wash. The resulting pellet of protoplasts was then washed again. Finally the protoplast pellet was re-suspended in protoplast maintenance media () and returned to 25°C.

2.2.20 *Arabidopsis* Transformation: The Dipping Method.

Arabidopsis thaliana were sown in 3.5' pots, 5-10 plants per pot with plastic mesh placed over the soil. Plants were then grown for 3-4 weeks until they were approximately 10-15cm tall and displaying a number of immature, unopened flower buds. 2-3 days before prior to dipping open flowers and any siliques were removed. *Agrobacterium tumefaciens* strain C58C3 were grown for 48 hours at 30C in 200ml LB (100mg/ml streptomycin, 25mg/ml Nalidixic Acid + plasmid). The culture was pelleted by centrifugation and re-suspended in 1L 5% sucrose solution. Once re-suspended Silwett L-77 (Lehle Seeds, Texas, USA) was added to a final concentration of 0.05% v/v. The plants were fully dipped into the bacterial solution and gently agitated for 10-15 seconds. Dipped plants were placed in transparent bags to maintain humidity and placed in a shaded position overnight. The following day, plants were removed from bags and grown under standard conditions. The dipping procedure was repeated 7 days after the first dipping. Following the final dipping, the plants were returned to the greenhouse. Seeds were collected from individual pots over a period of 2-4 weeks, sterilized and germinated on 1/2 MS10 agar with appropriate antibiotic selection.

2.2.21 Transformation of BY2 suspension cells

Binary plasmids containing a plant promoter such as 35s and a plant selectable marker such as hygromycin are transformed into the *agrobacterium* strain LBA4404 by electroporation. A 5ml culture of the transformed *agrobacterium* is

grown for approximately 2 days in YEB (Meat extract 5g/l, yeast extract 1g/l, sucrose 5g/l $MgSO_4.7H_2O$ 0.5g/l) media and then 100ul is added to xml of 3days old BY2 suspension culture and incubated at 25°C for 2 days. The BY2 cells are then washed 3 times in sterile BY2 media to remove *agrobacterium* and then plated out onto BY2 media agar containing the appropriate selection and carbenicillin to kill remaining agrobacteria. These plates are incubated at 25°C for several weeks until transformants start to produce calli, which are then subculture on to fresh media containing the same selection as before and maintained for analysis.

2.2.22 Transient expression in *N. benthamiana* leaves, Infiltration.

Agrobacterium strain GV3101 was transformed with a suitable plant expression vector such as pGWB6 for expression GFP fusion proteins. In addition GV3101 *agrobacterium* were transformed with the p19 vector, which contained a silencing suppressor and these bacteria were infiltrated along with the expression strain to prolong the period of expression. Both cultures were inoculated from a single colony and grown to an OD_{600} of 0.5-1.00 with suitable antibiotic selection (Rifampicin and Gentamycin for GV3010). Bacteria were pelleted at 4000rpm for 5 minutes and the pellet then washed twice in 3ml infiltration buffer (MES10g/l, $MgCl_2$ + 200μm Acetosyrigone (3,5-dimetoxy-hydroxy-acetophenone stock in DMSO)). The pellet was finally resuspended in 2ml infiltration buffer and incubated at room temperature for at least 2 hours. Following this period the bacteria were pelleted as before and resuspended in 1ml infiltration buffer. GV3101-contruct and GV3101-p19 solutions were mixed 1:1 and transferred to a 2ml sterile syringe. Three small nicks were made in the underside of the *N. benthamiana* Leaf using a scalpel blade. The circumference of the three nicks was small enough so that all three could be covered by the tip of the syringe. The solution was then infiltrated into the leaf and successful infiltration could be observed by the darkening of the surface of the leaf. Younger leaves of a diameter of approximately 4-5cm proved to be easier

for the fluid to infiltrate and in many cases the entire leaf, rather than a small area managed to be infiltrated.

Postranslational gene silencing (PTGS) is a major cause of lack of expression in such systems and to prevent this the co-expression of the viral-encoded suppressor of gene silencing, p19 of the tomato bushy stunt virus (TBSV) was used (Voinnet *et al.* 2003).

2.2.23 Transformation of plant cells/tissue by bombardment technique.

Plasmid DNA was precipitated onto fine gold particles.

The appropriate amount of gold particles was weighed out (each cartidge is coated with 0.5mg gold), to which 100ul of 0.05M spermidine was added. This solution was then briefly vortexed and sonicated to remove clumps. Each plasmid was added to a concentration of 1ug per cartridge (max concentration 5ug as higher induces clumping). Again mixture was briefly vortexed and whilst vortexing 100ul of 1MCaCl2 was added drop by drop (volume of $CaCl_2$ must equal that of spermidine). Plasmid was allowed to precipitate onto gold for a period of 10 minutes. This solution was centrifuged at 2000g for 15 seconds and the supernatant discarded. The pellet was washed 3 times in 100% ethanol and then resuspended in resuspended in 0.05 mg/ml PVP (0.12ml per 1mg).

Making cartridges.

Tubing was dried with nitrogen gas flow for 15 minutes. The gold suspension was injected into the tubing and allowed to settle. The ethanol was then removed by syringe and the tube rotated with low nitrogen gas flow to coat all surfaces and dry. The tube was then cut into 12cm sections or cartridges.

Shooting gold into cells.

Cartridges were inserted into a cartridge holder, which was then inserted into the BioRad Helios™ GeneGun. The barrel of the gun was held at a height of 30cm of above the sample. The gold particles were expelled from the cartridges by a burst of pressurised helium. Pressure ranged from 250psi to 600psi depending of the ability of the gold particles to penetrate the tissue being used. Tissue was maintained on agar media or in a sealed moist container for 3-24hrs and cells were analysed for GFP expression by viewing with a Nikon Eclipse TE 300 microscope or a Zeiss Axioskop microscope fitted with a Bio-Rad Radiance 2000 laser scanning system.

CHAPTER 3

Bioinformatic analysis of the MOR1/GEM1 and AtCMK genes and protein sequences.

3.1 Introduction

The objective of the work described in this chapter was to make use of publicly available bioinformatic software to identify *Arabidopsis* homologues of XMAP215/TOGp and Kinl kinesins. Following their identification to then analyse these proteins and their encoding genes to gain insights into their characteristics, such as domain architecture, motifs and possible transcriptional controls.

Bioinformatics is the analysis of nucleic acid and protein sequences and structures *in silico*. In particular the completion of genome sequencing projects and software, such as BLAST, which is capable of comparing these sequences at high speed, has allow researchers to identify homologous proteins within the same genome or genomes of other organisms. BLAST, Basic Local Alignment Search Tool, is an algorithm that compares one molecular sequence against either another specific sequence (paired BLAST) or an entire database containing millions of letters of sequence (eg BLASTN, BLASTP & TBLASTN)(Altschul et al 1990; Altschul et al 1997). BLAST can achieve this by breaking down the query sequence into 'words' and using each word to test for local alignments within the database. Matches are given a statistical score and returned to the user. In addition once a sequence has been identified *in silico* or by conventional techniques, further analysis can provide useful information about the possible function of a protein in the cell and stimulate the design of experiments. However such data is only a guide and must always be confirmed by experimental data. Here the genes/proteins studied in this work have been analysed with a variety of bioinformatic software to provide a portfolio of

putative homologues, domains and motifs for each. The algorithms used are described below:

SMART, Simple Molecular Architecture Search Tool was designed to identify protein sub-domains with a defined biological function within the context of a complete protein sequence (Schultz *et al.*; Schultz *et al.* 1998; Letunic *et al.* 2002). It is accessed through an EMBL web gateway and provides an easily interpretable graphical output of the domains identified within a query protein sequence. It uses HMMs (Hidden Markov Models) to compare the query primary amino acid sequence with alignments entered into its database of known protein domains. In addition SMART was instructed to refer to the PFAM protein database in addition to its own database and to use algorithms to screen for secretion peptide sequences and coiled coil regions.

PSORT is a computer program with a web gateway that attempts to assign a probability to the query protein being localized into a particular sub-cellular compartment (Nakai and Horton 1999). It is a collection of at least 12 algorithms that search for various signs of protein localization.

Rogers and colleagues proposed that polypeptide sequences enriched in proline (P), glutamic acid (E), serine (S) and threonine (T) were responsible for targeting proteins for rapid destruction (Rogers, Wells & Rechsteiner 1986). Further research has since provided evidence that these PEST regions do serve as proteolytic signals. The PESTfind program developed by Rechsteiner and Rogers, determines whether a protein contains a PEST region. The algorithim defines PEST sequences as hydrophilic stretches of amino acids greater than or equal to 12 residues in length, containing a minimum of one P, one E or one D and one S or T. These residues are flanked by lysine (K), arginine (R) or histidine (H) residues, but positively charged residues are disallowed. PESTfind produces a score ranging

between −50 to +50 and a score greater than zero denotes a possible PEST. However values greater than +5 are considered particularly significant.

3.2 Homologues, Domains and Motifs

3.2.1 At2g35630: MOR1/GEM1

To identify a XMAP215 homologue, the *Arabidopsis* genome was searched using NCBI BLAST and XMAP215 as the query. This resulted in a single 'hit' to gene/protein At2g35630, later named MOR1/GEM1, which showed 26% identity and 44% homology to XMAP215 over the full length of the protein. At2g35630 was used as the query to BLAST all genome databases and further plant members of the XMAP215 family were identified, along with previously identified members of the family from other organisms. These results are shown in Table 1 below.

TABLE 3.1

Species	Protein	Length	Score	Expect	Identities %	Positives %	Gaps %
Nicotiana tobacum	TMBP200	2029	2650	0.0	69	78	2
Oryza sativa	Putative MAP	1920	1483	0.0	57	69	8
Homo sapiens	TOGp	2032	514	e-143	27	46	4
Xenopus laevis	XMAP215	2065	469	e-130	26	44	9
Rattus norvegicus	Rat TOGp	1915	415	e-114	27	45	6
Drosophila melanogaster	Msps	2049	398	e-109	27	43	6
Anopheles gambiae	ENSANGP0 0000021996	1851	657	2e-66	26	44	8
Neurospora crassa	Hypothetical	944	509	2e-49	30	48	5
Pneumocystis carinii	Probable MAP	827	470	8e-45	31	47	5
Aspergillus nidulans	Hypothetical	891	451	1e-42	29	44	2

Gibberella zeae	Hypothetical	877	431	3e-40	29	46	4
Dictyostelium discoideum	DdCP224	2015	159	9e-37	25	49	5
Schrzosaccharomyces pombe	Alp14	809	158	2e-36	28	45	3
Caenorhabditis briggsae	Hypothetical	1419	135	7e-30	22	42	9
Schrzosaccharomyces pombe	P93dis1	882	124	3e-26	24	42	10
Caenorhabditis elegans	Zyg9	1415	115	8e-24	20	41	6
Eremothecium gossypii	ACL132Cp	954	108	2e-21	24	41	12
Arabidopsis thaliana	Unnamed protein product	97	91.3	2e-16	47	53	31
Arabidopsis thaliana	Hypothetical	102	73.2	7e-11	48	52	39

Here it was found that tobacco and rice both possess proteins which are highly similar to *Arabidopsis* At2g35630. In addition the *Arabidopsis* genome contains two small genes/proteins, which are almost identical to a central region of At2g35630. Further analysis of these gene entries revealed that these were both hypothetical splicing variants of the same gene, At3g28155. Members of the XMAP215 family revealed by BLAST were aligned using ClustalW and a phylogenetic tree calculated by PAUP (Swofford 1991) (**FIGURE 3.1**). The confidence of each node of a tree is represented by the bootstrap value associated with it. Here the software randomly substitutes regions of the sequence with other strings within the sequence and redraws the tree. This is repeated a specified statistically significant number of times. For the trees in this thesis a value of 1000 was selected; therefore the bootstrap values are the number of times out of 1000 that the alignment/tree produced that node.

Figure 3.1: Phylogenetic Trees of the XMAP215/TOGp Family of Proteins

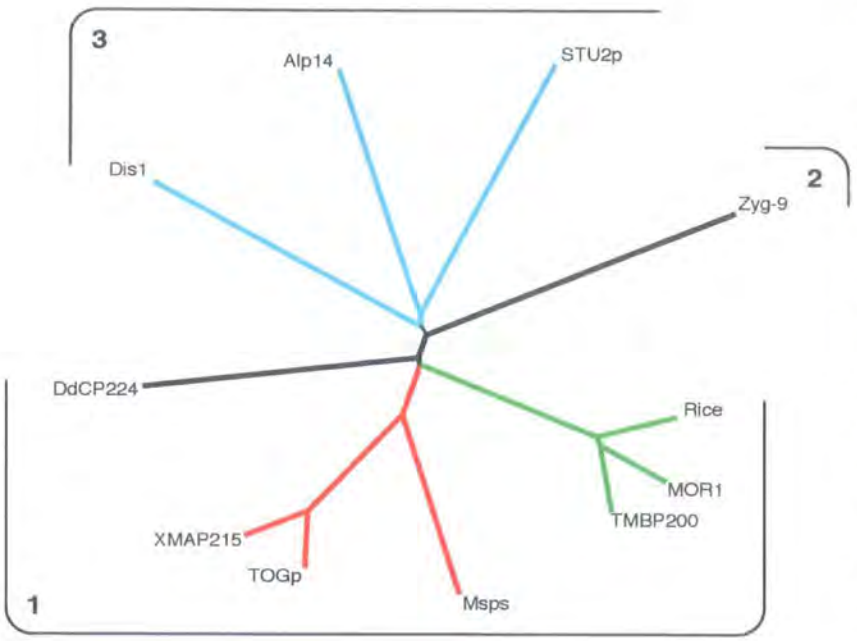

Radial Cladogram
On the tree there are 3 groups labelled 1-3. These are the groupings based on domain architecture (see Figure 1.4). Based on the size of the protein, the number of HEAT repeats that the N-terminal contains and the presence of a C-terminal conserved region. Within these based on primary sequence alignment the proteins can be separated into subgroups or clades. One clade contains examples from frogs (*Xenopus* XMAP215), insects (*Drosophila* Msps) and Humans (TOGp) (RED). A plant clade containing examples from Tobacco (TMBP200) , Rice (BAB64822) and *Arabidopsis* (MOR1/GEM1) (GREEN). A third clade contains yeast proteins, although they are very divergent (BLUE).

Retangular Cladogram
Here, the data from the same alignment is represented in a retangular cladogram. This phylogenetic tree shows the same 3 clades as above: insects, frogs humans, plants and finally yeast. *Dictostelium* CP224 is on the same greater branch as plants and humans. *C. elegans* Zyg9 appears to be an outlying protein, divergent from other members of the family. The numbers on the tree are the bootstrap values of each node or branch point. This figure is generated by the alignment software upon randomly changing amino acids in the sequence and redrawing the tree. The value is the number of times out of 1000 that this branch was created and as such is a confidence level in that node.

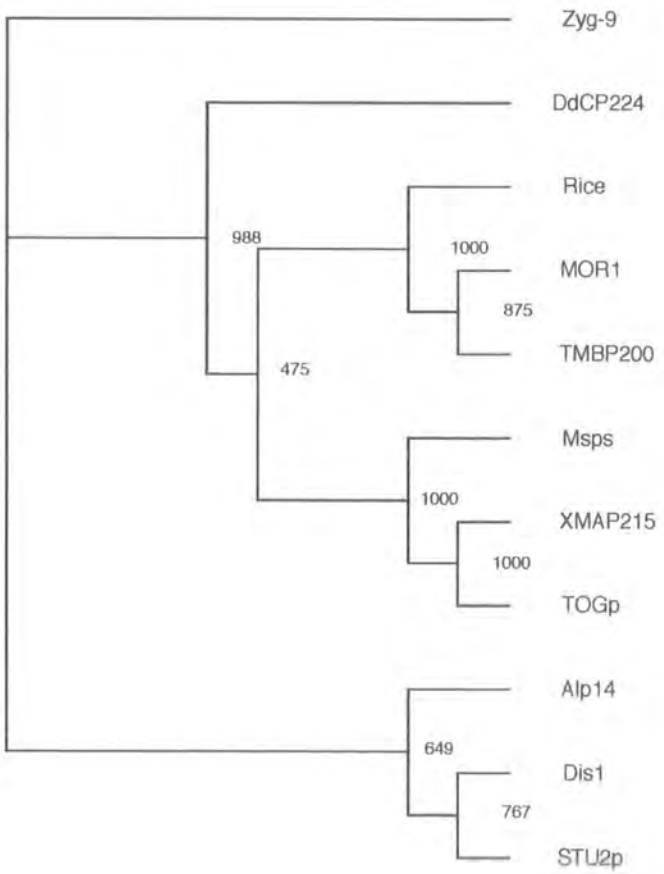

When the full length sequences are used to produce a tree, dis1, Alp14 and Stu2p align with the N-terminal section the rest of the family but the software is then required to compare the C terminal regions of these larger proteins to gaps and a tree with nodes with low bootstrap values is produced. This tree present in the appendix places the human and frog members of the family on a branch linked to that of the plant proteins with a node with a high bootstrap value. However this may be an artifact produced by the software because of their similar size. Therefore the alignment and tree were recalculated using only the N terminal half of each protein. This produced a different tree where the bootstrap values are higher. The XMAP215 and MOR1 branches are still linked yet here the bootstrap value is much lower. Although these trees differ, the radial cladograms still represent the same general clade structures. One clade contains XMAP215, TOGp, Msps, a second includes the plant members, TBMP200 and MOR1, and a third wide clade contains those yeast members, Alp14, dis1 and Stu2p. This leaves two outlying proteins DdCP224 and C. elegans Zyg-9. As more family members are found in other organisms these may represent a fourth or possibly a fifth clade.

XMAP215/TOGp proteins share a similar domain architecture consisting of a N terminal repeating region containing TOG domains each containing up to 5 HEAT repeats and a C-terminal non repeating domain (**FIGURE 3.2**). Members of the XMAP215/TOGp family appear to form three groups based on sequence length and their number of TOG domain/HEAT repeats. Examples from plants, humans, frogs and fruit flys are long proteins of approximately 2000 amino acids in length and each contain 5 TOG domains. The members of this group all have a total of 20 HEAT repeats with 3-5 Heat repeats per TOG domain apart from the plant members which, although still contain 5 TOG domains, each domain contains less HEAT repeats giving a total of 11 or 12. Furthermore the third TOG domain contains no HEAT repeats al all. Interestingly for this first group alone their C terminal no repeating domains are conserved. The second group only contains a single protein, Zyg-9, which has 3 TOG domains and a total of 13 HEAT repeats

Figure 3.2: XMAP215/TOGp family HEAT Repeats

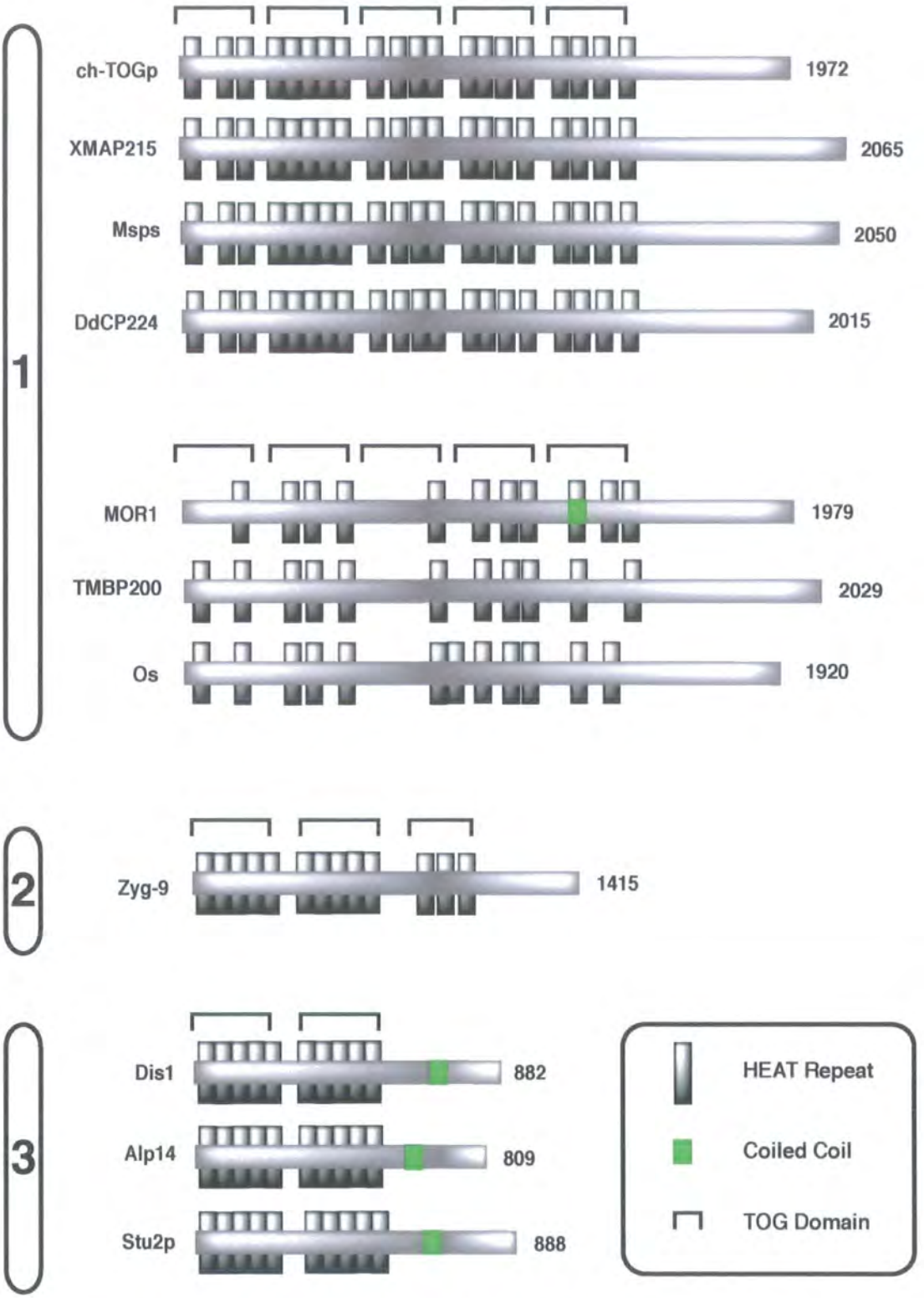

Figure 3.2: This figure shows the domain architecture of the XMAP215/TOGp family proteins. Based on this arrragement they can be separated into 3 broad groups. All contain a series of conserved HEAT repeats in the N-terminal region of the protein, although the number of these may range from 10-20. Group 1 contains long proteins ~2000 amino acids which contain 5 TOGp domains each containing between 1-5 HEAT repeats and a conseved C-terminal region. This region is only conserved in members of group 1. Group 2 only contains a single protein, Zyg9. The protein has 3 TOG domains, each with 3-5 HEAT repeats (total 13).Group 3 protein all come from yeast and contain 2 TOG domains with 5 HEAT repeats each. The C-terminal regions are not

but is approximately 600 amino acids shorter than those in the first group and its C-terminal non-repeat region shows no similarity to other members of the family. A third group consists of those from yeast, *S. cerevisiae* and *S. pombe.* These proteins are much shorter, only 800-900 amino acids, although they still contain two TOG domains with 5 HEAT repeats each and appear to correspond to the N terminal half of the other members of the family. Again their C-terminal non repeating regions show no similarity to each other nor do they to the rest of the XMAP215/TOGp family members. However these C terminal regions of Alp14, Dis1 and Stu2p all contain a coiled coil.

Motifs and domains contained within the At2g35630 protein sequence were identified by a series of servers and compared with those found in other members of the family. These features are shown in Table 3.2 below.

TABLE 3.2

At2g35630: MOR1/GEM1

Length: 1978
MW: 218 kDa
PI: 7.60

Motif/Domain	Location AA	Score	E Value	Comments
Low complexity	4-15 136-150 372-380 467-476 511-529 570-584 1602-1619 1886-1912	AST		
Coiled Coil	1268-1295	AST		
PEST	244-288 592-613 1884-1915	+9.35 +9.77 +7.37		
HEAT Repeat	164-202 321-359 362-400	1730 1560 2240	3.5e-08 4.1e-07 1.1e-05	

	443-481	2280	2.7e-06	
	854-892	1870	1.8e-08	
	937-975	1840	8.8e-08	
	1011-1051	1640	6.5e-08	
	1235-1258	1670	1.1e-07	
	1259-1296	1830	2.4e-08	
	1298-1371	1480	1.3e-07	
	1677-1618	1550	4.4e-07	

PSORT II		**TARGETP**		**iPSORT**
Subucellular Location	***%***	***Subucellular Location***	***Score***	Predicted as not having any of signal, mitochondrial targeting or chloroplast transit peptides
Nuclear	56.5	Chloroplast cTP	0.062	
Cytoplasmic	34.8	Mitochondrial mTP	0.102	
Cytoskeletal	4.3	Secretory sTP	0.095	
Secretory system	4.3	Other	0.929	

Most interestingly At2g35630 contains ten HEAT repeats between residues 164 and 1618. The HEAT repeat is a tandemly repeated 37-47 amino acid unit occurring in several cytoplasmic proteins, including the four proteins that give the repeat its name: Huntingtin protein, Elongation factor 3, Alpha regulatory unit of protein phosphatase 2A, and the yeast PI3-kinase TOR1. Arrays of HEAT repeats usually consist of 3 to 36 units, which produce a rod-like helical stricture and function as protein-protein interaction surfaces (Andrade & Bork 1995, Groves *et al.* 1999). The most amino terminal of these is the site of the MOR1 mutations. At2g35630 also contains: a coiled coil, a motif often involved in kinesin dimerisation, three potential PEST sequences, which control protein turnover and a series of putative phosphorylation sites, including CDK, concentrated at the carboxy terminal end of the protein.

The presence of such a large number of HEAT repeats suggests that At2g35630 probably interacts with one or more proteins. Importantly all other members of the XMAP215 family contain varying numbers of HEAT repeats. The coiled coil could indicate that At2g35630 can form dimers or alternatively this may be part of the

microtubule binding system of At2g35630 as is the case for the MURF protein. MURF is a striated muscle RING-finger protein and RING-finger motifs are found in proteins involved in signal transduction, ubiquitination, gene transcription, differentiation and morphogenesis (Spencer *et al.* 2000). MURF also contains a B-box (zinc finger) and a leucine rich coiled coil domain. The coiled coil domain was found to mediate the association of MURF with microtubules and expression of MURF establishes a cellular microtubule network that is resistant to microtubule depolymerisation induced by alkaloids, cold and calcium (Spencer *et al.* 2000). The PEST sequence and phosphorylation sites show the possible control of this protein in the cell. The ability of At2g35630 to bind microtubules and/or promote microtubule polymerization may be controlled by phosphorylation and with the presence of CDK sites it is tempting to suggest that this could be coordinated in a cell cycle dependent manner.

Predications for the subcellular location of MOR1/GEM1 are contradictory and inconclusive. It is reasonable to predict that MOR1/GEM1 would be found to locate to the cytoskeleton as for other members of the family. However the prediction of nuclear localization from PSORT II could also be possible, as the plant protein MAP190 is located to the phragmoplast during division but shows nuclear localization during interphase (Igarashi 2000). iPSORT which contains an algorithm specific for plant signals does not identify any localization sequence.

3.2.2 At3g16630 & At3g16060: AtCMK1 & 2

As an antagonistic relationship for XMAP215 with the Kinl kinesin XKCM1 has been demonstrated in Xenopus by Tournebize and colleagues, it was decided to interrogate the *Arabidopsis* genome for putative Kinl kinesins and investigate whether such a relationship exists in plants. As before, putative Kinl kinesins were identified using NCBI BLAST to search the *Arabidopsis* genome database using XKCM1 as the query (Table 3). This revealed two homologues with highly similar

motor domains to XKCM1. Although the motor domains are similar, the surrounding sequence is different, however this is seen for all Kinl kinesins.

TABLE 3.3

Species	Protein	Length	Score	Expect	Identities %	Positives %	Gaps %
Oryza sativa	KLP	800	822	0.0	59	69	12
Nicotiana tabacum	BY-2 KLP 10	703	548	e-154	61	73	5
Arabidopsis thaliana	At3g16060	684	539	e-151	61	72	7
Zea mays	KHC	430	347	6e-94	55	66	8
Dictyostelium discoideum	KFM6	1030	337	7e-91	49	62	9
Homo sapiens	KHC2	509	332	2e-89	50	65	10
Giardia lamblia	GLP_164...	714	329	2e-88	40	55	11
Xenopus laevis	XKIF2	706	328	4e-88	53	67	8
Homo sapiens	MCAK	725	327	9e-88	53	66	8
Mus musculus	KIF2C	721	326	1e-87	53	66	8
Macaca fascicularis	Hypothetical	671	832	3e-87	53	66	8
Homo sapiens	HsKIF2	679	323	9e-87	50	65	10
Leishmania major	LmMCAK	728	317	7e-85	52	66	8
Drosophila melanogaster	KLP10A	805	315	2e-84	50	63	7
Dictyostelium dicoideum	KLP K6	319	315	3e-84	55	67	7
Xenopus laevis	XKCM1	730	303	8e-81	50	65	8

The two genes were At3g16060 and At3g16630, and were named AtCMK1 and AtCMK2 respectively (*Arabidopsis thaliana* Central Motor Kinesin). As the name suggests, both have motor domains located centrally within their sequence, a characteristic common to all Kinl kinesins. AtCMK1/2 were aligned with other Kinl kinesins using ClustalX and a phylogenetic tree for the family calculated by PAUP

FIGURE 3.3: Phylogenetic Tree of KinI Kinesins and Domain Architecture of Arabidopsis KinI Kinesins

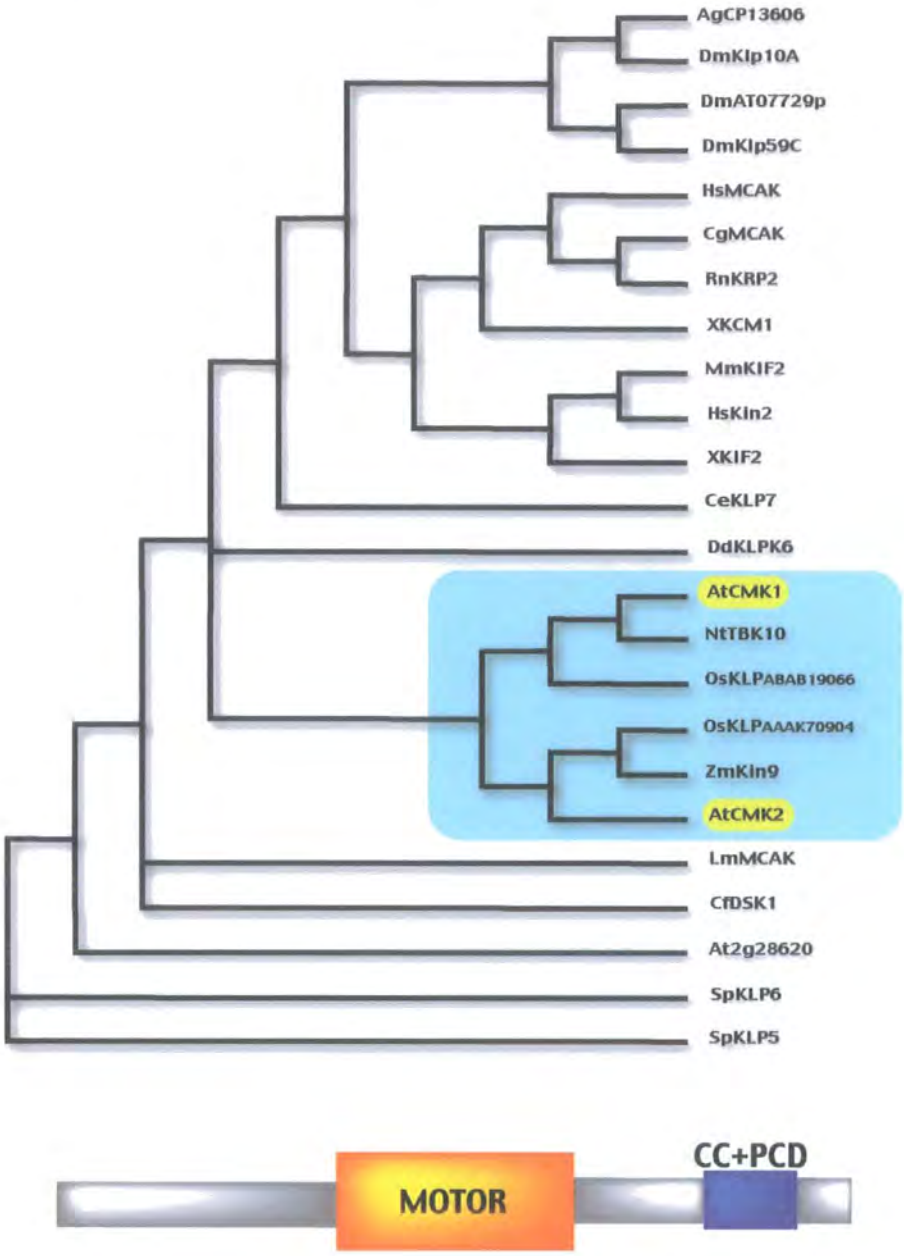

Figure 3.4: (A) Retangular Cladogram of members of the Kin I subfamily of Kinesins + plant examples. Several distinct clades can be seen: an insect clade, a second clade containing examples from mammals and frogs and a third plant clade, containing examples from *Arabidopsis* (AtCMK1 & AtCMK2), rice, maize and tobacco. It is likely that tobacco and maize may also have two such kinesins like rice and *Arabidopsis*, although these have yet to be identified as tobacco and maize do not have complete genome databases. All of these Kin I kinesins have the motor domain located centrally within the sequence. Some contain a coiled coil in the N-terminal section of the protein where as others do not. The plant members all have a highly conserved region in the C-terminal section of the protein which contains a coiled coil (B).

(**FIGURE 3.3**). In addition to check that these kinesins were of the Kinl subfamily, all kinesins in the genome databases were aligned as before and a phylogenetic tree calculated. Here the all the kinesin subfamilies were present including C-terminal motor kinesins and the BimC family. Importantly AtCMK1/2 fall into the Kinl (Kif2/MCAK) family branch or clade of the tree (data not shown). Therefore considering the sequence similarity, the central motor domain and their location in the kinesin, tree it is reasonable to conclude that AtCMK1/2 are good candidates for Kinl kinesins in *Arabidopsis*. When XKCM1 and AtCMK1/2 were used to query additional genome databases, further examples were found in plants including tobacco and rice. AtCMK1/2 were searched for motif and domain matches using web servers; the results are shown in the Tables 3.4 & 3.5 below.

TABLE 3.4

At3g16630: AtCMK2

Length: 749 aa
MW: 89 kDa
PI: 5.56

Motif/Domain	Location AA	Score	E Value	Comments
KISc, **BLAST: KISc** **Pfam: Kinesin** **SCOP: dlf9va** **PDB: 1l6l**	191-532 191-532 241-527 193-525 192-526	AST	6.1e-112 0.0e+00 9.9e-116 2.0e-90 4.00e-42	
P-Loop	282-289			ATP/GTP-binding site motif A
Coiled Coil	703-739	AST		
PEST	546-571	+5.18		
Low Complexity	1-13 703-720	AST		
Tandem Repeat: ETASRQY	684-690 691-697			

ETASRQY ET	698-699			

PSORT II		**TARGETP**		**iPSORT**
Subcellular Location	***%***	***Subcellular Location***	***Score***	Predicted as not having any of signal, mitochondrial targeting or chloroplast transit peptides
Nuclear	65.2	Chloroplast cTP	0.058	
Cytoplasmic	8.7	Mitochondrial mTP	0.220	
Mitochondrial	8.7	Secretory sTP	0.060	
Vacuolar	8.7	Other	0.658	
Extracellular, cell wall	8.7			

TABLE 3.5

At3g16060: AtCMK1				
Length: 684 aa MW: 76.8 kDa PI: 6.01				
Motif/Domain	**Location AA**	**Score**	**E Value**	**Comments**
KISc, **BLAST: KISc** **Pfam: Kinesin** **SCOP: dlf9va** **PDB: 1BG2**	167-498 178-498 217-493 169-491 178-492	AST	4.7e-114 1.0e-176 3.4e-129 1.0e-91 3.00e-39	
P-Loop	282-289			ATP/GTP-binding site motif A
Coiled Coil	596-630	AST		
PEST	514-551	+9.26		
Low Complexity	48-71 166-177 348-360	AST		
Tandem Repeat: NQLDG NQLDG	121-125 638-642			

PSORT II		TARGETP		iPSORT	
Subcellular Location	***%***	***Subcellular Location***	***Score***		
Nuclear	65.2	Chloroplast cTP	0.278		
Cytoplasmic	4.3	Mitochondrial mTP	0.665		
Mitochondrial	30.4	Secretory sTP	0.037		
		Other	0.169		

As mentioned earlier AtCMK1/2 both contain a kinesin motor domain in the centre of their sequence, which was identified by several databases including BLAST, SCOP, Pfam, Prosite, and as a 3D structure from PDB. Both also contain a coiled coil at the extreme carboxy terminus of the protein. This is common in kinesins and often represents the site through which dimerisation occurs. The majority of the Kinl subfamily possess coiled coils apart from a few insect examples. For the animal members, this is located in the amino terminal half of the protein rather than the carboxy terminus as for all plant examples.

Both Kinesins contain potential PEST sequences, suggesting that as for MOR1/GEM1, the turnover of these proteins may be important. Interestingly both kinesins contain simple tandem repeats, NQLDG and ETASRQY for AtCMK1 and AtCMK2 respectively. In the case of AtCMK1 this string is repeated once in 521 residues, whereas for AtCMK2, the string ETASRQY is repeated consecutively ETASRQYETASRQYET. It is likely that NQLDG may be a motif that is found twice within AtCMK1 rather that a true repeat. Both of these strings were used as queries at NCBI BLAST in order to identify proteins with similar repeats, which may suggest a possible function. Prediction of subcellular location for these kinesins is again inconclusive. Both have high scores for a nuclear localization as for MOR1/GEM1, however AtCMK1 also has an interesting score for a mitochondrial localization from PSORT II and TargetP gives its highest score to this location also. This is unusual, as both would be predicted to be predominately associated with the cytoskeleton as for other Kinl kinesins, although mitochondrial localization

Figure 3.4: Alignment of Several Plant Putative Kinl Kinesins

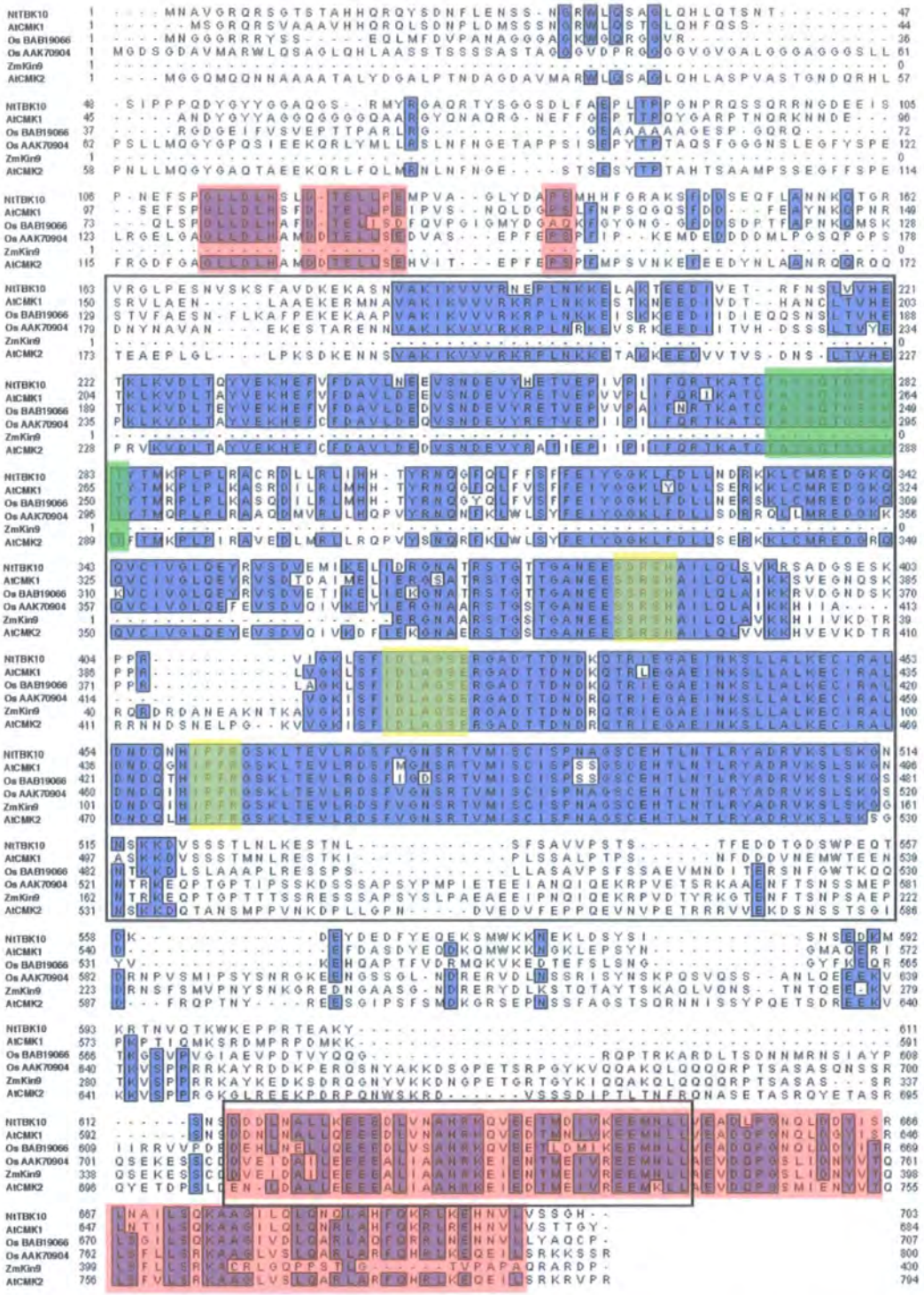

Blue - Regions of identity, Pink - Plant Conserved regions, Yellow - Microtubule binding sites, Green - ATP binding site, P loop, Upper box - Motor Domain, Lower Box - Coiled Coil

signals may represent a possible conventional kinesin-like transport role for AtCMK1.

In addition, when several plant putative Kinl kinesins are aligned as well as showing identity in their motor domains all possess a region at the extreme C-terminus of the protein which is highly conserved, and only in plant Kinl. This domain is referred to as the PSD, Plant Specific Domain from now on in this thesis. This may represent a domain, which is required in a role for Kinl kinesins limited to plants, however it does contain the coiled coil and therefore may be a conserved dimerisation site (**Figure 3.4**).

3.3 Analysis of Affymetrix Genechip, DNA Microarray Data.

With the advent of DNA microarray technology, the entire transcriptome of an organism or a particular tissue or cell type can now be analysed. The differences between tissues or perturbations in the levels of transcripts following treatments or in mutant lines can be particularly informative.

For this reason the Genechip data for the genes of interest in this thesis was analysed. The data for experiments using the Affymetrix *Arabidopsis* Genechip ATH1, which contain almost all transcripts, is made publicly available at the NASC website. Here there are several tools to mine the data, one of which is spot history. Here the data for your gene of choice is presented in the form of a histogram, which shows the distribution of signal values (gene expression). Along the x-axis are signal values for the selected gene, and along the y-axis frequency (No. of experiments which gave that level of signal). These bars can then be interrogated to identify the experiments and the variables, which gave these readings (**FIGURE 3.5**). The results in the centre of the graph tend to represent normal or global levels where as the outliers are the signal values for tissues or situations where the transcript is significantly up or down regulated and it is these regions which are of most interest.

Figure 3.5: Affymetrix GeneChip Data

A MOR1/GEM1 (At2g35630):

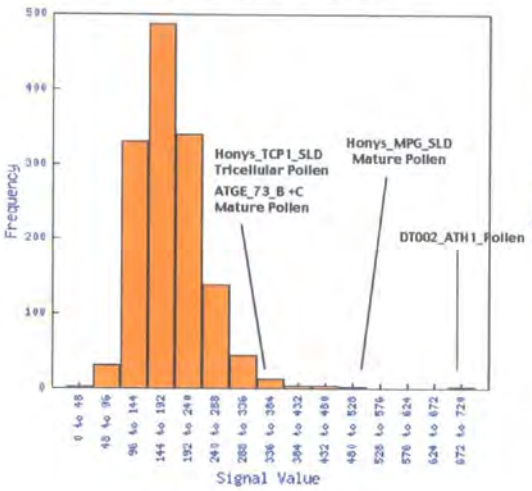

B AtCMK2 (At3g16630):

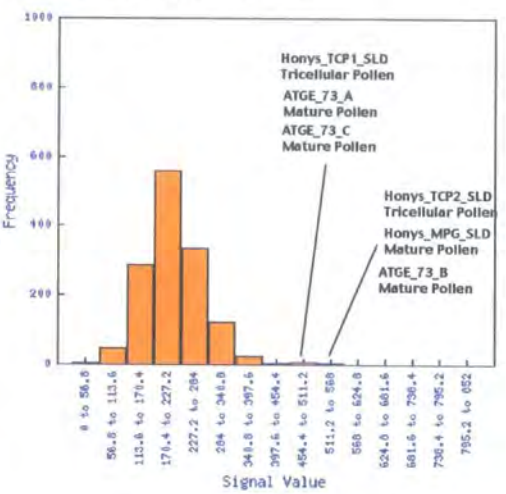

C AtCMK1 (At3g16060):

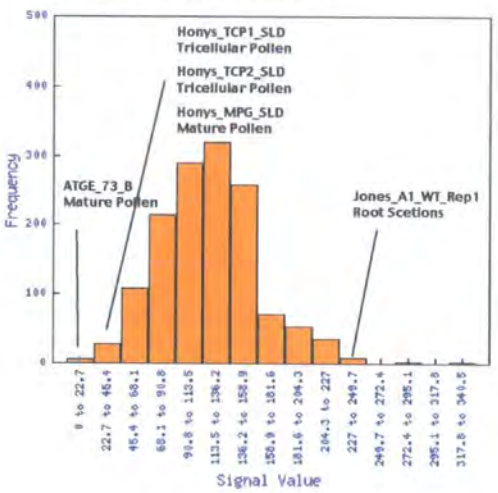

D Pollen Development

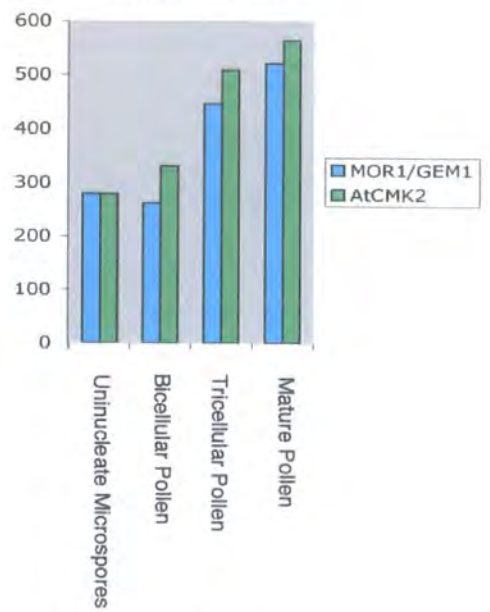

Affymetrix genechip spot history histograms.

A. MOR1/GEM1 transcript levels. Several pollen experiments show high signal values

B. AtCMK2 transcript levels. Several pollen experiments show high signal values.

C. AtCMK1 transcript levels.Root section experiments show high signal values.

D. MOR1/GEM1 & AtCMK2 signal values at four different pollen developmental stages

Each set of data for a slide contains four pieces of important information. They are StatPairsUsed, Signal, Detection P-Value and Detection call. The StatPairsUsed are the number of probe pairs used to calculate the other data for this probe for this chip. The Signal value is a number representing the amount of this probe pair. The Signal is the most important value in the spreadsheet, and is what most analysis is performed on and represents the level of gene expression. Any values below 150 are considered to be background noise rather than gene expression. The detection call states whether the gene was expressed. A detection call of 1 (present), wasn't expressed is a detection call of –1 (absent) and it is too close to say, is a detection call of 0 (Marginal). The detection p-value gives the probability that this amount of expression occurred through random chance. Low probabilities means that it is unlikely that this level of expression happened by accident. The detection call is calculated from the detection p-value. The signal value is a *quantitative* measurement for gene expression ("how much has this gene been expressed?"). The detection call is a *qualitative* measurement for gene expression ("has this gene been expressed or not?").

MOR1/GEM1

The MOR1/GEM1 spot history histogram shows that the majority of experiments gave signal values in the range of 144-240 and these analyse biosources including many different *Arabidopsis* tissues and organs. Interestingly, experiments which gave particularly high signals include those studying the transcriptome of pollen.

Slide	BioSource	Signal	Detection Call	p-value	StatPairsUsed
DT002_ATH_Pollen	Pollen	719.8	1	0	11
Honys_TCP1_SLD	Tricellular Pollen	381.4	1	0	11
ATGE_73_B	Mature Pollen	358.39	1	0	11
ATGE_73_C	Mature Pollen	357.23	1	0	11

DT002_ATH_Pollen and Honys_TCP1_SLD are two experiments by Twell and Honys of the transcriptome analysis of *Arabidopsis* microgametogenesis using

isolated microspores of pollen at 4 different developmental stages. ATGE_73_B and ATGE_73_C are experiments which are part of the AtGenexpress consortium developmental series of flowers and pollen. This is an international effort to develop a gene expression atlas of *Arabidopsis* and as such have generated expression data from 80 biologically different samples in triplicate. The focus of this data set is on different tissues and different developmental stages in wild type Columbia (Col-0) and various mutants.

AtCMK2

As for MOR1/GEM1 although signals give a present (1) detection call for AtCMK2 in many tissues and organs, particularly high signal values are seen in several independent pollen experiments.

Slide	BioSource	Signal	Detection Call	p-value	StatPairsUsed
Honys_TCP1_SLD	Tricellular Pollen	563.7	1	0	11
Honys_TCP2_SLD	Tricellular Pollen	516.6	1	0	11
Honys_MPG_SPC	Mature Pollen	512.51	1	0	11
ATGE_73_A	Mature Pollen	487.19	1	0	11
ATGE_73_C	Mature Pollen	486.49	1	0	11

AtCMK1

Slide	BioSource	Signal	Detection Call	p-value	StatPairsUsed
Jones_A1_WT_Rep1	Root Sections	236.1	1	0.01	11
Honys_TCP1_SLD	Tricellular Pollen	32.1	-1	0.17	11
Honys_TCP2_SLD	Tricellular Pollen	25.6	-1	0.11	11
Honys_MPG_SPC	Mature Pollen	32.6	-1	0.66	11
ATGE_73_B	Mature Pollen	18.6	-1	0	11

Jones_A1_WT_Rep1 is an experiment to assess the effect of mutations in AtrbohC on the pattern of gene expression in primary root tissue. ArbohC is allelic to rhd2, which has short root hairs, which burst at their ends (Schiefelbein & Sommerville). In this experiment RNA was prepared from a small excised region of the primary root, where root hairs are growing in hope that this tissue would be enriched for root hair RNAs. Interestingly unlike AtCMK2, signal values for AtCMK1 in pollen

experiments are very low, giving a detection call of –1, suggesting that AtCMK1 is not expressed in pollen.

Such data could suggest that MOR1/GEM1 and AtCMK2 are both highly express in pollen and AtCMK1 is highly expressed in areas of the root. Other experiments represented in these histograms also gave signals for MOR1/GEM1 and AtCMK2 in many other tissues and organs.

The limitation with such analysis is that although signal values can be compared between slides within an experiment e.g. different stages of pollen development, comparisons between experiments such as the signal value in leaves vs. pollen are restricted, as each experimenter may have used very different conditions. However high signals for genes in particular tissue or organs from independent experiments can at least indicate that transcript levels may be high. However one can still use the detection call to qualitatively say if a transcript is present or not. Therefore it can be concluded that the transcripts of MOR1/GEM1 and AtCMK2 are both present in pollen.

Further analysis of the pollen development transcriptome experimental data from Honys & Twell shows that the signal values for MOR1/GEM1 and AtCMK2 both increase as the pollen develops (**FIGURE 3.5D**). Possibly here the regulation of the microtubule cytoskeleton is tightly controlled and the relative levels of these two putative microtubule regulators is important. Such co-regulation could suggest a possible antagonistic relationship where the levels are similar within tissue and cell type, yet control through the cell cycle may produce differing transcript levels or their activity is postranslationally controlled by phosphorylation.

3.4 Promoter analysis; Plant cis-acting regulatory elements.

Expression of a gene is an essential part of its function and its expression profile a key element towards achieving a full functional description of a gene. PlantCARE is

a database of plant *cis*-acting regulatory elements, enhancers and repressors. The transcription site data is gained from literature and supplemented with *in silico* prediction data. In 2001 the database contained 417 *cis*-acting regulatory elements, of which 150 were from monocotyledous species, 263 from dicotyledonous species and 4 from conifers, describing approximately 160 individual promoters from higher plant genes (Lescot *et al.* 2002). Since these figures were published the data set has continued to grow with the addition of new regulatory elements from other researchers. Those response elements found within the putative promoters of the genes studied in this thesis are described in Tables 3.6., A, B & C. (Putative promoter area used = 2000bp upstream of ATG)

TABLE 3.6-A.

MOR1/GEM1		
Motif	**Sequence**	**Description**
A-box	AATAACAAACTCC	Sequence conserved in alpha amylase promoters
ABRE	tACGtg	Abscisic acid responsiveness (ABA)
ERE	ATTTcaaa	Ethylene response element
Skn-1	GTcat	Regulatory element associated with endosperm expression
TATA	TATAAA	Core promoter element ~ -30 of transcription start
WUN	TCATTACGAA	Wound responsiveness

TABLE 3.6-B

AtCMK1		
Motif	**Sequence**	**Description**
ABRE	tACGtg	Abscisic acid responsiveness (ABA)
Box-W1	TTGAcc	Regulatory element involved in fungal elicitation
MBS	CAAC(g/t)g	MYB binding site, associated with drought inducibility
Skn-1	GTcat	Regulatory element associated with endosperm expression
TGA-1	AACGac	Auxin responsiveness
WUN	aCATTacgt	Wound responsiveness
MeJA	CGTCa/TGACg	MeJA rsponsiveness
TATA	TATAAA	Core promoter element ~ -30 of transcription start
CAAT	aCCAAt	Common element in promoter and enhancer regions

TABLE 3.6-C

AtCMK2		
Motif	**Sequence**	**Description**
ABRE	tACGtg	Abscisic acid responsiveness (ABA)
MBS	CAACtg	MYB binding site, associated with drought inducibility
ERE	ATTTcaaa	Ethylene response element
Skn-1	GTcat	Regulatory element associated with endosperm expression
MeJA	CGTCa/TGACg	MeJA rsponsiveness
LTR	CCGAAA	Regulatory element involved in low temperature
TATA	TATAAA	Core promoter element ~ -30 of transcription start
CAAT	aCCAAt	Common element in promoter and enhancer regions

However, such an analysis does have limitations, including the fact that these strings of bases could occur randomly within the genome. For example an element such as ABARE, which is only 6 bases long, could occur once every 4096 bases ($4^6 = 4096$). Considering that the *Arabidopsis* genome is ~ $1x10^8$ bases, there could be $2.44x10^4$ random occurrences of a 6bp element. Such calculations assume that the genome is a random string of bases, but rather genomes contain duplications, and there is selective pressure for motifs to remain unchanged and as such areas become ordered and less random. The identification of such motifs in the promoter of a gene can suggest that the transcription of the gene could respond to these cues, yet such indications require corroboration by experimental evidence.

3.5 Discussion

For XMAP215/TOG family proteins the C-terminal non repeat regions are thought to be responsible for microtubule binding and localization to the centrosome, spindle pole body (SPB) or kinetochore. In XMAP215 and DdCP224 this region is sufficient for localization to the centrosome and SPB (Popov et al. 2001, Graef *et al.* 2000) and in Dis1 this region, although not conserved with group 1, is sufficient

for microtubule binding and localization to the kinetochore (Nakaseko *et al.* 1996, 2001). The TOG domains and HEAT repeats could represent another system of microtubule binding however, it is likely that this region is a protein-protein interaction domain for these proteins.

As described earlier MOR1/GEM1 contains HEAT repeats through which it may bind several other proteins, possibly forming complexes at points along or at the ends of microtubules and may even be necessary to locate some other proteins to the microtubule array. The conserved C-terminal non-repeating region of MOR1/GEM1 is likely to be responsible for microtubule binding, via an region which shows homology to the MT binding site of MAP2, possibly in conjunction with the coiled coil domain. Postranslationally MOR1/GEM1 may be controlled through the cell cycle via phosphorylation by CDK and degradation indicated by the inclusion of a PEST sequence. XMAP215 also contains a CDK site which when phosphorylated inhibits the ability of XMAP215 to promote the polymerization of tubulin in vitro (Vasquez *et al.* 1999). Considering these data and the model proposed in chapter 1 it is tempting to speculate that CDK is involved in regulation of this interplay between MOR1/GEM1 and a Kinl like kinesin. During interphase CDK1 activity is reduced and MOR1/GEM1 is unphosphorylated, and its activity predominates over that of a Kinl kinesin leading to long cortical microtubules. In mitosis, CDK1 activity is high and MOR1/GEM1 is hyperphosphorylated, its activity is reduced and the activity of XKCM1 prodominates leading to short microtubules (Hussey & Hawkins 2001, Heald 1999).

Expression of MOR1/GEM1 appears to up regulated in pollen where it may be involved in the control of microtubule dynamics during the important divisions as pollen develop. Furthermore analysis of the promoter reveals that

AtCMK1 & AtCMK2 both have kinesin motor domains in the centre of their sequence, a characteristic they share with other Kinl kinesins. The motor domains

are highly similar to those of Kinl kinesins and contain all of the important components. The coiled coil, another characteristic of kinesins could be the site through which AtCMK1 and AtCMK2 form hetero or homodimers. As with MOR1/GEM1 they may be controlled through the cell cycle by phosphorylation signified by the presence of CDK and PEST sites. Expression of AtCMK1 and AtCMK2 are very different with AtCMK2 up regulated in pollen (like MOR1/GEM1) and AtCMK1 is down regulated in pollen but up regulated in the root elongation zone. (**FIGURE 3.6**)

Figure 3.6: Summary of MOR1/GEM1 and AtCMK1/2 Bioinfomatic data

MOR1/GEM1 Domains

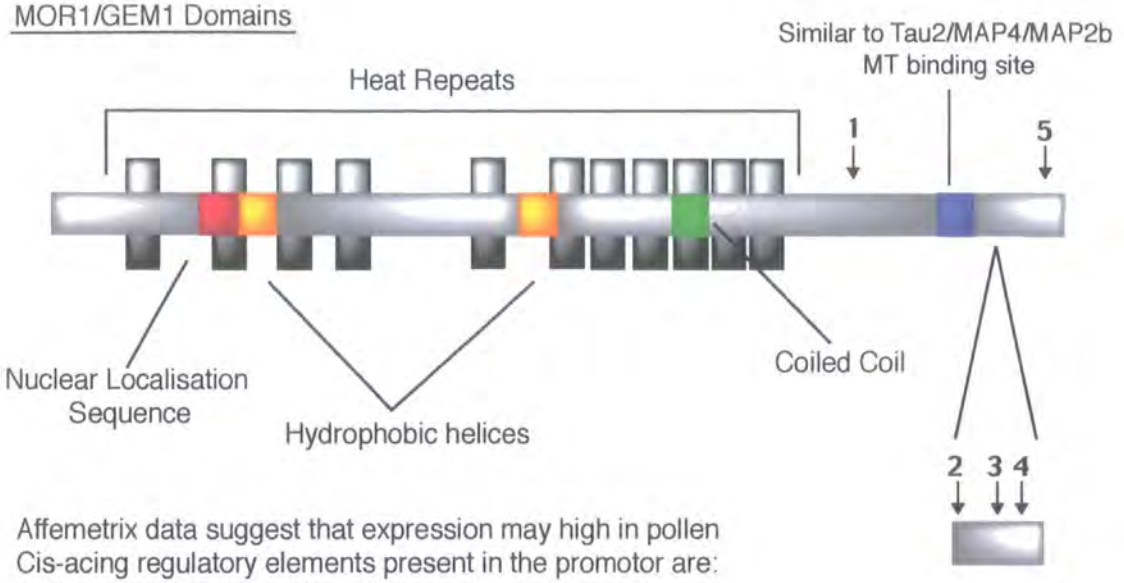

Affemetrix data suggest that expression may high in pollen
Cis-acing regulatory elements present in the promotor are:
A-Box, ABA, Ethylene, Wound response, endosperm
Expression.

1. Casein Kinase 1
2. Cyclin dependant kinase, CDK
3. Proline dependant Kinase
4. Proline dependant Kinase
5. Casein Kinase 1

AtCMK1 & AtCMK2 Domains

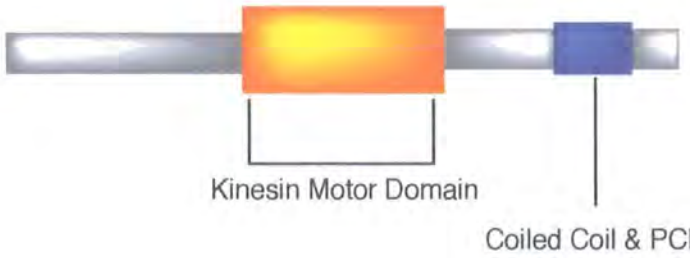

AtCMK1

Affemetrix data suggest that AtCMK1 may not be expressed in pollen
but expression maybe high in the root elongation zone

Cis-acing regulatory elements present in the promotor are: ABA, MeJA, Auxin,
Endosperm expression, MYB, Fungal elicitation & Wound response.

AtCMK2

Affymetrix data suggest that expression maybe high in pollen

Cis-acing regulatory elements present in the promotor are: ABA,MeJA, Ethylene,
Endosperm expression, MYB, & Low temperature.

CHAPTER 4

MOR1/GEM1 associates with all microtubules arrays and is essential for the function of the plant specific cytokinetic phragmoplast.

4.1 Introduction

As described in **CHAPTER 1**, the XMAP215/Ch-TOGp family of proteins are important regulators of microtubule dynamics in several organisms, including yeast, frogs and humans (Garcia *et al.* 2001, Wang & Huffaker 1997, Tournebize *et al.* 2000, Charrasse *et al.* 1998). Therefore, it was decided to identify whether a member of this family was present in the *Arabidopsis* genome. Although plants have a microtubule cytoskeleton, they only share a single array, the mitotic spindle, with these other organisms which posses this particular class of MAP. The plant cell produces three unique arrays: the interphase cortical array, the preprophase band and phragmoplast, and it is here, that an *Arabidopsis* MAP215 may exhibit novel functionality.

The objective of the work described in this chapter was to study the localisation of MOR1/GEM1 through the cell cycle, the proteins association with microtubules and if possible to apply this knowledge to known mutants. A further objective was to study the interaction of MOR1/GEM1 with itself and other proteins.

4.2 Production of an *Arabidopsis* MOR1/GEM1 Polyclonal Antibody

PCR primers were designed to amplify a ~ 2.5kb fragment of MOR1/GEM1. The fragment chosen consisted of the last 2545 bases of the sequence, encoding 855 amino acids of the C-terminal section of the protein. The PCR primer design also incorporated two endonuclease restriction sites, *Bam*H1 and *Nde*1, to allow cloning of the fragment into the bacterial expression plasmid, pET28a (Novagen). These

enzyme sites were chosen because digestion of the pET28a vector and the PCR product with *Bam*H1 and *Nde*1 allowed the fragment to be cloned, in frame with the pET28a histidine tag. Such a tag, in this case six consecutive histidine residues, allows the expressed protein to be specifically purified by a nickel column.

The primers named MAP215 FW and RV (**FIGURE 4.1**), were used in a PCR reaction using pGEM-T[MOR1/GEM1] as a template. A partial MOR1/GEM1 cDNA, isolated from a cDNA library screen, had previously been cloned into pGEM-T (Safina Khan). The constituents of the reaction mixture and the program used were based on those described in **CHAPTER 2** and the PCR product was analysed by agarose gel electrophoresis. The thermocycler program consisted of 35 cycles with a 2 minutes 30 second extension time and an annealing temperature of 55C. PCR products were separated on a 1% agarose gel (**FIGURE 4.2**). The PCR reaction produced a single product of ~ 2.5kb as desired, which was then cloned into TOPO2.1 (Invitrogen) by way of TA cloning. This system relies on the ability of Taq polymerase to produce fragments with single 3' adenosine overhangs. These allow the fragment to slot into the cloning site of the TA vector, which has corresponding thymidine overhangs. The insert is then permanently secured into the plasmid by the use of a ligase or in the case of TOPO2.1, topoisomerase (**SEE CHAPTER 2**). Following transformation into Oneshot™ *E. coli* cells, positive transformants were identified by blue/white selection and their plasmids analysed. Positive transformants appear as white colonies as upon insertion of the fragment into the cloning site of a vector such as TOPO2.1 or pGEMt Easy, the LacZ gene is disrupted. In negative transformants, where no insertion has occurred, the LacZ gene is intact and the β-galactosidase enzyme is expressed, which then converts the X-Gal present in the media into a blue precipitate. The LacZ gene encodes β-galactosidase an enzyme, which is responsible for the hydrolysis of D-galactopyranosides and is essential in *E. coli* for the hydrolysis of the disaccharide lactose to glucose and galactose. β-galactosidase also interacts with synthetic analogs including chromogenic X-gal.

Figure 4.1: Primer locations for MOR1/GEM1 Constructs

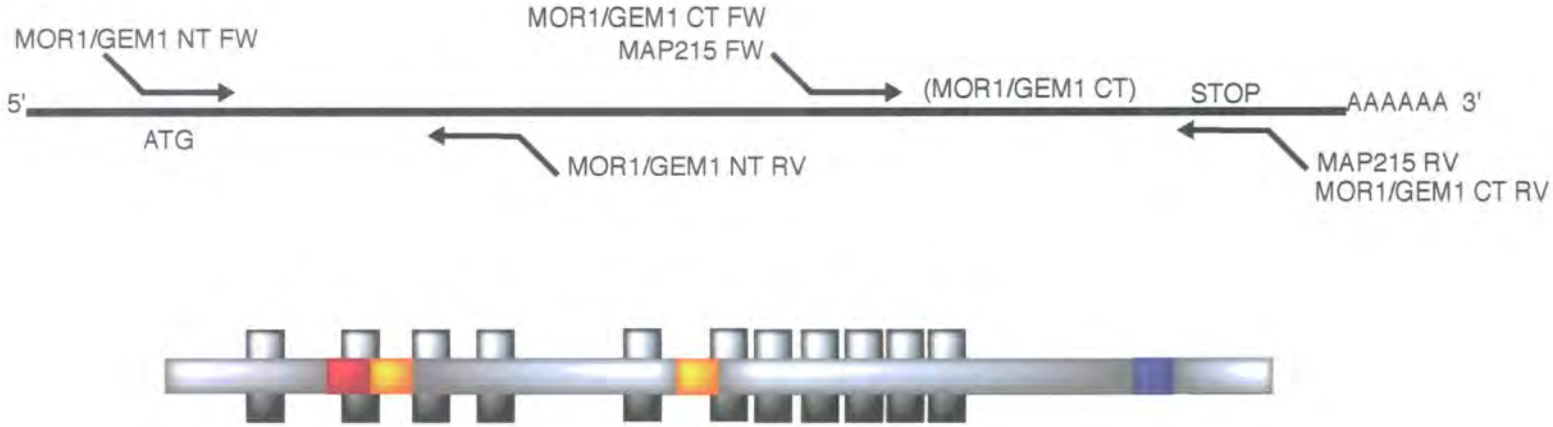

Figure 4.1: The horizontal black line represents the cDNA for MOR1/GEM1 and below is the corresponding protein architecture . Primers are shown aligned approximately with the regions of the cDNA to which they anneal. The purpose of this diagram is to illustrate the areas of the MOR1/GEM1 protein amplified with each combination of primers.

Figure 4.2: PCR of a MOR1/GEM1 CT fragment

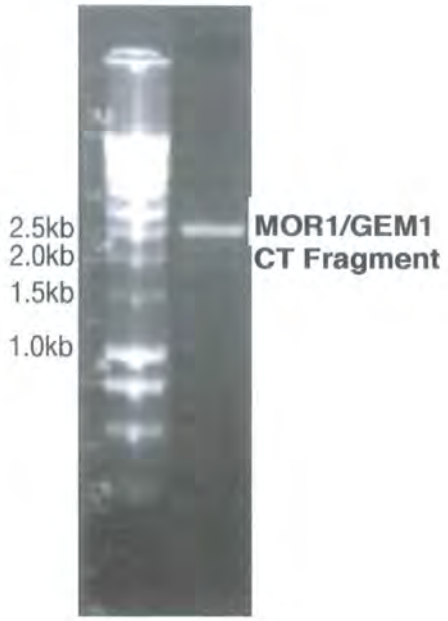

Figure 4.2: PCR of a MOR1/GEM1 CT fragment, to be expressed and used to raise polyclonal anti-MOR1/GEM1antisera in mice. Primers MAP215 FW and MAP215 RV were used to amplify MOR1/GEM1 CT from a partial MOR1/GEM1 cDNA clone. Pfu Taq was used and the extention time was 5 minutes. The MOR1/GEM1 CT Fragment gives a band of ~ 2500bp in size, which agrees with the predicted size of such a fragments based on the cDNA length from the MIPS and NCBI database. This PCR product was cloned into pGEMT Easy by TA cloning. Positive inserts were identified by bluw/white selection and confirmed by restriction digests and the sequence of the product was checked by DNA sequencing and checked against the MIPS/NCBI databases. The MOR1/GEM1 fragment was correct with no mutations. This PCR product was then subcloned from pGEMT Easy to pET28a by conventional restriction digest & ligation cloning.

The pET28[MOR1/GEM1] plasmid was transformed into the *E.coli* expression strain BL21 DE3. Expression of the recombinant fragment was induced by 1mM IPTG and allowed to proceed overnight at 15°C. Following expression the cells were lysed and the 6xHis-MOR1/GEM1 protein was purified on a nickel column. Here the imidazole ring found in the R groups of the histidine residues of the tag, bind the remaining ligand binding sites of the Ni coordination sphere and bind the recombinant protein to the column. Following elution with 250mM imidazole the recombinant fragment was analysed by SDS PAGE gel (4% Stack 7.5% resolving). Here a peptide of ~100kDa was observed corresponding to the correct molecular weight predicted for the MOR1/GEM1 fragment (**FIGURE 4.3B**). Following dialysis into an appropriate buffer, this protein was then used to immunize 3 mice in a course of 3 injections once every 2 weeks. The mouse α-MOR1/GEM1 polyclonal antibody serum was then used in the following experiments.

4.3 The MOR1/GEM1 is Expressed in All Plant Organs

To assess the quality of the MOR1/GEM1 antibody, the serum was used in a western blot to probe a membrane of total protein extract from *Arabidopsis* suspension culture cells (**FIGURE 4.3**). The protein extract was run on a 7.5% gel and electro-blotted on a nitrocellulose membrane. The anti-MOR1/GEM1 antibody was used at a dilution of 1:500 and film was exposed for a maximum of 10 minutes. Here a band of ~210kDa is seen, corresponding to the predicted size of full length MOR1/GEM1. In addition there are other smaller peptides, which show cross reactivity with the MOR1/GEM1 antibody. These are most probably degradation products of MOR1/GEM1, and rapid protein extraction by freezing in liquid nitrogen followed by immediate addition to boiling SDS sample buffer was found to improve yield of full length MOR1/GEM1.

FIGURE 4.3: Expression of Recombinant His-Tagged MOR1/GEM1 CT and the Anti-MOR1/GEM1 Antibody

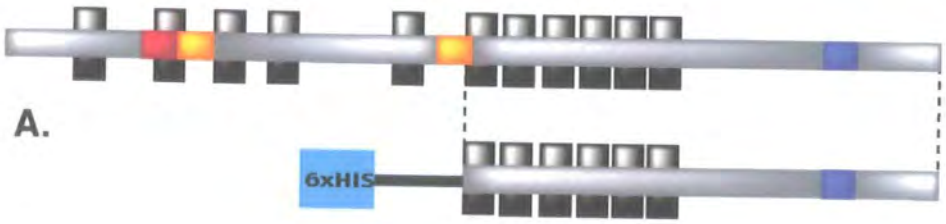

A. A carboxy terminal section of MOR1/GEM1, corrisponding to the last 844 aminoacids was cloned into pET28 and expressed as a recombinant histidine tagged protien in *E.coli* BL21 DE3. The protein was purified on a nickel column and the yield and purity assessed by PAGE gel.

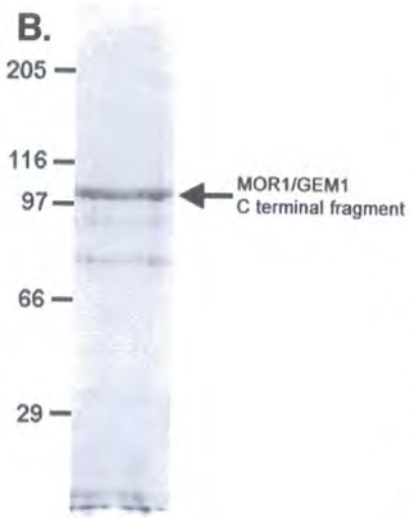

B. Here there is a band with a MW of ~ 100 kDa as predicted for the MOR1/GEM1 fragment. The recombinant protein was used to raise an anti-MOR1/GEM1 antibody in mice, which was then used in a western blot of several *Arabidopsis* tissues.

C. Here the antibody identifies a protein of ~ 210kDa, the correct size for MOR1/GEM1 CT. 10μg of protein was loaded for each tissue so that levels of MOR1/GEM1 expression could be compared.

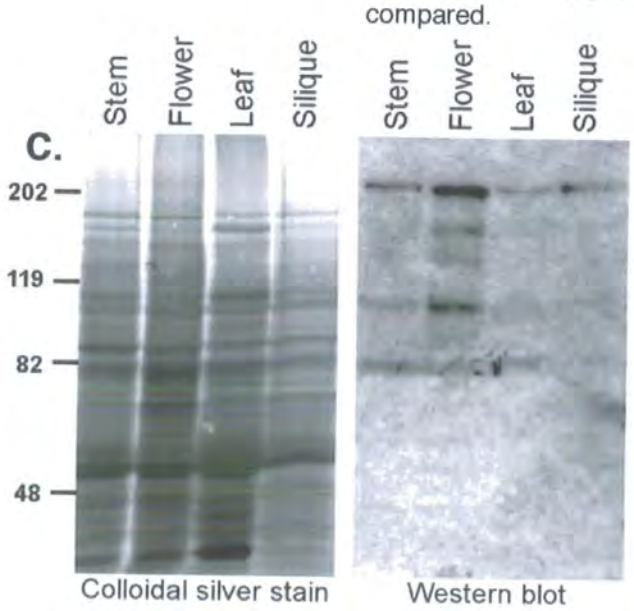

To identify the levels of MOR1/GEM1 expression in different plant tissues, total protein extracts were made as described from various plant tissues: flowers, leaves, stem, siliques, and roots. The total protein content of each of these samples was analysed by a Bradfords assay following removal of SDS sample buffer by a sephaphrose buffer exchange column. 10μg of each extract was used in the western blot and probed with anti-MOR1/GEM1 antibody (**FIGURE 4.3C**). The resulting blot suggests that the expression of MOR1/GEM1 is highest in flowers and is unexpressed in roots. However such a comparison assumes that the amount of MOR1/GEM1 degradation is equal in all tissue extracts. The lack of a MOR1/GEM1 210kDa band in roots does not agree with RT-PCR data for MOR1/GEM1 (Twell *et al.* 2002 Supp info). It is likely that there was significantly more MOR1/GEM1 degradation in the root protein extract. Although MOR1/GEM1 is highly expressed in flowers this may represent high expression in one of the structures it contains such as anthers, ovules or pollen. This is broadly consistent with the affymetrix data described in **CHAPTER 3**. Here the highest level of the MOR1/GEM1 transcript appears to be in pollen, identified by experiments where transcript levels in tricellular pollen were compared with those in whole tissue preparations.

4.4 Subcelluar Localization of MOR1/GEM1 Through the cell cycle.

The anti-MOR1/GEM1 antibody was used in immunofluorescence microscopy experiments to establish the sub-cellular localisation of MOR1/GEM1 and, more importantly whether it is found to co-localise to microtubule arrays. To achieve this, cells were double stained for MOR1/GEM1 and tubulin. *Arabidopsis* suspension culture cells were fixed with paraformaldehyde and stained as described in **CHAPTER 2**. MOR1/GEM1 was stained with the anti-MOR1/GEM1 antibody, raised in mouse and tubulin was stained with anti α-tubulin antibody, raised in sheep. These primary antibodies were visualized by anti-mouse IgG, conjugated with TRITC (Tetramethylrhodamine isothiocyanate) and anti-sheep IgG, conjugated

Figure 4.4 : Immunolocalisation of MOR1/GEM1 through the cell cycle

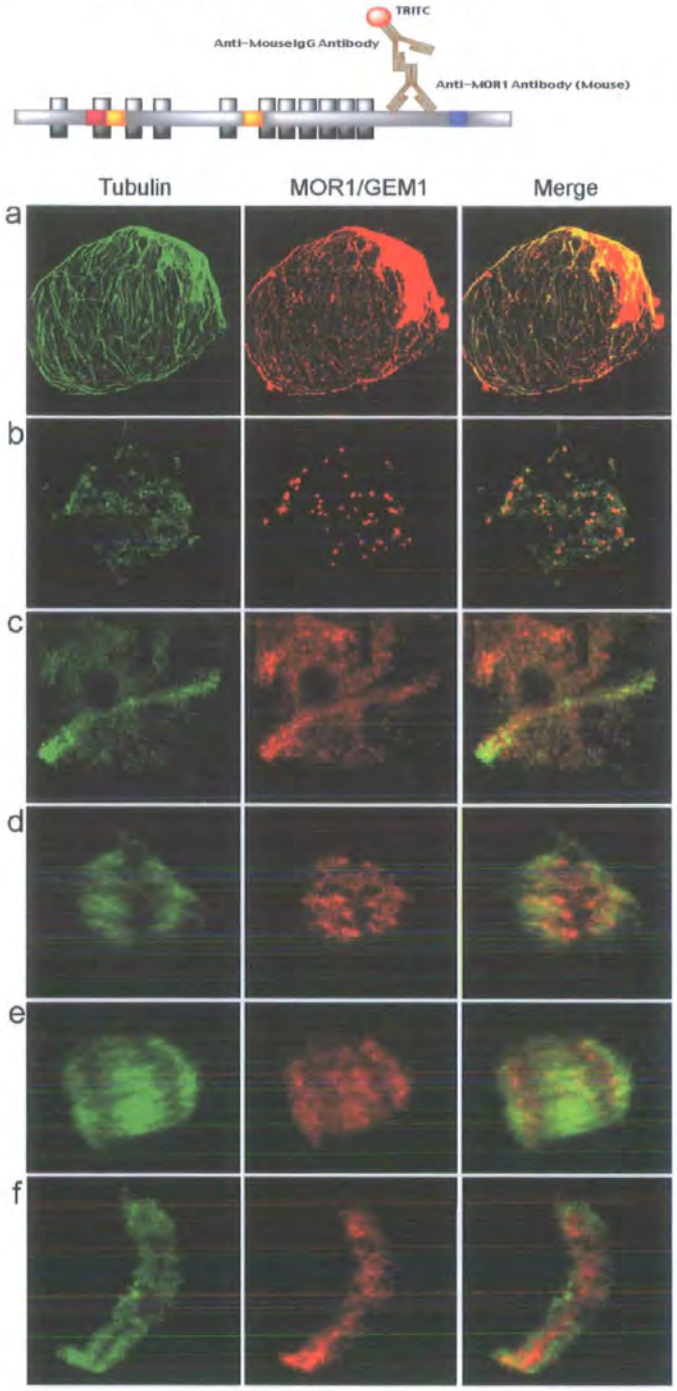

Figure 4.4 Tubulin is shown as green (FITC) and MOR1/GEM1 is shown as red (TRITC) regions of co-localisation appear yellow in the overlay. a-b Arabidopsis protoplasts. a, interphase array. b, Oryzalin treated. c-e Arabidopsis cells c, preprohase band. d, metaphase spindle. e, late anaphase spindle. f, phragmoplast. MOR1/GEM1 associates with all plant microtubule arrays. Images of the spindle show that although MOR1/GEM1 associates with microtubules throughout, it is concentrated at the plus end of microtubules where they meet the chromosomes. Also MOR1/GEM1 associates throughout the phramoplast but is concentrated at the midline where oppositely orientated microtubules overlap.

with FITC (Fluorescein isothiocyanate). In the images MOR1/GEM1 is RED (TRITC) and tubulin is GREEN (FITC) (**FIGURE 4.4**).

The two cortical arrays, the interphase array and the preprophase band are stained with anti-MOR1/GEM1. MOR1/GEM1 localises along the full length of the microtubule but with no distinguishable concentration at microtubule ends. Also all microtubules are labelled, rather than just a subset, as observed for MAP65 (Smertenko *et al.* 2001). Localisation of MOR1/GEM1 to interphase cortical microtubules was not observed in untreated *Arabidopsis* suspension culture cells. However, following the production of protoplasts by treatment with cell wall digestive enzymes, localization to the cortical microtubules could be seen. Possible explanations for this difference may include: the removal of epitope masking, due to a conformational change or the loss of a binding partner or reorganization of MOR1/GEM1 localisation, due to the proplasting process, such as involvement in the recovery of the cell wall. Localisation to the interphase cortical array is consistent with a role for MOR1/GEM1 at the cell cortex as observed in the *mor1* mutant. MOR1/GEM1 was also found to associate with the preprophase band in which it appears to label all microtubules along their length.

Tubulin and MOR1/GEM1 aggregates remained after the interphase cortical array was disrupted by the anti-microtubule herbicide, oryzalin. These data indicates that MOR1/GEM1 can bind small microtubule oligomers as well as the extended microtubule polymer. Similar experiments carried out using antiserum against MAP65 do not show co-localisation of MAP65 with tubulin aggregates following microtubule disassembly, which is consistent with the idea that MAP65 only binds microtubule polymers (Smertenko personal communication).

During mitosis, MOR1/GEM1 locates to the spindle and is seen to concentrate at the plus end of microtubules next to chromosomes (**FIGURE 4.4 & FIGURE 4.5A**). This may be suggestive of a kinetochore function, a property described for other

Figure 4.5: Localisation of MOR1/GEM1 to the spindle

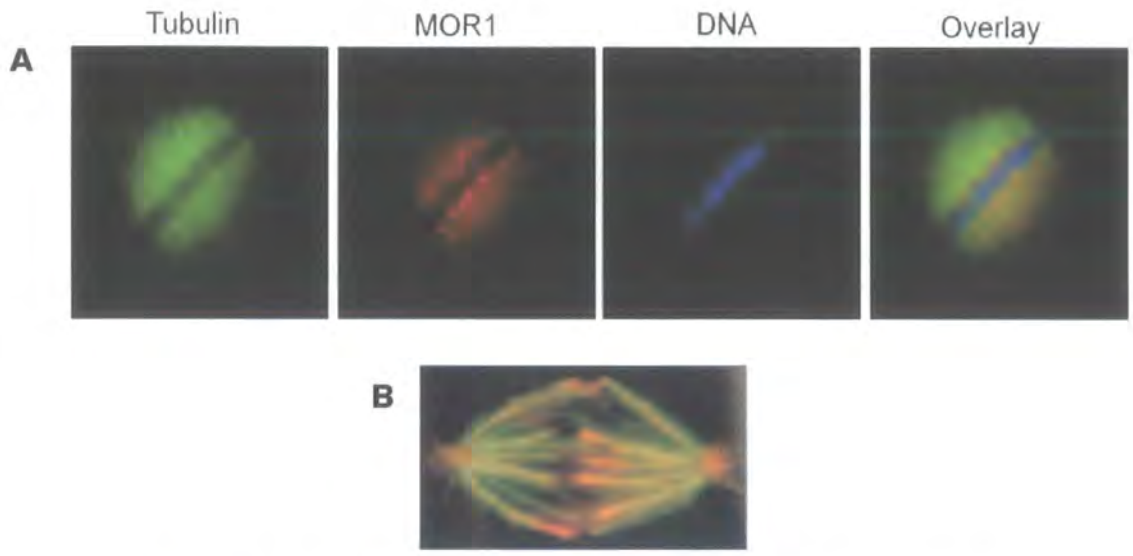

Figure 4.5: (A) MOR1/GEM1 association with the spindle. In this fluorescent microscope image of a metaphase spindle stained with anti-MOR1/GEM1 antibody (RED), There is a clear concentration at the interface between microtubules (GREEN) and chromosomes (BLUE). This is the location of the plus end of microtubules and the kinetochore. Considering this image and those presented in figure 4.4 it appears that MOR1/GEM1 is concentrated at the plus end of microtubules and/or the kinetochore. This localisation is consistent with that of Alp14, involving the capture of kinetochores by the kinetochore microtubules. (B) Image demonstrating that metaphase kinetochore microtubules add subunits at thier kinetochore-attached (Plus) end. Spindle contains fluorescein-labeled tubulin (green). Introduced rhodamine-labeled tubulin became incorporated into kinetochore microtubules at the plus end (red).Image (B) reproduced from Molecular Biology of the Cell, 3rd Edition, 925.

members of the XMAP215 family (Garcia *et al.* 2001). Here MOR1/GEM1 may be a member of those proteins found in complexes at the kinetochore, in particular the outer kinetochore which may be involved in connecting the centromere to the plus end of microtubules. Alternatively MOR1/GEM1 may stabilize these plus ends during attachment and/or stabilize and promote the growth of microtubules as they form the spindle, following the breakdown of the preprophase band. Spindle kinetochore microtubules have been shown to encorporate tubulin dimers (**Figure 4.5B**)

At cytokinesis, MOR1/GEM1 locates strongly to the phragmoplast, where it is concentrated in the midline where the plus ends of oppositely orientated microtubules overlap. It has been proposed that MAP65, which is believed to crosslink anti-parallel microtubules, stabilizes the line of overlap (Smertenko *et al.* 2000). In addition tubulin subunits are added at the overlapping plus ends at the midline (Asada, Sonobe & Shibaoka 1991). As members of the MAP215 family stimulate microtubule assembly at the plus ends (Charrasse *et al.* 1998, Gard & Kirschner 1987, Vasquez *et al.* 1994, Tournebize *et al.* 2000), it is possible that MOR1/GEM1 stabilizes the growing ends at the midline promoting the flux of tubulin through the microtubules.

As previously described, immunoblotting and RT-PCR analysis have shown that MOR1/GEM1 is expressed in all of the vegatative and reproductive tissues examined. What is intriguing about the immunolocalisation of MOR1 and its constitutive expression is that the spindle and phragmoplast arrays in both *mor1* mutations are apparently unaffected. This seems to indicate that the N-terminal HEAT repeat has a specific role at the interphase cortical array. Consistent with the localization of MOR1/GEM1 to the phragmoplast, the *gem1* mutation which gives rise to pollen with aberrant cell plate formation was positionally cloned and found to carry a mutation in the *MOR1* gene (Twell *et al.* 2002).

4.5 The *gem1* mutants

In the anther of the flower meiocytes undergo meiosis to form haploid microspores. Each microspore nucleus divides asymmetrically at pollen mitosis I to produce a larger vegative and smaller generative cell. Subsequently, only the generative cell divides at pollen mitotis II to form the two sperm cells of the mature tricellular pollen grain (Twell, Park and Lalanne 1998). The *gem1* mutation affects cytokinesis and the division pattern at pollen mitosis I (Park, Howden and Twell 1998, Park & Twell 2001). *gem1* plants produce microspores which fail to produce a cell plate at pollen mitosis I or produce incomplete and irregular branching cell walls, altering division symmetry (Park, Howden and Twell 1998, Park & Twell 2002) (**FIGURE 4.6 A +B**).

gem1 mutants contain two point mutations in the *MOR1/GEM1* coding region, the first in exon 22 (T > G) leads to a change of S745A and the second is in the splice acceptor of intron 38 (AG > AA). This produces a mis-spliced transcript in which the next downstream AG is used leading to a transcript, which encodes only the first 1326aa of MOR1/GEM1 with a 6aa C-terminal extension. In addition *gem1-2* contains a TDNA insert at exon12 giving a fusion transcript resulting in a 411aa truncated MOR1/GEM1 protein with a 48aa extension derived from the TDNA (Twell *et al.* 2002) (**FIGURE 4.6 C+D**).

4.6 The MOR1/GEM1 C-terminal Region Can Bind Microtubules.

The region missing in both *gem1-1* and *gem1-2* is the C-terminus, amino acids 1326-1978 in *gem1-1* and 411-1978 in gem1-2. The missing region common to both of these is residues 1326-1978 a region which includes a putative microtubule-binding site at position 1789. Mutation of this site in Xenopus MAP215 causes reduced microtubule binding but does not abolish it completely, suggesting that this is not the only microtubule-binding site (Popov *et al.* 2001).

FIGURE 4.6: The *gem1* Mutant and the MOR1/GEM1 Protein

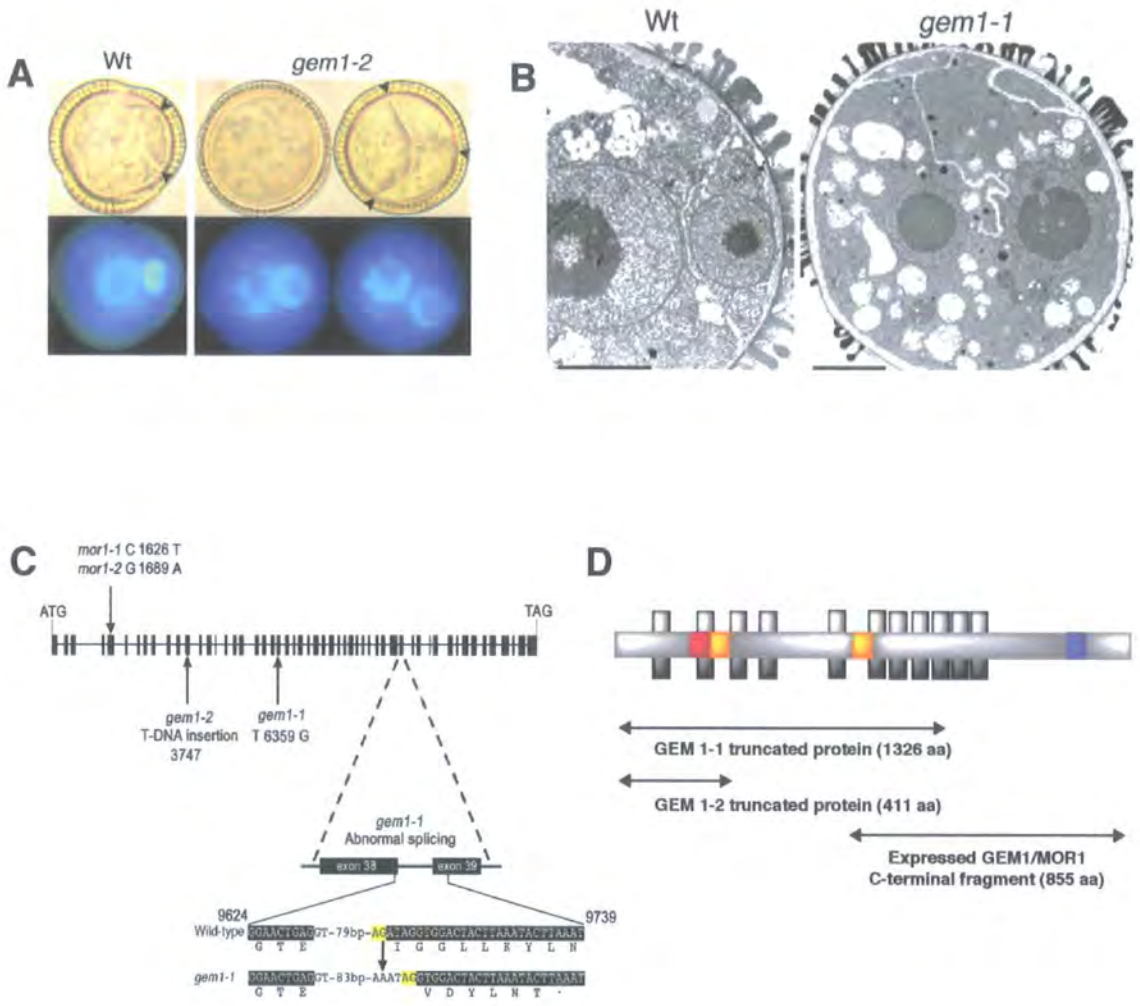

Figure 4.6: The *gem1* mutant and MOR1/GEM1 protein. (A) Binuclear stage pollen stained with DAPI. Bright field (bottom panals) & epi-fluorescence (bottom panals) of wild type and *gem1-2*. Wild type pollen shows a typical curved cell wall, but *gem1-2* like *gem1-1* pollen fail in cytokinesis or produce complex, branching cell walls after completion of karyokinesis (B) (Twell *et al.* 2002). (C) Diagram of MOR1/GEM1 exon structure showing the positions of the base changes in *mor1-1, mor1-2* (Whittington et al. 2001), *gem1-1* and the T-DNA isertion in *gem 1-2* (Twell et al. 2002).(D) Diagram showing the motif content of MOR1/GEM1, the expected GEM1 truncation products and the expressed C-terminal fragment used in microtubule cosedimentation assays (see section 4.7).

To investigate whether the aberrant phragmoplasts in *gem1* were as a result of reduced microtubule binding of MOR1/GEM1, a recombinant C-terminal fragment of MOR1/GEM1 (residues 1,123-1,978), which included the missing 652aa segment, was used in a microtubule binding co-sedimentation assay. The recombinant fragment was mixed with tubulin and incubated at 30°C to allow the tubulin to polymerize. Following this, the microtubules were pelleted at high speed and the pellet and supernatant analysed by SDS PAGE (4% stacking 7.5% resolving). Here the C-terminal fragment pellets with microtubules, indicating a binding interaction (**FIGURE 4.7**). This region of MOR1/GEM1 contains a series of phosphorylation sites as well as a coiled coil and as previously mentioned a motif, which shows homology to a conserved region in XMAP215 and TOGp, which is similar to a microtubule binding site from MAP2 (Popov *et al.* 2001). Therefore it is tempting to conclude that the errors in cell plate positioning are as a result of a compromised phragmoplast, possibly caused by the reduced affinity of MOR1/GEM1 for microtubules, due to the loss of the C-terminal region.

4.7 The Yeast Two-Hybrid System.

The yeast two-hybrid system is a powerful tool for examining the physical interactions between proteins. Yeast two-hybrid is a molecular genetic technique and has been utilized to investigate the protein-protein interactions between many of the predicted proteins from yeast (Uetz *et al.* 2000) and the large scale mapping of interactions in *C. elegans* (Walhout *et al.* 2000) and *H. pylori* (Rain *et al.* 2001) In plants the technique has been used to identify interactions involved in floral development (Davies *et al.* 1996), self-incompatibility mechanisms (Mazzurco *et al.* 2001), the circadian clock (Jarillo *et al.* 2001), plant disease resistance (Ellis *et al.* 2001) and phytohormone signaling (Ouellet *et al.* 2001) The technique was first described by Fields and Song (Fields and Song 1989) and is based on the observation that eukaryotic transcription factors have separate DNA binding and transcriptional activation domains. Interactions are tested by the fusion of protein one to the GAL4 activation domain and protein two to the GAL4 DNA binding

domain. These fusions were expressed in yeast and an interaction assayed by the expression of the GAL4 responsive reporter gene (Fields and Song 1989).

The yeast two-hybrid system has many advantages over biochemical approaches including; it can be more sensitive than many *in vitro* techniques, better suited to the detection of weak or transient interactions and proteins expressed *in vitro* often are lacking post-translational modifications which are require for the interaction (Causier & Davies).

The most widely used yeast two-hybrid system and the one used in this thesis is that which uses the reconstitution of an active transcription factor to assay protein-protein interactions. The technique base on that of Fields and Song (Fields and Song 1989) monitors an interaction by the expression of reporter genes, which contain upstream elements to which the DNA-binding domain (BD) binds. The ClonTech Matchmaker II used here, exploits the GAL4 system. The yeast strains used for two-hybrid, such as Y187 and AH109, carry mutations in several genes required for amino acid biosynthesis, such as *TRP1*, *LEU2*, *HIS3*, and *ADE2.* If these amino acids are omitted from growth media the yeast fail to grow (Causier & Davies). The expression plasmids used in yeast two hybrid contain genes, which encode these amino acids and as such allow for the selection of transformants.

4.8 MOR1 Yeast 2 Hybrid screen for interacting proteins.

Considering the high number of the HEAT repeat protein interaction motif in MOR1/GEM1 and its homologues it is reasonable to speculate that the protein may interact with a variety of proteins, possibly altering through the cell cycle or reflecting separate roles at discrete locations such as the kinetochore. Such interactions have only been elucidated for the yeast member of the protein family Stu2p through yeast two-hybrid experimentation. These interactors are Bik1, Bim1 and Spc72p (Chen *et al.* 1998) and MOR1/GEM1 may form similar interactions, although no Spc72p homologue is present in the *Arabidopsis* genome. In addition,

FIGURE 4.7: A 855 aa C-terminal fragment of the MOR1/GEM1 Protein can bind microtubules

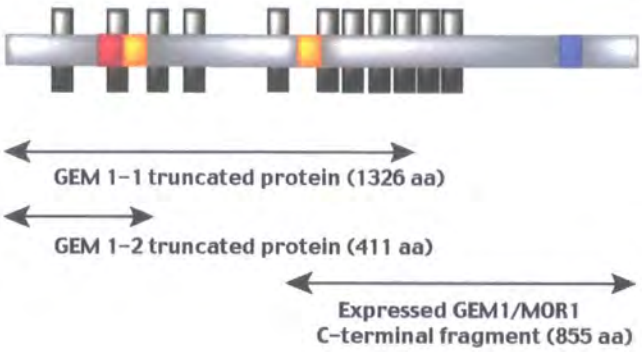

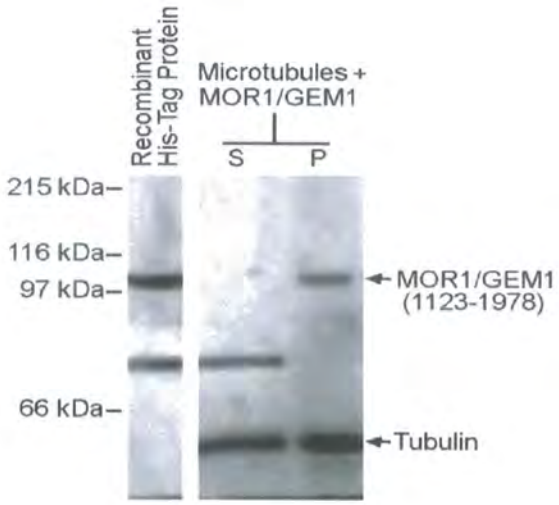

Figure 4.7: MOR1/GEM1 C-terminus binds to pig brain microtubules. Co-sedimentation of recombinant MOR1/GEM1 (aa 1123-1978) with microtubules analysed by SDS-PAGE and stained with Coomassie. S, supernatant. P, microtubule pellet.

MOR1/GEM1 should be involved in interactions that are unique to plants, thus reflecting the three microtubular arrays that only exist in plant cells.

To elucidate these interactors, MOR1/GEM1 was used as the bait in an *Arabidopsis* cDNA library yeast two-hybrid screen. Because of the size of the MOR1/GEM1 cDNA and to limit the possibility of autoactivation, the MOR1/GEM1 protein was split into two sections, MOR1/GEM1 NT, Middle, CT. The sections were ~ 1.8Kb (600 aa), 1.6Kb (534 aa) and 2.5Kb (855 aa) in length respectively. The 2.5kb CT fragment was chosen to match exactly the sequence used in previous experiments and the NT fragment contains the HEAT repeat, which contains the point mutations in *mor1*. The fragments were amplified by PCR with gateway primers using *Arabidopsis* suspension cell culture cDNA as the template. The PCR reactions were analysed by agarose gel electrophoresis and all produced products of the expected size (**FIGURE 4.8a**). These fragments were inserted into pDON207 by the BP recombination and checked by restriction digestion and DNA sequencing. Following this the fragments were transferred by LR recombination into the pACT2 (AD) and pAS2 (BD) yeast 2 hybrid vectors and checked as before. Sequencing was carried out using Gal4 BD and AD primers to check fusion and linker. Although the MOR1/GEM1 middle section was amplified it could not be cloned by gateway or traditional TA cloning therefore the following experiments used only MOR1/GEM1 NT and CT constructs, however these are the two regions previously show to have an effect on the functionality of the MOR1/GEM1 protein.

However yeast two-hybrid library screening requires efficient growth of yeast and mating of the two strains. The expression fusion proteins in the vectors ACT2 and AS2 is driven by a constitutive yeast promoter which can be problematic if the protein of interest is toxic or has an effect in yeast. Yeast cells, strain Y187 expressing either the N or C terminal fragments of MOR1/GEM1 showed reduce growth and viability and did not mate efficiently with AH109 (library). In addition when the cells expressing the N-terminal fragment of MOR1/GEM1 where

Figure 4.8a: PCR of MOR1/GEM1 Sections

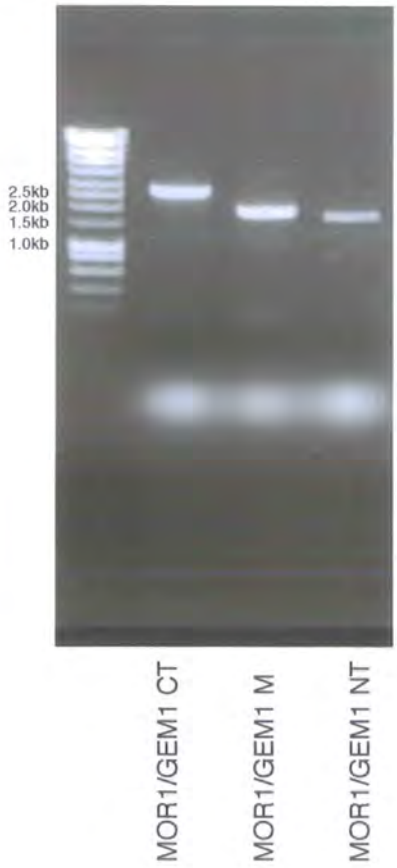

Figure 4.8a: PCR of MOR1/GEM1 sections. Three sections of MOR1/GEM1 CT, M and NT were amplified from Arabidopsis total cDNA using primers MOR1/GEM1 CT FW & RV, MOR1/GEM1 M FW & RV and MOR1/GEM1 NT FW & RV. Pfu Taq was used and extention times were 4, 4 and 6 minutes respectively. The PCR reactions gave bands of ~ 2.5kb, 1.8kb and 1.6kb in as expected for each section. The CT and NT PCR products were cloned by BP gateway recombination into pDONR207 and positive inserts were identified by restriction digests and the sequence of each product was checked by DNA sequencing and checked against the MIPS/NCBI databases. Both sections were correct with no mutations.

examined by microscopy it was found that these cells had morphological defects, with the average size of cells several times larger than wild type, typically cells were approximately 4x larger, spherical and showed no buds (**SEE APPENDIX G**). The N-terminal region used contains a high concentration of HEAT repeats and shows identity to the N-terminal region of the budding yeast member of the XMAP215/TOGp family, Stu2p (**SEE CHAPTER 3**). Therefore it is probable that the N-terminal fragment of MOR1/GEM1 is active in the yeast cell, either affecting microtubule dynamics, but lacking essential regulation or acting in a dominant negative respect, competing with Stu2p. Hence such aspects limit the effectiveness of yeast two-hybrid screening techniques, although in current and future experiments these are being resolved and parallel interaction techniques such as pull-down systems are being utilized. Interestingly during one on one, yeast two-hybrid experiments carried out on plates these factors do not appear to restrict the assay. Therefore these MOR1/GEM1 constructs were used to investigate MOR1/GEM1 interactions with itself (below) and *Arabidopsis* Kinl-like kinesins (**SEE CHAPTER 5**)

4.9 MOR1/GEM 1 vs 1 Yeast 2 Hybrid interactions.

In addition to the *Arabidopsis* cDNA screen, yeast two-hybrid analysis was used to check specific MOR1/GEM1 interactions. A table listing the interactions is shown below and **FIGURE 4.8**:

Bait Construct (pAS2)	Activator Construct (pACT2)
MOR1/GEM1 NT	MOR1/GEM1 NT
MOR1/GEM1 NT	MOR1/GEM1 CT
MOR1/GEM1 CT	MOR1/GEM1 NT
MOR1/GEM1 CT	MOR1/GEM1 CT
MOR1/GEM1 NT	AtCMK1
MOR1/GEM1 CT	AtCMK1
MOR1/GEM1 NT	AtCMK2
MOR1/GEM1 CT	AtCMK2

These experiments were designed to examine two possible sets of interactions:

Figure: 4.9 MOR1/GEM1 Yeast Two-Hybrid Constructs

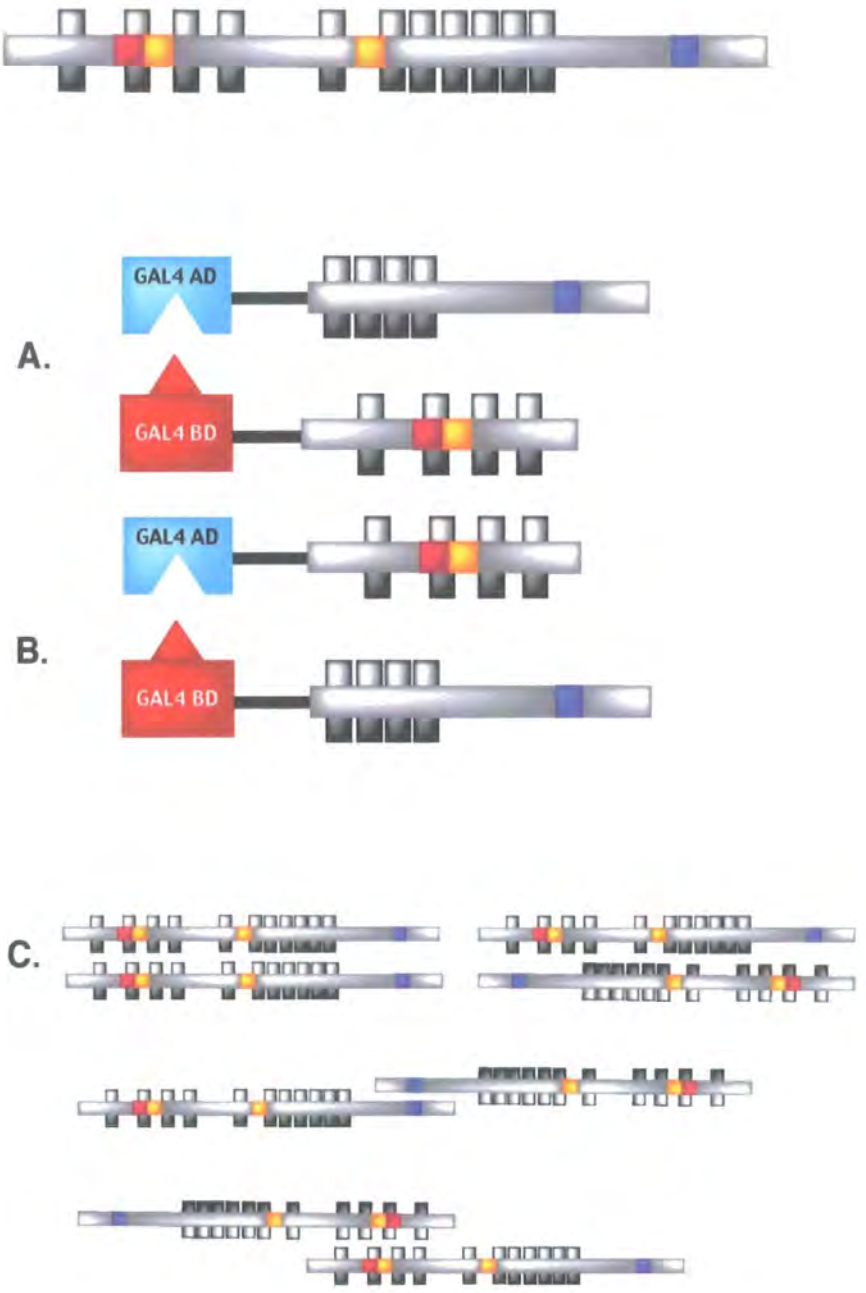

Figure 4.9: Yeast two-hybrid contructs used to test for the physical interaction of MOR1/GEM1 with itself. Two regions of MOR1/GEM1 were chosen and were expressed as GAL4 AD and GAL4 BD fusions to test interaction in both orientations. An N-terminal fragment which contained the HEAT repeat in which a point mutation occurs in the *mor1* mutant and a C-terminal fragment which is identical to that used in the microtubule binding assay as described earlier and contains those regions missing in the *gem1* mutants. The test for an interaction between the C-terminal fragment and the N-terminal fragment is shown in (A) and (B). Also CT-AD vs CT-BD and NT-AD vs NT-BD were also tested to see if each section could interact with itself. Possible orientations in which MOR1/GEM1 could dimerise if the N-terminal or C-terminal fragments showed an interaction (C).

Is MOR1/GEM1capable forming dimers and if so in which orientation and secondly does MOR1/GEM1 physically interact with *Arabidopsis* Kinl kinesins, AtCMK1 and AtCMK2 discussed later in **CHAPTER 5**.

Mating strains Y187 and AH109 were transformed with the relevant construct and allowed to mate as described in **CHAPTER 2**. Protein A was transformed into mating type a and protein B was transformed into mating type α. Three yeast transformants or colonies were used for each protein and cells were spotted onto media in triplicate. This was repeated for protein B on top of the colonies of protein A to give the grid system shown in **FIGURE 4.9**. Following mating and selection for diploids these yeast lines were spotted on to 3 types of media: either lacking adenine, histidine or neither in order to test activation of the three reporter gene systems, adenine, histidine or LacZ. If the yeast grow on the –A or –H media or give a blue colour in the LacZ assay, then this indicates that the chosen proteins interact.

FIGURE 4.9

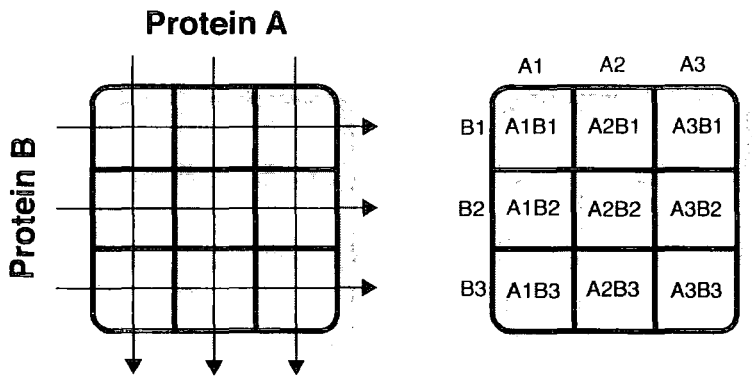

There was no activation of the reporter genes for any of the MOR1/GEM1 interactions tested (**FIGURE 4.10**). Therefore these data could suggest that MOR1/GEM1 does not form dimers like Stu2p (Huffaker, Plant and fungal cytoskeleton GRC 2004) or as speculated for other stabilizing MAPs such as MAP65. However, to assess whether this is a true negative result, it must be ascertained as to whether the MOR1/GEM1:gal4 fusion proteins are being

Figure 4.10: MOR1/GEM1 Dimerisation Yeast Two-Hybrid Experiments

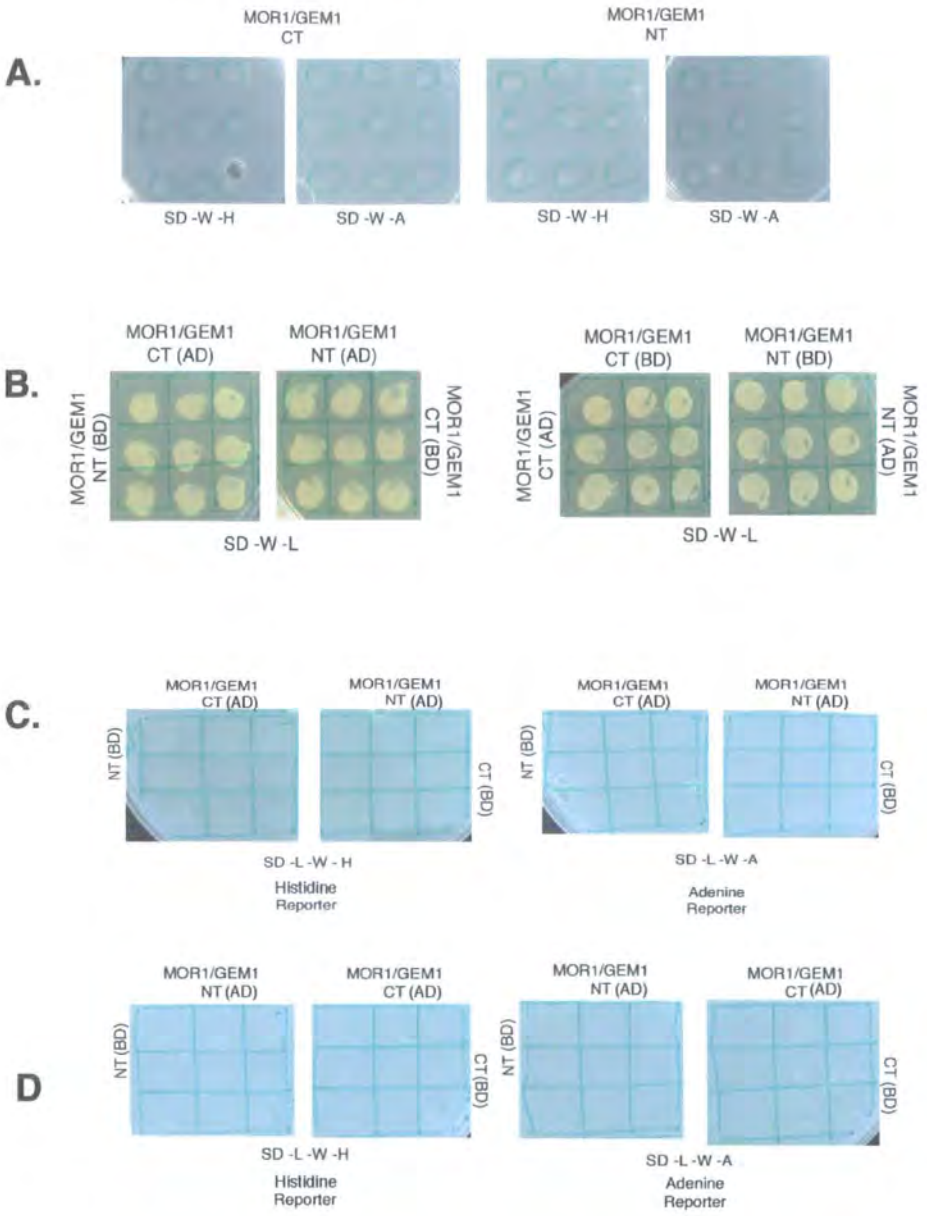

Figure 4.10: The MOR1/GEM1 BD constructs were tested for their ability to autoactivate the reporter genes and were spotted onto media lacking adenine or histidine and a LacZ assay was performed. The MOR1/GEM1 BD constructs showed no auto activation of any of the reporter gene systems (A). Yeast cells were spotted onto each other and allowed to mate in a variety of combinations. These were then streaked out and diploids selected. These diploid cells were then spotted on to -W-L media for use in LacZ assay(B) media lacking adenine or histidine to test for activation. None of the combinations of MOR1/GEM1 fragments grew on these media and gave negative results in a LacZ assay (no blue precipitate), therefore none of these combinations interact. (C) NTvsCT in both orientations (D) NTvsNT and CTvsCT.

expressed. To test this extracts from the yeast strains should be probed in a western blot using either a gal4 or MOR1/GEM1 specific antibody. Although the ability for the yeast to grow on –L –W media indicates that they contain the yeast two-hybrid plasmids, because of the possibly detrimental effects of the MOR1/GEM1 fusion proteins, there may be selection for those individuals, which do not express the protein.

4.10 Discussion/Summary.

MOR1/GEM is the *Arabidopsis* member of the XMAP215/TOGp family of proteins. These proteins are microtubule stablising MAPs and promote microtubule polymerization *in vitro*. Mutants of these proteins result in the formation of aberrant spindles and other cell division defects. To further study MOR1/GEM, a recombinant fragment of MOR1/GEM was expressed in *E. coli* and used to raise an anti-MOR1/GEM1 polyclonal antibody in mice.

Immunolocalisation of MOR1/GEM1 shows that the protein is associated with all microtubule arrays throughout the cell cycle. Association with the interphase cortical array is consistent with the *mor1* phenotype in which interphase microtubules are disorganized and shortened. Here MOR1/GEM1 may stabilize the long cortical microtubules from a destabilising factor such as a Kinl kinesin. At the preprophase band the MOR1/GEM1 protein could be involved the establishment of the guide, which delineates the plane of division and may stabilize the microtubules in the preprophase band or promote the polymerization of microtubules to form the PPB following the disassembly of the cortical array. At the spindle MOR1/GEM1 labels throughout the spindle but is concentrated at the end of microtubules next to chromosomes. This is the location of the kinetochore, a structure which connects kinetochore microtubules to the centromere. Such localization is consistent with other members of the XMAP215/TOGp family including Alp14 (Garcia *et al.* 2001). Alp14 mutants have dense short spindle microtubules at mitosis believed to be due

to the failure to capture the kinetochore, moreover Stu2p is believed to be required for tension at these sites (He *et al.* 2001).

MOR1/GEM1 is associated with the phragmoplast where it is concentrated at the midline where oppositely orientated microtubules overlap. In the *gem1* mutants the MOR1/GEM1 gene has been disrupted either by a premature stop codon or the insertion of a TDNA. These mutants show defects in the asymmetric division of pollen mitosis I, with incomplete or irregular cell plate formation leading to multinucleate pollen. Therefore the localization of MOR1/GEM1 to the cytokinetic phragmoplast is entirely consistent with this. In the *gem1* mutants a truncated protein is produced where the C-terminal region of MOR1/GEM1 is missing. This region was expressed as a recombinant protein in *E. coli* and used in a microtubule co-sedimentation assay where it was found to bind the microtubule polymer. Therefore it can be concluded that the errors in division during pollen mitosis I in the *gem1* mutants can be attributed to a compromised phragmoplast due the reduction in the ability of MOR1/GEM1 to bind microtubules.

The yeast homologue of MOR1/GEM1 is Stu2p, which has been shown to dimerise through a region in the C-terminus of the protein via a coiled coil and a microtubule binding site. To investigate whether MOR1/GEM1 could also interact with itself constructs of a N-terminal fragment containing the HEAT repeat in which the point mutation occurs in *mor1* and the C-terminal fragment missing in *gem1* which is capable of binding microtubules and contains a coiled coil, were used in a yeast two-hybrid interaction assay. However no interaction was observed for NT:NT, CT:CT or NT:CT. Therefore it is unlikely that MOR1/GEM forms dimers but rather exist as a monomer as suggested for XMAP215 (Charasse *et al.* 2002). Although the yeast two-hybrid experiment may have missed an interaction as neither the middle section or the full-length MOR1/GEM1 protein were used. In addition there may have been selection for those yeast, which did not express the fusion protein due to its possibly detrimental effects on the cell. To disregard this, expression

should be assessed by a western blot of yeast extracts with gal4 or MOR1/GEM1 antibodies.

Chapter 5

AtCMK kinesins show different subcellular localisations and expression patterns; AtCMK2 depolymerises microtubules *in vivo*

5.1 Introduction

It was established that the control of microtubule dynamics in Xenopus egg extracts involved the antagonistic relationship between two factors, the microtubule growth promoting XMAP215 and the microtubule destabalising factor, XKCM1, a Kinl kinesin (Tournebize *et al.* 2000). As an *Arabidopsis* MAP215 had been identified this posed the question as to whether plants and *Arabidopsis* in particular, possessed Kinl kinesins and if so, did such an antagonistic relationship exist. As described in chapter 3, two such Kinl kinesins were identified in the *Arabidopsis* genome, AtCMK1 and 2, along with further examples from other plants including rice and tobacco.

The objectives of the work described in this chapter were to study the localisations of AtCMK1&2 through the cell cycle and their effects on microtubules. Further objectives were to study the different expression patterns of these two kinesins and their interactions with each other and MOR1/GEM1.

5.2 The Expression of AtCMK1 and AtCMK2 Through the Cell Cycle.

The expression pattern of AtCMK1 and AtCMK2 through the cell cycle was analysed using the publicly available Affymetrix microarray data of two synchronization experiments using *Arabidopsis* tissue culture cells (Menges *et al.* 2003). In the first experiment, the cell cycle was arrested in G1 by sucrose deprivation and re-started by the addition of sucrose. In the second, the cells were blocked in S-phase using the DNA synthesis inhibitor aphidicolin and washing out

Figure 5.1: Fragments of AtCMK1/2 used to raise Polyclonal antisera

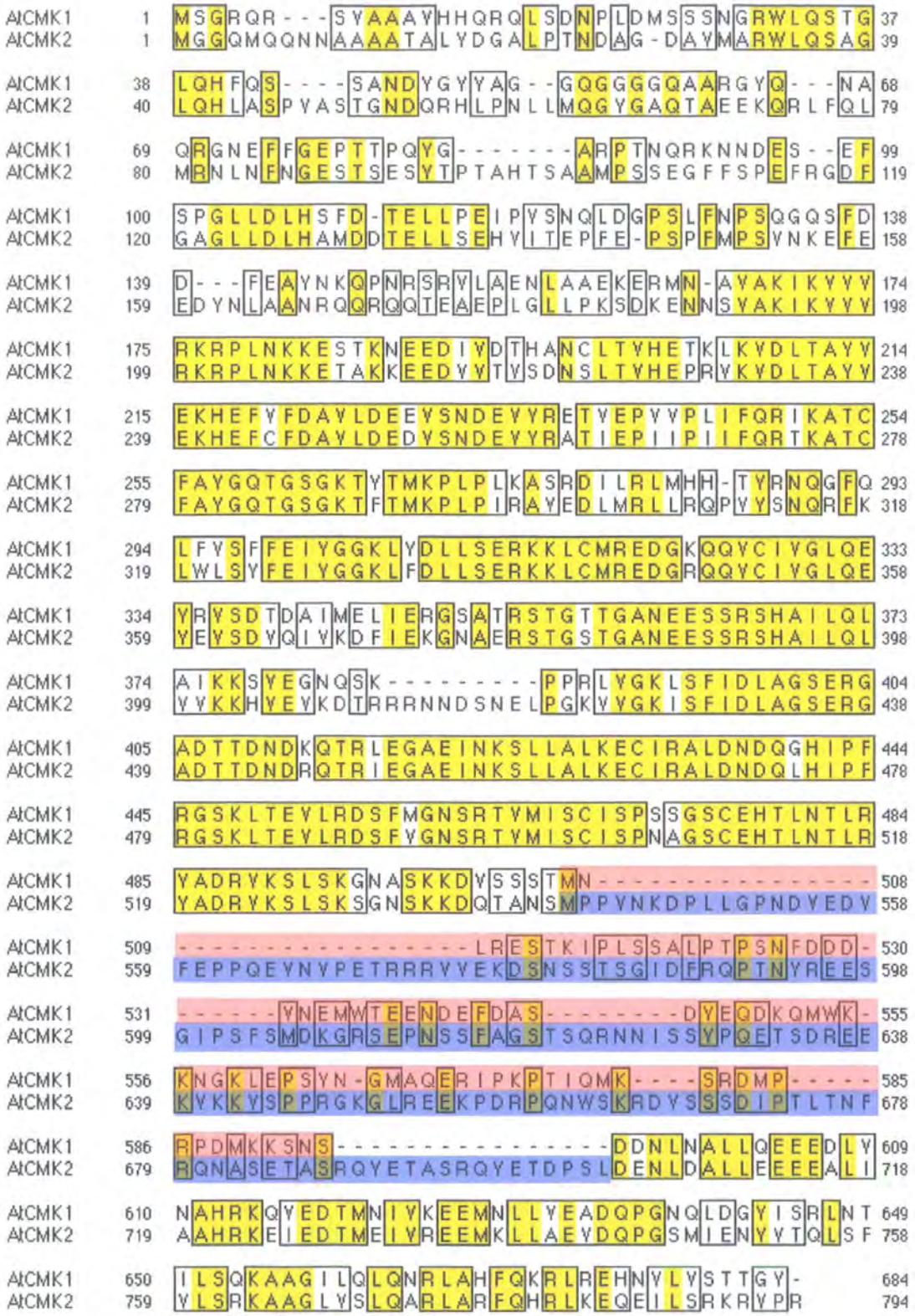

Red shaded area is the region of AtCMK1 used to raise the anti-AtCMK1 antibody.Blue shaded area is the region of AtCMK2 used to raise the anti-AtCMK2 antibody.

Figure 5.2: Primer locations for major constucts of AtCMK Kinesins

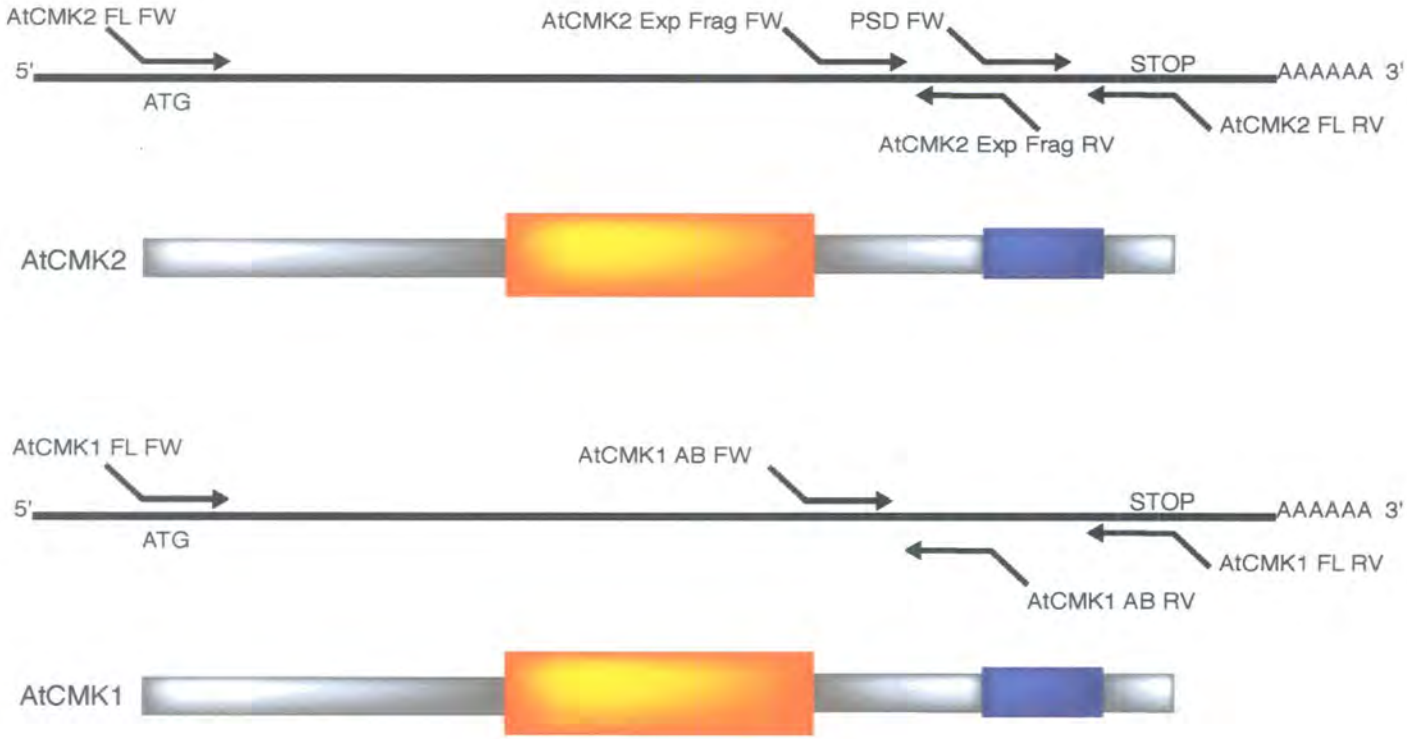

Figure 5.2: The horizontal black line represents the cDNA for the kinesin and below each is the corresponding protein architecture . Primers are shown aligned approximately with the regions of the cDNA to which they anneal. The purpose of this diagram is to illustrate the areas of each protein amplified with each combination of primers.

Figure 5.3: PCR of AtCMK Kinesin fragments

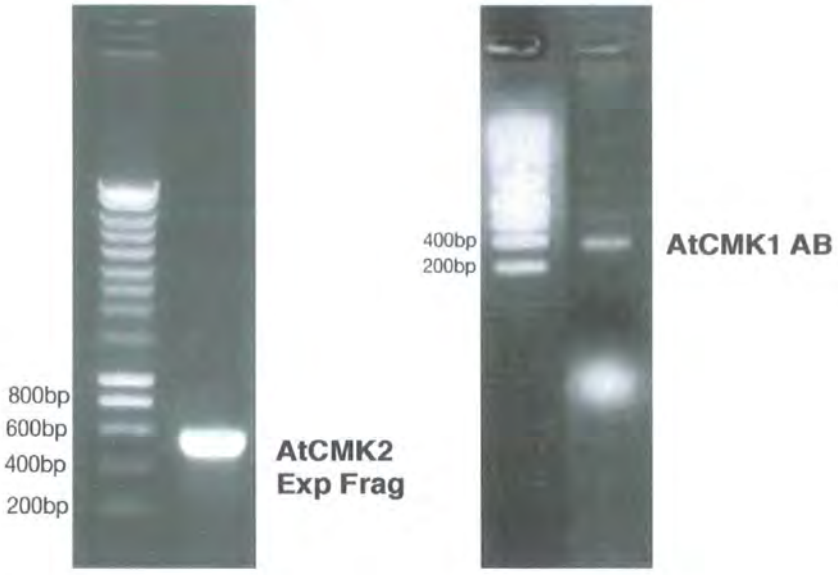

Figure 5.3: PCR of AtCMK Kinesin fragments, to be expressed and used to raise polyclonal anti-AtCMK1 or AtCMK2 antisera in mice. Primers AtCMK1 AB FW and AtCMK1 RV, and AtCMK2 Exp frag FW and AtCMK2 Exp frag RV were used to amplify AtCMK1 AB and AtCMK2 Exp Frag from total Arabidopsis cDNA respectively .Pfu Taq was used and extention times were 1 and 1.5 minutes. AtCMK2 Exp Frag gives a band of ~ 500bp in size and AtCMK1 AB gives a band of ~ 300bp in size both of which agree with the predicted sizes of such fragments based on the cDNA lengths from the MIPS database. These PCR products were cloned into pDONR207 by BP gateway recombination. Positive inserts were identified by restriction digests and the sequence of each product was checked by DNA sequencing and checked against the MIPS/NCBI databases. Both fragments were correct with no mutations.

this inhibitor allowed the cell cycle to resume. The level of AtCMK1 and AtCMK2 transcripts changed 2.96/2.55 and 1.29/1.19 fold in each experiment for each protein respectively, which is far below known cell cycle regulated transcripts (e.g. 14.9 and 97 folds for Cyclin A1 and Cyclin B1 transcripts respectively). The results of both experiments demonstrate that the amount of AtCMK transcripts does not change significantly throughout the cell cycle. It is interesting to note however that the level of both transcripts peaks during M phase. A polyclonal antiserum against AtCMK1 and AtCMK2 was prepared and the localization of these proteins through the cell cycle was examined.

5.3 Production of anti-AtCMK1 and anti-AtCMK2 polyclonal antibodies.

When the two *Arabidopsis* Kinl type kinesins, AtCMK1 and AtCMK2 are aligned it can be seen that although they share identity in their motor domains and a conserved plant domain at the extreme C-terminus of the proteins, regions surrounding these are quite dissimilar (**FIGURE 5.1**). Therefore in order to produce an antibody, which would specifically locate AtCMK2, one of these regions was used. Following the motor domain there is an insertion of sequence in AtCMK2, which is completely absent from the sequence of AtCMK1. Gateway primers were designed to this section (In frame for fusion) and this section amplified by PCR (**FIGURE 5.2 & FIGURE 5.3**) and cloned by a BP recombination in to the entry vector pDONR207. This was confirmed by restriction digest and DNA sequencing. As this region is highly divergent between the two kinesins, this section in AtCMK1 was used to raise a specific antibody to AtCMK1 and was cloned as for AtCMK2. In addition to the consideration of amino acid identity, these regions were chosen for their antigenicity as analysed by the Hopp and Woods (1981) algorithm and their dissimilarity at the DNA level. Although other regions show amino acid differences they are highly similar at the DNA level preventing specific PCR amplification. To prevent cross reactivity with other protein the amino acid sequences of the

fragments to be expressed were checked for similarity against the database of all *Arabidopsis* proteins using BLASTP. Neither of these recombinant fragments showed significant similarity to other proteins.

These fragments were transferred to the destination His-tag expression vector pGAT4 by means of an LR recombination. The pGAT4 vector is based on the pET28a system and again the recombination and particularly the resulting frame of the 6xHis-tag fusion was confirmed by restriction digest and DNA sequencing. The 6xHis-AtCMK2$_{541\text{-}703}$ and 6xHis-AtCMK1$_{502\text{-}594}$ fusion proteins were expressed and purified on a nickel column as described in **CHAPTER 2**. The purified recombinant proteins were analyzed by SDS-PAGE (**FIGURE 5.4 A & B**). Here bands of approximately 24kDa & 22kDa are present which are the same as the predicted molecular weight for these recombinant His-tagged fragments. These proteins were transferred to PBS buffer and used to raise anti-AtCMK2 and anti-AtCMK1 polyclonal antibodies in mice as described previously.

The Anti-AtCMK antibodies were used in western blots of *Arabidopsis* cell suspension culture total protein. The nitrocellulose membrane was probed by 1:500 Dilution of anti-AtCMK1 or anti-AtCMK2 mouse sera and visualised by the ECL reaction and recorded on a FujiFilm LAS-1000 Intelligent Dark Box II (**FIGURE 5.4 C**). Here bands of the predicted sizes were observed along with some smaller peptides. These may be degradation products of the AtCMK proteins or other proteins, which show some cross reactivity to the antibody. To further test that the antibody specifically identifies the correct protein in *Arabidopsis* extracts, the serum should be preabsorbed against the recombinant protein used to raise the antibody. This serum can then used to probe *Arabidopsis* protein extracts and if the antibody is specific for the kinesin of interest the correct molecular weight band should be absent or significantly reduced. In addition the antibody could be used to probed an extract of an *Arabidopsis* line where the protein of interest was known to be 'knocked out'.

FIGURE 5.4: Production of Anti-AtCMK1 and Anti-AtCMK2 Polyclonal Antibodies

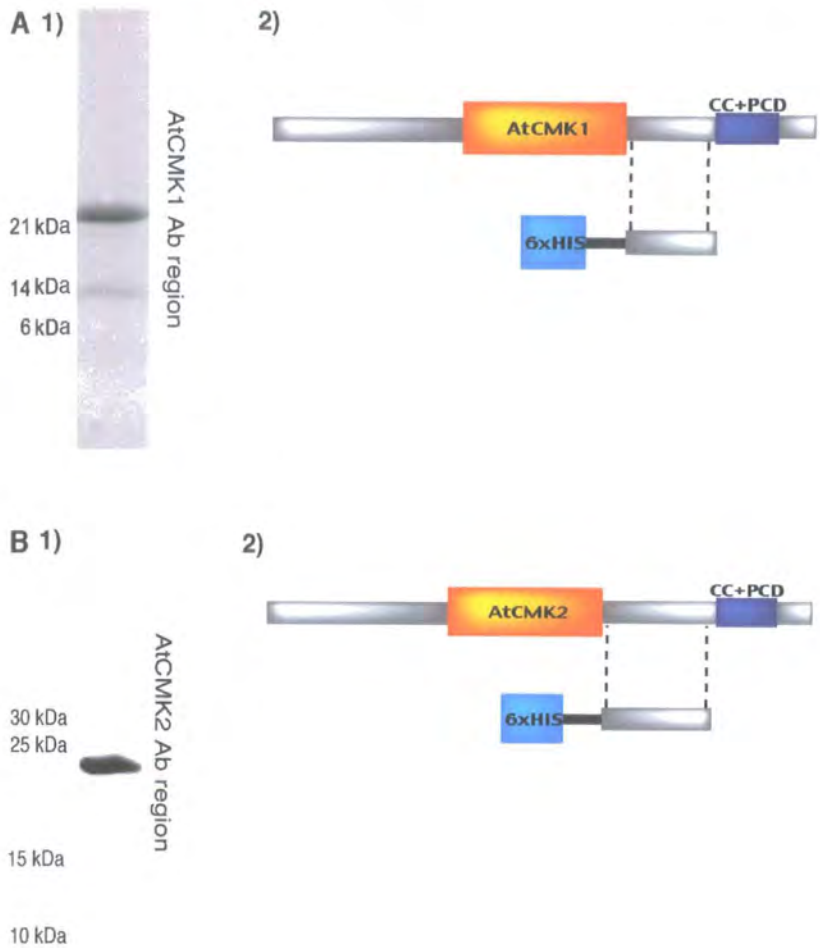

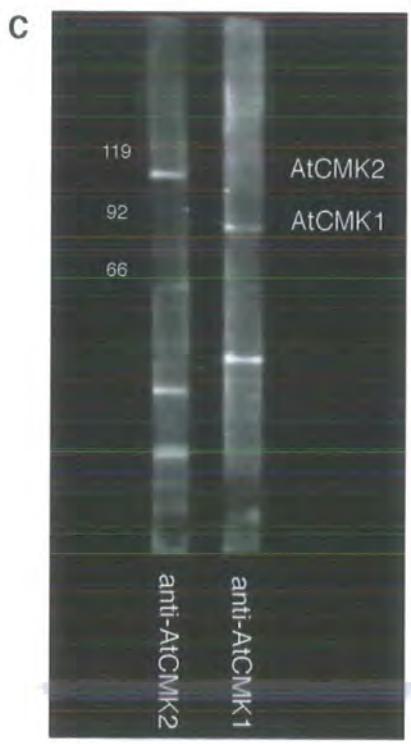

A. 1) PAGE gel of recombinant His tagged AtCMK1 Ab fragment. 2) Diagram of AtCMK1 region expressed

B. 1) PAGE gel of recombinant His tagged AtCMK2 Ab fragment. 2) Diagram of AtCMK2

C. Western Blot of Arabidopsis suspension culture cell total protein extract probed with anti-AtCMK1 and anti-AtCMK2.

5.4 Subcellular localization of AtCMK1 and AtCMK2 through the cell cycle.

The subcellular localizations of AtCMK1/2 were studied by immunofluorescence microscopy. Three day old *Arabidopsis* suspension culture cells were fixed as described in chapter 2 and allowed to adhere to poly-Lysine coated coverslips. These were then stained using the mouse polyclonal anti-AtCMK1 or 2 antibody and the rat monoclonal anti-tubulin antibody. Secondary antibodies were anti-mouse Ab conjugated to TRITC (no rat cross-reactivity) and anti-rat Ab conjugated to FITC (no mouse cross-reactivity). In the following microscopy images AtCMK proteins are represented on the red channel and tubulin on the green channel (**FIGURE 5.5**).

AtCMK2 is associated with the preprophase band and is particularly concentrated in the spindle. In this image AtCMK2 can be seen to associate with individual microtubules in the spindle and no preferential concentration at the spindle poles or kinetochore can be seen, although the kinesin is present at these sites. This localization to the spindle is consistent with the localization and mitotic roles of its homologues such as XKCM1 in other organisms (Walczak *et al.* 1996). In addition AtCMK2 is concentrated in the vicinity of the phragmoplast. However AtCMK2 shows no localization to cortical microtubules in untreated suspension culture cells or protoplasts (data not shown).

The localization of AtCMK1 appears to be dramatically different to AtCMK2. AtCMK1 was not found to associate with mitotic or cytokinetic microtubule arrays but rather locates to objects within the cytoplasm which may be structures such as Golgi derived vesicles (**FIGURE 5.6**). Further experiments using markers for other cellular components such as golgi, will enable the association of AtCMK1 to be studied further. Despite the sequence similarity to other Kinl kinesins, AtCMK1 may

FIGURE 5.5: Immunolocalisation of AtCMK2 Through the Cell Cycle

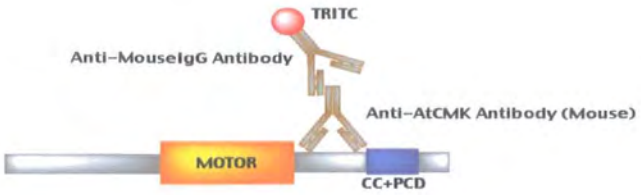

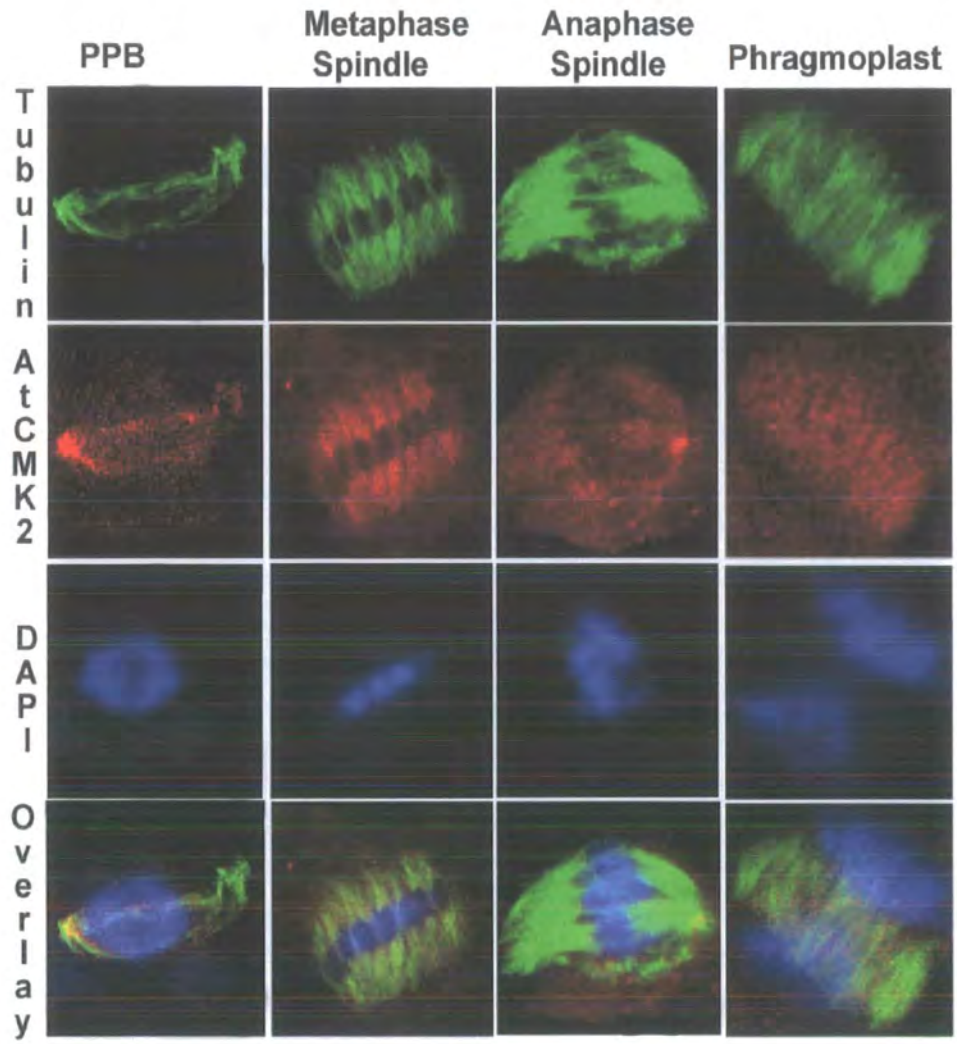

Figure 5.5: subcellular localisation of AtCMK2. Arabidopsis suspension culture cells were fixed and stained with mouse anti-AtCMK2 and rat anti-tubulin. Secondary antibodies were anti-mouse TRITC and anti-rat FITC. In the images above AtCMK2 is represented in red and tubulin is respresented in green. AtCMK2 associates here with all the plant microtubule arrays, exept the interphase cortical array. Staining is particularly strong within the metaphase spindle and AtCMK2 can be seen to clearly associate with individual microtubules/bundles.

Figure 5.6: AtCMK1 Subcellular Localisation

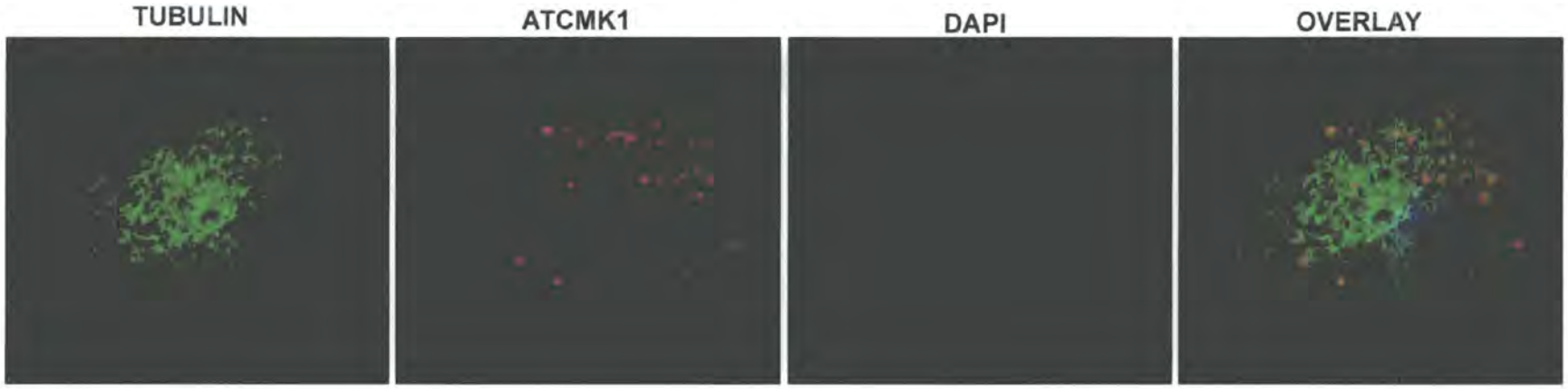

Figure 5.6: AtCMK1 subcellular localisation. Unlike AtCMK2 immunostaining of *Arabidopsis* cell suspension culture cells with anti-AtCMK1 showed that AtCMK1 does not associate with any of the four microtubule arrays. AtCMK1 appeared as descrete spots or structures within the cytoplasm which could be golgi vesicles. Future localisation experiments with different markers will help to identify what these structures may be.

not be a microtubule destabilser, but rather a conventional translocating kinesin and as such, these structures could represent cargo.

As the transcript levels of AtCMK2 do not vary significantly through the cell cycle yet the association of the kinesin with microtubules does, these data suggest that microtubule binding by AtCMK2 is regulated through the cell cycle. A plausible mechanism for this could be through control of the phosphorylation state of the kinesin. A kinase known to phosphorylate a Kinl kinesin is Aurora B, which phosphorylates XKCM1 (Cimini *et al.* 2002). Such kinesins are present in the *Arabidopsis* genome.

5.5 AtCMK Subcellular localization in live cells using GFP fusions.

To study the subcellular localization of AtCMK2 in living cells and the dynamics of this localization, N-terminal GFP-AtCMK fusion constructs were made. The full length AtCMK1&2 cDNAs were amplified by PCR using *Arabidopsis* suspension cell culture total cDNA as a template (**FIGURE 5.**). These full-length transcripts were then inserted into pDONR207 by means of a BP recombination reaction and then recombined into the GFP fusion destination vector, pGWB6 via a LR reaction. The sequence and frame of the GFP-AtCMK fusion was confirmed by DNA sequencing. PGWB6[AtCMK1/2] were transformed into *agrobacterium* strain LBA4404 and used to transform BY2 cell suspension cultures to form stable cell lines. To transform BY2 cells LBA4404 are mixed with BY2 cells and this mixture is incubated on a flat surface at 25°C for three days. Following this period the BY2 cells are washed and plated out onto selective media to select for transformants based on the resistance of the plasmid used, in the case of pGWB6 this was Hygromycin. Remaining *agrobacterium* are killed by addition of carbenicillin to the media. After several weeks successful transformants produce calli. For further details see **CHAPTER 2.**

Figure 5.7: Stable GFP-AtCMK1 BY2 Cells

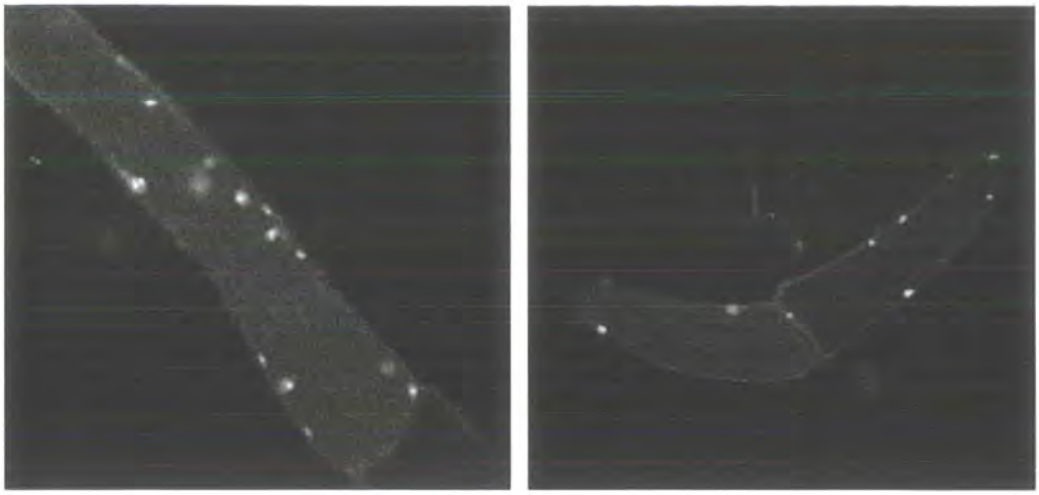

Figure 5.7: Stable GFP-AtCMK1 BY2 Cells. BY2 cells were mixed with agrobacterium LBA4404 containing the pGWB6[GFP-AtCMK1] plasmid. BY2 cells were plated out on selective media to identify positive transformants. Positives produced cali which were maintained on selective media. Unlike AtCMK2 stably tranformed GFP-AtCMK1 expressing cells do not die and continue to grow well. These cells showed only fluorescent dots in the cytoplasm and particularly at the cell cortex. No cytoskeletal structures were seen. These images are similar to those achieved with immunolocalisation with anti-AtCMK1 antibodies.

Several calli for each construct were produced and these were propagated on selective media for analysis. All calli containing the GFP-AtCMK2 expressing plasmid rapidly degenerated within days and upon observation by microscopy only dead cells and detritus could be observed with any possible GFP signal either lost or masked by the resultant auto-fluorescence.

However GFP-AtCMK1 stable BY2 tissue culture lines were maintained and analysed. Cells were observed here have a similar localization to structures within the cytoplasm was observed for all ten line analysed (**Figure 5.7**). Time lapse of these cells revealed that these structures did not appear to move (data not shown). As discussed previously these structures could be organelles or golgi.

As expression of GFP-AtCMK2 appeared to be lethal, to further study the localization of AtCMK2, transient transformants were also created by shooting the GFP construct into wild type tobacco (BY2) suspension culture cells and onion epidermis. The bombardment technique involved precipitation of the GFP-AtCMK2 plasmid onto fine gold beads, which were then coated onto small sections of tubing to create cartridges. The cartridges were loaded into the BioRad Helios™ GeneGun and the gold particles expelled from these by a burst of pressurized helium. The gold particles penetrate the tissues and within single cells the DNA from these particles is transcribed and translated. Full descriptions of the bombardment technique and the GeneGun are provided in **CHAPTER 2**.

Onion epidermal cells transformed with pGWB6[GFP-AtCMK2] showed fluorescent tubular or filamentous structures in the cell cortex which appear to be the cortical microtubules array (**FIGURE 5.8 A**). However the 'microtubules' were short and unaligned giving a disorganised arrangement. Although some onion epidermal cells can exhibit an apparently random matrix of microtubules, all of those cells expressing GFP-AtCMK2 possessed such arrangements. In addition these cells showed short microtubular 'fragments', which are not observed in the cortex of wild

Figure 5.8: GFP-AtCMK2 in Onion Epidermal Cells and BY-2 Suspension Cells (Bombardment Technique)

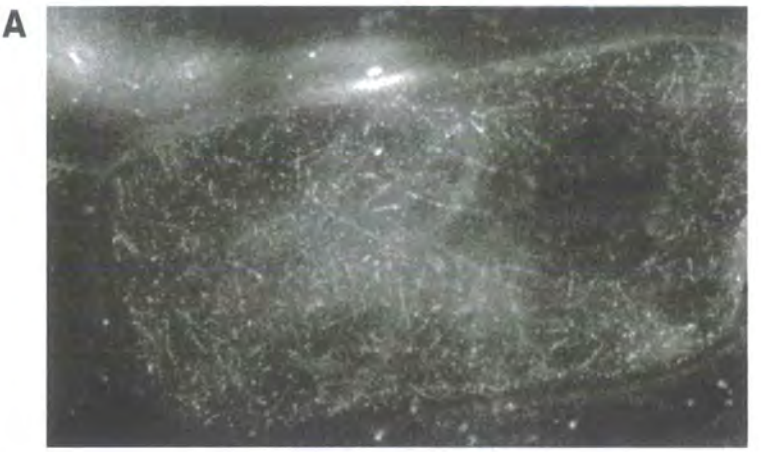

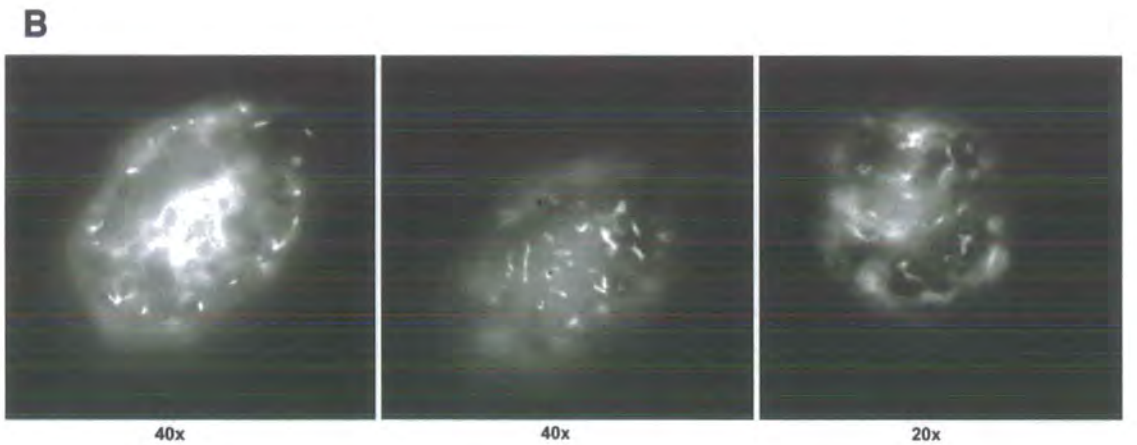

Figure 5.8: The GFP-AtCMK2 construct was coated onto gold beads and shot into onion epidermal cells (A) and BY2 tobacco supension cell culture cells (B). The fusion protein is transcribed and translated by the cell. It is important to note that expression of GFP-AtCMK2 is under the 35S strong consitutive promoter and as such is being over-expressed with levels of GFP-AtCMK2 much higher than endogenous AtCMK2. The onion cell shows what appears to be fluorescent cortical microtubules suggesting that AtCMK2 can bind the cortical array (A). These possible microtubules appear disorganised and shorter microtubules are also seen. BY2 cells, show only short highly fluoresent filamentous structures at the cell cortex, which could be microtubule fragments (B). As AtCMK2 is over-expressed in these cells it is reasonable to suggest that perhaps GFP-AtCMK2 is binding to cortical microtubules in both cells and promoting their disorganisation and depolymerisation.

type onion epidermal cells. When the same construct was shot into tobacco BY2 suspension culture cells, a similar effect was observed (**FIGURE 5.8 B**). All cells that expressed GFP-AtCMK2 showed small fluorescent tubular fragments at the cell cortex. It is tempting to conclude from these observations that AtCMK2 labels or binds to cortical microtubules and at this location disassembles the microtubule.

To further investigate the localization and effects of transient GFP-AtCMK2 expression, *N. benthamiana* leaves were infiltrated with *agrobacterium* strain GV3101 containing pGWB6[AtCMK-GFP]. In order to prolong expression, the leaves were co-infiltrated with *agrobacterium* containing a silencing suppressor. Postranslational gene silencing (PTGS) is a major cause of lack of expression in such systems and to prevent this the co-expression of the viral-encoded suppressor of gene silencing, p19 of the tomato bushy stunt virus (TBSV) was used (Voinnet *et al.* 2003). Six days after infiltration, sections of leaf were examined using the confocal microscope (**FIGURE 5.9**). Strong GFP expression was seen in the majority of cells and two types of GFP localization were observed. Some cells contained bright spots or aggregates at the cell cortex, secondly, those cells which appeared to exhibited a lower level of expression showed structures which appeared to be small filamentus fragments. Interestingly, this localization is practically identical to that observed following shooting of BY2 cells and therefore is unlikely to be an artifact of the bombardment process.

A possible explanation for the fluorescence spots is that these may be organelles such as peroxisomes where following such high expression, GFP-AtCMK2 is being packaged away for degradation. It is tempting to conclude from these observations that AtCMK2 labels or binds to cortical microtubules and at this location disassembles the microtubule. The expression of GFP-AtCMK2 is under the control of the 35S viral promoter and is, essentially, an over-expression system. Without the endogenous control on transcription the disassembly and

Figure 5.9: GFP-AtCMK2 in Infiltrated *N. benthamiana* Leaf Epidermal Cells

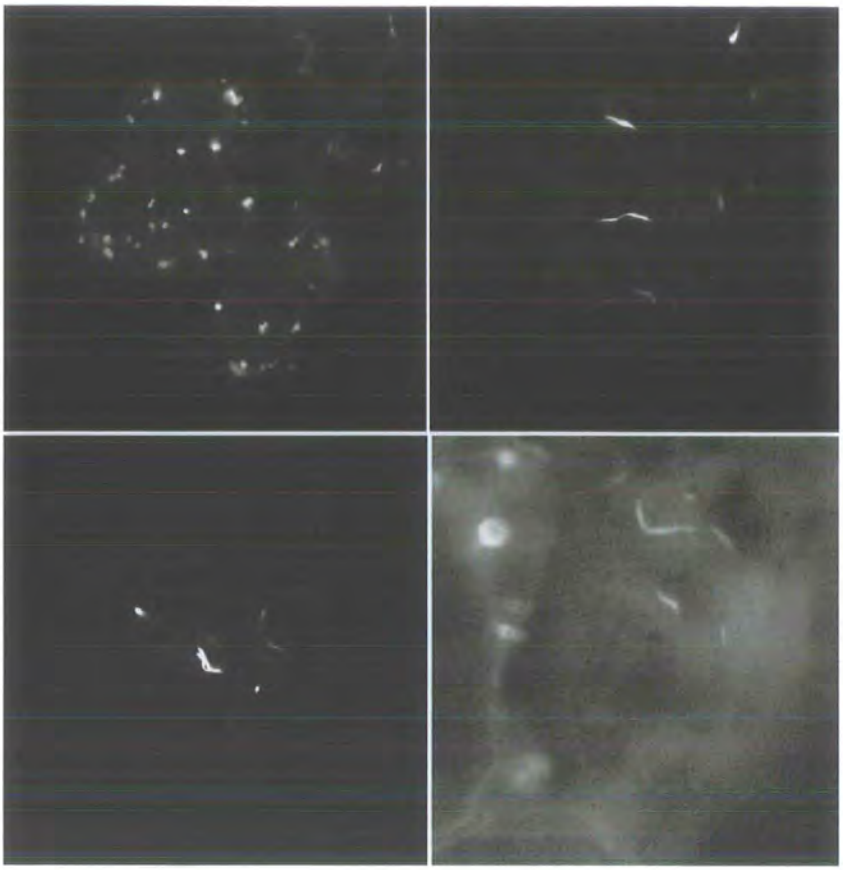

Figure 5.9: These images are GFP-AtCMK2 in *N.benthamiana* leaf epidermal cells which have been infiltrated with *Agrobacterium* GV3101 containing the pGWB6[GFP-AtCMK2] plasmid. These cells which show high levels of expression, as inferred by the intensity of the GFP signal, showed dots or aggregates in the cytoplasm, possibly inclusion bodies or organelles such as peroxisomes breaking down the large quantities of GFP-AtCMK. However other cells which appeared to have a lower level of GFP-AtCMK2 expression showed filamentous structures similar to those observed in BY2 cells bombarded with the same construct. These fragments sometimes appeared to clump together and some cytoplasmic fluorescence was also observed.

disorganisation of cortical microtubules would be overwhelming leading to the short microtubule fragments observed.

5.6 GFP-AtCMK2 destabilises microtubules *in vivo.*

These infiltrated leaves were then freeze shattered and stained for tubulin with a anti-tubulin primary antibody and anti-mouse IgG conjugated to FITC (**FIGURE 5.10**). The process of freeze shattering involves the fixation of the sample in a mixture of formaldehyde and gluturaldehyde before being frozen in liquid nitrogen and then force applied to 'smash' the sample creating cracks in cell walls, which allow the antibodies to penetrate. This technique is preferable for use on whole tissue such as leaves, as solutions of cell wall digestive enzymes are inadequate for rapidly producing holes within the tough cell walls. Freeze shattering has been used successfully to image microtubules and actin in leaves and even structures such as trichomes (Whittington *et al.* 2001, Deeks *et al.* 2004).

Pavement cells of wild type leaves showed clear organized arrays of cortical microtubules (**FIGURE 5.10 A**). There are long microtubules which transverse the cell and are typical of those seen in pavement cells. In contrast, those cells which had been infiltrated with GV3101 containing pGWB[GFP-AtCMK2] and as such exposed to over-expression of AtCMK2, exhibited small microtubule fragments or tubulin aggregates. These data suggest that AtCMK2 is responsible for the depolymerisation of microtubules in these cells consistent with AtCMK2 being a true Kinl catastrophic kinesin.

These images are very reminiscent of those observed in the *mor1* (microtubule organisation) mutant, an observation which could imply the existence of a Atcmk2 vs MOR1/GEM1 antagonistic relationship in plants. Furthermore, the area of the *N. benthamiana* leaf, which was infiltrated, began to degenerate or die, an observation not seen following infiltration with other constructs. This leads to the possibility that disruption of the interphase cortical array could induce or be

Figure 5.10 Tubulin Staining in AtCMK2-GFP Infiltrated *N. bethamiana* Leaf Epidermal Pavement Cells.

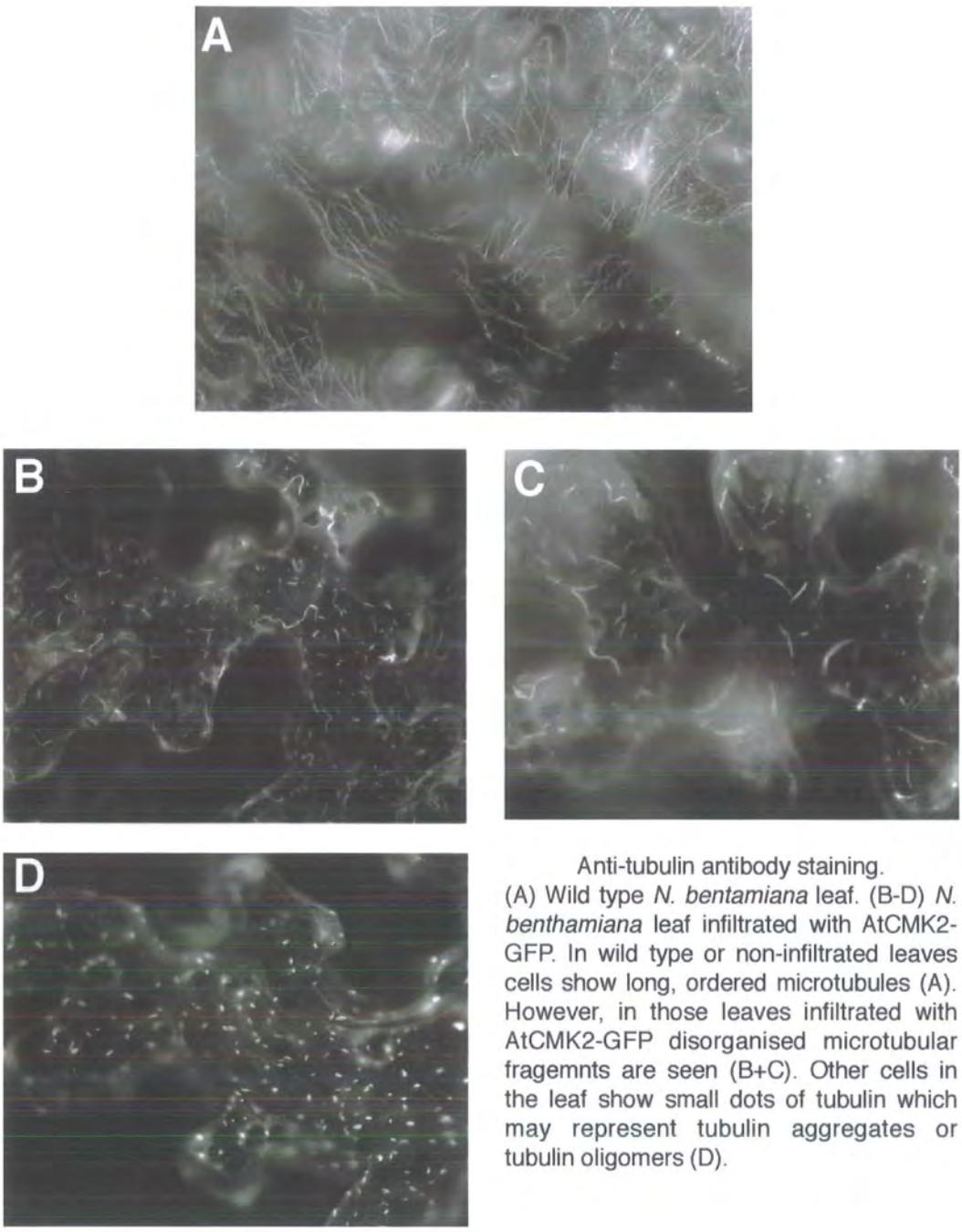

Anti-tubulin antibody staining.
(A) Wild type *N. bentamiana* leaf. (B-D) *N. benthamiana* leaf infiltrated with AtCMK2-GFP. In wild type or non-infiltrated leaves cells show long, ordered microtubules (A). However, in those leaves infiltrated with AtCMK2-GFP disorganised microtubular fragemnts are seen (B+C). Other cells in the leaf show small dots of tubulin which may represent tubulin aggregates or tubulin oligomers (D).

involved in programmed cell death. Reorganisation of the cytoskeleton has been shown to be associated with developmental programmed cell death in *Picea abies* embryos (Smertenko *et al.* 2003). Successful embryogenesis is reliant on programmed cell death and organisation of microtubules and F-actin changes successively from the embryonal mass towards the distal end of the embryo suspensor (Smertenko *et al.* 2003). The microtubule arrays appear normal in the embryonal mass cells, but the microtubule network is partially disorganized in the embryonal tube cells and the microtubules are disrupted in the suspensor cells (Smertenko *et al.* 2003).

5.7 Cloning and expression of Full Length AtCMK proteins.

Gateway primers were designed to the 5' and 3' of the predicted AtCMK coding regions and used to amplify the 2384bp and 2055bp cDNA from *Arabidopsis* total cDNA (**FIGURE 5.11**). The cDNA was cloned into the pDONR207 entry vector by a BP recombination and confirmed by restriction digest and DNA sequencing. AtCMK1/2 were recombined into pGAT4 and expressed as 6xHis-tagged fusion proteins and purified on a nickel column as described in Chapter 2. Cells were grown to a OD of 0.45 at 37°C, upon which they were transferred to 4°C and expression induced with 1mM IPTG. Expression was allowed to proceed overnight. The purified recombinant AtCMKs, were analyzed by SDS-PAGE (stacking 4% resolving 7.5%) where bands of the correct predicted molecular weights are present (**FIGURE 5.12**). The elusion buffer was exchanged for Microtubule buffer (MTSB) by ultrafiltration or dialysis for using in further microtubule experiments. Expression of these two kinesins was found to be low in BL21 DE3 and pLysS cells but with the use of BL21 Rosetta 2 pLysS yield was substantially improved, suggesting that the coding sequence of these kinesins contains plant codons which have low codon usage in E. *coli*. Also the kinesins were particularly susceptible to destruction by proteases, this was reduced with the addition of five protease

Figure 5.11: PCR of Full Length AtCMK Kinesins.

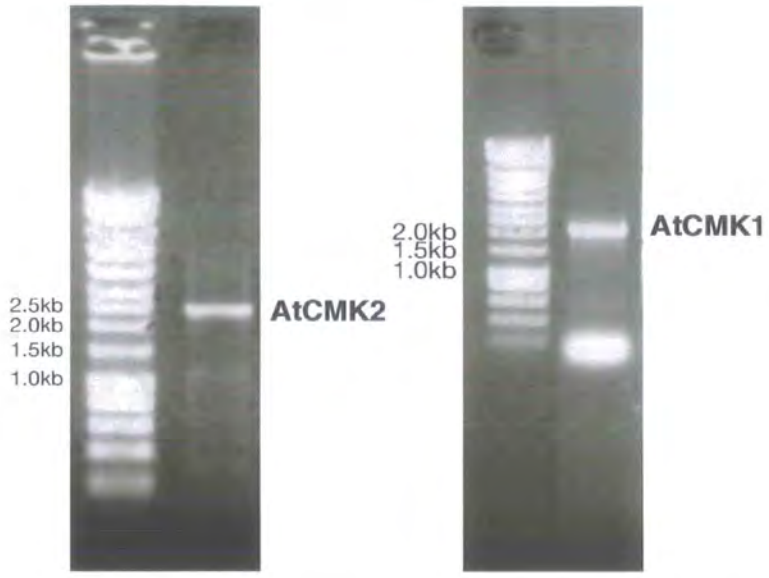

Figure 5.11: PCR of full length AtCMK Kinesins. Primers AtCMK1FL FW and AtCMK1FL RV, and AtCMK2FL FW and AtCMK2FL RV were used to amplify AtCMK1 and AtCMK2 from total Arabidopsis cDNA.Pfu Taq was used and extention times were 5 minutes. AtCMK2 gives a band of ~ 2500bp in size and AtCMK1 gives a band of ~ 2000bp in size both of which agree with their predicted cDNA lengths from the MIPS database. These PCR products were cloned into pDONR207 by BP gateway recombination. Positive inserts were identified by restriction digests and the sequence of each product was checked by DNA sequencing and checked against the MIPS/NCBI databases. Both cDNA were correct with no mutations.

Figure 5.12: Expression & Purification of 6xHis-tagged Recombinant Full Length AtCMK1 and AtCMK2

Figure 5.13: Full length AtCMK1 and AtCMK2 were expressed as recombinant His-tagged proteins in *E. coli* strain BL21 DE3 Rosetta 2. Following purification by nickel column proteins were run on a SDS PAGE gel (4% stacking & 7.5% resolving). Here protein bands of the approximate predicted size for each kinesin can be seen.

inhibitors to all purification solutions (PMSF; Aprotonin, Pepstatin A, Leupeptin, and TAME, **TABLE 2.1**). For further biochemical assays, the recombinant AtCMK kinesins were transferred into MTSB buffer by ultrafiltration or dialysis. However AtCMK1 proved to be particularly unstable during buffer exchange and possessed low solubility in the MTSB buffer. Therefore sufficient amounts of intact and soluble AtCMK1 could be obtained for microtubule assays. Currently different expression systems and buffers are being used to try and obtain sufficient amounts of active AtCMK1 to study the kinesin's biochemistry and effect on microtubules *in vitro.*

5.8 The effect of AtCMK2 on microtubules *in vitro.*

The effect of AtCMK2 on microtubule polymerization was assessed using a turbidometric assay. AtCMK2 was added to a MAP-free porcine brain tubulin solution (final concentration 20 μm) at the AtCMK2 to tubulin dimer ratio of 1:2. The turbidity of the mixture was monitored at 350nm (**FIGURE 5.13**). AtCMK2 induced a dramatic increase in the turbidity of the polymerizing microtubule mixture compared to the control. Such data could indicate two possibilities: AtCMK2 may increase the total amount of microtubule polymer or it could induce bundling of assembled microtubules. However this is at conflict with the characterized effects of Kinl type kinesins on microtubules. The expected effect on a microtubule solution would be one of a reduction in the total amount of microtubule polymer or the rate of polymerization. Therefore either plant Kinl like kinesins possess unique abilities for this type of kinesin or a third possibility could be evident. The effective amount and rate of microtubule polymeristion could be increased by the production of new microtubule ends from which to polymerise or seeds. The kinesin at these levels, may bind the microtubule, bending the protofilament not only at the end but along the microtubule, disrupting the structure and possibly breaking the microtubule into fragments creating free ends. Such an effect on actin solutions is seen for the actin binding protein, ADF. However in similar experiments with katanin, a protein which severs microtubules this is not seen, but rather a drop in turbidity concomitant with

Figure 5.13: AtCMK2 Microtubule Turbidometric Assay

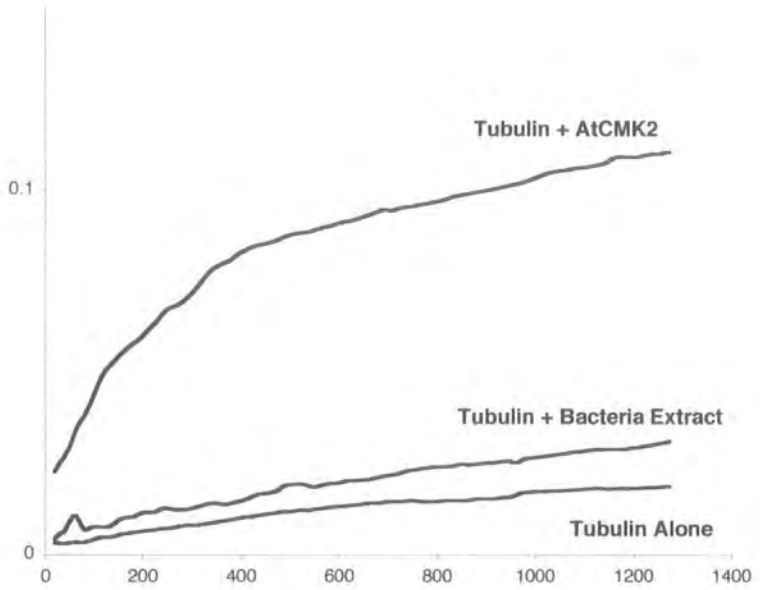

The effect of AtCMK2 on microtubule polymerization was assessed using a turbidometric assay. AtCMK2 was added to a MAP-free porcine brain tubulin solution (final concentration 20 μm) at the AtCMK2 to tubulin dimer ratio of 1:2. The turbidity of the mixture was monitored at 350nm. AtCMK2 induced a dramatic increase in the turbidity of the polymerizing microtubule mixture compared to the control and tubulin alone. Such data could indicate two possibilities: AtCMK2 may increase the total amount of microtubule polymer or it could induce bundling of assembled microtubules (Similar results are seen for AtMAP65). However this is at conflict with the characterized effects of Kinl type kinesins on microtubules. .

breakdown of the microtubule polymer (Stoppin-Mellet, Gailard & Vantard 2002). Further experiments will used fluorescently labeled tubulin and electron microscopy to analyse these microtubule solutions to further to identify if microtubules are longer than the control or bundled.

Therefore it is difficult to reconcile these results with the idea that AtCMK2 is a catastrophic kinesin. Bacterially expressed AtCMK2 may not be active due to incorrect folding or lack essential posttranslational modifications. *Arabidopsis* katanin has also been found to be inactive when expressed in bacteria (Marilyn Vantard personal communication.) Therefore in future experiments AtCMK2 will be expressed in a baculovirus system and the correctness of its folding will be assayed but measuring whether the kinesin has ATPase activity.

5.9 AtCMK Kinesins May Form Dimers.

To identify binding partners of AtCMK kinesins, full length AtCMK1 and 2 were recombined from pDONR207 into yeast two-hybrid vectors, pACT2 (AD) & pAS2 (BD). Both were confirmed by restriction digest and DNA sequencing.

Initially the yeast two-hybrid investigation was designed to establish which proteins interact with AtCMK kinesins. The binding domain AtCMK1/2 vectors were transformed into yeast and the activity of the three reporter gene systems were assessed to check for auto-activation. Unfortunately in all cases the reporter genes were activated. Therefore yeast two-hybrid screens with these full-length constructs were ruled out due to their ability to auto-activate (**SEE APPENDIX F**).

To continue the investigation of the specific question whether AtCMK kinesins dimerise, a new region was selected. The domain at the carboxyl terminus of the plant members of the Kinl family, referred to here as the PCD, contains a coiled coil. The coiled coil motif is a common feature of kinesins and is often the site at

Figure 5.14: PCR of the Plant Conserved Domain (PCD) from AtCMK2 for Yeast two-hybrid.

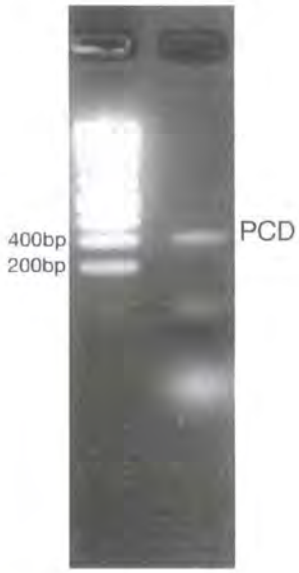

Figure 4.14: PCR of of the Plant Conserved Domain (PCD) from AtCMK2 to be used as the bait in further yeast two-hybrid interaction experiments. Primers AtCMK2PCD FW and AtCMK2FL RV were used to amplify the PCD using pDONR207[AtCMK2 FL] as a template. Pfu Taq was used and extention time was 2 minutes. The PCD gives a band of ~ 400bp in size, which agrees with the predicted size for the fragment (392bp + gateway) based on the cDNA lengths from the MIPS database. The PCD PCR product was cloned into pDONR207 by BP gateway recombination. Positive inserts were identified by restriction digests and the sequence of the PCR product was checked by DNA sequencing and checked against the MIPS/NCBI databases. The PCD was correct with no mutations.

which they dimerise (Thormahlen *et al.* 1998). It was therefore concluded that this region of AtCMK2 should by cloned into the binding vector and used to look for an interaction with the full length AtCMK1/2 activator clones. Gateway primers were designed to the PCD region of AtCMK2 and the sequence amplified from *Arabidopsis* total cDNA (**FIGURE 5.14**). Again this was transferred into pACT2/pAS2 via pDONR207 by means of gateway BP and LR recombinations. These contracts were transformed into the mating lines Y187 and AH109, allowed to mate and diploids selected (See **CHAPTER 2**). These diploids were spotted onto plates lacking adenine or histidine to test for reporter gene activation. In addition the activity of the LacZ reporter gene was also assayed. The yeast two-hybrid assay was conducted for AtCMK2 vs PCD by a slightly different co-transformation method, where both constructs were transformed into a single yeast strain, which removes the requirement for mating. Following the selection for yeast which contained both constructs by selection on –W –L SD media, a colony was grown up and plated out onto –L –W –H –A SD media to test for an interaction.

FIGURE 5.15

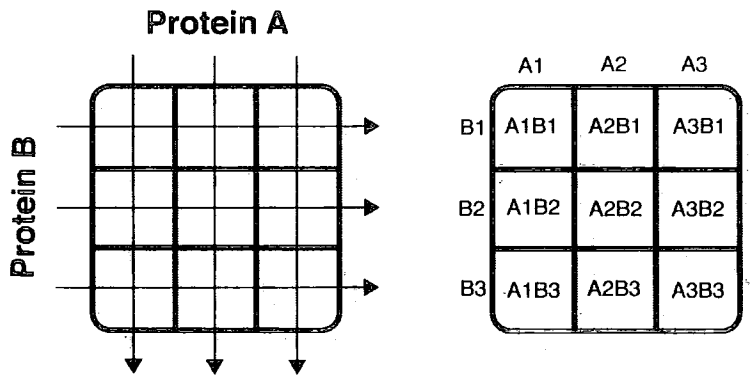

AtCMK2:PCD and AtCMK1:PCD colonies grew on both media and gave a blue precipitate in the LacZ assay (**FIGURE 5.16 & FIGURE 5.17**). However low auto-activation of the histidine reporter gene with PCD alone was observed. No auto-activation was seen for the adenine or lacZ reporter systems.

Figure 5.16: AtCMK Kinesins Can form Dimers

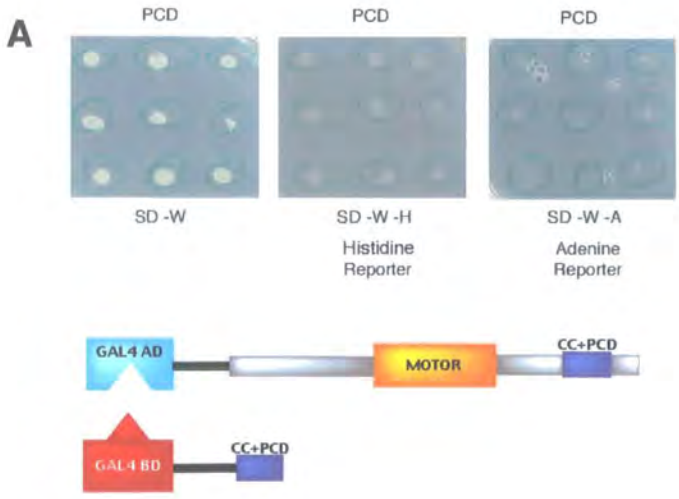

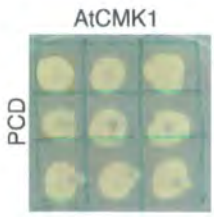

Figure 5.16: (A) Yeast containing the BD-PCD binding domain contruct grown on media lacking adenine or histidine to test for autoactivation. Yeast did not grow on either and no blue precipitate was formed in the LacZ assay. Therefore BD-PSD does not autoactivate and may be used in yeast two-hybrid experiments

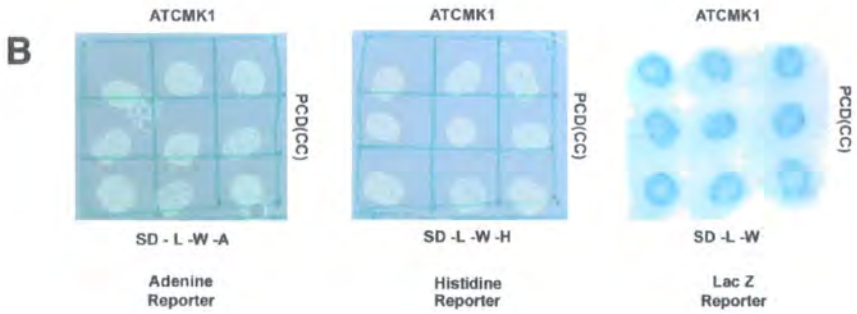

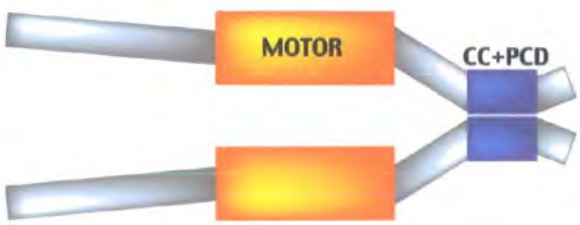

(B) Following the selection for diploid yeast by streaking out onto -L -W media these cells were then spotted onto media lacking adenine or histidine. Cells grew on both media and gave a blue precipitate rapidly in the LacZ assay suggesting that the PCD domain can interact with the full length AtCMK1

Figure 5.17: AtCMK2 interacts with the Plant Conserved Domain

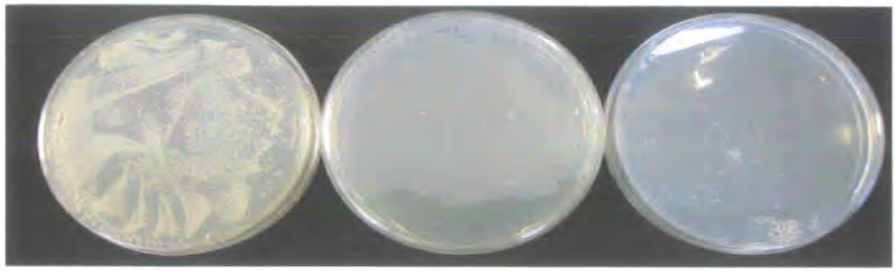

-W -L -W -L

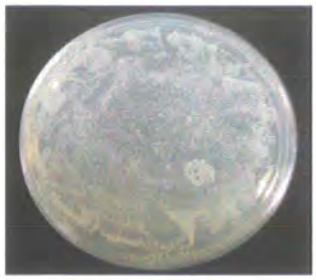

-W -L -H -A

Figure 5.17: PCD-BD and AtCMK2-AD were co-transformed into AH109 and plated out onto -W, -L and -L-W to assess the quality of transformation. The PCD-BD clone appeared to transform more efficiently than the AtCMK2-AD clone. However co-transformants were obtained, <10. One of these colonies was grown up and plated out onto -W-L-H-A media to test for activation of the adenine and histidine reporter genes. Colonies grew suggesting that, like AtCMK1, AtCMK2 can bind the PCD and as such possibly form dimers.

Therefore these data suggest that AtCMK1 and AtCMK2 can form homodimers as the PCD region is almost identical. As the PCD region used was from AtCMK2 this leads to the possibility of the formation of heterodimers, which is the case for the yeast Kinl kinesin KLP5 and KLP6 (Garcia *et al.* 2001). It is unlikely that these kinesins form heterodimers when it is considered that their subcellular localizations are very different and their sites of expression within the tissues of the plant are also different. Secondly only the PCD region was used here, and *in vivo* the geometry of the full protein could hinder the formation of a dimer between AtCMK1 and AtCMK2.

5.10 AtCMK1 and AtCMK2 May Not Physically Interact With MOR1/GEM1.

As described in Chapter 4, MOR1/GEM1 CT and NT fragments were amplified and recombined into yeast two-hybrid vectors via pDONR207. To test whether MOR1/GEM1 and AtCMK1 or AtCMK2 can physically interact with each other MOR1/GEM1 NT and CT were used as bait (MOR1/GEM1 NT or CT-BD) and tested against AtCMK1 or AtCMK2 activator clones (AtCMK1-AD & AtCMK2-AD) (**FIGURE 5.18**). The procedure was as described for the above dimerisation assays. Contructs were transformed into the relivant mating starins and allowed to mate in several combinations, MOR1/GEM CT vs AtCMK1, MOR1/GEM1 CT vs AtCMK2, MOR1/GEM1 NT vs AtCMK1 and MOR1/GEM1 vs AtCMK2. None of the interactions tested gave activation of any of the reporter gene systems, with no growth on media lacking histidine or adenine and a negative result in the LacZ assay (**FIGURE 5.19 & FIGURE 5.20**). Therefore these data suggest that AtCMK1 and AtCMK2 may not interact with the C-terminal region or N-terminal region of MOR1/GEM1 used. However an interaction could require the middle region of MOR1/GEM1, which was not included in the assay, full length MOR1/GEM1 or a third component such as tubulin. In addition, as described in chapter 4 the negative results obtained in interaction experiments using MOR1/GEM1 fusions may be

Figure 5.18: AtCMK vs MOR1/GEM1 Yeast Two-Hybrid Constructs

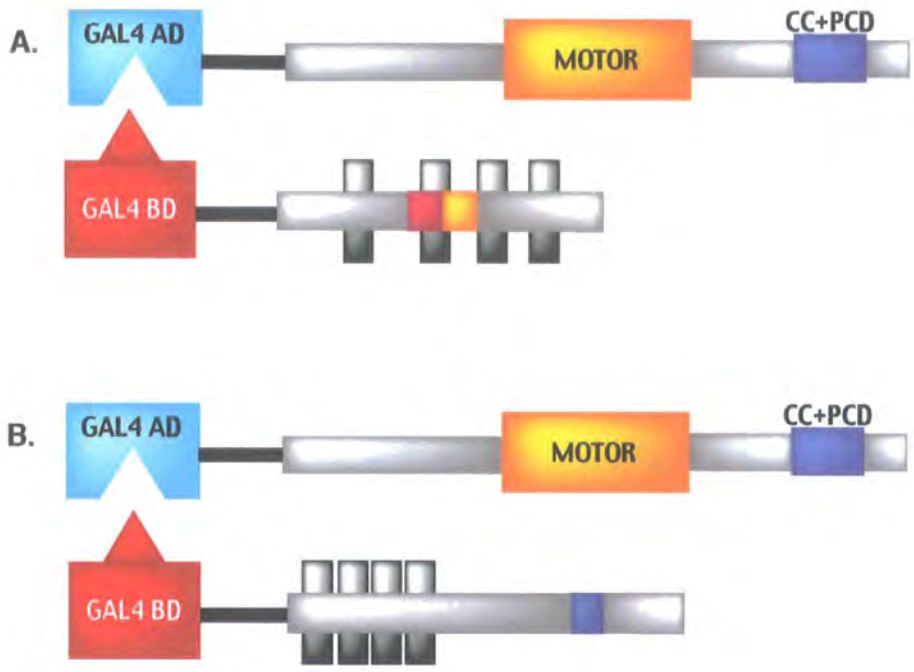

Figure 5.18: Yeast two-hybrid contructs used to test for a direct physical interaction between MOR1/GEM1 and AtCMK kinesins. Because of the ability of AtCMK kinesins to cause autoactivation in yeast two-hybrid reporter gene assays, these full lenth contructs were only used as activator clones, shown here as a fusion protein with the GAL4 AD or activation domain. As such interactions could only be tested in one orientation. The bait in these assays was one of two CT and NT fragments of MOR1/GEM1 shown here as fusions proteins with the GAL4 BD or binding domain. (A) A N-terminal fragment which contained the HEAT repeat in which a point mutation occurs in the mor1 mutant and (B) a C-terminal fragment which is identical to that used in the microtubule binding assay as described earlier and contains those regions missing in the *gem1* mutants.

Figure 5.19: AtCMK1 vs MOR1 CT and NT Y2H

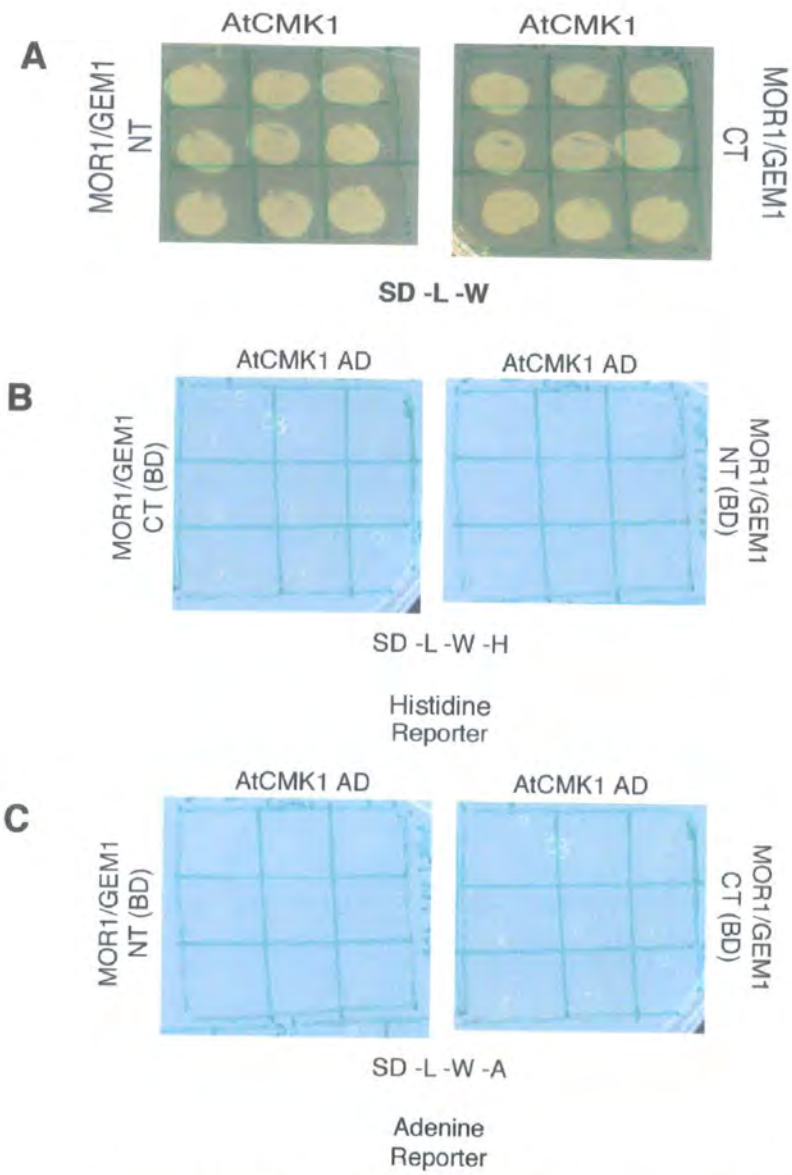

Figure 5.19: AtCMK1 vs MOR1/GEM1 CT and NT Yeast two-hybrid assay. MOR1/GEM1 BD fusion construct had previously been checked for autoactivation see Chapter 4. Yeast cells were spotted onto each other and allowed to mate. These were then streaked out onto -L -W media and diploids selected. These diploid cells were then spotted on to -L -W media (A) media also lacking histidine (B) or adenine (C) to test for activation.Those cells on -L -W were lifted on filterpaper and assayed for LacZ activity. Cells did not grow on -H (B) or -A (C) and the LacZ assay gave negative results. Therefore AtCMK1 did not show an interaction with either the N-terminal or C-terminal fragments of MOR1/GEM1.

Figure 5.20: AtCMK2 Does not interact with MOR1/GEM1 NT or CT fragments

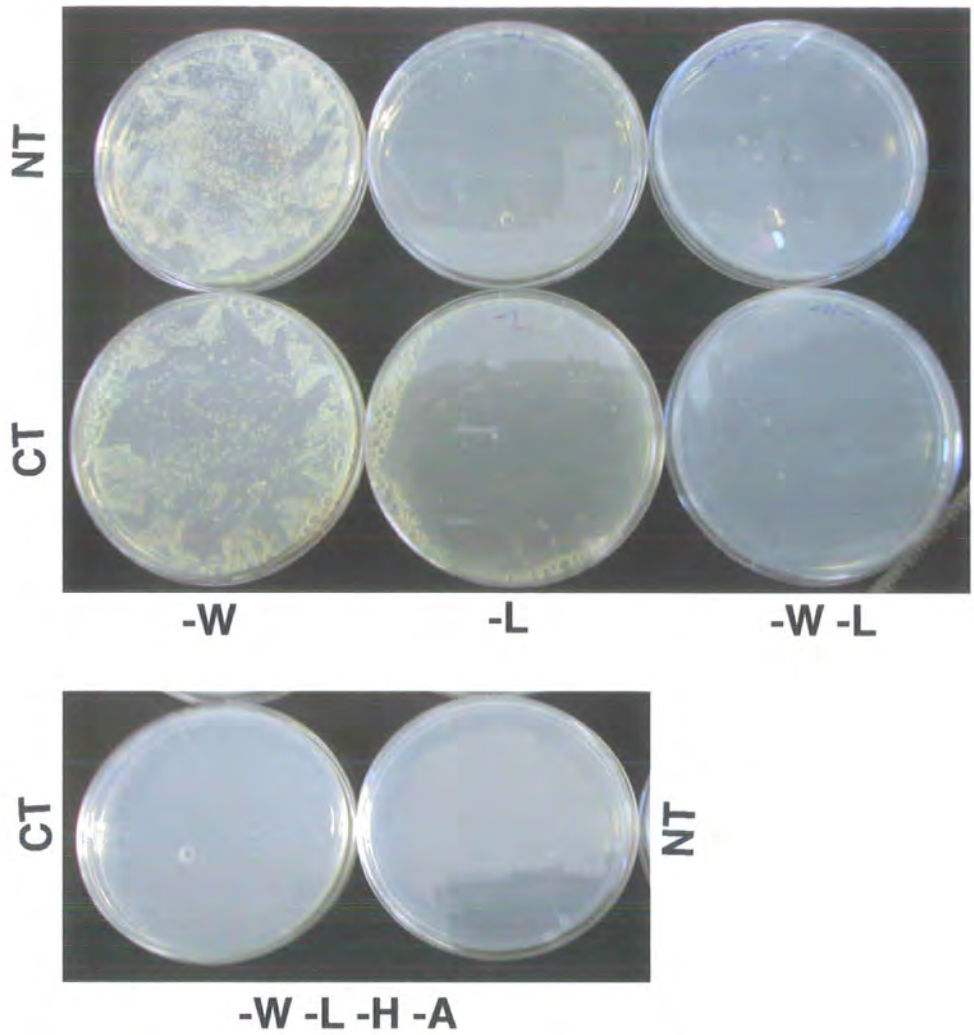

Figure 5.20: MOR1/GEM1-BD and AtCMK2-AD were co-transformed into AH109 and plated out onto -W, -L and -L-W to assess the quality of transformation. The MOR1/GEM1-BD clones appeared to tranform more efficiently than the AtCMK2-AD clone. However co-transformants were obtained for each, <10. One of these colonies was grown up and plated out onto -W-L-H-A media to test for activation of the adenine and histidine reporter genes. However no colonies grew suggesting as for AtCMK1 no interaction occurs.

because the proteins are not being expressed by the yeast. Here there may be selection for those yeast cells, which do not express the MOR1/GEM1 fusion proteins because of the proteins possibly detrimental effects on the yeast cell. For such negative results the expression of the fusion protein should be checked with the use of a western blot for gal4 or the protein of interest.

5.11 Analysis and comparison of AtCMK1 & 2 Expression Patterns.

The expression programme of AtCMK1 and AtCMK2 in various organs and tissues was determined by transforming *Arabidopsis* with an AtCMK1 or AtCMK2 promoter:GUS reporter gene transcriptional fusion construct and ten transformed lines were analysed.

The AtCMK promoters were identified and 2kb of the genomic sequence immediately prior to the ATG was amplified from *Arabidopsis* genomic DNA with gateway primers, PROCMK1 FW & RV AND PROCMK2 FW & RV (**FIGURE 5.21**). The promoters were cloned into the binary GUS expression vector, pBI101G, using BP and LR gateway recombinations via pDONR207. Correct recombinants were confirmed by restriction digest and DNA sequencing. PBI101G[AtCMK1/2 Pro] were transformed into *agrobacterium* strain C58C3 and used to transfect wild *Arabidopsis* ecotype Columbia by the dipping method. Here the flowers and bud of several *Arabidopsis* plants are dipped into a sucrose solution into which C58C3 *agrobaterium* containing the plasmid of interest have be resuspended. The plants are allowed to recover and the process is repeated one week later. The recombinant seedlings were selected for kanamycin resistance and tissues were stained for GUS activity as described in **CHAPTER 2**. Seedlings are placed within a buffered solution containing X-gluc and a vacuum is applied to allow the solution to penetrate the tissue. The seedlings, still within the solution, are incubated at 37°C for several hours. If the promoter is active in a certain tissue then this will initiate

Figure 5.21: PCR of AtCMK Kinesin Promoters

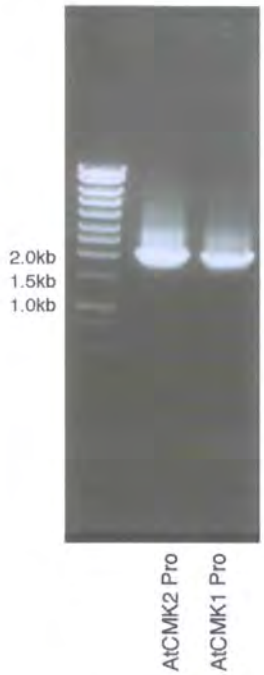

Figure 5.21: PCR of AtCMK kinesin promoters. A 2kb region immediately prior to the ATG of each gene was amplified from Arabidopsis genomic DNA using Primers AtCMK1 Pro FW & RV and AtCMK2 Pro FW & RV. Pfu Taq was used and extention times were 4 minutes. Promoters givs a band of ~ 2000bp in size as expected. These PCR products were cloned by BP gateway recombination into pDONR207 and positive inserts were identified by restriction digests and the sequence of each product was checked by DNA sequencing and checked against the MIPS/NCBI databases. Both promoters were correct with no mutations.

the transcription and translation of GUS, β-Glucuronidase. GUS substrates such as X-Gluc (5-bromo-4-chloro-3-indolyl-beta-D-glucuronic acid) are β-glucuronic acid substrates in which a sugar D-glucopyranoduronic acid is attached by a glycosidic linkage to hydroxyl group of a detectable molecule. The GUS enzyme cleaves this linkage with high efficiency releasing the detectable molecule, which in the case of X-Gluc is blue. In the following photos a blue pigment identifies those cells where the AtCMK promoter is active.

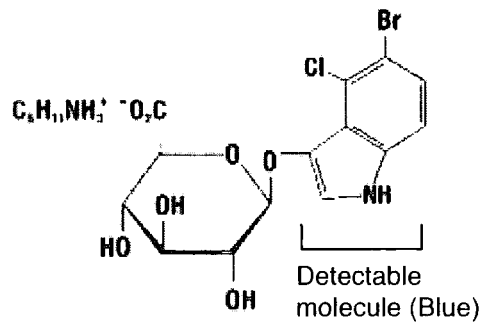

AtCMK2 GUS activity was detected in all organs and tissues and this pattern was similar in all ten lines (**FIGURE 5.22**). AtCMK2 is highly transcribed in all tissues examined, including flowers (pollen), siliques, stems, leaves and roots. The blue precipitate was particularly strong in roots and was visible quickly following vacuum infiltration, however this may be as a result of the ease of penetration in this tissue. This suggests that AtCMK2 is a house keeping protein which is required in all cells, rather than in particular tissues at particular times. This kind of expression pattern is similar to that for MOR1/GEM1 as inferred from organ specific immunoblotting (Chapter 4, Section 4.3) and RT-PCR analysis (Twell *et al.* 2002 & **APPENDIX E**).

Interestingly the expression pattern for AtCMK1 is very different from that of AtCMK2. As oppose to universal expression like AtCMK2, expression of AtCMK1 is only seen in several specific locations within those tissues examined (**FIGURE 5.23**). One is the funiculus, a structure which supports and connects the ovule to the silique, containing vascular tissue to supply the developing ovule/embryo with nutrients. Secondly, and most interestingly, strong GUS expression was seen at

FIGURE 5.22: AtCMK2 Expression Pattern

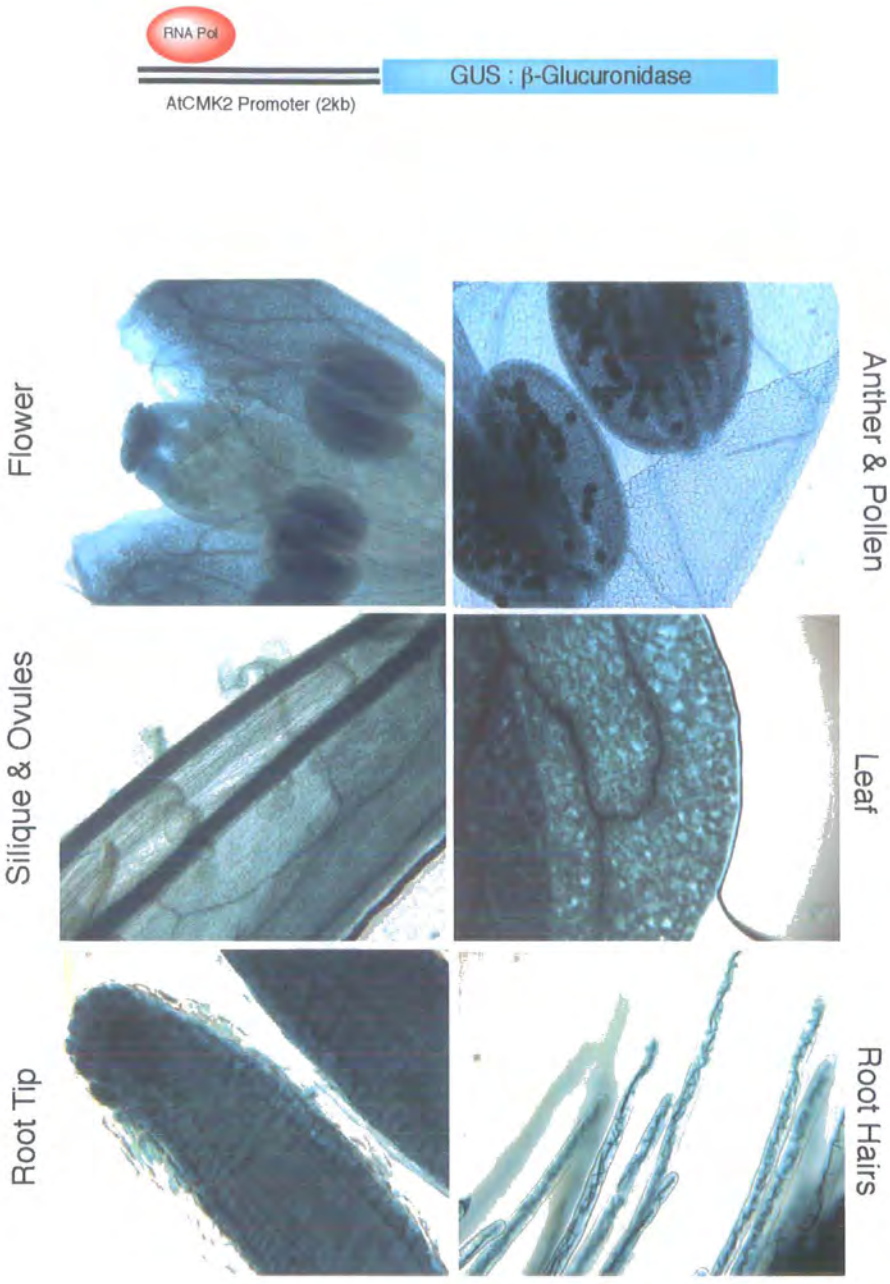

Figure 5.22: The expression programme of AtCMK2 in various organs and tissues was determined by transforming Arabidopsis with an AtCMK2 promoter:GUS reporter gene transcriptional fusion construct and ten transformed lines were analysed. The AtCMK2 promoter was identified and 2kb of the genomic sequence immediately prior to the ATG was amplified from *Arabidopsis* genomic DNA. AtCMK2 is expressed highly in all tissues and organs examined. This suggests that AtCMK2 is a house keeping gene required for regulation of microtubule dynamics in all cells. Similar expression is seen for MOR1/GEM1 in tissue specific immunostaining and RT-PCR.

FIGURE 5.23: AtCMK1 Expression Pattern

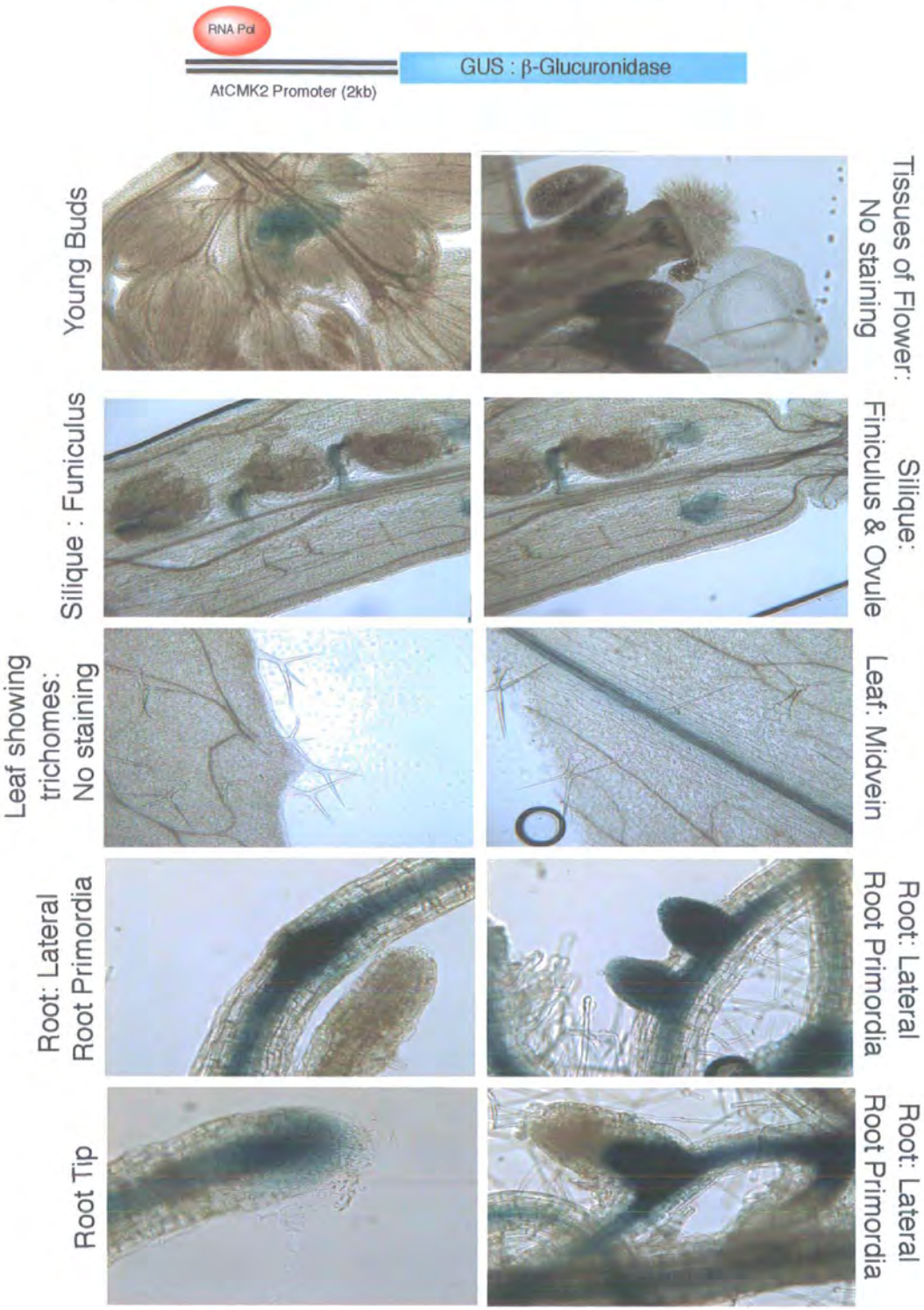

Figure 5.23: The expression programme of AtCMK1 in various organs and tissues was determined by transforming Arabidopsis with an AtCMK1 promoter:GUS reporter gene transcriptional fusion construct and ten transformed lines were analysed. The AtCMK1 promoter was identified and 2kb of the genomic sequence immediately prior to the ATG was amplified from Arabidopsis genomic DNA. Unlike AtCMK2, AtCMK1 is only expressed in specific locations including the funiculus and is particularly highly expressed at the lateral root primordium, even before the new lateral root emerges and remains at this point as the root extends. Many of these locations have the presence of vasculature in common.

the point from which the lateral root develops and emerges, a region known as the lateral root primordium.

5.12 Discussion/Summary.

Kinl kinesins were first identified as a major microtubule destabalising factor in *xenopus* egg extracts and as such are referred to as catastrophic kinesins (Walczak *et al.* 1996, Desai *et al.* 1999). Further studies revealed that the Kinl subfamily of kinesins, is present in many diverse organisms including: parasites, insects, frogs, humans and yeast and one common feature appears to be a centrally located motor (Walczak et al. 1996, Wordeman & Mitchinson 1995, Moores et al. 2002, Garcia et al. 2002) Moreover in *Xenopus* the catastrophic activity of such kinesins is balanced by the opposing stabilization provided by XMAP215. Following the identification of the *Arabidopsis* XMAP215 homologue, MOR1/GEM1, this posed the question as to whether the *Arabidopsis* genome contained Kinl-like kinesins, a subfamily of kinesin previously uncharacterized in plants.

Two putative Kinl kinesins were identified in the *Arabidopsis* genome, AtCMK1 (Atg316060) & AtCMK2 (At3g16630), both have central motors, which show identity to those of other Kinl kinesins such as MCAK and XKCM1, and when these two proteins are added to a phylogenetic tree of all kinesin families they fall into the Kinl clade.

To study the localization of these two kinesins within the cell, fragments of each were expressed as recombinant proteins in *E. coli* and used to raise anti-AtCMK1 and anti-AtCMK2 polyclonal antibodies in mice. AtCMK2 is associated with all of the microtubule arrays except the interphase cortical array, however association here can be seen when AtCMK2 is expressed as a GFP fusion protein within plant cells. AtCMK2 associates with the PPB. The strongest association of AtCMK2 is to

the metaphase spindle, a localization consistent with other Kinl kinesins. Kinl kinesins are essential for spindle assembly and XKCM1 depleted *Xenopus* egg extracts, rather than forming bipolar spindles, form large asters with centrally located chromatin from which long microtubules emanate (Walczak *et al.* 1996). In addition Kinl kinesins are located at the kinetochore where they required for the correct capture of this structure by kinetochore microtubules (Garcia *et al.* 2002). AtCMK2 is also associated with the phragmoplast and although other Kinl kinesin associate with the cytokinetic midbody the phragmoplast is a unique structure. In plants, during cytokinesis, vesicles fuse to form the new membrane compartment, the cell plate, which then expands laterally to the cell margin (Strompen *et al.* 2002, Simarro *et al.* 2004). The targeting of vesicles is co-ordinated by the reorganisation of the phragmoplast, from a solid cylinder to an expanding ring shaped structure (Grainger & Cyr 2000, Strompen *et al.* 2002). Such expansion laterally is achieved by the depolymerisation of microtubules in the centre of the phragmoplast, giving way to the cell plate and the polymerisation of microtubules along the edge of the phragmoplast (Strompen *et al.* 2002, Yasuhara *et al.* 1993, Lauber *et al.* 1997). Therefore at the phragmoplast a Kinl kinesin such as AtCMK2 could depolymerise the microtubules in the centre of the phragmoplast, required for lateral expansion. As described above further to this immunolocalisation AtCMK2 was seen to associate with interphase cortical microtubules when expressed as a GFP fusion protein in onion epidermal cells. The kinl kinesins, XKCM1 and MCAK are found to be a pool within the nucleus during interphase which is then redistributed upon mitosis to the spindle, however no nuclear localization for AtCMK2 has been observed.

Yeast two-hybrid experiments demonstrate that both AtCMK1 and AtCMK2 can interact with a domain in their C-terminal regions and as such are likely to form homodimers. The domain responsible is a region, which is only conserved between the plant Kinl kinesin homologues, referred to in this thesis as the PCD, Plant Conserved Domain. The PCD contains a coiled coil, a motif commonly implicated

in dimerisation. Here proteins are joined together by the ability of two coils to twist around each other in an attempt to hide their highly hydrophobic faces (Thormahlen *et al.* 1998). Further yeast two-hybrid assays have indicated that AtCMK1 and AtCMK2 may not physically interact with MOR1/GEM1 via the chosen N-terminal or C-terminal sections, although expression of the fusion protein needs to be assessed. However if these data are correct it could suggest that a physical interaction between a KinI kinesin and the N-terminal HEAT repeats of MOR1/GEM1 as proposed in model 1 (**SEE CHAPTER 1**) may not be the case. The second model, suggests that MOR1/GEM1 and a KinI kinesin compete for a microtubule binding site, however, the association of MOR1/GEM1 is not lost in the *mor1* mutant (Wasteneys personal communication). These considerations lead to a third model in which MOR1/GEM1 and a KinI kinesin are genetic rather than physical interactors, where their effects on microtubule dynamics oppose each other.

Data concerning the intergrity of microtubules within cells expressing GFP-AtCMK2, suggests that the *Arabidopsis* KinI-like kinesin with catastrophic activity, which may oppose MOR1/GEM1 could be AtCMK2. As described previously GFP-AtCMK2 is seen as either dots or aggregates or small filaments, randomly orientated within the cytoplasm. If these cells are also stained for tubulin similar structures are seen. There is a gradation ranging from short disorganized microtubules, through small microtubular fragments or oligomers to dots, which could be aggregates of tubulin and AtCMK2. Similar results have been seen upon over-expression of XKCM1-GFP, a well characterized catastrophic kinesin (Kline-Smith & Walczak 2002). Recent studies have identified differences in the three-dimensional structure of the motor core of pKinI, when compared to other kinesins and those residues uniquely conserved between KinI kinesins, which are required for it catastrophic activity (Shipley *et al.* 2004). All of these residues are conserved within AtCMK2, consistent with the kinesins *in vivo* microtubule destabilising activity.

Finally, to further compare the two Kinl kinesins in *Arabidopsis* the expression programmes of these two genes were analysed. The expression programme of AtCMK1 and AtCMK2 in various organs and tissues was determined by transforming *Arabidopsis* with an AtCMK1 or AtCMK2 promoter:GUS reporter gene transcriptional fusion construct and ten transformed lines were analysed for each. AtCMK2 is expressed in all tissues and organs examined, suggesting that like MOR1/GEM1, AtCMK2 is a house keeping protein required to control the dynamicity of microtubules in all cells. AtCMK1 however, is expressed in a very different pattern. AtCMK1 is expressed in specific tissues and organs unlike AtCMK2. These locations include the embryo, cell files associated with the vasculature, the funiculus and most strongly the lateral root primordium, the site from which the lateral root emerges.

The level of the AtCMK2 transcript does not vary significantly through the cell cycle and as such it is likely that the association and activity of this kinesin is regulated by modifications including phosphorylation. A good candidate for such a kinase would be an AuroraB kinase, which has been shown to phosphorylate XKCM1 (Lan *et al.* 2004) and homologues of which have been identified in *Arabidopsis*. The Aurora B complex associates with centromeres and the midline of the spindle during mitosis and has been implicated in the resolution of erroneous connections of kinetochores to spindle microtubule. Studies have suggested that AuroraB controls these connections by phosphorylation of XKCM1 which is required for its localization to the centromere where it depolymerises these incorrectly orientated kinetochore microtubules (Lan *et al.* 2004). A second possible interactor and regulator of AtCMK kinesins could be an *Arabidopsis* ICIS. ICIS stimulates MCAK activity and depletion of ICIS results in excessive microtubule growth and inhibited spindle formation The ICIS protein also appears to be part of the complex of proteins associated with the Aurora B complex at the kinetochore/centromere. (ICIS: (AURORA B : INCENP : SURVIVIN) : MCAK).

CHAPTER 6

Discussion

6.1 MOR1/GEM1 Through the Cell Cycle

6.1.1 *MOR1/GEM1 at the cell cortex and the interphase cortical array.*

The *mor1* mutants identified that the MOR1/GEM1 protein plays a role at the interphase cortical array. Close examination of *mor1* mutant plants expressing tubulin-GFP show that on shifting to the restrictive temperature, cortical microtubules become disorganised and shortened (Whittington *et al.* 2001). Consistent with this, the results presented here, show that the MOR1/GEM1 protein locates to the cortical microtubules of the interphase cortical array. However, it is important to note that the *mor1* mutants did not exhibit mitotic or cytokinetic phenotypes and no spindle or phragmoplast phenotypes were observed.

It is likely that MOR1/GEM1 has similar properties to that of its homologues, such as XMAP215, which can increase microtubule growth and stability by 10 fold and following immunodepletion from *Xenopus* egg extracts, microtubule catastrophe is increased and microtubule length is reduced (Tournebize *et al.* 2000). This agrees with the short disorganised microtubules observed in *mor1,* suggesting that MOR1/GEM1 is also capable of promoting microtubule growth and stability.

But how exactly does the point mutation in *mor1* abolish this effect? There are two possible models based on the role of the amino terminal HEAT repeat in which the point mutations are. As described previously, HEAT repeats are motifs responsible for protein:protein interactions (Andrade 1995, Groves *et al.* 1999). At the permissive temperature, a Kinl-like kinesin protein (possibly AtCMK1 or AtCMK2) may bind to MOR1 at the N-terminal HEAT repeat. At the restrictive temperature, a conformational change in the protein caused by the *mor1* mutations releases the

kinesin, which is now capable of depolymerising the microtubules. Alternatively, MOR1 decorates the microtubules at the permissive temperature, stabilising the long microtubules in the cortex. A shift to the restrictive temperature causes a loss of the N-terminus catastrophe-suppressing activity (as in XMAP215) or the microtubule- binding capability (as in TOGp) of MOR1, enabling a Kinl-like kinesin to depolymerise the long cortical microtubules (Hussey & Hawkins 2001). However, our results now suggest that of the two models, the latter is more feasible. Yeast two-hybrid experiments between the two putative *Arabidopsis* Kinl kinesins AtCMK1 and AtCMK2, and the C- and N-terminal fragments or MOR1/GEM1 show no interaction. However, there are possibilities that, *in vivo,* the two proteins do interact but the yeast two-hybrid experiments failed to identify this. The kinesins may interact with the middle of MOR1/GEM1, which was not used in the interaction experiments. Secondly, the kinesin may require a full length MOR1/GEM1 protein to interact with, possibly due to three-dimensional structural considerations. Finally a third factor may be required to complex these two MAPs together.

mor1 mutant plants at the restrictive temperature also exhibit root epidermal cells which show left-handed twisting and radial swelling. It is speculated that these characteristics were as a result of incorrect cellulose microfibril deposition or organisation. This focuses on the cellulose synthase model where cortical microtubules are thought to constrain the movement of cellulose synthase complexes and thus align newly deposited cellulose microfibrils (Giddings & Staehelin 1991). However, studies with the *mor1* mutant suggest that in growth anisotropy such a relationship does not exist; rather cortical microtubules regulate growth anisotropy by a mechanism independent of cellulose microfibril alignment. Although the cortical microtubule network is disorganised in *mor1* root tips, cellulose microfibrils remain transverse to the long axis of the root, with no random network or partial disorder (Sugimoto *et al.* 2003). Unaffected cellulose levels in *mor1* suggest that synthesis and parallel microfibril deposition continues at the

restrictive temperature. Double mutants of *mor1-1* and *rsw1-1*, a cellulose synthase mutant with a root tip swelling phenotype, exhibit an additive phenotype with extensive swelling (Sugimoto *et al.* 2003). Therefore, the mechanism by which *mor1-1* produces root tip swelling, through microtubule disorganisation, is independent of cellulose microfibril orientation/structure and cellulose synthesis.

An appealing alternative to the cellulose synthase model is a geometric one, as proposed by Emons and Mulder (Emons & Mulder 1998). Here complex order microfibril arrangement can be generated by simple geometric considerations and that these can be mathematically modeled. This could explain why ordered transverse microfibril arrangements are still apparent in epidermal cells at the restrictive temperature, which lack order cortical microtubules. However, a pre-requisite of this model is the space limiting condition. When, experimentally, the space between membrane and wall is enlarged by plasmolysis, wall texture deposition becomes irregular (Reis *et al.* 1985).

Following disruption of the cortical array at the restrictive temperature, *mor1* roots begin to show right handed twisting (Whittington *et al.* 2001). So why does this occur and particularly why right and not left? As described in chapter 1, the *lefty* mutation is the substitution of a single amino acid in plant tubulin and *lefty*, plants show left hand twisting of various organs including roots (Furutani *et al.* 2000, Thitamadee *et al.* 2002, Hashimoto 2002). However the *spr1-1* mutant shows right handed twisting like *mor1*. Here the cortical microtubules, rather than being shortened or disorganised, showed a left-handed helical arrangement instead of the normal transverse arrangement. It is important to note that *lefty* has left handed organ twisting with right handed helical microtubule arrangement and therefore it appears that the direction of microtubule deflection results in organ twisting of the opposite orientation. Although examination of a second *SPIRAL* allele, *sku6* or *spr1-6*, revealed that although there is the right handed twisting of organs, microtubules are transverse or the pitch is slightly left or even right handed, leading

the authors to speculate that the pitch of cortical microtubules in epidermal cells does not guide epidermal cell file twisting (Sedbrook *et al.* 2004). Therefore it is suggested that SPR1 affects microtubule dynamic instability by promoting polymerisation and/or discourage pausing and catastrophe events. In addition the authors suggested that considering the predicted rod-like structure of SPR1, could act to stabilise microtubule polymers by cross-linking proteins in the plus end complex. Alternatively, SPR1 may recruit growth machinery to the plus end complex, stabilise or guide microtubules by linking them to the cell cortex (Sedbrook *et al.* 2004).

It is tempting to speculate that as *mor1* and *spr1* both create right handed twisting of organs, perhaps there could be a common mechanism or link here. SPR1 is located to the plus end of the microtubules, a localisation suggested for MOR1/GEM1 in our spindle staining and shown for the MOR1/GEM1 homologue, Alp14. However, no specific concentration of MOR1/GEM1 at plus ends could be observed in our experiments during interphase, although it is present at these sites. Furthermore, SPR1 has a domain, which is repeated at the N and C terminus of the protein and show some similarity to the microtubule binding repeats in classical MAPs such as Tau. However, these domains, when expressed as recombinant proteins do not bind microtubules (Sedbrook, personal communication). As GFP-SPR1 clearly locates to microtubules *in vivo,* it is possible that rather than a direct interaction, a second factor is required to locate SPR1 to the microtubule. Could MOR1 be this factor? It has been demonstrated that MOR1 homologues are required for associating proteins to microtubules in other organisms; examples include the requirement of XMAP215/TOGp for cyclinB1 and Alp14/TOGp for TACC. Maybe the HEAT repeats in MOR1 and the N and C terminal domains of SPR1 (one of which is disrupted in *spr1-6*) are required for this interaction.

6.1.2 *MOR1/GEM1 in Preprophase Band*

There are no structures in animal or yeast cells which are comparable to the preprophase band and therefore less can be gained from considering XMAP215 and TOGp. It is likely that MOR1/GEM1 may possess a plant specific role at this location, possibly forming interactions with proteins, which are unique to plants. Could it be involved in the creation or maintenance of the invisible guide, established by the PPB, which is then followed by the phragmoplast? The use of GFP linked MOR1/GEM1 could reveal whether MOR1/GEM1 remains at the division plane following the disassembly of the PPB. Alternatively, a role for MOR1/GEM1 may simply be to promote microtubule growth and stabilisation at the PPB, as microtubules disassembled from the cortical array, repolymerise to form the PPB. The *Arabidopsis ton2* mutants have disorganised interphase microtubules and lack the preprophase band (Mayer *et al.* 1991, Torres-Ruiz & Jurgens 1994, Traas *et al.* 1995). The *TON2* gene is highly conserved in higher plants and encodes a protein whose C-terminal region is similar to B" regulatory subunits of type 2A protein phosphatases, PP2A (Camilleri *et al.* 2002). TON2 may be involved in the formation of a PP2A complex, which presumably controls the phosphorylation status of proteins important for the structure of the plant cortical cytoskeleton. It is tempting to speculate that proteins such as MOR1/GEM1 and MAP65 could be candidate targets for the TON2-PP2A phosphatase.

6.1.3 *MOR1/GEM1 in the spindle*

MOR1/GEM1 localises to the spindle and spindle microtubules. Other members of the XMAP215 family also locate to the spindle and their mutants result in errors in spindle formation. Not only does MOR1/GEM1 associate with the spindle, it is concentrated at the plus end of microtubules next to the DAPI stained chromosomes. This region contains the kinetochore and hence MOR1/GEM1 may be located and function at the kinetochore during mitosis. This is consistent with observations for the *Schizosaccharomyces pombe* MOR1-like protein Alp14.

Imaging of Alp14-GFP shows that during mitosis, Alp14 is associated with peripheral region of the kinetochore (Garcia *et al.* 2001). Furthermore, this has been supported by ChIP (chromatin immunoprecipitation) and co-localisation with the kinetochore marker Mis6 (Garcia *et al.* 2001). From studies with the *alp14* mutant it is believed that Alp14 is required for the interaction between the kinetochore and chromosome microtubules. Dense short spindles seen at early mitosis in *alp14* mutants could be due to the failure to capture the kinetochore. Mad2 localises to these dots and in addition to its structural role, Alp14 is believed to a component of the Mad2 mediated spindle checkpoint at the kinetochore (Garcia *et al.* 2001). The *Saccharomyces cerevisiae* Stu2p has also been implicated in kinetochore function where it may be required for tension (He *et al.* 2001, Pearson *et al.* 2002), however kinetochore localisation has not been reported for any other members of the XMAP215 family.

6.1.4 *MOR1/GEM1 at the phragmoplast and cytokinesis*

There is some evidence that members of the XMAP215 family may have a role in cytokinesis. Cells expressing GFP-DdCP224 show defects in cytokinesis (Graf *et al.* 2000) and TOGp has been shown to be present in the midbody (Charrasse *et al.* 1998), an apparatus in which microtubules are arranged similarly to those in the phragmoplast (Euteneuer and McIntosh 1980), although the phragmoplast is specific to plant cells.

The MOR1/GEM1 protein localises to the cytokinetic phragmoplast and particularly to the midzone. Clues as to its role here can be gained from the *gem1* or *Gemini pollen1* mutant which disrupts microspore polarity, division symmetry and pollen cell fate. In the anther of the flower, meiocytes undergo meiosis to form the haploid microspores. Each microspore nucleus divides unequally at pollen mitosis 1 to form a larger vegetative and smaller generative cell. Subsequently, only the generative cell divides at pollen mitosis II to form the two sperm cells of the mature tricellular pollen grain (Twell *et al.* 1998). The *gem1* mutation has been identified

as a mutation affecting cytokinesis and the cell division pattern at pollen mitosis I (Park *et al.* 1998, Park & Twell 2001). *gem1* plants produce a significant proportion of microspores that either fail to establish a cell plate at pollen mitosis I or produce partial or irregular branching cell walls altering division symmetry. Internal cell walls are frequently incomplete and show highly irregular profiles in *gem1* (Park *et al.* 1998, Park & Twell 2001). Nuclear divisions at pollen mitosis I are always complete in mutant *gem1* cells, producing binucleate or bicellular pollen. These data have strongly suggested a direct role for GEM1 in cytokinesis. Moreover, *gem1* mutants are homozygous lethal and can only be maintained as heterozygotes, demonstrating that *GEM1* is an essential gene. Complementation of the *gem1-1* phenotype with the wild type MOR1/GEM1 sequence further suggests that *gem1-1* also acts recessively in pollen.

The 14 kb genomic region containing MOR1 was sequenced from *gem1* heterozygotes and found to contain two point mutations in the coding sequence. The first in exon 22 (T to G) resulted in a change from serine at position 745 to alanine and the second in the splice acceptor (AG to AA) in intron 38 (Twell *et al.* 2002). The Ser745 is not conserved in the MAP215 family. Sequencing of transcripts amplified from *gem1-1* heterozygotes identified the wild-type and a mis-spliced transcript in which the next downstream AG was used to create a transcript encoding the N-terminal 1326 aa of MOR1/GEM1 with a 6 amino acid C-terminal extension. *gem1-2* harboured a T-DNA insertion into exon12 and was confirmed to be expressed as a fusion transcript. The putative truncated protein is predicted to contain the N-terminal MOR1/GEM1 411 amino acids with a 48 amino acid C-terminal extension derived from T-DNA sequences (Twell *et al.* 2002).

The region of GEM1 missing in both *gem1-1* and *gem1-2* is the C-terminus that includes a putative microtubule-binding site at position 1786. Mutation of this site in XMAP215 causes reduced microtubule binding, but does not abolish microtubule binding indicating that this is not the only microtubule binding site. A recombinant

C-terminal fragment of MOR1/GEM1 (aa 1123-1978) was used in a microtubule-binding co-sedimentation assay. In this assay, the C-terminal fragment pellets with microtubules, indicating a binding interaction. These data suggest that the loss of function in the *gem1* mutants is at least in part due to the lack of this microtubule binding domain. Other domains known to be missing from the *gem1* mutants include five potential kinase sites and two and eight HEAT repeats in *gem1-1* and *gem1-2* respectively. Lack of potential regulation by reversible phosphorylation or protein-protein interactions through the HEAT repeats may also contribute to the *gem1* phenotype.

The fact that the *gem1* mutants are homozygous lethal strongly suggests that sporophytic cell divisions may also be affected in a similar way. However, MOR1/GEM1 localises to all microtubule arrays so one cannot rule out the possibility that other MOR1/GEM1 mediated processes are also severely disrupted in sporophytic cells.

Phenotypic and genetic analyses of *gem1-1* and *gem1-2* suggest that MOR1/GEM1 is essential for the correct functioning of the phragmoplast at pollen mitosis I and that partial or complete lack of a microtubule-binding domain may be a cause of this defect. In *gem1-1* it is reasonable to propose that the longer truncated GEM1-1 product retains partial function, allowing normal cytokinesis in a proportion of *gem1-1* mutant spores. In the more severe *gem1-2* allele all *gem1-2* mutant spores are affected, indicating that the shorter GEM1-2 product does not maintain its function in the phragmoplast at pollen mitosis I. Although one cannot rule out conditional semi-dominant effects on cytokinesis, the fact that heterozygote *gem1* mutant plants have no constituitive phenotype strongly suggests that both are loss of function alleles.

The *mor1* mutants highlighted a role for the N-terminal HEAT repeat in the interphase cortical array. In contrast, the *gem1* mutants specify a role for the C-

terminus of MOR1/GEM1 in phragmoplast organisation. Neither *mor1* or *gem1* mutants are defective in nuclear division, indicating that these domains are not required for spindle function.

Our data indicate that MOR1/GEM1, like other members of this family, can bind microtubule polymers and small tubulin aggregates. MOR1/GEM1 concentrates at the midline of the phragmoplast where the plus ends of opposing microtubules overlap. It has been proposed that MAP65, which is believed to cross-link anti-parallel microtubules, serves to stabilise the line of overlap (Smertenko *et al.* 2000). Moreover, it has been shown that exogenous tubulin subunits are added at the overlapping plus ends at the midline (Asada et al. 1991). As members of the MAP215 family stimulate microtubule assembly at the plus ends (Charrasse *et al.* 1998, Gard & Kirschner 1987, Vasquez *et al.* 1994, Tournebize *et al.* 2000), it is possible that MOR1/GEM1 serves to stabilise the growing ends at the midline, promoting the flux of tubulin through the microtubules. The predicted diminished microtubule-binding capabilities of GEM1-1 and GEM1-2 may cause destabilisation of the line of overlap resulting in the aberrant cell plate formation seen in the *gem1* mutants.

A role for MOR1/GEM1 in the cytokinetic phragmoplast is supported by work with the tobacco homologue of MOR1/GEM1, TMBP200. TMBP200 was purified from telophase tobacco BY2 cells and when added to microtubules, bundles microtubules with cross bridges of lengths similar to those observed in phragmoplasts (Yasuhara *et al.* 2002, Kakimoto & Shibaoka 1988).

6.2 MOR1/GEM1 interacting proteins.

The large number of HEAT repeats present in MOR1 suggests that it may interact with other proteins and it is likely that such interactions are important in the

protein's functionality and that these interactions change through the cell cycle. The HEAT repeats are conserved in all members of the XMAP215 family, many of which have been shown to interact with several different proteins. One common interactor is the transforming acidic coiled-coil-containing TACC family of proteins, the mammalian members of which have all been implicated in cancer (Chen *et al.* 2000, Still *et al.* 1999, Still *et al.* 1999, Conte *et al.* 2002). These proteins are essential for mitotic spindle function and have been found to associate with centrosomes and microtubules during mitosis (Gergely *et al.* 2000, Gergely *et al.* 2000). However, this microtubule association was believed to be indirect as it could not be replicated with purified microtubules and a mediating protein was sought (Gergely *et al.* 2000). The *Drosophila* XMAP215, Msps was found to co-purify with recombinant *Drosophila* D-TACC when mixed with embryo extracts and this was confirmed by immunoprecipiation experiments where each protein specifically co-immunoprecipited the other (Lee *et al.* 2001). This interaction appears to be important for the efficient localisation of Msps to centrosomes as in 50% of mutants where D-TACC expression is <1%, Msps is absent from spindle centrosomes (Lee *et al.* 2001). In addition, overexpression of human and drosophila TACC proteins recruit extra Msps/TOGp to the centrosome. spindle pole and there is a concomitant increase in the number and length of centrosomal microtubules (Lee *et al.* 2001). TAC-1 and Zyg-9 have also been found to interact in *C. elegans* and this complex promotes assembly of microtubules and is essential for long astral and spindle microtubules (Le Bot et al. 2003, Bellanger & Gonczy 2003, Strayko 2003).

A second protein found to interact with multiple members of the XMAP215 family is Cyclin B1. The reorganisation of the cytoskeleton, which leads to the formation of the mitotic spindle, is M-phase specific and is controlled by maturation promoting factor (MPF: p43cdc2-cyclinB1 complex). This complex associates with spindle microtubules and MAPs are believed to be responsible for this. Charrasse and collegues (Charasse *et al.* 2000) have shown that XMAP215 and TOGp associate

with p34cdc2 kinase and direct it to the microtubule cytoskeleton. Co-staining of *Xenopus* cells with anti-TOGp and anti-Cyclin B1antibodies demonstrate that these proteins co-localise throughout the cell cycle and co-sedimentation of Cyclin B1 with microtubules is dependent on the presence of TOGp (Charasse *et al.* 2000). The region responsible for this interaction is the proline rich domain of TOGp, residues 723-790, which contains a consensous p34cdc2 phoshorylation site (Charasse *et al.* 2000). Interestingly this region is highly conserved and is present at the same location (730) in MOR1/GEM1. The identity between these regions is 36% with a homology of 70% with no gaps. Therefore it is highly likely that such an interaction between MOR1/GEM1 and CyclinB1 exists in the plant cell.

The *Saccharomyces cerevisiae* XMAP215, Stu2p is a component of the spindle pole body and has been found to interact with a second SPB component, Spc72p. Stu2p and Spc72p associate in yeast two-hybrid and immunoprecipitation experiments and can also interact with themselves to possibly form multimeric Stu2p:Spc72p complexes. Spc72p does not bind or localise to microtubules but is an essential component of the SPB. *Spc72* mutants have defects in SPB morphology, lack cytoplasmic microtubules and spindle elongation and chromosome segregation rarely occur (Chen *et al.* 1998). Further studies with Stu2 have identified two further interactors, Bim1p (EB1) and Bik1p (Clip170) (Kosco *et al.* 1999). In addition, these proteins bind each other and themselves. The site of interaction between Bik1/Bim1 and Stu2 is located in the C-terminus of the protein and the smallest fragment to do so consisted of the C terminal region after the coiled coil. In addition, the smallest fragment of Stu2, capable of binding of Stu2, contained the MT binding domain and a section of the coiled coil. Fragments containing the MT binding domain but not the coiled coil, do not bind, as do C terminal fragments containing the coiled coil but not the MT binding domain, suggesting that both are required (Chen *et al.* 1996, Kosco *et al.* 1999, Huffaker, Plant and Fungal Cytoskeleton GRC 2004) (**FIGURE 6.1**).

Figure 6.1: Interactors of XMAP215 Family Proteins

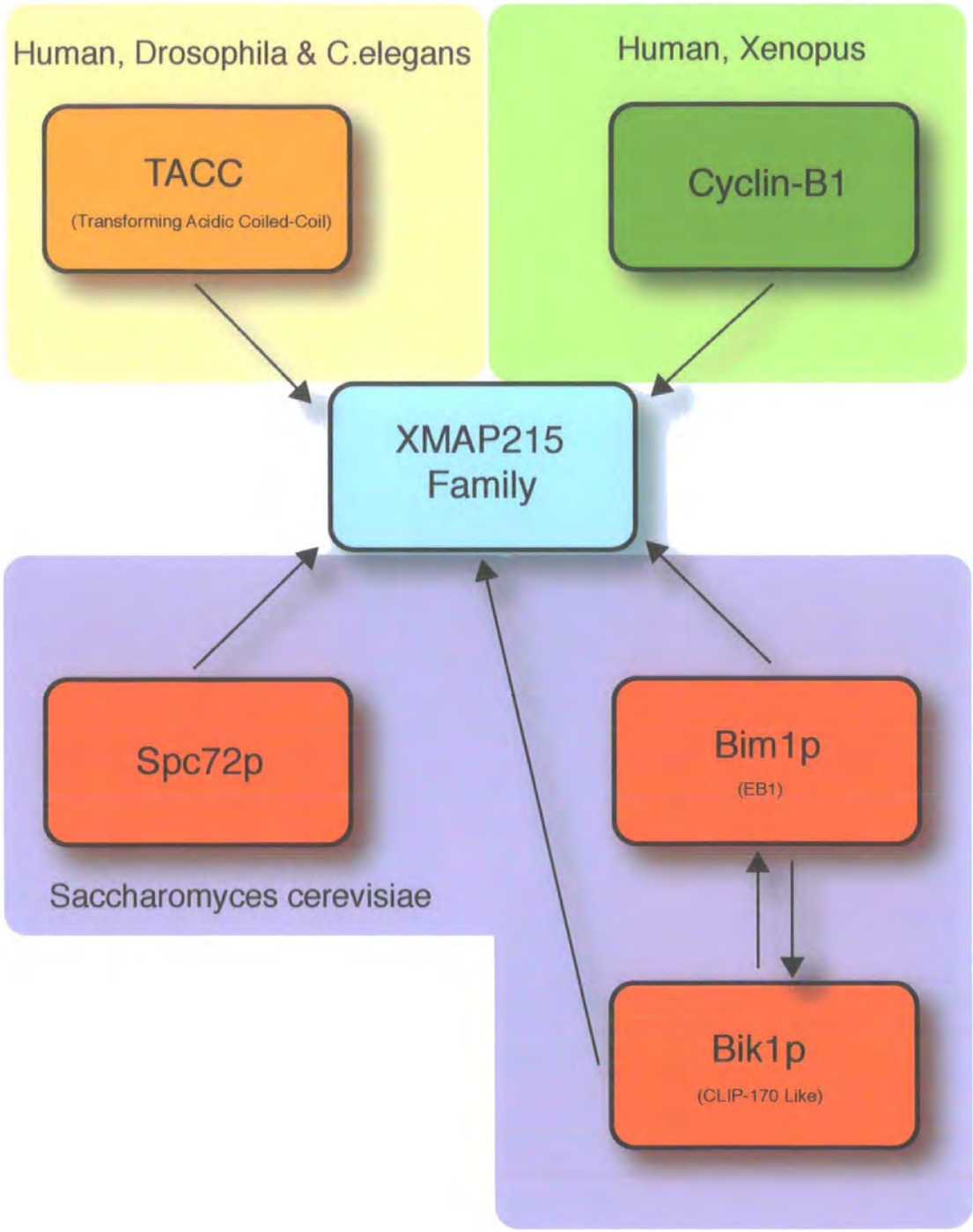

Figure 6.1: XMAP215/TOGp family proteins have been shown to interact with a variety of proteins in several organisms. TACC, transforming acidic coiled coil proteins are essential for mitotic spindle function and associate with microtubules and centomeres. Cyclin-B1 is part of the maturation promoting factor (MPF) complex which controls the reorganisation of the cytoskeleton to form the spindle at M-phase. The association of both of these interacting proteins with microtubules has been shown to require the XMAP215/TOGp family protein. Spc72p is an essential componant of the spindle pole body and Bim1p and Bik1p are homologues of EB1 and CLIP170 respectively. Homologues of CyclinB1, EB1 and CLIP170 are present in *Arabidopsis* and as such similar interactions may occur with MOR1/GEM1.

Therefore considering these data it is temping to speculate whether such interactions occur in plants. The first consideration is whether homologues of these proteins exist in the *Arabidopsis* genome. Spc72p is not present, this is not unexpected as plants do not have spindle pole bodies. Secondly, no conclusive TACC sequence can be identified. However, homologues of Cyclin B1, three EB1 proteins and Clip170 have been identified (Wang *et al.* 2004, Gardiner & Marc 2003, Chan *et al.* 2003). GFP-EB1 labels microtubule plus ends and therefore perhaps plus end complexes may also be conserved (Chan *et al.* 2003). Although the C-terminal region of group 1 XMAP215/TOGp proteins is conserved, it is not conserved with the yeast examples of group 3 (Ohkura *et al.* 2001, **SEE CHAPTER 3**). As discussed above, the C-terminal region of Stu2p contains those motifs, which interact with Bim1 (EB1) and BIK1 (CLIP170). The C-Terminal region of MOR1/GEM1 does contain a coiled coil so could MOR1/GEM1 form dimers like Stu2. Our data of yeast two hybrid interaction experiments with the N and C-terminal regions of MOR1/GEM1 may suggest that it does not, an observation consistent with electron microscopy of XMAP215 solutions (Cassimeris *et al.* 2001). But in our experiments, no full length or middle fragments of MOR1 were used, and as such dimerisation may require these regions. In addition the fusion protein may not have been expressed. Although such experiments would be very informative, the most insightful experiments would be those, which identify novel plant MOR1/GEM1 interactors, which could then provide new insights into how the unique microtubule arrays are co-orordinated.

Of the models provided in chapter one for an antagonistic relationship for MOR1/GEM1 and AtCMK1/2, model one, in which there is a direct interaction between these two factors, may not be correct, as our Yeast two-hybrid analysis showed no interaction with the N or C-terminal regions of MOR1/GEM1. However, again the full length MOR1/GEM1 could be required. This does not exclude model two in which following loss of MOR1/GEM1 binding Kinl-like kinesins can access a common binding site. But interestingly, anti-MOR1 staining of *mor1* mutant tissues

at the restrictive temperature show that, consistent with our localisation, MOR1/GEM1 labels all microtubule arrays, yet this means that the mutation in the N-terminal HEAT repeat does not abolish binding (Wasteneys, Plant and Fungal Cytoskeleton GRC 2004). These findings agree with our data that the C-terminal region is capable of binding microtubules and *in vivo* this may be sufficient to locate MOR1 to microtubular arrays, although the HEAT repeat may help to stabilise this interaction. So if the N-terminal HEAT repeat is not the major site of microtubule binding and it is not responsible for a AtCMK1/2 interaction, what could this protein-protein interaction motif do. Interactions with other factors, such as EB1 or SPR1, could be disrupted in the *mor1* mutant or perhaps the HEAT repeats may directly be responsible for the speculated microtubule polymerisation promotion activity of MOR1/GEM1. The mechanism by which the XMAP215/TOGp family of proteins do this has yet to be elucidated.

6.3 Signalling to MOR1/GEM1

In common with MOR1/GEM1, XMAP215 also contains a CDK site which when phosphrorylated inhibits the ability of XMAP215 to promote the polymerisation of tubulin *in vitro* (Vasquez *et al.* 1999). Considering these data and the model proposed in chapter 1, it is tempting to speculate that CDK is involved in regulation of this interplay between MOR1/GEM1 and a Kinl like kinesin. During interphase, CDK1 is reduced and MOR1/GEM1 is unphosphorylated, and its activity predominates over that of a Kinl kinesin leading to long cortical microtubules. In mitosis, CDK1 activity is high and MOR1/GEM1 is hyperphosphorylated, its activity is reduced and the activity of XKCM1 prodominates leading to short microtubules (Hussey & Hawkins 2001, Heald 2000).

Many other microtubule associated proteins are controlled through the cell cycle and posses CDK sites. Such regulation is understandable as the arrangement and dynamicity of the cell's microtubules has to be attenuated in order to disassemble,

create and maintain the different arrays required for progression through the cell cycle.

AtMAP65-1 can be phosphorylated by a protein extract prepared from *Arabidopsis* tissue culture cells and this phoshorylation is inhibited by roscovitine, suggesting that CDK may be responsible for this activity (Smertenko *et al.* 2004). However, phosphorylated AtMAP65-1 still co-sediments with microtubules and increases the turbidity of a tubulin solution. Therefore phosphorylation alone is not the sole factor that controls the association of AtMAP65-1 with microtubules (Smertenko *et al.* 2004).

In addition to such phosphorylation events, a phosphatase is required to remove the phosphate group and dephosphorylate the protein. Considering data for XMAP215 (Vasquez *et al.* 1999), such dephosphorylation could be responsible for reactivating MOR1/GEM1, allowing it to again bind and promote microtubule polymerisation. One candidate for such a phosphatase could be the type 2A phosphatase complex of which TON2 is a part. MOR1/GEM1 is strongly associated with the PPB, an array which *ton2* mutants lack (Camilleri *et al.* 2002). Could MOR1/GEM1 be phosphorylated, allowing the interphase cortical array to disassemble and then be reactivated by the PP2A phosphatase, promoting and stabilising the formation of the PPB? Also during interphase, *ton2* mutants have disorganised cortical microtubules similar to those seen in the *mor1* mutant. Again, perhaps this is because MOR1/GEM1 is in the phosphorylated state and inactive. The HEAT repeat protein-protein interaction motif found in MOR1/GEM1 gets its name from those proteins which contain the motif, one of which is the regulatory subunit of type 2A protein phosphatase (HEAT) (Andrade & Bork 1995, Groves *et al.* 1999). Perhaps this could be a mechanism for interaction of MOR1/GEM1 to a PP2A. However, although irregular preprophase bands are observed in *mor1* mutants, these defects are less severe than those of the cortical array or phragmoplast (Wasteneys Plant & Fungal Cytoskeleton GRC 2004). This may

suggest that MOR1/GEM1 alone is not solely required for maintenance of the PPB. A second candidate would be MAP65 which is also located to the PPB and could be responsible for bundling the PPB microtubules (Smertenko *et al.* 2004). Although MAP65 certainly plays a role at the PPB, the phosphorylation status of the protein and the activity of a PP2A may not be involved as the interaction of MAP65 with microtubules, as discussed earlier, is not solely reliant in phosphorylation (Smertenko *et al.* 2004).

6.4 A Paradox in the effect on Microtubule Dynamicity.

XMAP215 and Stu2p as microtubule depolymerising factors:

Although members of the XMAP215/TOGp family have been characterised as microtubule growth promoters, recent work, in contrast, has identified a microtubule depolymerisation role for two members of the family, XMAP215 (Shirasu-Hiza *et al.* 2003) and Stu2p (Breugel *et al.* 2003).

Shirasu-Hiza and colleagues (Shirasu-Hiza *et al.* 2003) identified a novel source of microtubule depolymerisation independent of previously characterised factors, XKCM1, OP18 and Katanin in *Xenopus* egg extracts. The factor responsible for this novel MT depolymerisation was biochemically purified and found to be XMAP215. This ability was confirmed by experiments with recombinant XMAP215 and GMPCPP microtubules and was found to be confined to microtubule plus ends. At these ends microtubule depolymerisation was increased by 5-10 fold in the presence of recombinant XMAP215. The mechanism by which XMAP215 achieved this depolymerisation was thought to be one of three possibilities: promotions of GMPCPP hydrolysis, Sequestration of GMPCPP-tubulin dimers or disruption of the lattice. Experiments with ^{32}P labelled GMPCPP showed that hydrolysis was not increased and CPP MT depolymerisation was not found to increase in the presence of the tubulin sequestering drug, Nocodazole. In further experiments, CPP MT ends were imaged by negative-stain electron microscopy. Here in buffer alone CPP MT ends appeared blunt wereas in the presence of full

length or N-terminal XMAP215, bulbs of material at the ends of depolymerising microtubules, which may contain curled protofilaments were observed. The final conclusion of this work was based on the microtubule system used. It was suggested that the CPP MT system is a model for the pause state of microtubules, proposed as a mid state between polymerisation and depolymerisation in dynamic instability by Tran *et al.* (1997). XMAP215 may destabilise the pause state, acting as an antipause factor. In the pause state, MTs may shift to growth or shrinkage and a pause destabilising, antipause factor would increase MT dynamicity.

Parallel work by Breugel and colleagues (Breugel *et al.* 2003) with the yeast member of the family, Stu2p, provided similar conclusions but here they suggest that it induces microtubule catastrophes by sterically interfering with tubulin addition to microtubule ends. Recombinant Stu2p was expressed in baculovirus and used in experiments monitoring the growth of rhodamine labelled microtubules from purified centrosomes where it was found to lead to a clear reduction in microtubule length. The temperature sensitive mutant *stu2-10* was studied to examine whether this activity of Stu2p was evident *in vivo.* After shifting to the restrictive temperature cytoplasmic microtubules of *stu2-10* were found to be on average ~30% longer than those of wild type cells. Further experiments showed that Stu2p destabilised microtubules by inhibiting growth as opposed to promoting catastrophe. In experiments with sheared taxol stabilised microtubules, where microtubule ends are increased; more Stu2p was found in the sheer microtubule pellet, indicating that Stu2p preferentially binds to microtubule ends. The authors concluded that Stu2p destabilises microtubules by preferentially binding to their plus ends and sterically hindering tubulin addition. As a result, microtubule growth would decrease and the probability of hydrolysis of stabilising GTP cap would increase.

These studies show that XMAP215 and Stu2p, and perhaps other members of the family, constitute a new class of microtubule destabilisers as they do not require

ATP like Kinl kinesins and Katanin do, nor do they sequester tubulin dimers like Op18/Stathmin. To reconcile this destabilising activity with the stabilisation abilities previously described in other studies it is intriguing to propose that the destabilising activity might be regulated in a cell cycle-dependant manner in vivo where these proteins can switch from a stabiliser to a destabiliser.

In further experiments to analyse the effects of MOR1/GEM1 on microtubule dynamics it would be interesting to establish whether MOR1/GEM1 also exhibits this anti-pause behaviour. Such findings could be particularly important considering that plant microtubules are more dynamic than their animal and yeast counterparts. (Hush *et al.* 1994, Yaun *et al.* 1994, Moore *et al.* 1997, Shaw *et al.* 2003)

6.5 AtCMK1 & AtCMK2 Through the Cell Cycle.

6.5.1 *Kinl at the cell cortex and the interphase cortical array.*

The interphase cortical array of *Arabidopsis* cell suspension cells does not stain with anti-AtCMK2 antibody. However, in experiments with onion and tobbaco cells expressing GFP AtCMK2 interphase arrays are clearly labelled. Antibody staining of other kinl kinesins such as MCAK and XKCM1 during interphase, show the protein as a soluble pool present in both the nucleus and cytoplasm (Wordemann & Mitchison 1995, Walczak *et al.* 1996 cell). The inability to stain AtCMK2 at the cortex with anti-AtCMK2 antibody may be due to epitope masking at this site, possibly due to binding of an interacting protein. However, the location of AtCMK2 to the cortical array when expressed as a GFP fusion could be a result of over-expression as the construct is driven by the strong 35s promoter. Uniquely the two yeast members of the Kinl family, KLP5 and KLP6 have been located to interphase microtubules (Garcia *et al.* 2002) and it is tempting to speculate that short microtubules in *mor1* cells are cut back by a destabilizing factor. Why would a catastrophic kinesin be required at the interphase cortical array? One consideration could be that Interphase cortical microtubules do need to depolymerise to

breakdown and repolymerise to for the PPB. Secondly, at interphase, during the process of generating parallel ordered microtubule bundles, cortical microtubules encounter each other and there are believed to be several potential out comes, two of which involve catastrophe and depolymerisation (Hashimoto 2003). When the leading end encounters another microtubule at an acute angle, the microtubule depolymerises and finds another route, or following an encounter the microtubule loses its stabilizing association with the inner plasma membrane and depolymerises (Hashimoto 2003). Although this switch of microtubules to catastrophe could be explained by physical and kinetic considerations, such as stalling due to the physical contact with another microtubule, could destabalising factors such as Kinl kinesins regulate such encounters? It is likely however that during interphase Kinl kinesin activity is reduced by phosphorylation or opposed by the stabalisation provided by MAPs such as MOR1/GEM1 in order to produce long microtubules and an ordered array.

6.5.2 Kinl at the Preprophase band.

As discussed previously, studies with MAP4-GFP have shown that PPB formation consists of four stages: PPB initiation, PPB narrowing, PPB maturation, and PPB breakdown (Dhonukshe *et al.* 2003). During PPB formation microtubules form a broad ring, which covers two thirds the cell length, this structure then gradually narrows to form a ring structure with a width of 2-5 μm. During maturation there is the flow of tubulin or microtubules from the cell cortex towards the region of PPB (Dhonukshe *et al.* 2003).

Further studies with YFP-CLIP170, a plus end binding protein, identified the importance of altered microtubule dynamic instability in driving the formation of the PPB. During PPB formation the growth rate and catastrophe frequency of PPB microtubules double, whereas the shrinkage rate and rescue frequency remain unchanged, making microtubules shorter and more dynamic (Dhonukshe *et al.*

2003). It is also interesting to note that breakdown of the PPB is very rapid compared to initiation, 90 minutes and 5-10 minutes respectively.

Dhonukshe and colleagues proposed a model of the mechanisms, which govern the microtubular events,which occur during PPB formation. At PPB initiation a broad PPB forms, overlapping almost two thirds of the cell length. At this stage the catastrophe frequency increases gradually (possibly as a result of the inactivation of microtubule-stabilising proteins or the activation of microtubule-destabilising proteins) destroying the microtubules and creating an enhanced free tubulin pool that is used for the formation of new microtubules. During PPB narrowing, the cycle of gradual increase in catastrophe frequency and subsequently increased growth rate makes microtubules increasingly dynamic (Dhonukshe *et al.* 2003).

The factors which produce this increase in the dynamic instability, required for formation of the PPB could be MOR1/GEM1 and AtCMK2, both of which locate to the PPB. In addition the rapid breakdown of the PPB could as a result of the activity of AtCMK2 as well as other destabilising factors such as katanin.

6.5.3 Kinl during mitosis and the spindle.

Immunolocalisation of XKCM1 in tissue culture cells during mitosis revealed that the cytoplasmic pool of the protein, present during interphase, persists through mitosis. However, a portion of XKCM1 localised to the centromeric region of the mitotic chromosomes and to the centrosomal region of the spindle from prometaphase to anaphase. These findings were confirmed with in vitro assembled spindles, although here a diffuse staining of the entire spindle was also observed (Walczak *et al.* 1996).

Immunolocalisation of AtCMK2 in *Arabidopsis* tissue culture cells shows that it localises strongly to the spindle during mitosis. This staining is to individual spindle microtubules as well as diffusely throughout the entire spindle. However no

concentrated staining at the kinetochore was observed although the kinesin is present at these sites.

KinI kinesins appear to be required for correct spindle assembly and its maintenance. If XKCM1 is immunodepleted from xenopus egg extracts, rather than forming bipolar spindles these extracts create abnormally large microtubule asters with centrally located chromatin from which microtubules emanate. Finally, these extracts form huge aggregates from which long microtubules radiate (Walczak *et al.* 1996). *klp5* and *klp6* mutants spend a longer time (x2) in mitosis where the initiation of anaphase B is delayed (Garicia *et al.* 2002). In these mutants two indicators of this delay are the observations that sister centromeres move back and forth between the poles and that Cut2 securin is retained (Garicia *et al.* 2002, Nakamura *et al.* 2002). Suggested reasons for such a delay are: capture of kinetochores by the spindle is delayed or both sister kinetochores are captured, but tension is compromised (Garicia *et al.* 2002). Therefore KinI kinesins are required for the establishment and maintenance of mitotic spindles and are involved in capture of kinetochores and spindle checkpoint processes.

In addition to this, Walczak proposed a model, which implicates XKCM1 function at the kinetochore. Based on observations that kinetochores oscillate throughout mitosis (Skibbens *et al.* 1993), and that these oscillations are thought to be a result of switching between phases of growth and shrinkage of kinetochore microtubules. XKCM1 may act to regulate these transitions of kinetochore microtubules and on locating to the end of the microtubule would trigger catastrophe, causing chromosomes to move back towards the pole concomitant with microtubule depolymerisation (Walczak *et al.* 1996) In addition, isolated chromosomes can modulate microtubule dynamics in vitro and kinetochores increase the catastrophe rate of their bound microtubules in a ATP dependant manner (Hyman & Mitchison 1990). It is suggested that XKCM1 represents the ATP-dependant kinetochore-bound catastrophe factor described in these experiments.

Therefore AtCMK2 may participate in the capture of kinetochores and then trigger catastrophe of kinetochore microtubules causing chromosomes to move back towards the pole.

6.5.4 Kinl during cytokinesis and the phragmoplast.

Kinl kinesins are found associated with cytokinetic apparatus as Skop *et al.* isolated MCAK from mammalian midbodies, as described previously. Further experiments with *Ce*lMCAK RNAi showed that knocking out this protein caused mitotic defects, including cell cycle progression or spindle defects consistent with those observed in other studies. In addition, *Ce*lMACAK RNAi also showed defects in cleavage furrow termination (Skop *et al.*).

Although these are examples of Kinl kinesins functioning during cytokinesis, the phragmoplast is an array which is unique to plants and is very different to the midbody. In addition, plant cytokinesis as a whole, is unique as it involves the creation of a new cell plate, co-ordinated by the phragmoplast. During cytokinesis, vesicles fuse to form the new membrane compartment, the cell plate, which then expands laterally to the cell margin (Strompen *et al.* 2002, Simarro *et al.* 2004). The targeting of vesicles is co-ordinated by the reorganisation of the phragmoplast, from a solid cylinder to an expanding ring shaped structure (Grainger & Cyr 2000, Strompen *et al.* 2002). Such expansion laterally is achieved by the depolymerisation of microtubules in the centre of the phragmoplast, giving way to the cell plate and the polymerisation of microtubules along the edge of the phragmoplast (Strompen *et al.* 2002 Yasuhara *et al.* 1993). Therefore, within this series of events there is a clear requirement for a factor, which can induce the depolymerisation of microtubules in the centre of the phragmoplast, required for lateral expansion. The depolymerised tubulin may then repolymerise along the edge. A good candidate for such a role would be a Kinl kinesin, in *Arabidopsis* probably AtCMK2. However, staining of the phragmoplast is throughout the array

and not restricted to the centre. Possibly, this diffuse staining is because of the transient association of AtCMK2 with microtubules or the kinesin is throughout the phragmoplast yet its depolymerising activity is restricted to the centre by modulation of the activity of central and peripheral populations by a kinase (two tobacco Aurora B kinases have been found to associate with the phragmoplast, Van Damme, Plant and Fungal cytoskeleton GRC 2004).

The HIK kinesin has also been implicated in the depolymerisation of central phragmoplast microtubules. In the *hik* mutants, lateral expansion is not affected yet microtubules appear to persist in the centre of the phragmoplast. Therefore, it is suggested that HINKEL plays a role in the reorganisation of the phragmoplast microtubules during cell plate formation (Strompen *et al.* 2002). Two explanations for the cytokinetic defects of the *hik* mutants are that the persistence or delay of depolymerisation of overlapping microtubules may destabilise the nacent cell plate, resulting in cell wall stubs or that cell plate formation may be compromised, resulting in abnormal stability of phragmoplast microtubules due to the failure to transport some necessary regulatory protein to the plane of division (Strompen *et al.* 2002). HINKEL is a kinesin with an N-terminal motor (Strompen *et al.* 2002) and no microtubule depolymerising activity has be described. Perhaps the required cargo described above could be an Aurora B kinase, AtCMK2 or another microtubule destabilising factor, Katanin.

6.6 Kinl Kinesin dimerisation.

Maney and collegues have shown that native MCAK appears to form homodimers (Maney *et al.* 1998). Furthermore, the majority of this dimerisation ability was focused in the N-terminus of MCAK, although to produce an interaction as strong as that of the full (motorless) protein the C-terminus is also required (Maney *et al.* 2001). However, dimerisation studies with MCAK demonstrated that the smallest functional constructs of MCAK exist as monomers, suggesting that the

depolymerisation activity of MCAK is not dependant on quaternary structure (Maney *et al.* 2001).

In contrast, the two fission yeast Kinl kinesins, Klp5 and Klp6 form a hetrocomplex rather than a homocomplex (Garcia *et al.* 2002). The non-additive phenotypes of *klp5 klp6* double mutants suggest that these kinesins either act sequentially in a linear pathway or work together. Klp5 and klp6 show co-localisation throughout the cell cycle and are capable of immunoprecipitating each other in a reciprocal manner (Garcia *et al.* 2002). Further experiments demonstrated that klp6 can not immunoprecipitate itself and hence only forms a hetercomplex; although whether Klp5 is capable of forming a homocomplex has yet to be determined.

Our yeast two-hybrid data suggest that *Arabidopsis* CMK kinesins can form dimers through a plant conserved domain situated at the extreme amino terminus of the protein via a coiled coil. This is a common motif through which many proteins, including kinesins, dimerise. The primary sequence of a coiled coil produces a helix where hydrophobic residues are concentrated on one side of the helix. The interactions produced between two of these helicies or coils is in part an attempt for the two coils to bury their hydrophobic faces, positioning these together leaving only the hydrophilic sides exposed (Thormahlen *et al.* 1998). The interaction causes the two coils to twist around each other tethering the two kinesins together. The plant conserved domain of AtCMK2 was used to test dimerisation of AtCMK1 as this region is almost identical. However this raises the possibility that the CMK kinesins could form heterodimers as well as homodimers. *In vivo* this is unlikely to occur as the localization of these two kinesins within the cell are very different. In addition to this the tissues and organs where the kinesins are expressed are also very different although AtCMK2 is present in those tisse which express AtCMK1. In our assay only the PCD, Plant Conserved Domain, was used and as such *in vivo* the geometry of the full-length protein may prevent the formation of heterodimers.

In further experiments it would interesting to identify whether such dimerisation is required for the activity of AtCMK kinesins.

6.7 Kinl kinesin interacting proteins.

As yet, only a single Kinl interacting protein has been identified, ICIS (Inner Centromere Kinl Stimulator), which was identified in a Xenopus screen of uncharacterised MAPs. ICIS stimulates MCAK activity in vitro and ICIS antibodies cause excessive microtubule growth and inhibited spindle formation when introduced to xenopus extracts (Ohi *et al.* 2003). ICIS was found to localise to inner centromeres and the chromosomal region located between kinetochores, in a MCAK dependent manner. Furthermore, ICIS co-immunoprecipitates MCAK and the inner centromere proteins ICENP and Aurora B, an association supported by Immunoelectron microscopy, which finds ICIS located on the surface of inner centromeres (Ohi *et al.* 2003). Interestingly Aurora B kinase with which ICIS immunoprecipitates, has been shown to phosphorylated MCAK/XKCM1 (Lan *et al.* 2004, & discussed later in **SECTION 6.11**). Therefore at the kinetochore there appears to be a complex containing MCAK, Aurora B, ICIS and ICENP. ICIS could be required to associate Aurora B kinase to MCAK, which it then phosphorylates, a signalling system believed to control correct attachment of kinetochore microtubules to kinetochores/centromeres (Lan *et al.* 2004).

Figure 6.2

Previously discussed in section 1.x, model 1 for the involvement of a Kinl kinesin in *mor1* phenotype required a physical interaction between a Kinl kinesin and

MOR1/GEM1 (Hussey & Hawkins 2001). To test this hypothesis a yeast two-hybrid interaction assay was performed between AtCMK1 and AtCMK2 with N and C-terminal fragments of MOR1/GEM1. As described previously no interaction was found between either of the kinesins with either the N or C terminal fragments of MOR1/GEM1, although the MOR1/GEM1 fusion proteins may not have been expressed. In addition, the full length MOR1/GEM1 or a third factor may be required for interaction. If such a negative result is correct, it is probably that MOR1/GEM1 and *Arabidopsis* Kinl kinesins, specifically AtCMK2, are genetic rather than physical interacting partners i.e. they interact in the same pathway but not directly.

6.8 Over-expression can induce microtubule depolymerisation

As described previously AtCMK2 was transiently expressed as a N-terminal GFP fusion protein in *N. benthamiana* leaves. Here cells showed highly flouresecent aggregates in the cytoplasm or small fluorescent filaments with levels between the two. To examine the state of microtubules in these cells and whether these filamentous objects could be microtubules, leaves expressing GFP-AtCMK2 were stained for tubulin. Here wild type cells showed extensive intact and ordered interphase cortical arrays with long microtubules. In contrast those cells expressing GFP-AtCMK2 showed short disorganized microtubules. There appeared to be a scale of the level of disruption, with some cell with short fragments, others with very small fragments and then cells where no microtubule fragments could be seen, but rather aggregates which stain with anti-tubulin antibody (**FIGURE 6.3**).

PtK2 cells transfected with a GFP-XKCM1 fusion construct have yielded similar results (Kline-Smith & Walczak 2002). GFP-XKCM1 protein was present in a soluble pool in the cytoplasm and the nucleus and to examine the effect of GFP-XKCM1 expression on the MT array, cells were fixed and stained for tubulin. Cells expressing low levels of GFP-XKCM1 had morphologically normal MT arrays, however cells expressing moderate levels of GFP-XKCM1 had disruptions of the

Figure 6.3: Summary of the effects of AtCMK2-GFP over-expression in N.*bethamiana* leaf epidermal pavement cells

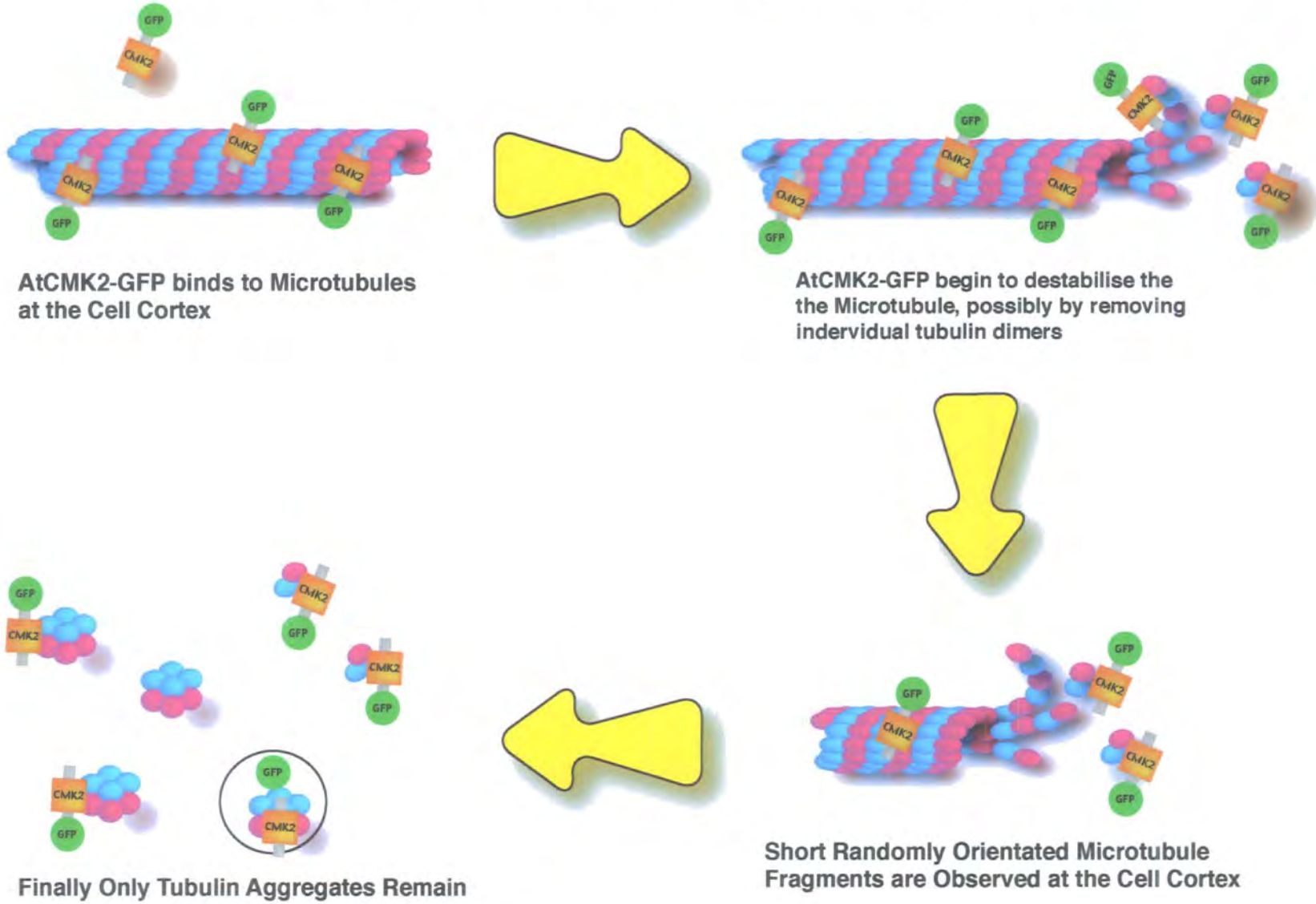

interphase MT array consistent with the role of XKCM1 as a MT destabiliser. In cells expressing high levels of GFP-XKCM1, the entire MT array was nearly abolished and a lightly staining tubulin pool was present in the cytoplasm. MT destabilisation was not observed in cells expressing GFP alone (Kline-Smith & Walczak 2002). Further experiments showed that the extent of MT destabilisation was tightly correlated with the levels of GFP-XKCM1 expression. Maximal destabilisation of MTs was achieved at a 10-20 fold excess expression of GFP-XKCM1 over endogenous XKCM1 levels (Kline-Smith & Walczak 2002). Cells expressing low levels of GFP-XKCM1, a 4-6 fold excess, were used to study MT dynamics and mitotic spindle integrity. In these cells, the frequency of MT catastrophe was increased by 4.5 fold, with a decrease in MT rescue frequency of 1.7 fold when compared to GFP controls. GFP control cells were found to have a mitotic index of ~2% whereas GFP-XKCM1 expressing cells had a mitotic index of ~6%, suggesting that cells expressing GFP-XKCM1 exhibited a mitotic arrest or a mitotic delay. In addition, 62% of mitotic cells expressing GFP-XKCM1 had abnormal spindles compared with GFP control cells (Kline-Smith & Walczak 2002).

Considering the data for the effect of transient expression of GFP-AtCMK2 on microtubules and comparing this to those findings for GFP-XKCM1, it is reasonable to suggest that both kinesins are microtubule destabilsing proteins. The observations for GFP-AtCMK2 and GFP-XKCM1 are strikingly similar and both cases severity of disruption varies and appears to be linked to kinesin expression. It is interesting to note that images of short disorganised microtubules following over-expression of AtCMK2 are similar to microtubules in epidermal cells of *mor1* at the restrictive temperature (**FIGURE 6.4**). This suggests that the short microtubules in *mor1* are as a result of the destabilizing activity of AtCMK2 predominating in the absence of stabilisation provided by MOR1/GEM1.

6.9 *Arabidopsis* Kinl Kinesin Expression Pattern.

Figure 6.4: Comparison of Microtubules in *mor1* and GFP-AtCMK2 Expressing Cells

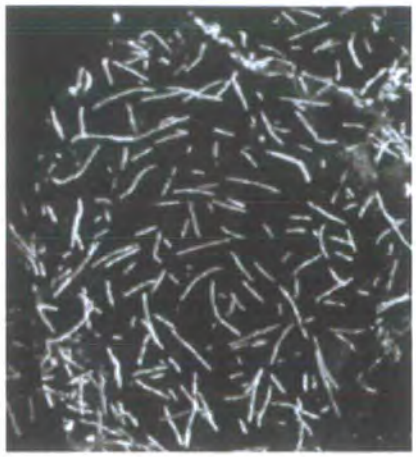

A. thaliana mor1

(Whittington *et al.* 2001)
Tubulin-GFP

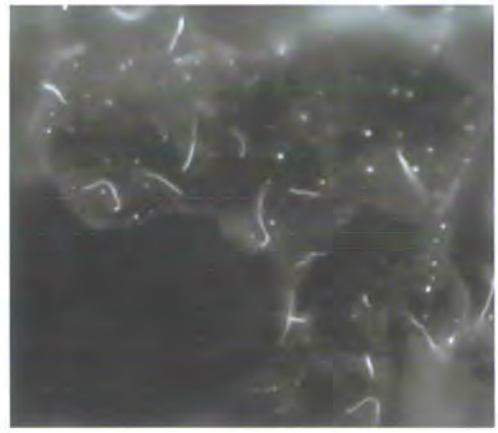

***N. benthamiana* GFP-AtCMK2**

(This study)
Anti-Tubulin Antibody

Short disorganised microtubules following over-expression of AtCMK2 in *N. benthamiana* epidermal cells are similar to microtubules in epidermal cells of *mor1* at the restrictive temperature. This could suggest that the short microtubules in *mor1* are as a result of the destabilizing activity of AtCMK2 predominating in the absence of stabilisation provided by MOR1/GEM1.

The expression pattern of *AtCMK1* and *AtCMK2* as assessed by GUS activity shows that the two kinesins are expressed differentially. *AtCMK2* is highly transcribed in all tissues examined, including pollen. These findings, agree with the Affymetrix microarray data described in **CHAPTER 3** and are similar to the expression programme of MOR1/GEM1. Immunolocalisation data suggest that AtCMK2 does not locate to interphase cortical microtubules, but rather the mitotic spindle, therefore why is it expressed in non-dividing cells? It is possible that AtCMK2 does not stain cortical microtubules due to epitope masking and AtCMK2-GFP studies show what appear to be fluorescent cortical microtubules. If AtCMK2 does bind cortical microtubule it is here that it may have a role in non-dividing cells. Alternatively, at interphase AtCMK2 may have a secondary role. The constitutive expression of AtCMK2 suggests that the kinesin is a house keeping protein like MOR1/GEM1, which is required for the control of microtubule dynamics in all cell types.

AtCMK1 expression is particularly interesting as it only appears to be expressed in several locations during specific processes. One is the funiculus, a structure which supports and connects the ovule/embryo to the silique and contains vascular tissue to supply the developing ovule/embryo with nutrients. The most interesting GUS expression was seen at areas of high expression at the point from which the lateral root develops and emerges. This region is known as the lateral root primordial.

The initiation of a lateral root.

The vascular cylinder compromises the vascular tissues and one or more layers of nonvascular cells, the pericycle. The pericycle of the root arises from the same part of the apical meristem as the vascular tissues and is composed mainly of parenchyma cells. Parenchyma cells carry out a variety of functions in relation to their position in the plant and although they may be more or less highly specialised they are capable of changing their functions and can even resume meristematic activity.

FIGURE 6.5

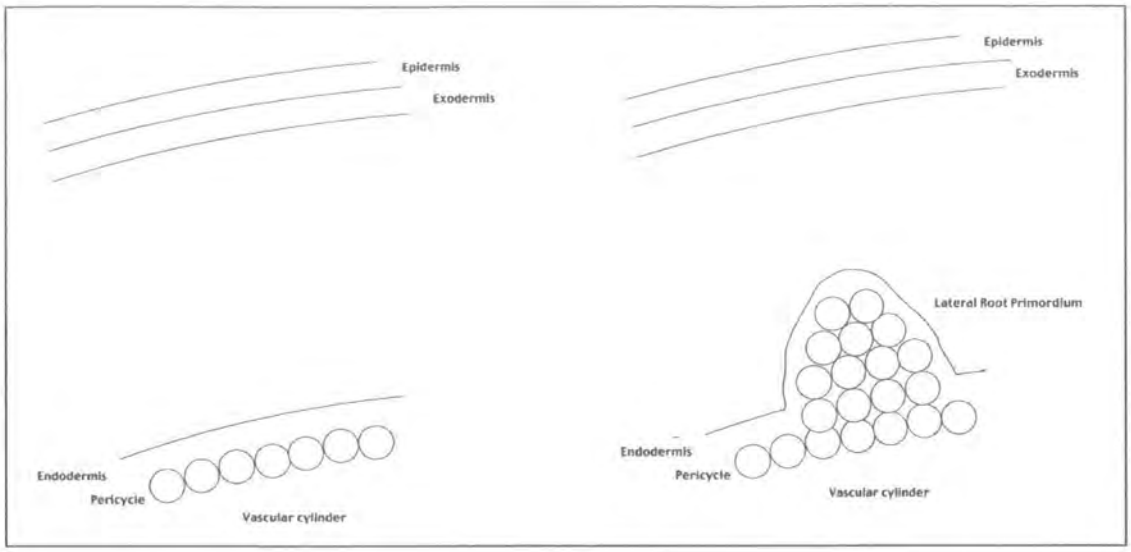

Lateral roots arise at the periphery of the vascular cylinder at variable distances from the apical meristem. They originate, most commonly, in the pericycle, but the endodermis may also contribute some cell layers to the lateral root primordium (Bell 1970, Guttenberg 1968). However, often the cells provided by the endodermis are sloughed off after the lateral root emerges from the parent root (Street 1952). Due to the pericyclic origin of the lateral root it is located closely to the vascular tissues of the parent root with which the vascular tissues of the lateral root will be connected. When a lateral root is initiated, several contiguous pericyclic cells acquire dense cytoplasm and divide periclinally (parallel with the circumference or the nearest surface of an organ). The products of these divisions then divide again, periclinally and anticlinally (perpendicular to the nearest surface). The accumulating cells form a protrusion, the lateral root primordium. As the primordium increases in length, it penetrates the cortex and emerges on the surface.

Therefore, it is tempting to speculate that AtCMK1 plays a role in the differentiation and development of the pericycle into the lateral root primordium and the vascular tissues. Interestingly both locations of expression, lateral root primordium and

funiculus both contain developing vascular tissue. We are awaiting the analysis of insertions in AtCMK1 to see if defects in lateral root formation occur.

6.10 Dissecting KinI microtubule destabilizing activity

Lessons from HIV-1

Interestingly, the HIV-1 virus may posses the ability to modulate microtubule dynamics via viral proteins with similarity to MAPs, a proposition consistent with the disruption of microtubules following HIV-1 infection (Watts *et al.* 2000). The N-terminal half of HIV-1 reverse transcriptase (Rev) has unexpected sequence similarity to the tubulin-binding portion of the catalytic/motor domains of the microtubule-destabilizing Kin I kinesins (Watts *et al.* 2000). HIV-1 Rev binds microtubules and results in the formation of bi-layered rings with an external diameter of 44-49 nm. Although this ring formation is not sensitive to taxol, colchicine, or MAPs, it does requires Mg^{2+} and is inhibited by maytansine (Watts *et al.* 2000). This small area of similarity between HIV-1 rev and KinI kinesins may identify the minimal amino acid sequence sufficient to cause microtubule depolymerisation. If this region is compared with AtCMK kinesins and XKCM1 it can be seen that all of those residues conserved between XKCM1 and HIV-1 and HIV-2 are also conserved in AtCMK kinesins (**FIGURE 6.6**). However the residues, which are conserved, differ between HIV-1 and HIV-2. Previous molecular dissection techniques with MCAK have identified that an additional 'neck' domain, consisting of 30 amino acids to the amino terminus of the motor domain, is required for efficient depolymerising activity (Maney *et al.* 2001). Although these 30 residues are conserved in classical members of the KinI family, XKCM1, MCAK, they are absent in AtCMK1/2. However studies with the *Plasmodium falciparum* pKinI have identified that the motor core alone is sufficient for microtubule destablisation (Moore *et al.* 2002).

Figure 6.6: Alignment of AtCMK1+2 and XKCM1 with the MT destabilisation domains of HIV-Rev1/2

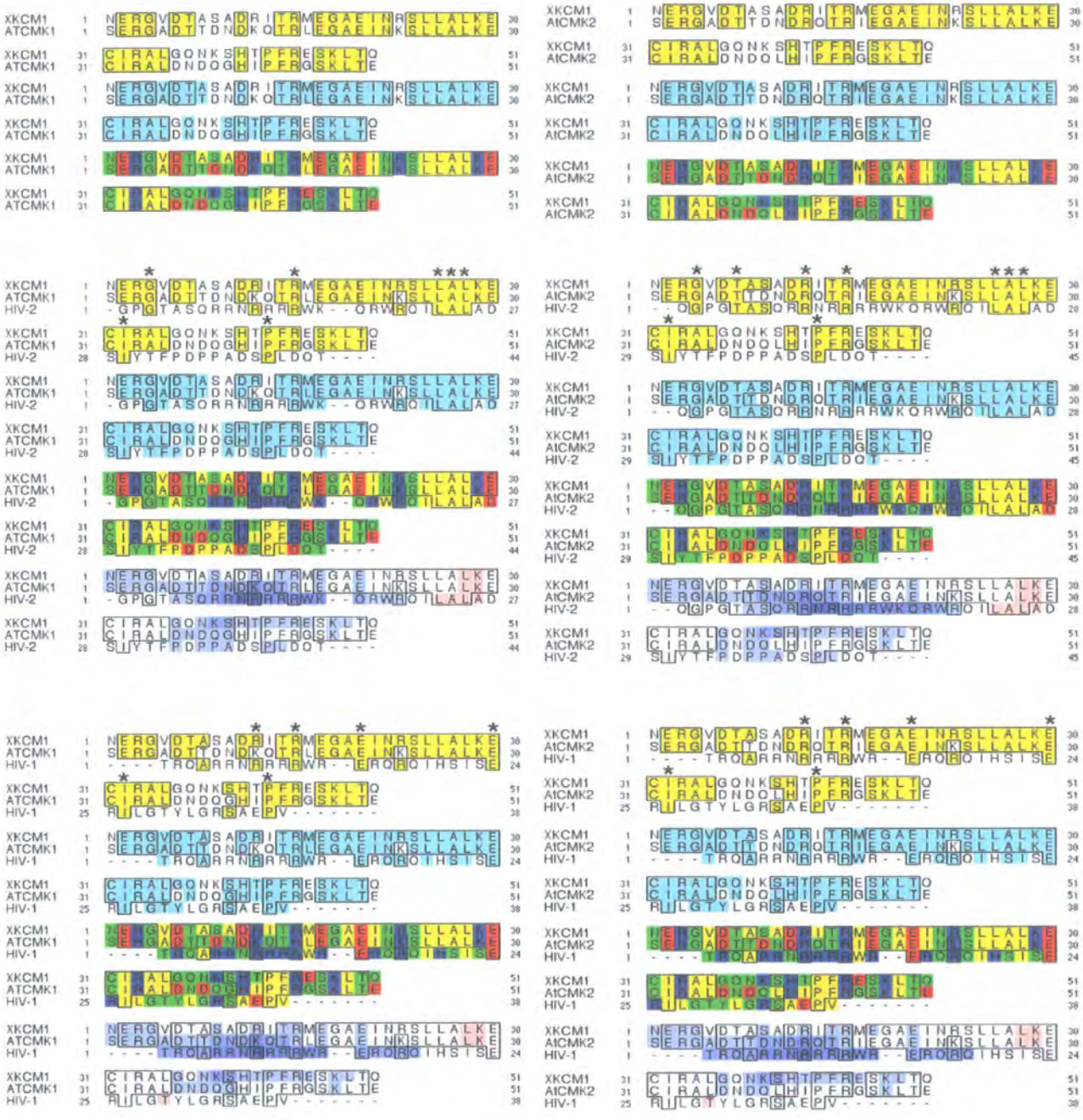

Figure 6.6: Alignments of AtCMK kinesins with XKCM1 and the region of HIV Rev 1 and 2 which shows similarity to Kin I kinesins. Conserved residues are marked with a *. This region of HIV Rev is not highly similar to Kin I kinesins, yet those residues which are identical are conserved between AtCMK kinesins and other Kin I kinesin. As HIV Rev has been shown to have microtubule depolymerising activity, perhaps these residues, in this arrangement, are the minimal requirement for microtubule depolymerisaing activity

Furthermore HIV-1 intergrase (IN) has also been shown to have an involvement with microtubules and MAPs. HIV-1 IN was used as the bait in a yeast 2 hybrid screen, which identified several interacting proteins associated with the microtubule network. One of these MAPs was the C-terminal half of the yeast member of the MOR1/XMAP215 family. (de Soultrait, 2002). In vitro, recombinant Stu2p-CT is capable of inhibiting HIV-1 IN and when co-expressed in yeast cells with HIV-1 IN, the lethal phenotype observed upon HIV1-IN expression alone is abolished (de Soultrait, 2002).

In future, it would be useful to mutate these residues conserved between HIV-1 Rev and AtCMK1/2 and identify which, if not all, are essential for the microtubule depolymerisation activity of AtCMK1/2. In addition this may shed light on the binding interaction between this class of kinesins and tubulin, indicating why upon binding, Kinl kinesins cause protofilaments to bend and tubulin dimers to disassociate. This interaction may be similar for HIV-1 and therefore could be a further possible site for therapeutics. However, if this interaction is as conserved as it appears to be, such therapeutics could also be detrimental to endogenous microtubule based cellular processes.

The recent 3D Structure of pKinI

Shipley and collegues have resolved the crystal structure of the pKinI motor core from *Plasmodium falciparum* at a resolution of 1.6 A. This motor core alone is sufficient for depolymerisation *in vitro* (Moore *et al.* 2002). The pKinI structure is very similar to other kinesin structures although there are differences in the loop regions, L6 and L10 (the plus-end tip), L2 and L8 and in switch II (L11 and helix4)(Shipley *et al.* 2004). In addition, KinI-conserved amino acids were mutated to alanine and studied for their effects on depolymerisation and ATP hydrolysis. Mutation of three residues in L2 primarily affect depolymerisation rather than microtubule binding and ATP hydrolysis (Shipley *et al.* 2004).

Figure 6.7: Structure of pKinI Motor Core

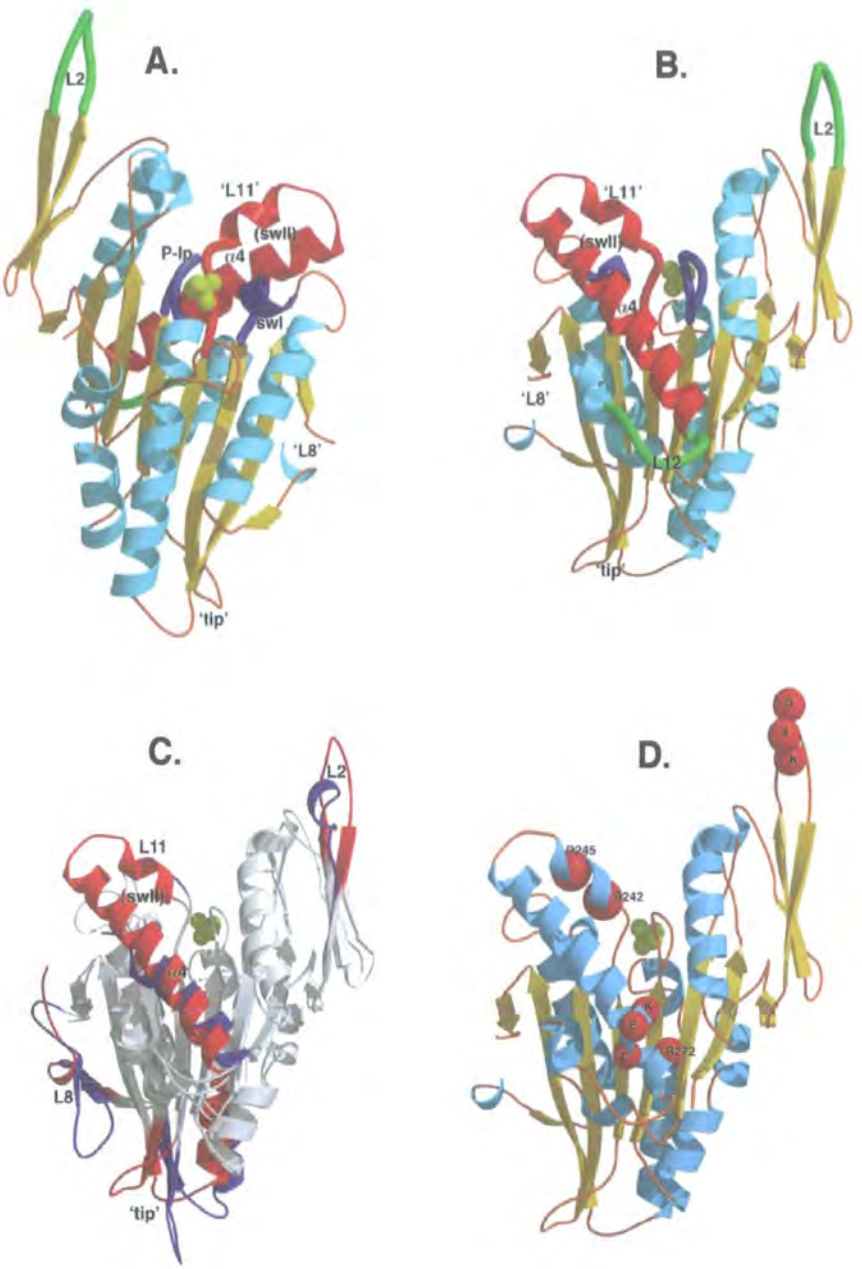

Structure images reproduced from Shipley *et al.* 2004 EMBO 23, 1422-1432 Structure of a kinesin microtubule depolymerisation machine.

Figure 6.7: (A-B) 3D structure of pKin I, MT binding surface (GREEN), nucleotide binding pocket (BLUE), Switch II (RED) Sulphate at β-phosphate position (YELLOW balls).(C) Comparison of pKin I with NCD, common elements (GRAY), differing pKinI parts (RED), differing NCD parts (BLUE). (D) Locations of pKinI amino acid substitutions in the Shipley *et al.* study (RED balls).

Kinesin core structures are usually 'arrowhead' shaped, with a central β-sheet region surrounded by α-helicies, and have always been found complexed with adenosine nucleotide (Kull and Enddow 2002). Most strikingly, the pKinI structure does not have a nucleotide in the ATP-binding site (Shipley *et al.* 2004) (**FIGURE 6.7 A & B**). Comparison of pKinI with the most structurally similar kinesin, NCD reveals that the largest differences are in the length of microtubule contacting L2, the positioning of the 'tip', the direction of L8 and the stability of switch II, which is ordered and forms a short two-turn helix (Shipley *et al.* 2004) (**FIGURE 6.7 C**). L8 does not form a long strand pair pointing towards the microtubule binding face as is the case for most gliding kinesins, but rather points in the opposite direction. In addition, the 'tip' is bent when compared to other kinesins but this region is also bent in Eg5 (Turner *et al.* 2001), however, in the opposite direction (Shipley *et al.* 2004).

Several residues conserved between KinI kinesins, which are located in the MT-binding regions, were mutated to alanines and their effects on MT depolymerisation and ATP hydrolysis assayed (**FIGURE 6.7 D**). The residues mutated include: Arg 242 and Asp 245 which are located in the switch II and stabilise L11, KVD (Lys40-Val41-Asp42) a conserved KinI insertion in loop L2 and KEC (Lys268-Glu269-Cys270) and Arg272 which are located in the major MT binding region (Woehlke *et al.* 1997) Mutation of most of these selected residues affect the depolymerisation activity of pKInI with KEC and KVD mutants showing no depolymerisation activity, R272A and R242A displaying significantly lower activities than wild type. The exception was mutation D245A, whose depolymerisation activity was the same as wild type. The KEC mutant no longer bound microtubules and had no ATPase activity in the presence of microtubules but had 27% activity in the presence of tubulin. In contrast, KVD was still capable of binding the microtubule lattice and also had little ATPase activity in the presence of microtubules but retained its full ATPase activity in the presence of tubulin. Also,

Figure 6.8: Alignment of KinI Kinesin Motor Domains with Mutated Residues

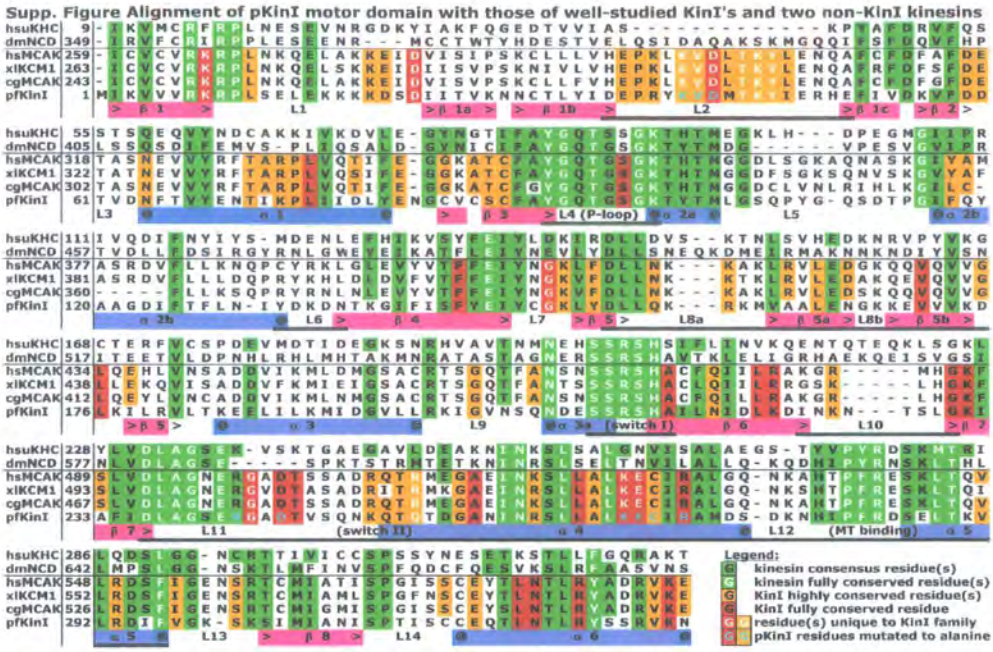

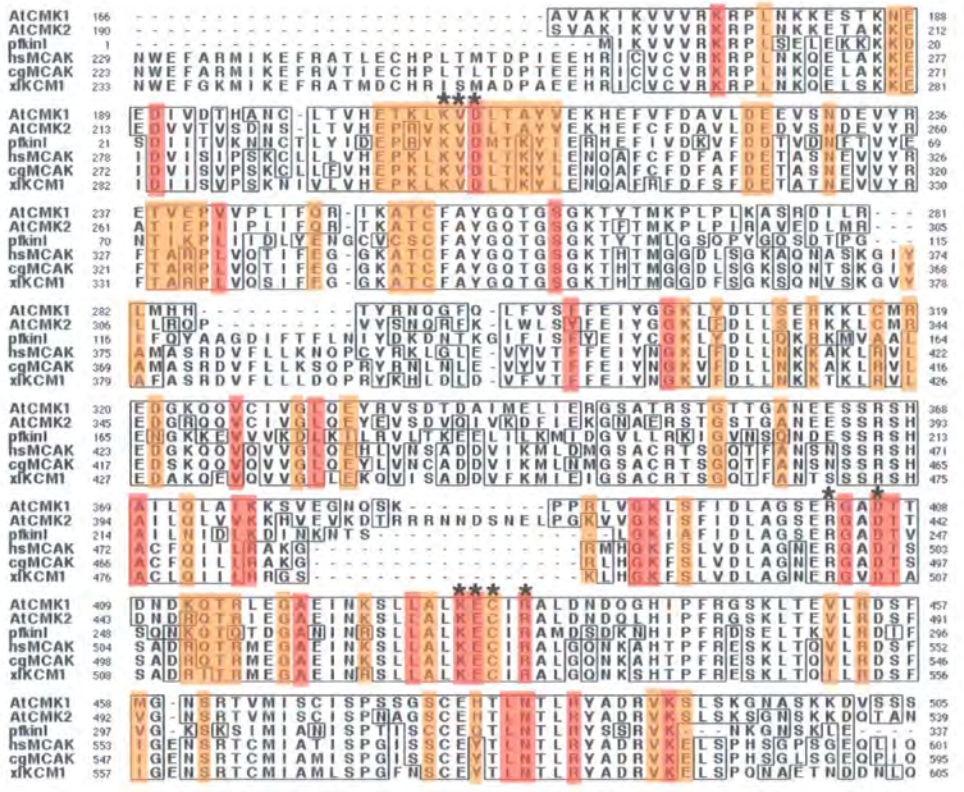

R242A and R272A showed only a half or third ATPase activity respectively. As with depolymerisation, the ATPase activity of D245A was unaffected.

The authors proposed that, based on these data, when the KinI has reached the microtubule end and lost its ADP, the switch II makes contact with tubulin at the interdimer interface, while L2 and the N terminal 'neck' provide anchor points. ATP binding induces a conformational change resulting in L2, the neck, L12 and L8 tugging and bending the protofilament. In the resulting curved filament, contacts between KinI and tubulin are maximized, possibly enabling L8 to contact tubulin. This stabilises the activation state, triggering ATP hydrolysis weakening the association of KinI with tubulin, leaving the kinesin free to bind a protofilament again (Shipley *et al.* 2004).

AtCMK2 has all of these residues (**FIGURE 6.8**)

6.11 Post-translational control, Phosphorylation of AtCMKs.

Sister kinetochores must attach to microtubules from opposite poles of the spindle for correct segregation to occur, a process known as amphitelic attachment (Cimini *et al.* 2002). However, there may also be incorrect attachment processes. Merotelic attachment is where a single kinetochore is bound by microtubules from both poles or syntelic attachment, where sister kinetochores incorrectly bind microtubules from the same pole, both of which result in mis-segregation of chromosomes (Nasmyth 2002).

(**FIGURE 6.9**)

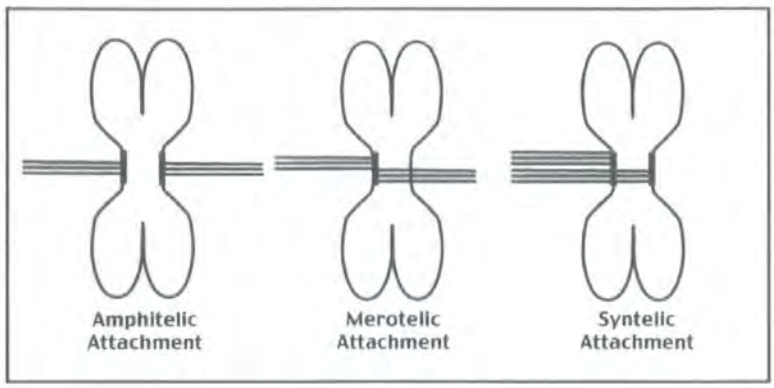

Therefore, cells must resolve these erroneous connections, a process in which the Aurora B family of kinases has been implicated (Tanaka *et al.* 2002). The Aurora B complex (**AURORA B : INCENP : SURVIVIN**) is found associated with chromosomes, concentrating at centromeres through the cell cycle and ending up at the spindle midzone where it later has a role during cytokinesis (Adams, Carmena & Earnshaw 2001). As discussed before XKCM1 is also found at the centromere, inhibition of which also results in missegregation (Walczak *et al.* 2002, Kline-Smith *et al.* 2003).

Considering their localisation and overlapping mitotic functions, Lan and colleagues speculated that Aurora B kinase was likely to promote chromosome biorientation by regulating kinetochore-microtubule attachment via XKCM1 (Lan *et al.* 2004). Indeed Aurora B kinase was found to phosphorylate XKCM1 at six sites within the neck domain and a region implicated in centromeric targeting of XKCM1 (Lan *et al.* 2004). Such phosphorylation was required for localisation of XKCM1 to centromeres and more specifically phosphorylation of serine 196 within the neck inhibited the ability of XKCM1 to depolymerise microtubules (Lan *et al.* 2004). Therefore, the authors concluded that Aurora B kinase biorients chromosomes by directing XKCM1 to depolymerise incorrectly orientated kinetochore microtubules.

Although the specific serine 196 and its surrounding area is not conserved between XKCM1 and AtCMK1 or AtCMK2, both do contain several putative Aurora

B kinase phosphorylation sites. In addition, Aurora B like kinases have been identified in plants.

6.12 Interplay of MOR1/GEM1 and AtCMK2

A model was proposed, based for MOR1/GEM1 and AtCMK interplay to explain the *mor1* phenotype (Hussey & Hawkins 2001). Considering these and other findings, it is possible to suggest two models to describe the effect of the *mor1* mutations on microtubule dynamics. At the permissive temperature a Kinl-like kinesin can bind to MOR1 at the N-terminal HEAT repeat. At the restrictive temperature a conformational change in the protein, caused by the *mor1* mutations releases the kinesin, which is now capable of depolymerising the microtubules (Model 1.). Alternatively, MOR1 decorates the microtubules at the permissive temperature, stabilising the long microtubules in the cortex. A shift to the restrictive temperature causes a loss of the N-terminus catastrophe-suppressing activity or microtubule binding capability of MOR1, enabling a Kinl-like kinesin to destabilise the long cortical microtubules (Model 2.) (**FIGURE 1.6**).

Kline-Smith and Walczak proposed a model for this interplay during the transition to mitosis from the point of view of XKCM1. XKCM1 is active in interphase cells, but its effect is suppressed by the stabilising activity of MAPs, such as XMAP215. On entry into mitosis, there is a sudden increase in MT turnover (Salmon *et al.* 1984, Saxton *et al.* 1984, Zhai *et al.* 1996), MT catastrophe frequency doubles and MT rescue frequency decreases 4 fold during mitosis (Rusan *et al.* 2001). Concurrent with this, the increase in MT turnover, the stabilising activity of MAPs, is decreased by phosphorylation (Cassimeris & Spittle 2001). This would then allow the catastrophe-promoting activity of XKCM1 to predominate as the cell transits into mitosis. The increase at this transition enables the cell to rapidly reduce the length of interphase MTs and increase their dynamic behaviour, thereby

promoting spindle formation and allowing MTs to effectively search and capture the kinetochores on chromosomes (Reider and Salmon 1998).

Recently, further studies have lead Holmfeldt and colleagues to suggest that the functional interplay of TOGp and MCAK proteins in human somatic cells can be separated into three distinct phenotypes during the cell cycle. The first involves a role for TOGp in protecting spindle microtubules from MCAK activity at the centrosome, a function essential to prevent the formation of disorganised multipolar spindles. The second phenotype involves TOGp-dependant counteraction of excessive MCAK activity during mitosis. The third involves the destabilisation of the interphase microtubules by over-expression of TOGp, a process which requires endogenous MCAK (Holmfeldt *et al.* 2004). (**FIGURE 6.10 A**).

The interplay between MOR1/GEM1 and AtCMK2 is unlikely to involve a direct interaction and therefore model 2 may be more probable. However, rather than simple competition for a MT binding site, the interplay between these two factors may be more complex, involving two antagonistic activities in the cell. Evidence suggests that MOR1/GEM1 may have a positive effect on microtubule polymerisation and stabilisation and AtCMK2, when over-expressed, can cause the depolymerisation and destabilisation of microtubules *in vivo*. AtCMK2 activity, although apparent, is opposed during interphase by MAPs, such as MOR1/GEM1. At the transition to mitosis, the stabilising activity of MOR1/GEM1 is reduced due to phosphorylation by a CDK. This allows the catastrophe-promoting activity of AtCMK2 to predominate, leading to reduction in length and an increase in dynamicity of interphase MTs, promoting spindle formation and capture the kinetochores as suggested by Kline-smith & Walczak. AtCMK2 may regulate kinetochore attachment by depolymerising incorrectly orientated kinetochore microtubules (Merotelic or Syntelic attachment), a process possibly co-ordinated by an *Arabidopsis* Aurora B kinase. Further to this, MOR1/GEM1 may still be involved

Figure 6.10: MCAK and TOGp Interplay

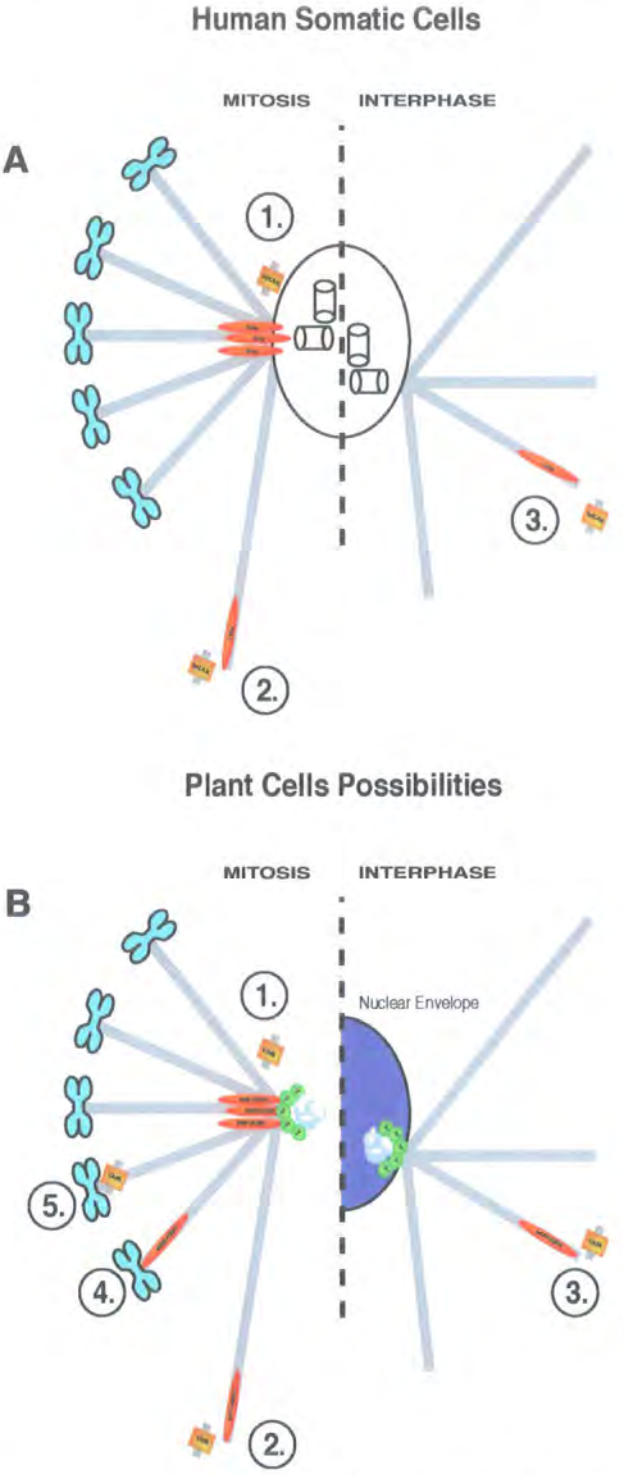

Holmfeldt three stage model of model of TOGp and MCAK interplay in human somatic cells (A). The first involves a role for TOGp in protecting spindle microtubules from MCAK activity at the centrosome, a function essential to prevent the formation of disorganised multipolar spindles (1). The second phenotype involves TOGp-dependant counteraction of excessive MCAK activity during mitosis (2). The third involves the destabilisation of the interphase microtubules by over-expression of TOGp, a process which requires endogenous MCAK (XMAP215/Stu2 previously shown to have destabilising anti-pause capabilities) (3). Such interplay may also exist in plants between MOR1/GEM1 and AtCMK2 (B). Further posibilities could be that MOR1/GEM1 and AtCMK2 both fuction at the kinetochore. MOR1/GEM1 could be required for capture of kinetochores and the promotion of stabilisation and addition of tubulin dimers at the + end (4). AtCMK could be required at the kinetochore to regulate the correct attachment of kinetochores to kinetochore microtubules, depolymerising those which are incorrect (5). The control of these to opposing activites is likely to be controlled and balanced through the cell cycle by kinases such as CDK and Aurora B.

in counteraction of excessive AtCMK2 activity during mitosis and protection of the minus end of spindle microtubules at the poles from AtCMK2 (**FIGURE 6.10 B**). There is also the consideration that MOR1/GEM1 may exhibit the properties of an antipause factor, as identified for XMAP215 and Stu2p.

6.13 Conclusions.

MOR1/GEM1 associates with all microtubule arrays throughout the cell cycle. During mitosis, in addition to labelling spindle microtubules, MOR1/GEM1 concentrates at kinetochores and during cytokinesis, labels the phragmoplast, where it is concentrated at the midzone. The *mor1* and *gem1* mutants have shown that MOR1/GEM1 is essential for the interphase cortical array and the cytokinetic phragmoplast. In *gem1* mutants, the MOR1/GEM1 protein is truncated and the missing C-terminal section can bind microtubules in *vivo*. Therefore, the phragmoplast defects exhibited in *gem1* may be due to the reduced microtubule binding of MOR1/GEM1. The yeast homologue of MOR1/GEM1, Stu2p, has been shown to interact with itself via a coiled coil and MT binding domain within the C-terminus of the protein, however such oligomerisation has not been shown for other members of the family. Yeast two hybrid studies have shown that the C or N termini of MOR1/GEM1 do not interact with each other or themselves indicating that MOR1/GEM1 may act as a monomer. Further experiments have shown that the N terminus of MOR1/GEM1 is also capable of binding microtubules and causes a significant increase in the turbidity of microtubule solutions, however whether this is due to increased polymerisation or bundling is as yet unknown.

The MOR1/GEM1 contains several HEAT repeats, one of which contains a point mutation in the *mor1* mutant. The presence of these protein - protein interaction sites suggest that MOR1/GEM1 is likely to be capable of interacting with several proteins and these interactions may be important for the role of MOR1/GEM1 within the cell. Several interactors have been identified in other organisms such as

Spc72p, Cyclin B1, TACC, Bik1 (EB1) and Bim1 (CLIP170), however not all of these proteins have been found to have reliable homologues in plants. In addition to these, it is essential to identify plant specific interactors of MOR1/GEM1, which may help to further characterise the involvement of MOR1/GEM1 in the unique plant microtubule arrays; one such candidate could be SPR1.

Arabidopsis contains two Kinl-like kinesins, AtCMK1 and AtCMK2. AtCMK2 associates with all microtubule arrays through the cell cycle and is particularly concentrated at the PPB and Metaphase spindle where individual microtubules are labelled. AtCMK2 shows no significant concentration at kinetochores or spindle poles although the kinesin is present at these sites. In confirmation of the localization of the kinesin *in vivo*, recombinant AtCMK2 also binds purified pig brain microtubules *in vitro*. AtCMK2 GUS promoter fusions indicate that AtCMK2 is expressed in all *Arabidopsis* tissues and organs during development, a similar programme as for MOR1/GEM1. AtCMK2 can form dimers via a coiled coil situated in a domain within the C terminus of the kinesin, which is highly conserved between plant Kinl homologues. Further interaction experiments have shown that neither AtCMK2 or AtCMK1 interact with the C or N terminal regions of MOR1/GEM1. Over-expression of AtCMK2 as a GFP fusion protein in *N. benthamiana* results in short, disorganised microtubules suggesting that AtCMK2 can depolymerise microtubules *in vivo*. Considering these data, AtCMK2 appears to be a true functional plant Kinl kinesin.

AtCMK1 is very different from AtCMK2. AtCMK1 does not locate to any of the plant microtubule arrays but rather locates to structures within the cytoplasm, which may be organelles such as golgi vesicles. As for AtCMK2, AtCMK1 can form dimers via a coiled coil. AtCMK1 GUS promoter fusions show that AtCMK1 is expressed in specific organs and tissues in contrast to AtCMK2. AtCMK1 is expressed in ovules/embryos, funiculus and the vasculature or cell files associated with it. The strongest and most striking expression of AtCMK1 is in the lateral root primordium,

Figure 6.11: Summary of the Localisations of MOR1/GEM & AtCMK1 and AtCMK2 Through the Cell Cycle.

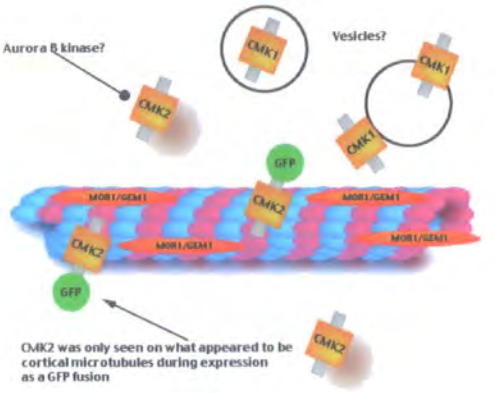

Interphase, Cortical Array

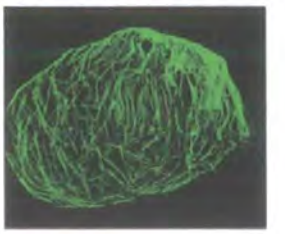

Interphase, Preprophase Band

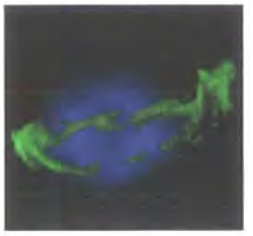

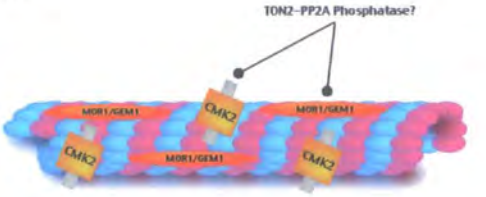

Mitosis, Spindle

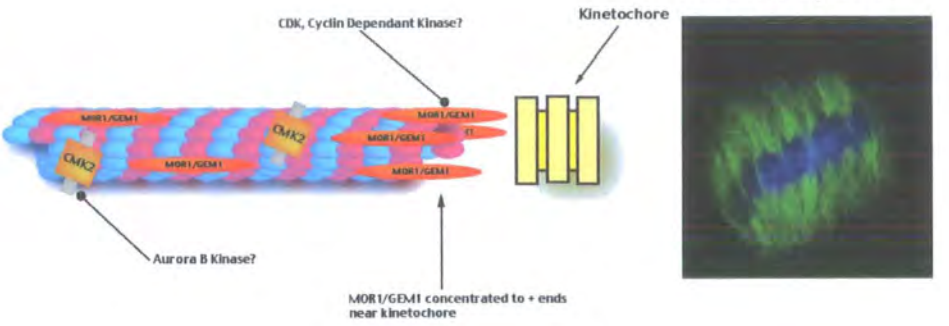

Cytokinesis, Phragmoplast

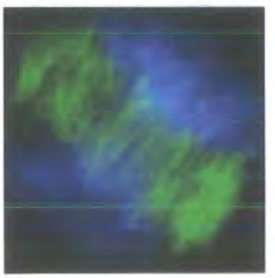

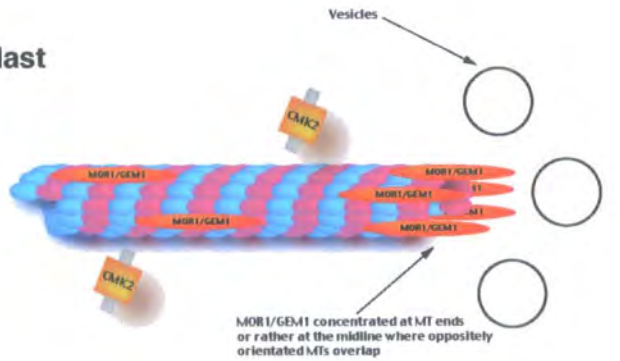

appearing at the site during early divisions even before a protrusion is observed. AtCMK1 may have a role in these divisions and differentiation of the pericycle to form the lateral root.

FIGURE 6.11 shows a summary of the localizations of MOR1/GEM1 and AtCMK kinesins through the cell cycle and the some of the possible signals which may control this localization and the balance of these to factors activities.

6.14 Future Work and Perspectives.

The work outlined in this thesis, when coupled with observation by other researchers, supports the existence of XMAP215 and Kinl proteins in *Arabidopsis* and that the function and possible interplay of these factors may be generally similar to the antagonistic relationships in animal and fungal cells. Although the plant microtubule cytoskeleton and its associated proteins show similarities to those of animals and yeast there are also many differences. The plant cell has three unique arrays, the cortical array, the preprophase band and the phragmoplast which coordinate several processes absent in animal cells, in particular the formation of the cell wall. In addition to this plant tubulin and microtubules show differences in dynamicity where plant microtubules are more dynamic and persist in the treadmilling state for longer (Hush *et al.* 1994, Yuan *et al.* 1994, Moore *et al.* 1997, Shaw *et al.* 2003). These fundamental differences would suggest that MOR1/GEM1 and AtCMK kinesin also show unique properties in the plant cell. The dynamics of the interaction with plant microtubules for MOR1/GEM1 and AtCMK kinesin may be different from their counterparts. Recent evidence suggest that the interaction of MAP65 with microtubules is extremely dynamic with the rate of MAP65 recover following photo-bleaching several times faster than the recovery of tubulin itself (Smertenko, personal communication). Moreover identification of novel plant MOR1/GEM1 and AtCMK kinesin interactors, could then provide new insights into how the unique microtubule arrays are co-ordinated.

With these aspects in mind, future work with MOR1/GEM1 will involve the identification of interacting partners both through yeast two-hybrid and biochemistry. Also the *in vivo* and *in vitro* dynamics and interplay of both MOR1/GEM1 and AtCMK2 will be studied further.

Appendices

Appendix A. Vectors & Contructs.

Vectors.

pACT2	Kan	Y2H-Activator
pAS2	Kan	Y2H-Binding
pBI101G	Kan	GUS Expression
pDONR207	Gen	Gateway Entry Plasmid
pET28a	Kan	6xHis-Tag Fusion Protein Expression
pGAT4	Amp	6xHis-Tag Fusion Protein Expression
pGEMT Easy	Amp	TA cloning
pGWB6	Kan/Hyg	Plant GFP Fusion Protein Expression, 35s
pTOPO2.1	Kan/Amp	TA cloning

Contructs used in this study.

pACT2[AtCMK1]
pACT2[AtCMK2]
pACT2[MOR1 CT]
pACT2[MOR1 NT]
pACT2[PCD]

pAS2[AtCMK1]
pAS2[AtCMK2]
pAS2[MOR1 CT]
pAS2[MOR1 NT]
pAS2[PCD]

pBI101G[AtCMK1 Pro]
pBI101G[AtCMK2 Pro]

pDONR207[AtCMK1 AB]
pDONR207[AtCMK1 Pro]
pDONR207[AtCMK1]
pDONR207[AtCMK2 Exp Frag]
pDONR207[AtCMK2 Pro]
pDONR207[AtCMK2]
pDONR207[MOR1 CT]
pDONR207[MOR1 NT]
pDONR207[PCD]

pET28a[MOR1 CT]

pGAT4[AtCMK1 AB]
pGAT4[AtCMK1]

pGAT4[AtCMK2 Exp Frag]
pGAT4[AtCMK2]
pGAT4[MOR1 CT]
pGAT4[MOR1 NT]

pGWB6[AtCMK1]
pGWB6[AtCMK2]

pTOPO2.1[MOR1 CT]

Cloning Strategies.

PCR Product	→ Entry Clone	→ Destination Clone
MOR1/GEM1 CT	TOPO2.1[MOR1/GEM1 CT]	pET28[MOR1/GEM1 CT]
MOR1/GEM1 CT GW	pDONR207[MOR1/GEM1 CT]	pACT2[MOR1/GEM1 CT]
		pAS2[MOR1/GEM1 CT]
MOR1/GEM1 NT	pDONR207[MOR1/GEM1 NT]	pACT2[MOR1/GEM1 NT]
		pAS2[MOR1/GEM1 NT]
AtCMK1 AB	pDONR207[AtCMK1AB]	pGAT4[AtCMK1AB]
AtCMK2 Exp Frag	pDONR207[AtCMK2 Exp Frag]	pGAT4[AtCMK2 Exp Frag]
AtCMK1	pDONR207[AtCMK1]	pGAT4[AtCMK1]
		pACT2[AtCMK1]
		pAS2[AtCMK1]
		pGWB6[AtCMK1]
AtCMK2	pDONR207[AtCMK2]	pGAT4[AtCMK2]
		pACT2[AtCMK2]
		pAS2[AtCMK2]
		pGWB6[AtCMK2]
AtCMK1 Pro	pDONR207[AtCMK1 Pro]	PBI101G[AtCMK1 Pro]
AtCMK2 Pro	pDONR207[AtCMK2 Pro]	PBI101G[AtCMK2 Pro]
PCD	pDONR207[PCD]	pACT2[PCD]
		pAS2[PCD]

Appendix B: Web Addresses Bioinfomatic servers used.

BLASTP	http://www.ncbi.nlm.nih.gov/BLAST/
BLASTN	http://www.ncbi.nlm.nih.gov/BLAST/
TBLASTN	http://www.ncbi.nlm.nih.gov/BLAST/
SMART	http://smart.embl-heidelberg.de/
PSORT	http://psort.nibb.ac.jp/form.html
IPSORT	http://www.hypothesiscreator.net/iPSORT
TargetP	http://www.cbs.dtu.dk/services/TargetP/
PlantCARE	http://intra.psb.ugent.be:8080/PlantCARE/

Affymetrix GeneChip Data
http://affymetrix.arabidopsis.info/narrays/spothistory.pl

Appendix C: CDNA & Protein Sequences

Arabidopsis thaliana MOR1/GEM1

DNA Sequence:

ATGTCGACGGAGGATGAGAAGTTATTGAAGGAGGCGAAAAAACTTCCTTGGGAGGATCGGCTT
GGGCATAAGAATTGGAAAGTTAGGAACGAAGCTAACGTCGATTTAGCTTCTGTTTTTGATTCGA
TTACTGATCCTAAGGACCCTCGTCTTCGCGATTTTGGTGAGTTTCTCTACCTCGTTTTTTTATTA
TTATTATGTTAGGGTTTTTGTTTTTGAAGCTCAGATCTGATTAGGGTGGTTTATATCGGTGTGGA
TCTGTTTTGAATTTGGATTGTTGAGTGGGAATGTGATTGGTCTAGGGTTCCATTTTGCTTTACTT
TTGATTGAATTTCTGATTATTATTTTTTATTCGCAGGTCACTTGTTTAGGAAGACGGTGGCAGAT
TCTAATGCGCCGGTGCAAGAGAAAGCGCTTGATGCATTGATTGCGTTTTTGCGAGCAGCCGAT
TCAGATGCTGGAAGGTATGGTGTTGTTTATTTTTATTGCTTTAGAAATGGGCAGAGTGGAGTGT
TCGTTTGCATGTGAATAATTAGTTTGTTTCTGCTTTTGAAGGTATGCAAAGGAAGTTTGCGATGC
TATTGCGCTCAAATGCCTTACGGGTCGGAAGAATACTGTGGACAAGGCGCAGGCTGCTTTCTT
GCTTTGGGTAGAATTAGAGGCCGTCGATGTTTTTCTGGTATGTCATTCATTCTATGTTTTTGCAA
CACTGCTAGGGTTATCTAGACACATACGGTTAACCCTTGCACTCTGATGTATAGGTTCACCATC
TAGCCATAGAGTTACTTGCTAGATTGCTGATACTGGTATCTGAAACTAGATAGGTGAGCTGACA
TAGAAATGAAAGTGCTTTATAACCCAGAATTCAACCATATACTGATCTTAGAAGGAGTGACGTA
GAATATAGCATTGTGGCTCTTTGTCCAGTTCTGTGTTATGCTAGGTATCTAGTGTGGCATAGGA
AAAGAGCAATTTAAATAACGATGACTGACAGATGTCCTGAGCATCCTGTGTTCAAGGTCAAGAA
ACAGAATCAACTTTCTGGGGTCTGTTCCTATAATCACCCTCTTCAGTAACCAACATTTCCAGTTT
TGAGTTGTTGTCACCGTGTCTCAAGCTGTTGGACTTCTGCTATGAATAATACTTATTTCTGAAG
GAGAAAGGAATCTAGATACCTTCTTTATTGTTGTTTTCAAGATATCTACCATAGTGTTTTGTTCA
AAACATCATTTCCTTCAGAAGTTTTAATTCACTTCCCAAGTATAAAGTTGCAATAACTCTACTTGA
TATGCATTGTTTCAGTCATTTCAATTTTCAACTGCCAACAAGATATATATTGGGAGACTGGGAGT
TGTATAGTTTATAGGATAACATCGTTTTTATACATGCTAACAGATTTGGCATGATTGTAGGATAC
GATGGAGAAAGCTATAAAGAATAAAGTTGCAAAGGCTGTGGTACCTGCAGTAGACGTTATGTTT
CAAGCTCTAAGGTCTGTTTTCAACTCCTTGTTAGTTTTCTCCATTGGTTCATGAAATCTTTTATCT
GAAATATCGACACTACTTTATTTCTACCTTAGTGAATTTGGATCAAAAGTTATTCCACCTAAAAG
GATTTTAAAGATGCTTCCTGAACTTTTCGACCATCAAGATCAGAATGTCCGTGCATCTGCCAAA
GGAGTGACTCTTGAGCTATGCCGTTGGATTGGAAAAGACCCTGTAAAGTCTATATTGTTTGAAA
AAATGAGGGATACGATGGTAAGATTTATGTTGAGCCGCACATTTGCAACTTAGCTATGCTGCCA
AGTTGATATGAACTGGATTAAATCCTCTTGATTTTTCTTGGAATTGGAAAACTGAAACAGGGGTT
TCTAGTCATAACAGATAGATAGATGATAGATCCCATTGCGGATAAGAACCACACCTTACCTGTA
AATTCTGCCCATGATTTGCGTTTTTCTTTAATCAGTGGAAGAAGTTACACTTGAATTTTTATTTAT
TCTCTTGTGCTTTGTTGCAAACCCTAATATTCCGTTTCATTGTTACTATGTAAGAAAAAAGAGCT
GGAGGCTGAGCTTGCCAATGTTACAGCGGGTGCCAAGCCTACTCGAAAGATAAGGTTACTACC
ACATACGATAATAATTGTTGAATTTTCCTAATTATTCATTGGCACATACATCTAATATATTTTGAC
ATTTATTGGTAAGGTAAAACCAGATCCAGTTTCACCGTAATTCAGCCTATGCTTTGTGAATACTC
AATGTGCCTCTGTCAAATTTCTGAATAATTGAATTGATATGCATGAGTATTTCTTTTTGGTTTCAA
GACCTTTTTCTAGCCTGTGTGAATTTTAAAGTTGAAAAAGTAAAGCTGCAATGAGATTATTTCTG
TATTTGGCTTTCAAGATCTGAGCAAGACAAGGAACCAGAGGCAGAAGCTAGTTCTGATGTTGT
GGGTGATGGGCCCAGTGAAGAAGCTGTTGCTGACGGTAAGTAGCTTGTACCTCAATGAATTGT
TCTTCATCAAGTAATAATGAGAAGTCTGCTTACATTGTTTTTTCTTTTATCTACCCGTACTATCAG
CGCCTCAAGAAATAGATGAGTATGATCTTATGGATCCTGTGGACATTTTGACACCTTTGGAGAA
GTCTGGGTTCTGGGACGGAGTGGTGAGTTTTGATGCTTAATGCACATTTTACTATGTTTTATTT
CTTGTGGTTGTCTTTCACTGAAAGAACTTTTTTATACTATACCACTTACTTCTCATGTTGATTGCA

TGTGGCACATTACACTAACTAACGATGTATCCCTTATAGAAAGCTACAAAGTGGTCCGAACGTA
AAGAAGCTGTTGCAGAGCTAACAAAGCTTGCTTCGACTAAAAAGATAGCTCCTGGTGATTTTTC
AGAAATTTGTCGGACTTTAAAGAAGGTAGTTAACTTTCCATGATAAGAAGTTTAGGCAGCATTG
ATTATATGTATATGTTATAATCCTTGTTATGTTTTATTCCGTAAGTGGAATATTATCTAATTGGTG
ATGATGCAGCCTGCAAACATCTGTGCTTATTGATTAATCTGAAGTTCGAAGTTCATGCGTTTCA
AAATGTTTTCTGGTCGCAATCATAGTTTGTGGATGCTGCTATTGTTCAGGATTCAATACTGCATA
ACTAATTTTGCTTTCGTTTTGATAATATTTGTAAATATTTCCAATTGCAGCTTATCACGGATGTGA
ACTTGGCCGTTGCAGTTGAAGCTATTCAAGCCATTGGAAATCTTGCATGTGGTTTAAGAACACA
TTTCTCTGCTAGTTCACGGTTTATGCTGCCTGTTTTACTTGTGAGTCATGTAGCATCTTTGATCG
AAAAGTATAATTGGAGGAAGACGCTTCCAGTCTTATGAGTGTTAATACTATTTCTTAGATATTAA
TGGGCTTAAGTAGCTGACTTGGTTTTAGTCCAGGAATTGATACAAAATTGCTGTCTGTTTGTTC
CTTGAACAGGAAAAATTGAAAGAGAAAAAGCAATCAGTCACAGACCCACTTACACAAACGCTAC
AAACAATGTACAAAGCCGGGTGTTTGAATCTTGTTGACGTTATAGAAGGCAAGAGTCAGTTTAT
CTTGGATTTTATTTTATGAAGCTCTACTGATTTGCTTATGATTATCTTTTTTAGATGGCGACCAAT
TTTGCTTAAGCATCTGTCTTTCATCAGTTTCCAATCAACTTTACTCTCTTTTGCAGATGTGAAGA
CAGCAGTGAAAAACAAAGTTCCACTTGTGCGTTCTTCAACTTTGACCTGGTTGACATTCTGCCT
TGAAACAAGTAACAAAGCTCTTATTCTAAAGGCTCACAAAGAATATGTCCCTTTATGTATGGAG
GTTAGTTTTCTTGCGCCAAATGGCTCCTAATAATACTTTGACTGAACTTTAAAGCATGGCACTGT
TAGATTAGCTATATGCAACAAGTTAGTGCTAAAAAGACAGACAACGTATGTCATGTTGCAGTAT
TATGATTAGTTGGTGTAGCGAAAGCCTGGAGTTTTGATTGCAGTTACCCCTTCTAAGTTTGAAA
TTAATCAATGGTTTGAACTTATAACTTAATTGGATGCCTGAAATTTGTAATGATGTAGTGTCTCA
ACGATGGAACTCCTGATGTGAGGGATGCAGCATTTTCGGCTTTGGCTGCAATAGCTAAGGTAT
TAATTTTATATTGTGCTTTGTAACAGCAACCTTTTTGCGTTGTTGTCTGTGGTACATTAATGTTGT
ACACATGTTAGAATATGTGGATAAATGAGTATCGTTTACTTCATGTTTTACTATTCCCGTTTGTTT
ATTATCTTTTGGTTATTTTAGTCTGTAGGTATGAGACCTTTGGAAAGGTCGTTGGAAAAACTTGA
TGATGTTAGAAAAAAGAAACTTTCAGAAATGATTGCAGGCTCTGGTGGTGGTGACCAAGCTGG
TACAAGCTCAGGTTTGTGGACTTTTCGTACTCGTTAGCTAAACATCAAGTTTTGTTTGCGGGGG
TTTTCCCATTCTAATTGGATGCTCTTTTCATATTAAAGTGACAGTTCAGTCTTCAGTTGGGAGCA
CAGCCACAGGGGTACGCTTCTATCTATATCTTCAGGGTCAAATAATATTTAGTTCTATAAAACGT
TTTCTCTTCCCCTTTTGATGGGATAAGGGTAGGGCATCTGGGATGTGGAGATGTAGCTGGTAT
TAGATGCCTTGTCTTTTCCCATCGTGTTGTCTAAGAGTTTGAATGGGTTTTATGTCTTGTATCTA
TTTGCCTAGTCGCTCTTATAACATTAGTGTCTCCACAATCGTTATACCACTTCAAAATTTATGCA
GAACTCAGACGCTTCCTTTGTAAGGAAATCAGCTGCAAGCATGTTGAGCGGCAAAAGACCCGC
TCCTTCGGCTGTGAGTTTTTTCATACTTTTTCTTTTGTGGCTGTTGAATCCTGCAATCATTTGGG
GTTTCATGACACTTGCACGCCTTTTCCTTTTCTCTTTTGTTCTCAATTCCACTATGACTTGGACG
TCACATTGTATGTTAACATTTTATAGCAGGCGAGCAAGAAGGTTGGGACTGGCAAACCGGGTG
GAGGCAAAAAAGATGGATCTGTAAGGAATGAAGGTTCAAAATCTGTTGAACCACCTGAAGATG
TCGAGGTACATAGAAATATAATTATAAATGGTTATGTGATTTACTATGTCCTTCTTCAGACTTTG
ATGGTATTAATATCTTATTCTTCTTTGCATTTTAGCCTGCCGAGATGGGTCTTGAAGAGATTGAA
AACAGATTAGGTTCTCTTGTGAAACCAGAAACTGTATCTCAGTTAAAGAGCTCTGTTTGGAAAG
AAAGACTTGAAGGTTTGTTAAAGGCCTTGAGGACTCTTTTATTCTCAAATACTGTTATCTTCATC
ATTAGTTCTTACTTCCTTCTTTGTTCATTTCTTTTTGCGTTTTGCTTGGGTGGTTAATCTCATTTT
AAGTGGTTCATCATCAAATTTTACCACACATAGGATAAATCTGTTGCGCAAGGTTCCTGAATTG
ATATTAAAGCTCTATTTCATGTTGCCTCTTATTGCTTCAGATCAAAGCTGCATTAGCACATGTCA
CAGAATCTCTTTGCTAGCTCTTTAAAAAAAAAGTATTTATCAGTTTGGTGATTTTTTGCATTATAT
TGCCGTGCAGCAACTTTGGCTTTGAAAGAAGAGATAGAAGGTCTACAAGAACTAGACAAGTCG
GTGGAAATCTTGGTCCGGTTGCTGTGTGCTGTTCCTGGTTGGAATGAGAAAAATGTGCAGGTA
TGCTCTAATTCTATCTAAAATCTTCTTATTTGTAGTTTTAAGAATTGATTTCCCCCAAAATATTTAA
AGAAGTACATGAGCATATTACTTGAAAATGCAGGTTCAGCAACAGGTCATTGAAATCATCACTT
ATATATCTTCGACTGCAGCGAAGTTTCCTAAGAAATGTGTCGTACTTTGTATTACCGGTTAGTAT
CATATGAAGAAATACCTAGTTTCAGTTGATGAATGCTATTTTCTGACCTCAGTTGGTCTCTTTTG
AGAATTATTTCTTTTCTAATTTGCCTGATTTTTCTATTAATTCATTAGGCACTAGTGAACGAGTTG
CAGATATAAAAACAAGAGCCTCTGCTATGAAGTGCCTTACTGCTTTCTGTGAAGCAGTTGGTCC

TGGATTTGTTTTCGAGAGGGTATGTGCTGGTTCGGTCAACTTTCTTTGACTTTCATTTTATTCTG
ATCATAATGACATATGGCTTTTGTTTGTAGCTTTTCAAAATCATGAAAGAGCACAAGAATCCCAA
GGTTCTTAGTGAAGGCTTGTTATGGATGGTTTCGGCAGTTGATGACTTTGGTGTCTCACTTTTG
AAACTTAAGGTTTTGAAGATTTTTCTACTTGGAAATTCCCATATCCTGATTTCCCTGTTTATGTAA
CTGCAGTATCTAGGTTATTAATATTATGACCCAGGAGACTTTTGTGTTCATTTGGCAGGATTTGA
TAGATTTTTGTAAGGATGTTGGGCTGCAATCTAGTACAGCTGCCACCAGAAATGCTACAATTAA
ACTCTTGGGTGCTTTACACAAGTTTGTTGGTCCAGGTGGCTACGAATTCCTTTAAGCTGGTTCA
GCTTTGTCTAAATTCTGTTTGGTAGAATAACTTATCTTAACACTGAATCAAACTTATGTTTTTCTG
TTTTCAGACATTAAAGGGTTTCTTAATGATGTCAAACCTGCACTACTAAGTGCACTTGACACCG
AATATGAGAAAAACCCTTTCGAGGTACAGTTGTGTGGATTGCCTTGATTTGTCTAGTTCTTGTTT
TTCTTGCTGTACTTATATTATGTTCATCAGGGGACTGCGGCTCCAAAGAGAGTTGTTAAGACGT
CAGTTTCAACATCAACATCTTCTGGAGGGTTGGATAGCTTACCTAGAGAAGATATCAGTACCAA
GATTACACCTAATCTCCTTAAGGGCTTTGAGAGTCCTGATTGGAAGGTGCTCTTGAAATTGGAA
GTCTTCTTTTGTTGTCTAAACCTATCAATTTCTTTGCGGAAATTTATTTGAAGCTGTAGAGTTAAA
ATTGAGTCTTTTAAACTTTTGTAGATGCGTTTGGAGTCAATTGAAGCTGTCAATAAAATTCTGGA
AGAGGCTAATAAACGTATCCAACCAACTGGAACTGGTATGAAGTCAGAAATTTCCCCCATAATT
CTCTCATTCTCTGTTATTTTAGATTTATCATACCAATGTTAAGTCACGATTCCTTATTGTTTATAT
GAACCCTTCCTGTTCAATAGGAGAATTATTTGGTGGTCTTCGAGGACGTCTGTTGGATAGTAAC
AAAAATCTTGTTATGCAAACATTGACTACTATTGGAGGTGTTGCAGCAGCTATGGGACCAGCTG
TCGAGAAGGCGAGCAAGGTTGGTTATACATGTCATGCATTGAAAATAGTATGTACACTGTAATC
ATAGTATCACTGTCTGCCATTTTTACCAAGTACTTGAGTTATCTACCTCAGGGAATTCTGTCTGA
TGTTCTGAAATGCCTCGGTGACAACAAGAAGCACATGAGAGAGTGTACCTTGGCTGCTCTTGA
CTTGTGGCTTGGTGCTGTGCATCTTGACAAAATGGTTGGTGATAATCTTTTTGAGCCATGTCTT
CGCTTGTTGATATAATTTCGTTGACTTCAAATATTTTTTATTCTGTTAATGCAGATTCCTTACATT
ATAATAGCCCTAACAGATGGGAAAATGGGAGCAGAAGGTCGTAAAGATCTTTTTGATTGGTTGA
CAAAACAACTTACTGGATTAAGTGACTTTGTGGATGCCATACATTTACTAAAACCTGCGAGCAC
TGCAATGACGGTGACTCATCTAAAAATGTTATACCGTCTTATCAGTTTCCAACAGTGATTACGA
CTGTTTGTAATGATTTCAATTTGTTATGCTTCAATGTATCTTTCCAGGACAAATCAGCAGATGTG
AGAAAAGCAGCCGAAGGATGCATTTCTGAGATCTTGAGAGTCAGTGGACAAGAAATGGTAGAT
ATCCTTGGGTTAACTTGTTCTATTCAGGGCTAGAATTCAATATCTGATTAGATGTCTGTATTTGT
CTCAGATTGAAAAGAATCTTAAAGATATCCAAGGCCCAGCATTAGCTCTTGTGCTTGAAAAAGT
AAGACCAGGATTCGTTCAAGGTACCTCTCCATGATCTGGTTGTCTGATTAGCATGTTTTCTCCT
CGTTGTTTGCTTTTTTCTGTTCATGCTAATGATGTTGTTTTCAGAACCATTTGAATCATCAAAAG
CTATGGCGGGGCCAGTGTCAAAAGGTGTTACAAAGATTTCAAAATCAACTTCTAATGGTACCTT
AAAGCAAGGAAACAGATCAGTAAGTTTCTGTCTCCTAACATTTTTTTTGTTTTCAATTTATATTAT
CTGACTTGTTTTGTGTTTCTGAAGAGAGCCGTACCAACAAAGGGCTCAAGTCAAATTACGTCTG
TCCATGATATAGCTATCCAGTCACAGGCTTTGCTAAATACTAAGGACTCCAATAAGGTGGGATG
AGTTTTCCAAAGGTTTACAAAATATTTCCACAGGTATTGTATAGGATGATGTAAGGTTGATTTTT
GTGTGTTTAATCTGCAGGAGGACAGGGAGAGGGTGGTGGTTCGTAGAATTAAATTTGAGGAGC
TGCGACCAGAACAGATTCAGGATCTTGAGGTTTGTTTTCTAGAGCATTTAACCAATGTTGGGTG
GTTGTTGGTGTTATAACCAATGTTGGGTGGTTGTTGGTGCAGAATGATATGATGAAATTTTTTA
GGGAAGACTTGCAAAAACGGTTGTTGAGTCCCGACTTCAAGAAACAAGTAGATGGGCTGGAAA
TCCTACAGAAGGTAGCAGCTATCTTATGTTAGAATGCGGATATCTTGTGTTGGAATCTTATTCAT
CTGCTAGATCTTTGTAATTTTCTTTAAAGTATTCTTCTTCCTTCTCACCACAGGCACTTCCATCT
GTTTCGAAGGAAATTATAGAAGTATTAGATGTACTTCTCAGGTGGTTTGTGTTGCAATTCTGTAA
ATCCAACACAACCTGTCTGCTAAAGGTAATTTGTAATGAATCTTCTGCTATTGTAGTTCATGTTT
GACACTGTTTTTCTTGCAAGAACAATGAAATTTATTTGCTCTGGGTAAGAATAGGTGCTTGAGTT
TCTTCCAGAACTTTTCAACACATTGAGGGATGAGGAATACTGCATGACGGAAGCAGAAGCTGC
AATATTTCTGCCTTGTTTAGCGGAGAAGGTTAGGCATCTGATATTAATCCAATTTCCTATGGTGT
TGGCCTCTTTCTAATCATTCCCGTTTATCTTTCTGTTTTAGAAAAAGATTGGTGCTTCAGTGTCT
TTATATTTAACTCCTTGTCCTTGGTGCAGTTGGGGCATAACATTGAAAAAGTAAGAGAAAAAAT
GCGGGAGCTGATGAAGCAGATCATTCAGGCATATTCTGTAGGAAAGACGTATCCCTATATTTTG
GAAGGTTTACGTTCCAAAAACAACCGGACGAGGATAGAGTGTACTGATCTCATAGGATATCTAC

TCGAGACTTGTGGAACTGAGGTAGTAGCAAGACTTGACAAATTATCTGATAGTCCTGTACTCCT
GTTCTGTTTGAATTCTAATATGCCTTTCTAAGCAGATAGGTGGACTACTTAAATACTTAAATATC
GTTGCAAGCTTGACAGCAGAAAGAGATGGTGAACTCAGGAAAGCTGCTTTGAACACCATGGCT
ACTGGTTATCAGATTCTTGGTAGGACATGAAATTCATGAGCTATTGCGAAGTTATAGTGGAATT
TTCTCAAAACATGCTGCCATGTCTCGCAGTGATTAGTGCACAATTTTGGCTTCTCAACGTTTCAT
AAAAACCTGGAATCTAACTATGATTTTGAAACGAATGTCGCACTTGGTTATCCATTCCCTTGAGA
GAACTATTTGCACTCGTTTCTTATTGTTTGGCTTGTTATTGCAGGTGCTGACATCTGGAAATATG
TTGGGAAGCTTACAGATGCTCAAAAGAGTATGATTGATGATAGATTTAAGTGGAAAGTAAGCTC
AAAATATGAACCATTTTTCTGCTTCCGTCTTGTATTTTTGAGTTTTATTTTCATAGTTTTGCCTGC
ATCAGGCCAAGGATATGGAGAAAAGAAGAGAAGGGAAACCTGGGGAGGCACGAGCAGCATTA
AGGCGTTCTGTTAGAGATAGCGGGTGCGTAGGTTACAGCATTAAGATGTTTTGGTAGCGACTT
ATTTGTACTTAGCATTAGCAATTAGCTGAAAGTGGAAGCCAAAAAGATAATCACATAAATTCCAA
GGCCTAATAATGCATTTTAGAATCACAAAATTATTTTAATGTTGTTTTTTGAGTAATCAGAAGCA
GAAAAGGAGTCTATGATGGGTTTAGTGTCTATAATTTATGACTTTCTGTTTGTTTCCAGACCTGA
GGTGGCAGAGCAAAGTGGTGACATTTCTCAAACAGTCCCTGGTCCTTTATTTCCAAGGTAAACA
TATACATAAGATTCTGGTGTTCACGTGGCTTCTATACACAACTCAATCTTTTTGCCCTCCCAGG
CAAAGCTATGGTATTTCCGAACAAATGCTGGAGAGGACCCCGGTACCTCGGACAATTGCTGGA
GTTAATGGCCCTACAGACTGGAATGAGGCTTTAGACATCATTATGTTTGGTTCTCCAGAGCAGG
TATCTGGCTTATGTGGTCCGATCTTGATATTATTTGTTTTGTTTGTTATGGAATAGCTTGTTCTGT
TTTTAAGGTAACAAAGAAATTTACTTGATATAGTTATAGTAATTCAGTTATCTAGTCAGTAACAAA
GACTTGGTTGTGAGGGGACGTTGACCATACTTATCACTTAACAGTTTTGTCATTTGAAAACTTA
GGTGATGCATATTTGAAGATCCTGCAAGTGTTGGTTTGTTTTTTATTTTCTTTTTTTTTTGTTTTA
ATGTGTTGCAGTCCGTTGAAGGGATGAAAGTTGTGTGTCATGAGTTGGCACAGGCTTCTAATG
ATCCTGAAGAGAGTGCAATTGATGAACTTGTGAAGGATGCAGATGGGCTTGTTTCATGCTTAG
CAAATAAGGTTTGCCTGAATAAACTTTCTTTGTCCATTTGTCATGAAGAACTACTTCCAATAATA
GTTTTTGCTGACCACCACTTAATTATTTTTGTTTTCTGTTAGGTTGCCAAAACATTTGATGTTAGC
TTGATGGGAGCTTCATCGAGGTCGTGTAAATATGTTTTGAACACACTTATGCAGGTAACTTCGT
GTGAATTAGTGATGCTGCTCTTCTTCATTAGCTGGCTAGCCCACTTAGATTTGTTTGTGAAGTT
CACTACTCATAAGTATGTATTTTTGCAGACATTCCAAAATAAAAAGCTTGCCCATGCAGTCAAAG
AAGGGACTCTTGAAAGCCTTATAACAGAGCTCTTGCTTTGGCTTCTGGATGAAAGAGTTCCACG
CATGGAAGATGGGAGTCAACTTCTTAAAGCTCTGAATGTTTTGATGCTTAAGATCCTGGTCAGA
TATTCGTTCCATGCTAAAGGTTTTCATCATATGTGGCTATGAAGTTCTCTGACTTCATTATTTTTA
TTTCTTGTTTTATTTAATTCAGGATAATGCAGATCGGACATCTTCGTTTGTGGTGCTTATTAGCT
TGCTACGTCCTCTAGATCCATCTAGATGGCCTTCACCTGCTACGGCTGAAGTTTATGCTGTCCG
GAATCAGAAATTCTCTGATTTGGTAGTTAAATGCCTTATTAAACTTACAAAGGTATTTTAGGACA
ATCATTGTTCACATAACTCAAGTAGTTGTTACGTACAGCCCTACTGTCTATTATGCAACACTTGC
CTTTCCTACTTGCTACAATCACAGTGTCAAATTGTTTAGTATTGTATATCTGATAATTGCTTGTCC
TTGTTAAGCTCCTCCAAAGCACCATATATGAAGTTGATCTTGATAGACTTCTTCAGAGTATCCAT
GTATATCTGCAAGATCTGGGAATGGAAGAGATACGTAGGAGGTACATCTCTTTAAATGCACTCT
TAGAAATTTTGCAAATCTATGTCTGTTTATTATGTGGAGATTTTTCGTACTTGGCAATACTAATG
CATTCTCGGTTGGTATTTTTTCCAATGAAAAGAGCTGGGGCAGATGATAAACCTCTGAGGATGG
TGAAAACTGTTCTACATGAACTTGTTAAGCTCCGCGGAGCCGCAATTAAGGGCCACTTGTCTCT
TGTCCCTATTGACATGAGGCCACAACCCATCATTCTCGCTTACATCGATCTAAACCTTGAGGTG
AGACCTCCTTAGTCGTCTAACTTCATGTCCAGAAATTTTGACAAATTTGCTGAAGCTGAGGGTT
TGGTCAAAGAGCGCATCCAAACTATTTGCTGTTTTACTATGTTTTGAGAAATTTAGACGCCATTG
GTAGTAACTATTTAAATACCTGCAGACTTTAGCTGCAGCAAGAATGTTAACTGCAACAGGTCCT
GTGGGCCAAACCCATTGGACAGATTCAACAGCCAACAATCCTTCACCTCCTGCAAATTCTGCC
GATGTTCAGTTGAAGCAAGAGCTTGGGGCTATTTTTAAGAAAATAGGTGACAAACAAACTTCCA
CAATTGGTCTTTACGACCTCTACCACATCACAAAGTCATATCCAAAGGTAATAGATATGACTATG
TATTTCAAGTCTCAATGTTTCCTGTTCTTCATGAACAAACGAGCCAAATTGTATGTACTTACAAC
CTCATCTTAATGCTTGTAGGTTGATATATTTTCCCAACTTCAAAATGCTAGTGAAGCGTTTCGTA
CTTACATCAGAGATGGTCTGGCACAGGTCTGTAACTAGTCTCCTAGCTTTTTACTATGATTTCG
ATAAAACTCAAGTTTTTTGTCTTGAAGTTTTGCAATCGGTTCTGTAGGTTGAGAAGAATGCAGCT

GCGGGAAGAACACCTTCAAGCCTACCGTTGTCAACTCCTCCCCCTTCGTCCTTAGCTCTTCCA
TCTCCTGATATTCCTTCCTTGTCCTCTTTAGATGTGAAGCCTTTGATGAACCCTAGATCTGATTT
ATACACAGACGACATCCGAGCCAGTAACATGAATCCTGGAGGTAGTTTCCTAGATCCTTATCCT
TCTTTGTCCTTCCTTGCGGTGTTTATATATATCTGTTAAAAACAAACATCTTTGGCAGTGATGAC
AGGGACGCTAGATGCAATCAGAGAAAGGATGAAGAACATGCAACTGGCTTCATCAGAGCCAGT
AAGCAAACCGCTGATGCCAACAAACGATAACTTATCAATGAACCAACAGAGCGTTCCCCCGAG
CCAAATGGGACAAGAGACAGTCCACACACACCCAGTGGTTCTCCCAATGGATGAGAAAGCATT
GTCCGGTCTTCAAGCCCGAATGGAGAGGCTCAAAGGTGGATCACTGGAACATATGTAG

Protein Sequence:

MSTEDEKLLKEAKKLPWEDRLGHKNWKVRNEANVDLASVFDSITDPKDPRLRDFGHLFRKTVADS
NAPVQEKALDALIAFLRAADSDAGRYAKEVCDAIALKCLTGRKNTVDKAQAAFLLWVELEAVDVFLD
TMEKAIKNKVAKAVVPAVDVMFQALSEFGSKVIPPKRILKMLPELFDHQDQNVRASAKGVTLELCR
WIGKDPVKSILFEKMRDTMKKELEAELANVTAGAKPTRKIRSEQDKEPEAEASSDVVGDGPSEEAV
ADAPQEIDEYDLMDPVDILTPLEKSGFWDGVKATKWSERKEAVAELTKLASTKKIAPGDFSEICRTL
KKLITDVNLAVAVEAIQAIGNLACGLRTHFSASSRFMLPVLLEKLKEKKQSVTDPLTQTLQTMYKAG
CLNLVDVIEDVKTAVKNKVPLVRSSTLTWLTFCLETSNKALILKAHKEYVPLCMECLNDGTPDVRDA
AFSALAAIAKSVGMRPLERSLEKLDDVRKKKLSEMIAGSGGGDQAGTSSVTVQSSVGSTATGNSD
ASFVRKSAASMLSGKRPAPSAQASKKVGTGKPGGGKKDGSVRNEGSKSVEPPEDVEPAEMGLEE
IENRLGSLVKPETVSQLKSSVWKERLEATLALKEEIEGLQELDKSVEILVRLLCAVPGWNEKNVQVQ
QQVIEIITYISSTAAKFPKKCVVLCITGTSERVADIKTRASAMKCLTAFCEAVGPGFVFERLFKIMKEH
KNPKVLSEGLLWMVSAVDDFGVSLLKLKDLIDFCKDVGLQSSTAATRNATIKLLGALHKFVGPDIKG
FLNDVKPALLSALDTEYEKNPFEGTAAPKRVVKTSVSTSTSSGGLDSLPREDISTKITPNLLKGFESP
DWKMRLESIEAVNKILEEANKRIQPTGTGELFGGLRGRLLDSNKNLVMQTLTTIGGVAAAMGPAVE
KASKGILSDVLKCLGDNKKHMRECTLAALDLWLGAVHLDKMIPYIIIALTDGKMGAEGRKDLFDWLT
KQLTGLSDFVDAIHLLKPASTAMTDKSADVRKAAEGCISEILRVSGQEMIEKNLKDIQGPALALVLEK
VRPGFVQEPFESSKAMAGPVSKGVTKISKSTSNGTLKQGNRSRAVPTKGSSQITSVHDIAIQSQALL
NTKDSNKEDRERVVVRRIKFEELRPEQIQDLENDMMKFFREDLQKRLLSPDFKKQVDGLEILQKAL
PSVSKEIIEVLDVLLRWFVLQFCKSNTTCLLKVLEFLPELFNTLRDEEYCMTEAEAAIFLPCLAEKLGH
NIEKVREKMRELMKQIIQAYSVGKTYPYILEGLRSKNNRTRIECTDLIGYLLETCGTEIGGLLKYLNIVA
SLTAERDGELRKAALNTMATGYQILGADIWKYVGKLTDAQKSMIDDRFKWKAKDMEKRREGKPGE
ARAALRRSVRDSGPEVAEQSGDISQTVPGPLFPRQSYGISEQMLERTPVPRTIAGVNGPTDWNEA
LDIIMFGSPEQSVEGMKVVCHELAQASNDPEESAIDELVKDADGLVSCLANKVAKTFDVSLMGASS
RSCKYVLNTLMQTFQNKKLAHAVKEGTLESLITELLLWLLDERVPRMEDGSQLLKALNVLMLKILDN
ADRTSSFVVLISLLRPLDPSRWPSPATAEVYAVRNQKFSDLVVKCLIKLTKLLQSTIYEVDLDRLLQSI
HVYLQDLGMEEIRRRAGADDKPLRMVKTVLHELVKLRGAAIKGHLSLVPIDMRPQPIILAYIDLNLET
LAAARMLTATGPVGQTHWTDSTANNPSPPANSADVQLKQELGAIFKKIGDKQTSTIGLYDLYHITKS
YPKVDIFSQLQNASEAFRTYIRDGLAQVEKNAAAGRTPSSLPLSTPPPSSLALPSPDIPSLSSLDVKP
LMNPRSDLYTDDIRASNMNPGVMTGTLDAIRERMKNMQLASSEPVSKPLMPTNDNLSMNQQSVP
PSQMGQETVHTHPVVLPMDEKALSGLQARMERLKGGSLEHM

Arabidopsis thaliana CMK1

DNA Sequence:

ATGAGCGGAAGACAGAGATCTGTTGCAGCGGCGGTGCATCACCAGAGGCAGCTCTCCGATAA
CCCTCTCGATATGTCTTCATCCAATGGCAGATGGCTTCAATCCACTGGTCTTCAGCATTTTCAG
TCATCCGCCAATGATTATGGATACTATGCTGGTGGGCAAGGAGGTGGTGGTCAAGCAGCAAGA
GGATACCAGAATGCTCAGAGAGGAAACGAGTTCTTTGGGGAACCAACTACTCCTCAATACGGT
GCTCGTCCTACCAACCAAAGGAAGAACAATGATGAATCTGAGTTTAGTCCTGGGCTCTTAGATC

TGCATTCTTTTGATACTGAGCTTCTTCCTGAGATTCCAGTCTCTAACCAATTGGATGGTCCCTCA
CTTTTCAATCCTAGTCAAGGTCAAAGCTTTGATGACTTTGAAGCTTACAACAAGCAGCCTAACC
GTAGTCGCGTGTTGGCTGAAAACTTGGCTGCTGAGAAGGAGAGGATGAATGCTGTTGCAAAGA
TTAAAGTCGTTGTGCGTAAGCGACCACTTAACAAAAAGGAGTCGACAAAAAACGAGGAAGATA
TTGTTGACACCCATGCCAATTGCTTAACAGTTCATGAAACTAAACTTAAGGTCGACTTAACAGC
TTATGTTGAAAAGCATGAATTTGTGTTTGATGCCGTGCTAGATGAGGAAGTATCAAATGATGAG
GTATATCGTGAGACTGTGGAGCCTGTAGTCCCCCTAATTTTTCAGCGCATCAAAGCCACTTGCT
TTGCATATGGGCAAACAGGTAGTGGTAAAACCTATACTATGAAGCCTTTGCCTCTTAAGGCTTC
AAGGGACATCCTGCGGTTGATGCACCACACATACAGAAATCAAGGGTTTCAGTTGTTTGTCAG
CTTCTTTGAGATTTATGGAGGAAAGCTATATGATCTCCTCAGTGAGAGGAAGAAGCTGTGCATG
AGAGAGGATGGTAAGCAGCAAGTGTGCATCGTTGGTTTACAAGAGTACAGAGTATCTGATACA
GATGCTATTATGGAGCTTATTGAGAGAGGAAGTGCAACAAGAAGTACTGGAACCACTGGTGCA
AATGAAGAATCCTCTCGTTCACATGCTATACTACAGCTCGCGATAAAAAAATCAGTAGAGGGAA
ATCAGTCAAAGCCCCCTCGCCTTGTTGGCAAGCTTTCTTTCATTGATCTTGCTGGAAGTGAACG
TGGTGCAGATACAACAGACAATGACAAGCAGACAAGATTGGAAGGAGCAGAGATCAATAAGAG
CTTACTCGCCTTAAAGGAATGCATTAGAGCTCTGGATAATGACCAAGGTCATATCCCTTTTAGA
GGCAGTAAGTTAACTGAAGTTCTCAGGGACTCCTTCATGGGAAATTCTCGTACTGTAATGATAT
CGTGCATATCTCCAAGCTCTGGATCATGTGAGCACACCCTGAACACCCTAAGATATGCGGACA
GGGTTAAGAGTCTCTCAAAGGGAAACGCCTCTAAGAAAGATGTATCTTCTTCGACCATGAACTT
AAGGGAGTCCACGAAAATTCCTTTGTCTTCTGCACTTCCAACTCCATCTAACTTTGATGATGAC
GTGAATGAGATGTGGACTGAAGAGAACGATGAATTTGATGCATCGGATTATGAGCAAGATAAA
CAAATGTGGAAGAAAAACGGGAAGCTAGAGCCATCCTATAACGGTATGGCACAGGAGAGAATC
CCGAAACCTACTATTCAGATGAAGTCACGAGACATGCCAAGGCCCGATATGAAGAAGTCAAAC
TCTGATGACAATCTAAATGCGCTTCTGCAGGAAGAAGAAGACCTTGTGAATGCACACCGTAAA
CAAGTTGAGGATACCATGAACATAGTGAAAGAGGAGATGAACTTGCTGGTTGAGGCAGACCAA
CCCGGAAACCAGCTAGATGGTTACATTTCAAGACTGAACACAATTCTATCTCAGAAGGCTGCA
GGTATACTCCAACTACAGAACCGTCTTGCTCATTTCCAGAAACGCCTTAGAGAGCACAATGTAT
TAGTCTCTACCACTGGGTACTGA

Protein Sequence:

MSGRQRSVAAAVHHQRQLSDNPLDMSSSNGRWLQSTGLQHFQSSANDYGYYAGGQGGGGQAA
RGYQNAQRGNEFFGEPTTPQYGARPTNQRKNNDESEFSPGLLDLHSFDTELLPEIPVSNQLDGPS
LFNPSQGQSFDDFEAYNKQPNRSRVLAENLAAEKERMNAVAKIKVVVRKRPLNKKESTKNEEDIVD
THANCLTVHETKLKVDLTAYVEKHEFVFDAVLDEEVSNDEVYRETVEPVVPLIFQRIKATCFAYGQT
GSGKTYTMKPLPLKASRDILRLMHHTYRNQGFQLFVSFFEIYGGKLYDLLSERKKLCMREDGKQQV
CIVGLQEYRVSDTDAIMELIERGSATRSTGTTGANEESSRSHAILQLAIKKSVEGNQSKPPRLVGKL
SFIDLAGSERGADTTDNDKQTRLEGAEINKSLLALKECIRALDNDQGHIPFRGSKLTEVLRDSFMGN
SRTVMISCISPSSGSCEHTLNTLRYADRVKSLSKGNASKKDVSSSTMNLRESTKIPLSSALPTPSNF
DDDVNEMWTEENDEFDASDYEQDKQMWKKNGKLEPSYNGMAQERIPKPTIQMKSRDMPRPDMK
KSNSDDNLNALLQEEEDLVNAHRKQVEDTMNIVKEEMNLLVEADQPGNQLDGYISRLNTILSQKAA
GILQLQNRLAHFQKRLREHNVLVSTTGY*
(684aa)

Arabidopsis thaliana CMK2

DNA Sequence:

ATGGGCGGCCAAATGCAGCAAAACAATGCTGCGGCTGCGACGGCGCTTTACGATGGGGCTTT
ACCCACTAATGACGCAGGAGATGCAGTCATGGCACGGTGGCTTCAATCCGCTGGTTTGCAGC
ATTTGGCGTCTCCTGTTGCTTCTACAGGCAATGATCAGCGTCACCTCCCAAACCTTCTCATGCA
GGGTTATGGAGCTCAGACTGCTGAAGAGAAACAAAGACTGTTCCAACTAATGAGAAATCTCAAT

TTTAATGGGGAGTCGACTTCTGAATCATATACACCAACTGCTCACACATCAGCAGCTATGCCCT
CTTCGGAAGGATTTTTTTCACCTGAGTTCAGAGGTGATTTTGGAGCAGGATTATTGGATCTTCA
TGCAATGGATGATACAGAGCTTCTATCTGAGCATGTGATTACCGAACCCTTTGAGCCGTCACCT
TTCATGCCTAGTGTAAATAAAGAATTTGAAGAAGACTATAATTTGGCAGCTAATCGTCAACAGC
GGCAACAGACAGAAGCTGAACCTTTGGGTTTATTGCCTAAAAGTGATAAAGAAAATAACAGTGT
AGCCAAGATTAAAGTAGTGGTAAGGAAAAGACCCCTAAACAAGAAAGAAACAGCTAAAAAGGA
GGAGGATGTCGTGACGGTATCTGATAATTCTTTGACTGTCCATGAGCCCAGAGTGAAGGTTGA
TTTGACTGCTTATGTGGAAAAGCATGAGTTCTGCTTTGATGCTGTTCTAGATGAGGATGTTTCA
AATGACGAGGTGTATCGGGCCACAATTGAGCCAATAATTCCCATTATTTTCCAGAGAACTAAAG
CTACATGCTTTGCATATGGCCAAACAGGTAGTGGTAAGACATTTACAATGAAACCATTACCTAT
ACGAGCAGTTGAAGATCTTATGAGGTTGTTGCGTCAACCAGTATACAGCAATCAGAGGTTTAAA
TTGTGGCTCAGCTATTTTGAGATATATGGTGGAAAGCTGTTCGATCTTCTCAGTGAGAGAAAGA
AACTTTGCATGCGAGAAGATGGTAGACAGCAAGTTTGCATTGTTGGCCTGCAAGAATATGAAG
TTTCAGATGTACAAATTGTAAAGGATTTTATCGAGAAAGGAAATGCCGAAAGGAGCACAGGTTC
AACTGGAGCAAATGAGGAATCTTCTAGATCGCATGCCATCCTACAGCTTGTTGTAAAAAAGCAT
GTTGAGGTAAAAGACACTAGACGGAGGAATAATGATAGTAATGAATTGCCTGGGAAAGTTGTG
GGAAAGATTTCTTTCATTGACCTTGCTGGCAGTGAAAGAGGTGCAGACACCACAGACAATGAT
CGCCAGACAAGGATTGAAGGCGCAGAAATCAACAAGAGTCTCTTGGCTCTTAAGGAATGTATA
CGTGCACTGGACAATGACCAGCTACATATACCATTTCGTGGAAGCAAACTAACGGAAGTGCTC
CGTGACTCATTTGTTGGAAACTCAAGAACGGTGATGATTTCCTGCATCTCTCCAAATGCAGGAT
CGTGTGAACATACCCTCAATACTCTAAGATATGCTGATCGAGTCAAAAGTCTATCTAAAAGTGG
AAATAGCAAGAAAGATCAAACTGCGAATTCAATGCCTCCGGTTAATAAGGATCCTTTGTTGGGC
CCAAATGATGTAGAAGATGTCTTTGAGCCTCCACAGGAAGTGAATGTACCAGAAACCAGGAGG
AGGGTGGTCGAGAAGGACAGCAACAGCAGTACGTCGGGTATTGACTTCAGACAGCCTACAAA
TTATCGAGAGGAAAGTGGAATCCCATCATTCTCAATGGACAAGGGAAGATCAGAGCCGAACAG
TTCTTTTGCTGGCTCCACTAGTCAGAGAAACAACATTTCTTCATATCCCCAAGAAACTTCAGAC
CGTGAAGAGAAAGTAAAGAAAGTGTCACCACCTCGTGGGAAAGGGTTGCGGGAAGAAAAACC
AGACAGACCACAAAATTGGTCTAAAAGAGATGTCAGTTCGTCGGATATCCCTACCTTGACAAAT
TTTAGACAGAACGCAAGTGAAACTGCTTCAAGGCAATATGAAACCGCTTCAAGGCAATATGAAA
CCGACCCTTCGCTTGATGAAAACCTCGATGCACTGCTTGAGGAAGAAGAAGCTCTGATTGCAG
CGCACAGAAAAGAAATTGAGGATACAATGGAGATTGTTCGCGAGGAAATGAAACTTCTAGCGG
AGGTGGACCAACCGGGAAGCATGATAGAAAACTATGTGACGCAACTGAGCTTTGTGTTGTCCC
GGAAAGCAGCAGGGCTAGTCAGTCTTCAAGCCAGGCTTGCTCGGTTCCAACACCGTCTCAAG
GAACAAGAAATACTGAGCCGTAAGAGAGTTCCTCGGTAG

Protein Sequence:

MGGQMQQNNAAAATALYDGALPTNDAGDAVMARWLQSAGLQHLASPVASTGNDQRHLPNLLMQ
GYGAQTAEEKQRLFQLMRNLNFNGESTSESYTPTAHTSAAMPSSEGFFSPEFRGDFGAGLLDLHA
MDDTELLSEHVITEPFEPSPFMPSVNKEFEEDYNLAANRQQRQQTEAEPLGLLPKSDKENNSVAKI
KVVVRKRPLNKKETAKKEEDVVTVSDNSLTVHEPRVKVDLTAYVEKHEFCFDAVLDEDVSNDEVYR
ATIEPIIPIIFQRTKATCFAYGQTGSGKTFTMKPLPIRAVEDLMRLLRQPVYSNQRFKLWLSYFEIYGG
KLFDLLSERKKLCMREDGRQQVCIVGLQEYEVSDVQIVKDFIEKGNAERSTGSTGANEESSRSHAIL
QLVVKKHVEVKDTRRRNNDSNELPGKVVGKISFIDLAGSERGADTTDNDRQTRIEGAEINKSLLALK
ECIRALDNDQLHIPFRGSKLTEVLRDSFVGNSRTVMISCISPNAGSCEHTLNTLRYADRVKSLSKSG
NSKKDQTANSMPPVNKDPLLGPNDVEDVFEPPQEVNVPETRRRVVEKDSNSSTSGIDFRQPTNYR
EESGIPSFSMDKGRSEPNSSFAGSTSQRNNISSYPQETSDREEKVKKVSPPRGKGLREEKPDRPQ
NWSKRDVSSSDIPTLTNFRQNASETASRQYETASRQYETDPSLDENLDALLEEEEALIAAHRKEIED
TMEIVREEMKLLAEVDQPGSMIENYVTQLSFVLSRKAAGLVSLQARLARFQHRLKEQEILSRKRVPR
*

(794aa)

Appendix D: PCR primers

AtCMK2FLFWGate
*GGGGACAAGTTTGTACAAAAAAGCAGGCTTG*ATGGGCGGCCAAATGCAGCAA
AAC

AtCMK2FLRVGate
*GGGGACCACTTTGTACAAGAAAGCTGGGT*TCTACCGAGGAACTCTCTTACGG
CT

AtCMK1FLGatFW
*GGGGACAAGTTTGTACAAAAAAGCAGGCTTA*ATGAGCGGAAGACaGAGATCT
GTT

AtCMK1FLGatRV
*GGGGACCACTTTGTACAAGAAAGCTGGGT*TCaGTACCCAGTGGTAGAGAC

CMK1ABFW
*GGGGACAAGTTTGTACAAAAAAGCAGGCTTC*GTATCTTCTTCGACCATGAACT
TAA

CMK1ABRV
*GGGGACCACTTTGTACAAGAAAGCTGGGT*CAGAGTTTGACTTCTTCATATCGG
GC

CMK2PSDKoFW
*GGGGACAAGTTTGTACAAAAAAGCAGGCTTC*ACCATGGCAAGTGAAACTGCT
TCAAGG

PROCMK2Fw
*GGGGACAAGTTTGTACAAAAAAGCAGGCTT*CGTACAGACATGATGTCTTGAGA

PROCMK2Rv
*GGGGACCaCTTTGTACAAGAAAGCTGGGT*GAGGCGCTGTGATCTTCTTTGAG
G

PROCMK1Fw
*GGGGACAAGTTTGTACAAAAAAGCAGGCTG*GTACATCTAACAACTGTCTTACT
TAG

PROCMK1Rv
*GGGGACCACTTTGTACAAGAAAGCTGGGT*CTATTGACTCTAGCTCGAATCGG
AGC

MOR1 NT Y2H GW FW
GGGGACAAGTTTGTACAAAAAAGCAGGCTTGATGTCGACGGAGGATGAGAAG
TTA

MOR1 NT Y2H GW RV
*GGGGACCACTTTGTACAAGAAAGCTGGGTC*CGGTTTGCCAGTCCCAACCTTC
TTG

MOR1 M Y2H GW FW
*GGGGACAAGTTTGTACAAAAAAGCAGGCTTC*GGTGGAGGCAAAAAAGATGGA
TCTG

MOR1 M_Y2H GW RV
*GGGGACCACTTTGTACAAGAAAGCTGGGTC*CATTCTCAAGATCCTGAATCTGT
TC

MOR1 CT gat FW
*GGGGACAAGTTTGTACAAAAAAGCAGGCTAC*ACCATGGATATAGCTATC
CAGTCACAG

MOR1 CT gat RV
*GGGGACCACTTTGTACAAGAAAGCTGGGTT*CTACATATGTTCCAGTGATCCAC
C

AtCMK2 Exp Frag FW
*GGGGACAAGTTTGTACAAAAAAGCAGGCTCA*ATGCCTCCGGTTAATAAG

AtCMK2 Exp Frag RV
*GGGGACCACTTTGTACAAGAAAGCTGGGTT*TTAAAGCGAAGGGTCGGTTTCA
TA

Appendix E: MOR1/GEM1 RT-PCR (David Twell & Soon Ki Parks, Twell *et al.* 2002 Supp Info)

Supplementary Information; Figure 3.

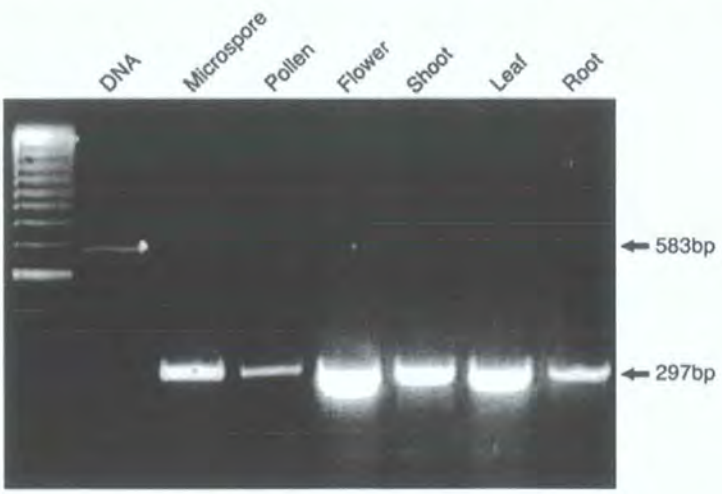

RT-PCR analysis of total RNA shows expression of *MOR1/GEM1* in all organs. Primer F (position 12-36 in exon1) and primer R (position 287-309) were used and gave the expected product sizes of 297 for RT-PCR reactions and 583bp for the genomic DNA control. DNA = genomic DNA control (Twell *et al.* 2002 supplementary information).

Appendix: F Yeast Phenotype upon expression of MOR1/GEM1 NT

All images of yeast are at the same magnification (20x) and were viewed using a Ziess Axioskop microscope. The control cells were also transformed with a yeast two-hybrid plasmid, pAS2, containing fragment 5 of Formin 4 clone 2C (52C). This construct had previously been used for yeast two-hybrid screens and yeast appeared and behaved as wild type (construct from Micheal Deeks). Here it can be seen that those yeast cells containing the pAS2[MOR1/GEM1 NT] construct are substantially larger than those cells of the control or yeast containing pAS2[MOR1/GEM1CT]. The MOR1/GEM1 NT cells are approximately 4x larger and none were seen to form buds.

Appendix: G AtCMK2 Yeast Two-Hybrid Auto-activation Tests

Appendix F: Yeast Phenotype upon Expression of MOR1/GEM1 N-terminal Section.

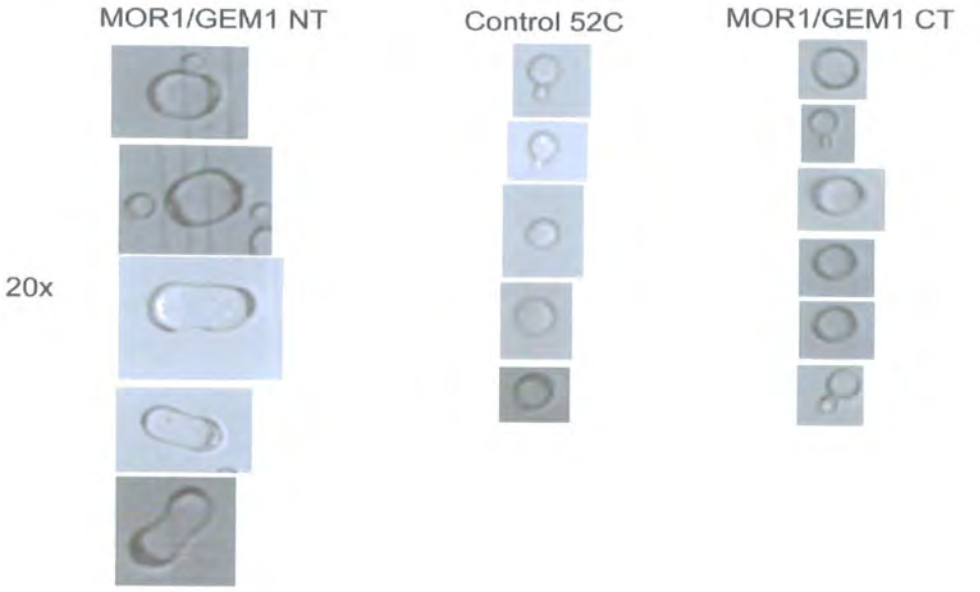

Appendix G: AtCMKFL-BD Yeast Two-hybrid Autoactivation Tests

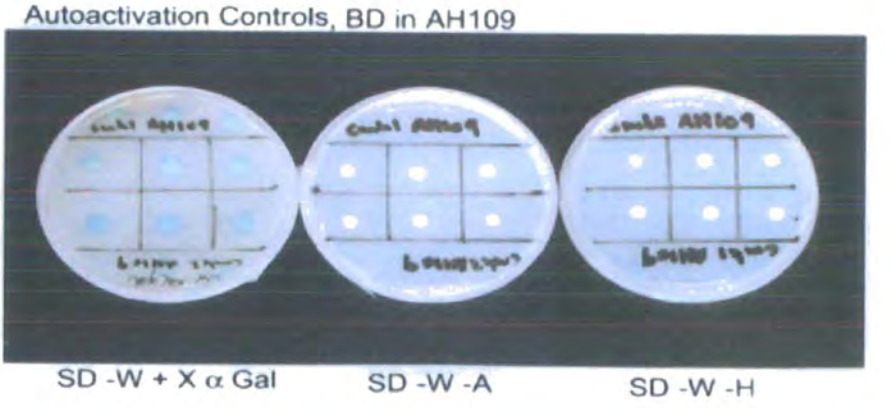

These plates show the auto-activation tests of the full length AtCMK1 and AtCMK2 yeast two-hybrid bait or GAL4 DNA binding constructs (pAS2). The contructs were transformed into yeast strain AH109 and plated onto SD media lacking adenine, histidine or +X-gal (MEL1 reporter). All clones grew on both –A and –H media and gave a blue colour on X-gal. Therefore the full length AtCMK2 (BD) constructs auto-activate the ADE3, HIS3 and MEL1 reporter gene systems.

Appendix:H Alternative XMAP215/TOGp family phylogenetic trees.

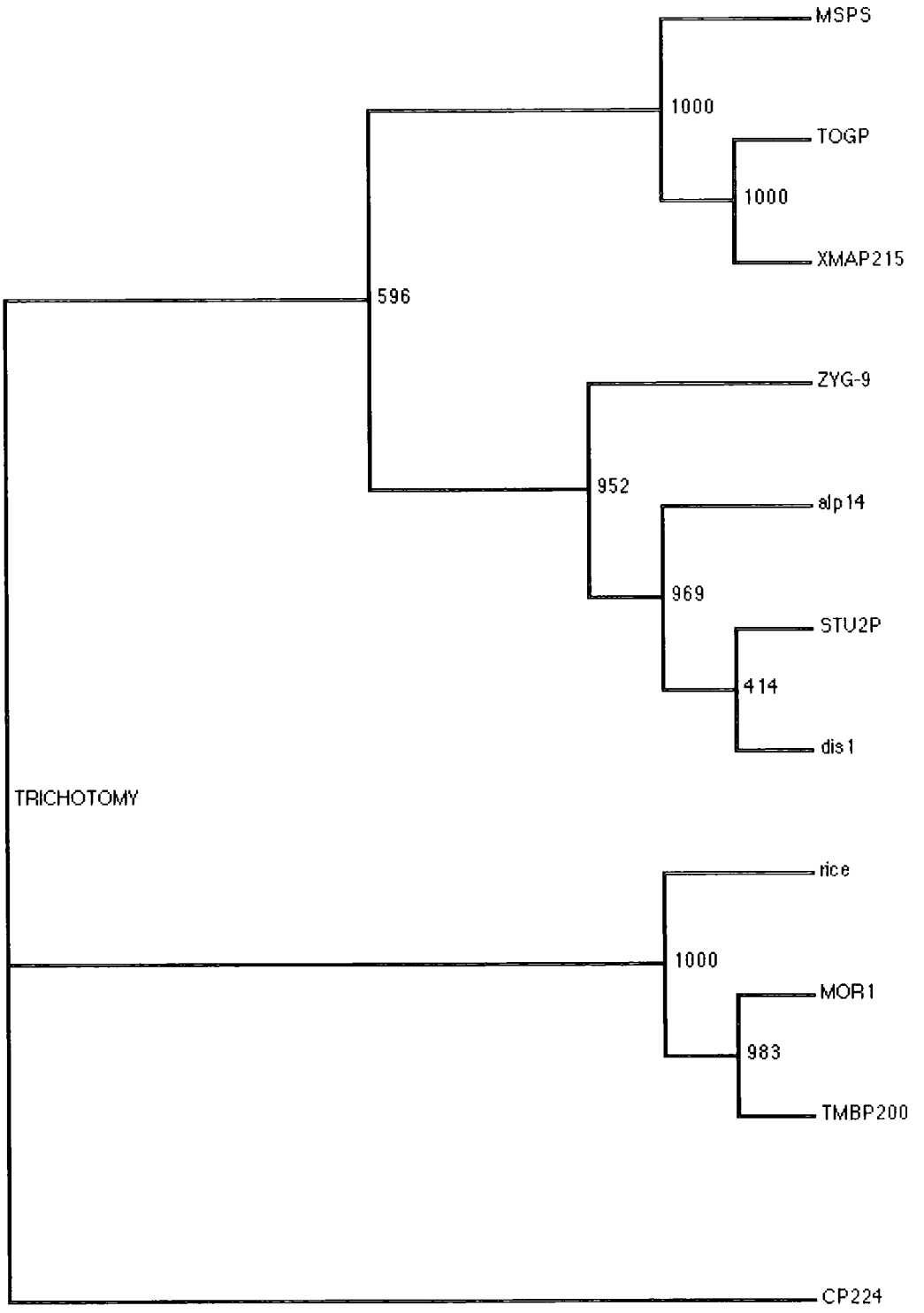
MSPS
1000
TOGP
1000
XMAP215
596
ZYG-9
952
alp14
969
STU2P
414
dis1
TRICHOTOMY
rice
1000
MOR1
983
TMBP200
CP224

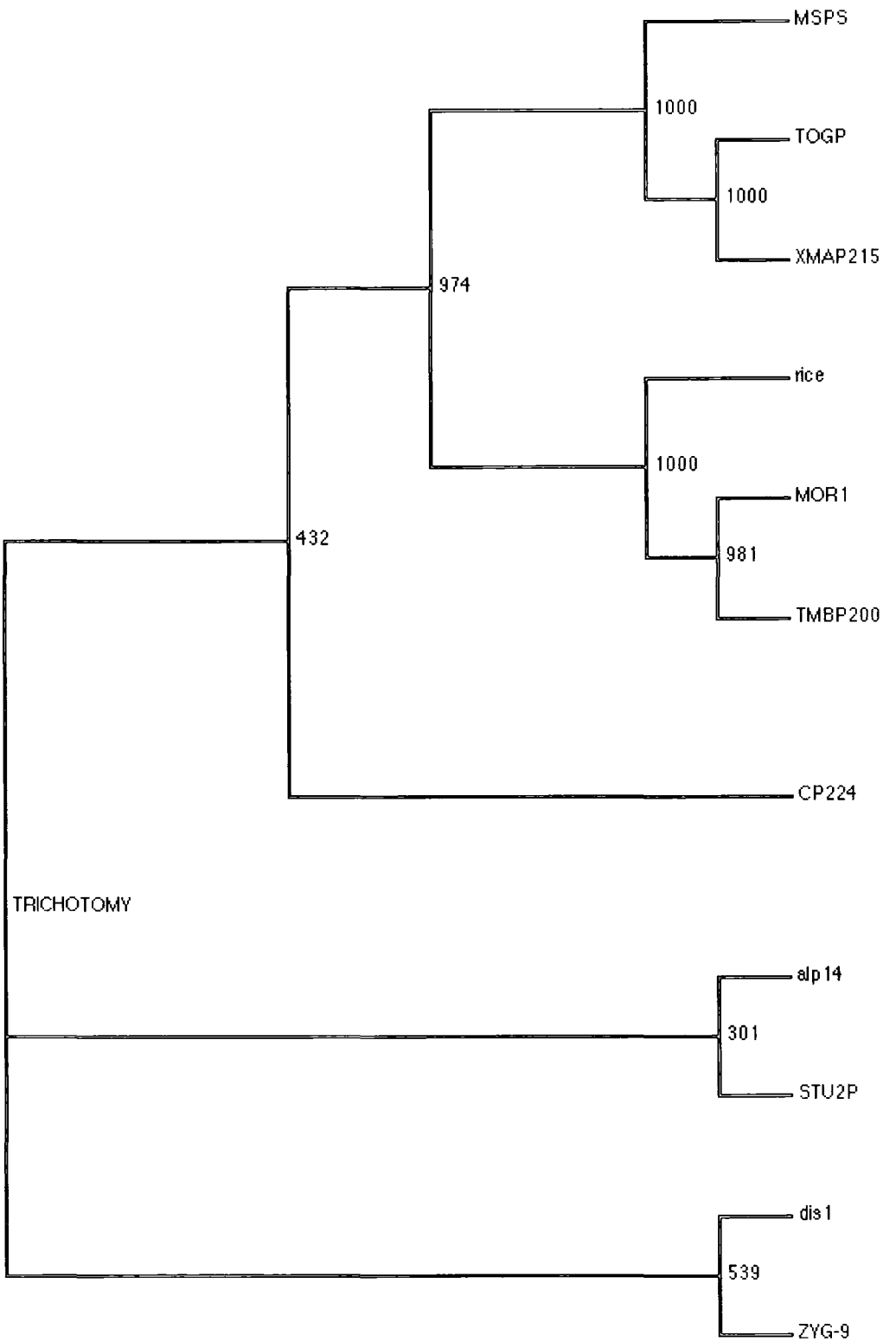
MSPS
1000
TOGP
1000
XMAP215
974
rice
1000
MOR1
981
TMBP200
432
CP224
TRICHOTOMY
alp14
301
STU2P
dis1
539
ZYG-9

Appendix I: Papers which include work from this thesis.

Hussey, P. J. and Hawkins, T.J. (2001). "Plant microtubule-associated proteins: the HEAT is off in temperature-sensitive *mor1*." Trends in Plant Science **6**(9): 389-392.

Hussey, P. J., Hawkins, T.J., Igarashi, H., Kaloriti, D., Smertenko, A. (2002). "The plant cytoskeleton: recent advances in the study of the plant microtubule-associated proteins MAP-65, MAP-190 and the Xenopus MAP215-like protein, MOR1." Plant Molecular Biology **50**(6): 915-924.

Twell[1], D., Park[1], S. K., Hawkins[1], T.J., Schubert, D., Schmidt, R., Smertenko, A. Hussey, P.J. (2002). "MOR1/GEM1 has an essential role in the plant-specific cytokinetic phragmoplast." Nature Cell Biology **4**(9): 711-714.

[1]These authors contributed equally.

Hawkins, T.J., Smertenko, A. Hussey, P.J. (2004) "AtCMK2 is an *Arabidopsis* Kinl Kinesin and causes microtubule depolymerisation *in vivo*" Current Biology (in press)

References.

Adams, R.R., Carmena, M. & Earnshaw, W.C. (2001): Chromosomal passengers and the (aurora) ABCs of mitosis. Trends in Cell Biology **11**, 49-54.

Alexander, J.E., Hunt, D.F., Lee, M.K., Shabanowitz, J., Michel, H., Berlin, S.C., Macdonald, T.L., Sundberg, R.J., Rebhun, L.I. & Frankfurter, A. (1991): Characterization of Posttranslational Modifications in Neuron- Specific Class-Iii Beta-Tubulin by Mass-Spectrometry. Proceedings of the National Academy of Sciences of the United States of America **88**, 4685-4689.

Altschul, S.F., Gish, W., Miller, W., Myers, E.W. & Lipman, D.J. (1990): Basic Local Alignment Search Tool. Journal of Molecular Biology **215**, 403-410.

Altschul, S.F., Madden, T.L., Schaffer, A.A., Zhang, J.H., Zhang, Z., Miller, W. & Lipman, D.J. (1997): Gapped BLAST and PSI-BLAST: a new generation of protein database search programs. Nucleic Acids Research **25**, 3389-3402.

Andersen, S.S.L. (2000): Spindle assembly and the art of regulating microtubule dynamics by MAPs and Stathmin/Op18. Trends in Cell Biology **10**, 261-267.

Andersen, S.S.L. & Wittmann, T. (2002): Toward reconstitution of in vivo microtubule dynamics in vitro. Bioessays **24**, 305-307.

Andrade, M.A. & Bork, P. (1995): Heat Repeats in the Huntingtons-Disease Protein. Nature Genetics **11**, 115-116.

Anthony, R.G. & Hussey, P.J. (1999): Double mutation in Eleusine indica alpha-tubulin increases the resistance of transgenic maize calli to dinitroaniline and phosphorothioamidate herbicides. Plant Journal **18**, 669-674.

Anthony, R.G. & Hussey, P.J. (1999): Dinitroaniline herbicide resistance and the microtubule cytoskeleton. Trends in Plant Science **4**, 112-116.

Arnal, I., Karsenti, E. & Hyman, A.A. (2000): Structural transitions at microtubule ends correlate with their dynamic properties in Xenopus egg extracts. Journal of Cell Biology **149**, 767-774.

Asada, T., Kuriyama, R. & Shibaoka, H. (1997): TKRP125, a kinesin-related protein involved in the centrosome- independent organization of the cytokinetic apparatus in tobacco BY-2 cells. Journal of Cell Science **110**, 179-189.

Azimzadeh, J., Traas, J. & Pastuglia, M. (2001): Molecular aspects of microtubule dynamics in plants. Current Opinion in Plant Biology **4**, 513-519.

Baskin, T.I., Wilson, J.E., Cork, A. & Williamson, R.E. (1994): Morphology and Microtubule Organization in Arabidopsis Roots Exposed to Oryzalin or Taxol. Plant and Cell Physiology **35**, 935-942.

Becker, B., Charrasse, S., Larroque, C. & Gard, D. (1997): Molecular cloning of XMAP215: A microtubule-associated protein from Xenopus eggs that is related to proteins depressed in human cells and tumors. Molecular Biology of the Cell **8**, 291-291.

Becker, B.E. & Gard, D.L. (2000): Multiple isoforms of the high molecular weight microtubule associated protein XMAP215 are expressed during development in Xenopus. Cell Motility and the

Cytoskeleton **47**, 282-295.

Becker, B.E., Romney, S.J. & Gard, D.L. (2003): XMAP215, XKCM1, NuMA, and cytoplasmic dynein are required for the assembly and organization of the transient microtubule array during the maturation of Xenopus oocytes. Developmental Biology **261**, 488-505.

Beinhauer, J.D., Hagan, I.M., Hegemann, J.H. & Fleig, U. (1997): Mal3, the fission yeast homologue of the human APC-interacting protein EB-1 is required for microtubule integrity and the maintenance of cell form. Journal of Cell Biology **139**, 717-728.

Bell, J.K. & McCully, M.E. (1970): A Histological Study of Lateral Root Initiation and Development in Zea-Mays. Protoplasma **70**, 179-&.

Bellanger, J.M. & Gonczy, P. (2003): TAC-1 and ZYG-9 form a complex that promotes microtubule assembly in C-elegans embryos. Current Biology **13**, 1488-1498.

Bibikova, T.N., Blancaflor, E.B. & Gilroy, S. (1999): Microtubules regulate tip growth and orientation in root hairs of Arabidopsis thaliana. Plant Journal **17**, 657-665.

Bichet, A., Desnos, T., Turner, S., Grandjean, O. & Hofte, H. (2001): BOTERO1 is required for normal orientation of cortical microtubules and anisotropic cell expansion in Arabidopsis. Plant Journal **25**, 137-148.

Bouquin, T., Mattsson, O., Naested, H., Foster, R. & Mundy, J. (2003): The Arabidopsis lue1 mutant defines a katanin p60 ortholog involved in hormonal control of microtubule orientation during cell growth. Journal of Cell Science **116**, 791-801.

Bowser, J. & Reddy, A.S.N. (1997): Localization of a kinesin-like calmodulin-binding protein in dividing cells of Arabidopsis and tobacco. Plant Physiology **114**, 1417-1417.

Brady, S.T. (1985): A Novel Brain Atpase with Properties Expected for the Fast Axonal-Transport Motor. Nature **317**, 73-75.

Brown, R.C., Lemmon, B.E., Nguyen, H. & Olsen, O.A. (1999): Development of endosperm in Arabidopsis thaliana. Sexual Plant Reproduction **12**, 32-42.

Burk, D.H., Liu, B., Zhong, R.Q., Morrison, W.H. & Ye, Z.H. (2001): A katanin-like protein regulates normal cell wall biosynthesis and cell elongation. Plant Cell **13**, 807-827.

Burns, R.G. (1991): Alpha-Tubulin, Beta-Tubulin, and Gamma-Tubulins - Sequence Comparisons and Structural Constraints. Cell Motility and the Cytoskeleton **20**, 181-189.

Camilleri, C., Azimzadeh, J., Pastuglia, M., Bellini, C., Grandjean, O. & Bouchez, D. (2002): The Arabidopsis TONNEAU2 gene encodes a putative novel protein phosphatase 2A regulatory subunit essential for the control of the cortical cytoskeleton. Plant Cell **14**, 833-845.

Carlier, M.F. & Pantaloni, D. (1978): Kinetic-Analysis of Cooperativity in Tubulin Polymerization in Presence of Guanosine Diphosphate or Triphosphate Nucleotides. Biochemistry **17**, 1908-1915.

Cassimeris, L. (2002): The oncoprotein 18/stathmin family of microtubule destabilizers. Current Opinion in Cell Biology **14**, 18-24.

Cassimeris, L., Gard, D., Tran, P.T. & Erickson, H.P. (2001): XMAP215 is a long thin molecule that

does not increase microtubule stiffness. Journal of Cell Science **114**, 3025-3033.

Cassimeris, L. & Spittle, C. (2001): Regulation of microtubule-associated proteins. In: International Review of Cytology - a Survey of Cell Biology, Vol 210, pp. 163-226.

Caudron, N., Valiron, O., Usson, Y., Valiron, P. & Job, D. (2000): A reassessment of the factors affecting microtubule assembly and disassembly in vitro. Journal of Molecular Biology **297**, 211-220.

Chan, J., Calder, G.M., Doonan, J.H. & Lloyd, C.W. (2003): EB1 reveals mobile microtubule nucleation sites in Arabidopsis. Nature Cell Biology **5**, 967-971.

Charrasse, S., Lorca, T., Doree, M. & Larroque, C. (2000): The Xenopus XMAP215 and its human homologue TOG proteins interact with cyclin B1 to target p34cdc2 to microtubules during mitosis. Experimental Cell Research **254**, 249-256.

Charrasse, S., Schroeder, M., Gauthier-Rouviere, C., Ango, F., Cassimeris, L., Gard, D.L. & Larroque, C. (1998): The TOGp protein is a new human microtubule-associated protein homologous to the Xenopus XMAP215. Journal of Cell Science **111**, 1371-1383.

Charrasse, S., Schroeder, M., GauthierRouviere, C., Cassimeris, L., Gard, D.L. & Larroque, C. (1996): The human ch-TOG protein is associated with mitotic spindles and is homologous to the xenopus microtubule associated protein, XMAP215. Molecular Biology of the Cell **7**, 1292-1292.

Chen, C.B., Marcus, A., Li, W.X., Hu, Y., Calzada, J.P.V., Grossniklaus, U., Cyr, R.J. & Ma, H. (2002): The Arabidopsis ATK1 gene is required for spindle morphogenesis in male meiosis. Development **129**, 2401-2409.

Chen, X.Y. & Huffaker, T.C. (1996): Isolation and characterization of proteins that interact with STU2p, an essential component of the yeast spindle pole bodies. Molecular Biology of the Cell **7**, 1189-1189.

Chen, X.Y.P., Yin, H.W. & Huffaker, T.C. (1998): The yeast spindle pole body component Spc72p interacts with Stu2p and is required for proper microtubule assembly. Journal of Cell Biology **141**, 1169-1179.

Chu, B.Y., Wilson, T.J., McCune-Zierath, C., Snustad, D.P. & Carter, J.V. (1998): Two beta-tubulin genes, TUB1 and TUB8, of Arabidopsis exhibit largely nonoverlapping patterns of expression. Plant Molecular Biology **37**, 785-790.

Cimini, D., Fioravanti, D., Salmon, E.D. & Degrassi, F. (2002): Merotelic kinetochore orientation versus chromosome mono- orientation in the origin of lagging chromosomes in human primary cells. Journal of Cell Science **115**, 507-515.

Cleveland, D.W. (1993): Tubulin and associated proteins in Guidebook to the cytoskeleton and motor proteins. Kreis, T. & Vale, R. (Ed), Oxford university press, 101-105

Cleveland, D.W. (1989): Use of DNA Transfection to Analyze Gene - Regulation and Function in Animal-Cells - Dissection of the Tubulin Multigene Family. Cell Motility and the Cytoskeleton **14**, 147-155.

Compton, D.A. (2000): Spindle assembly in animal cells. Annual Review of Biochemistry **69**, 95-114.

Compton, D.A., Sanchez, A. & Dionne, M.A. (1999): Ch-TOGp is required for microtubule aster formation in a mammalian mitotic extract. Molecular Biology of the Cell **10**, 745.

Conte, N., Charafe-Jauffret, E., Delaval, B., Adelaide, J., Ginestier, C., Geneix, J., Isnardon, D., Jacquemier, J. & Birnbaum, D. (2002): Carcinogenesis and translational controls: TACC1 is down-regulated in human cancers and associates with mRNA regulators. Oncogene **21**, 5619-5630.

Coy, D.L., Wagenbach, M., Howard, J. & Wordernan, L. (1998): Microtubule-stimulated ATPase activity of Mitotic Centromere- Associated Kinesin (MCAK). Molecular Biology of the Cell **9**, 2266.

Cullen, C.F., Deak, P., Glover, D.M. & Ohkura, H. (1999): mini spindles: A gene encoding a conserved microtubule- associated protein required for the integrity of the mitotic spindle in Drosophila. Journal of Cell Biology **146**, 1005-1018.

Cullen, C.F. & Ohkura, H. (2001): Msps protein is localized to acentrosomal poles to ensure bipolarity of Drosophila meiotic spindles. Nature Cell Biology **3**, 637-642.

de Soultrait, V.R., Caumont, A., Durrens, P., Calmels, C., Parissi, V., Recordon, P., Bon, E., Desjobert, C., Tarrago-Litvak, L. & Fournier, M. (2002): HIV-1 integrase interacts with yeast microtubule-associated proteins. Biochimica Et Biophysica Acta-Gene Structure and Expression **1575**, 40-48.

Deavours, B.E., Reddy, A.S.N. & Walker, R.A. (1998): Ca2+/calmodulin regulation of the Arabidopsis kinesin-like calmodulin-binding protein. Cell Motility and the Cytoskeleton **40**, 408-416.

Desai, A., Mitchison, T.J. & Walczak, C.E. (1997): Microtubule destabilization by XKCM1 and XKIF2 - Two internal motor domain subfamily kinesins. Molecular Biology of the Cell **8**, 13-13.

Desai, A., Verma, S., Mitchison, T.J. & Walczak, C.E. (1999): Kin I kinesins are microtubule-destabilizing enzymes. Cell **96**, 69-78.

Dhonukshe, P. & Gadella, T.W.J. (2003): Alteration of microtubule dynamic instability during preprophase band formation revealed by yellow fluorescent protein-CLIP170 microtubule plus-end labeling. Plant Cell **15**, 597-611.

Dionne, M.A., Sanchez, A. & Compton, D.A. (2000): ch-TOGp is required for microtubule aster formation in a mammalian mitotic extract. Journal of Biological Chemistry **275**, 12346-12352.

Dutcher, S.K. (2001): The tubulin fraternity: alpha to eta. Current Opinion in Cell Biology **13**, 49-54.

Edde, B., Rossier, J., Lecaer, J.P., Desbruyeres, E., Gros, F. & Denoulet, P. (1990): Posttranslational Glutamylation of Alpha-Tubulin. Science **247**, 83-85.

Emons, A.M.C. & Mulder, B.M. (1998): The making of the architecture of the plant cell wall: How cells exploit geometry. Proceedings of the National Academy of Sciences of the United States of America **95**, 7215-7219.

Endow, S.A., Kang, S.J., Satterwhite, L.L., Rose, M.D., Skeen, V.P. & Salmon, E.D. (1994): Yeast Kar3 Is a Minus-End Microtubule Motor Protein That Destabilizes Microtubules Preferentially at the Minus Ends. Embo Journal **13**, 2708-2713.

Ennulat, D.J., Liem, R.K.H., Hashim, G.A. & Shelanski, M.L. (1989): 2 Separate 18-Amino Acid

Domains of Tau Promote the Polymerization of Tubulin. Journal of Biological Chemistry **264**, 5327-5330.

Enos, A.P. & Morris, N.R. (1990): Mutation of a Gene That Encodes a Kinesin-Like Protein Blocks Nuclear Division in Aspergillus-Nidulans. Cell **60**, 1019-1027.

Erickson, H.P. (1997): FtsZ, a tubulin homologue in prokaryote cell division. Trends in Cell Biology **7**, 362-367.

Erickson, H.P. & Obrien, E.T. (1992): Microtubule Dynamic Instability and Gtp Hydrolysis. Annual Review of Biophysics and Biomolecular Structure **21**, 145-166.

Errington, J. (2003): Dynamic proteins and a cytoskeleton in bacteria. Nature Cell Biology **5**, 175-178.

Euteneuer, U., Jackson, W.T. & McIntosh, J.R. (1981): Structural Polarity of Spindle and Phragmoplast Microtubules in Haemanthus Endosperm Cells. Journal of Cell Biology **91**, A320-A320.

Euteneuer, U. & McIntosh, J.R. (1980): Polarity of Midbody and Phragmoplast Microtubules. Journal of Cell Biology **87**, 509-515.

Faulkner, N.E., Vig, B., Echeverri, C.J., Wordeman, L. & Vallee, R.B. (1998): Localization of motor-related proteins and associated complexes to active, but not inactive, centromeres. Human Molecular Genetics **7**, 671-677.

Fisher, D.D. & Cyr, R.J. (1998): Extending the microtubule/microfibril paradigm - Cellulose synthesis is required for normal cortical microtubule alignment in elongating cells. Plant Physiology **116**, 1043-1051.

Flyvbjerg, H., Jobs, E. & Leibler, S. (1996): Kinetics of self-assembling microtubules: An "inverse problem" in biochemistry. Proceedings of the National Academy of Sciences of the United States of America **93**, 5975-5979.

Furutani, I., Watanabe, Y., Prieto, R., Masukawa, M., Suzuki, K., Naoi, K., Thitamadee, S., Shikanai, T. & Hashimoto, T. (2000): The SPIRAL genes are required for directional central of cell elongation in Arabidopsis thaliana. Development **127**, 4443-4453.

Fygenson, D.K., Flyvbjerg, H., Sneppen, K., Libchaber, A. & Leibler, S. (1995): Spontaneous Nucleation of Microtubules. Physical Review E **51**, 5058-5063.

Galjart, N. & Perez, F. (2003): A plus-end raft to control microtubule dynamics and function. Current Opinion in Cell Biology **15**, 48-53.

Gan, E. & Walczak, C.E. (2000): Kinetic characterization of the microtubule destabilizing kinesin XKCM1. Molecular Biology of the Cell **11**, 1008.

Garcia, M.A., Koonrugsa, N. & Toda, T. (2002): Spindle-kinetochore attachment requires the combined action of Kin I-like Klp5/6 and Alp14/Dis1-MAPs in fission yeast. Embo Journal **21**, 6015-6024.

Garcia, M.A., Koonrugsa, N. & Toda, T. (2002): Two kinesin-like Kin I family proteins in fission yeast regulate of metaphase and the on the establishment set of anaphase A. Current Biology **12**, 610-

621.

Garcia, M.A., Vardy, L., Koonrugsa, N. & Toda, T. (2001): Fission yeast ch-TOG/XMAP215 homologue Alp14 connects mitotic spindles with the kinetochore and is a component of the Mad2-dependent spindle checkpoint. Embo Journal **20**, 3389-3401.

Gard, D.L. & Becker, B.E. (1999): XMAP215 expression during Xenopus development. Molecular Biology of the Cell **10**, 1468.

Gard, D.L. & Kirschner, M.W. (1987): A Microtubule-Associated Protein from Xenopus Eggs That Specifically Promotes Assembly at the Plus-End. Journal of Cell Biology **105**, 2203-2215.

Gardiner, J. & Marc, J. (2003): Putative microtubule-associated proteins from the Arabidopsis genome. Protoplasma **222**, 61-74.

Garner, C.C. & Matus, A. (1988): Different Forms of Microtubule-Associated Protein-2 Are Encoded by Separate Messenger-Rna Transcripts. Journal of Cell Biology **106**, 779-783.

Garrett, S. & Kapoor, T.M. (2003): Microtubule assembly: Catastrophe factors to the rescue. Current Biology **13**, R810-R812.

Gergely, F., Draviam, V.M. & Raff, J.W. (2003): The ch-TOG/XMAP215 protein is essential for spindle pole organization in human somatic cells. Genes & Development **17**, 336-341.

Gergely, F., Kidd, D., Jeffers, K., Wakefield, J.G. & Raff, J.W. (2000): D-TACC: a novel centrosomal protein required for normal spindle function in the early Drosophila embryo. Embo Journal **19**, 241-252.

Giet, R., McLean, D., Descamps, S., Lee, M.J., Raff, J.W., Prigent, C. & Glover, D.M. (2002): Drosophila Aurora A kinase is required to localize D-TACC to centrosomes and to regulate astral microtubules. Journal of Cell Biology **156**, 437-451.

Glotzer, M., Murray, A.W. & Kirschner, M.W. (1991): Cyclin Is Degraded by the Ubiquitin Pathway. Nature **349**, 132-138.

Graf, R., Daunderer, C. & Schliwa, M. (2000): Dictyostelium DdCP224 is a microtubule-associated protein and a permanent centrosomal resident involved in centrosome duplication. Journal of Cell Science **113**, 1747-1758.

Graf, R., Euteneuer, U., Ho, T.H. & Rehberg, M. (2003): Regulated expression of the centrosomal protein DdCP224 affects microtubule dynamics and reveals mechanisms for the control of supernumerary centrosome number. Molecular Biology of the Cell **14**, 4067-4074.

Graf, R. & Hestermann, A. (2002): DdCP224, the Dictyostelium XMAP215 homologue, is required for microtubule elongation and microtubule tip/cortex interactions in vivo. Molecular Biology of the Cell **13**, 1058.

Granger, C.L. & Cyr, R.J. (2000): Microtubule reorganization in tobacco BY-2 cells stably expressing GFP-MBD. Planta **210**, 502-509.

Green, P.B. (1962): Mechanism for Plant Cellular Morphogenesis. Science **138**, 1404-&.

Green, P.B. (1980): Organogenesis - a Biophysical View. Annual Review of Plant Physiology and

Plant Molecular Biology **31**, 51-82.

Green, P.B. (1994): Connecting Gene and Hormone Action to Form, Pattern and Organogenesis - Biophysical Transductions. Journal of Experimental Botany **45**, 1775-1788.

Groves, M.R., Hanlon, N., Turowski, P., Hemmings, B.A. & Barford, D. (1999): The structure of the protein phosphatase 2A PR65/A subunit reveals the conformation of its 15 tandemly repeated HEAT motifs. Cell **96**, 99-110.

Gu, X.J. & Verma, D.P.S. (1996): Phragmoplastin, a dynamin-like protein associated with cell plate formation in plants. Embo Journal **15**, 695-704.

Gu, X.J. & Verma, D.P.S. (1997): Dynamics of phragmoplastin in living cells during cell plate formation and uncoupling of cell elongation from the plane of cell division. Plant Cell **9**, 157-169.

Gunning, B.E.S. & Wick, S.M. (1985): Preprophase Bands, Phragmoplasts, and Spatial Control of Cytokinesis. Journal of Cell Science, 157-179.

Hashimoto, T. (2002): Molecular genetic analysis of left-right handedness in plants. Philosophical Transactions of the Royal Society of London Series B-Biological Sciences **357**, 799-808.

Hashimoto, T. (2003): Dynamics and regulation of plant interphase microtubules: a comparative view. Current Opinion in Plant Biology **6**, 568-576.

He, X.W., Rines, D.R., Espelin, C.W. & Sorger, P.K. (2001): Molecular analysis of kinetochore-microtubule attachment in budding yeast. Cell **106**, 195-206.

Heald, R. (2000): A dynamic duo of microtubule modulators. Nature Cell Biology **2**, E11-E12.

Hepler, P.K. & Lancelle, S.A. (1986): Cytoskeletal Details in Freeze-Substituted Meiotic Cells of Tradescantia Blossfeldiana. Journal of Cell Biology **103**, A555-A555.

Hestermann, A. & Graf, R. (2003): DdCP224, the Dictyostelium XMAP215 homologue, is involved in microtubule tip cell cortex interactions in a dynein-dependent pathway. European Journal of Cell Biology **82**, 66-66.

Hestermann, A., Rehberg, M. & Graf, R. (2002): Centrosomal microtubule plus end tracking proteins and their role in Dictyostelium cell dynamics. Journal of Muscle Research and Cell Motility **23**, 621-630.

Himmler, A. (1989): Structure of the Bovine Tau-Gene - Alternatively Spliced Transcripts Generate a Protein Family. Molecular and Cellular Biology **9**, 1389-1396.

Hoekema, A., Hirsch, P.R., Hooykaas, P.J.J. & Schilperoort, R.A. (1983): A Binary Plant Vector Strategy Based on Separation of Vir- Region and T-Region of the Agrobacterium-Tumefaciens Ti-Plasmid. Nature **303**, 179-180.

Hogan, C.J. (1987): Microtubule Patterns During Meiosis in 2 Higher-Plant Species. Protoplasma **138**, 126-136.

Holmfeldt, P., Brattsand, G. & Gullberg, M. (2002): MAP4 counteracts microtubule catastrophe promotion but not tubulin-sequestering activity in intact cells. Current Biology **12**, 1034-1039.

Holmfeldt, P., Stenmark, S. & Gullberg, M. (2004): Differential functional interplay of TOGp/XMAP215 and the Kinl kinesin MCAK during interphase and mitosis. Embo Journal **23**, 627-637.

Horio, T. & Hotani, H. (1986): Visualization of the Dynamic Instability of Individual Microtubules by Dark-Field Microscopy. Nature **321**, 605-607.

Hoshi, M., Ohta, K., Gotoh, Y., Mori, A., Murofushi, H., Sakai, H. & Nishida, E. (1992): Mitogen-Activated-Protein-Kinase-Catalyzed Phosphorylation of Microtubule-Associated Proteins, Microtubule-Associated Protein-2 and Microtubule-Associated Protein-4, Induces an Alteration in Their Function. European Journal of Biochemistry **203**, 43-52.

Howard, J. & Hyman, A.A. (2003): Dynamics and mechanics of the microtubule plus end. Nature **422**, 753-758.

Hunter, A.W., Caplow, M., Coy, D.L., Hancock, W.O., Diez, S., Wordeman, L. & Howard, J. (2003): The kinesin-related protein MCAK is a microtubule depolymerase that forms an ATP-hydrolyzing complex at microtubule ends. Molecular Cell **11**, 445-457.

Hush, J.M., Wadsworth, P., Callaham, D.A. & Hepler, P.K. (1994): Quantification of Microtubule Dynamics in Living Plant-Cells Using Fluorescence Redistribution after Photobleaching. Journal of Cell Science **107**, 775-784.

Hussey, P.J. (2002): Cytoskeleton - Microtubules do the twist. Nature **417**, 128-129.

Hussey, P.J. & Hawkins, T.J. (2001): Plant microtubule-associated proteins: the HEAT is off in temperature-sensitive mor1. Trends in Plant Science **6**, 389-392.

Hussey, P.J., Hawkins, T.J., Igarashi, H., Kaloriti, D. & Smertenko, A. (2002): The plant cytoskeleton: recent advances in the study of the plant microtubule-associated proteins MAP-65, MAP-190 and the Xenopus MAP215-like protein, MOR1. Plant Molecular Biology **50**, 915-924.

Hyman, A.A. & Mitchison, T.J. (1990): Modulation of Microtubule Stability by Kinetochores Invitro. Journal of Cell Biology **110**, 1607-1616.

Jiang, C.J. & Sonobe, S. (1993): Identification and Preliminary Characterization of a 65-Kda Higher-Plant Microtubule-Associated Protein. Journal of Cell Science **105**, 891-901.

Joly, J.C., Flynn, G. & Purich, D.L. (1989): The Microtubule-Binding Fragment of Microtubule-Associated Protein-2 - Location of the Protease-Accessible Site and Identification of an Assembly-Promoting Peptide. Journal of Cell Biology **109**, 2289-2294.

Kakimoto, T. & Shibaoka, H. (1987): A New Method for Preservation of Actin-Filaments in Higher-Plant Cells. Plant and Cell Physiology **28**, 1581-1585.

Kemphues, K.J., Wolf, N., Wood, W.B. & Hirsh, D. (1986): 2 Loci Required for Cytoplasmic Organization in Early Embryos of Caenorhabditis Elegans. Developmental Biology **113**, 449-460.

Khawaja, S., Gundersen, G.G. & Bulinski, J.C. (1988): Enhanced Stability of Microtubules Enriched in Detyrosinated Tubulin Is Not a Direct Function of Detyrosination Level. Journal of Cell Biology **106**, 141-149.

Kim, A.J. & Endow, S.A. (2000): A kinesin family tree. Journal of Cell Science **113**, 3681-+.

Kim, I.G., Jun, D.Y., Sohn, U. & Kim, Y.H. (1997): Cloning and expression of human mitotic centromere-associated kinesin gene. Biochimica Et Biophysica Acta-Molecular Cell Research **1359**, 181-186.

Kinoshita, K., Arnal, I., Desai, A., Drechsel, D.N. & Hyman, A.A. (2001): Reconstitution of physiological microtubule dynamics using purified components. Science **294**, 1340-1343.

Kinoshita, K., Habermann, B. & Hyman, A.A. (2002): XMAP215: a key component of the dynamic microtubule cytoskeleton. Trends in Cell Biology **12**, 267-273.

Kirchner, K. & Mandelkow, E.M. (1985): Tubulin Domains Responsible for Assembly of Dimers and Protofilaments. Embo Journal **4**, 2397-2402.

Kline-Smith, S., Park, S.J. & Walczak, C.E. (1999): Exploring the function of XKCM1 in cells. Molecular Biology of the Cell **10**, 31.

Kline-Smith, S.L., Gan, E., Lipkin, T.G. & Walczak, C.E. (2000): Dissection of domains of XKCM1 important in centromere- targeting and microtubule destabilization. Molecular Biology of the Cell **11**, 494.

Kline-Smith, S.L. & Walczak, C.E. (2000): XKCM1 destabilizes microtubules in cells. Molecular Biology of the Cell **11**, 1857.

Kline-Smith, S.L. & Walczak, C.E. (2001): XKCM1 regulates microtubule catastrophe in cells. Molecular Biology of the Cell **12**, 936.

Kline-Smith, S.L. & Walczak, C.E. (2002): The microtubule-destabilizing kinesin XKCM1 regulates microtubule dynamic instability in cells. Molecular Biology of the Cell **13**, 2718-2731.

Kline-Smith, S.L. & Walczak, C.E. (2002): Centromere-bound KCM1 is required for proper progression through prometaphase in cells. Molecular Biology of the Cell **13**, 981.

Koncz, C. & Schell, J. (1986): The Promoter of Tl-DNA Gene 5 Controls the Tissue-Specific Expression of Chimeric Genes Carried by a Novel Type of Agrobacterium Binary Vector. Molecular & General Genetics **204**, 383-396.

Kopczak, S.D., Haas, N.A., Hussey, P.J., Silflow, C.D. & Snustad, D.P. (1992): The Small Genome of Arabidopsis Contains at Least 6 Expressed Alpha-Tubulin Genes. Plant Cell **4**, 539-547.

Kosco, K.A., Adams, I.R. & Huffaker, T. (1999): STU2 interacts with BIK1 and BIM1 to modulate microtubule assembly in S-cerevisae. Molecular Biology of the Cell **10**, 1482.

Kosco, K.A., Pearson, C.G., Maddox, P.S., Wang, P.J.J., Adams, I.R., Salmon, E.D., Bloom, K. & Huffaker, T.C. (2001): Control of microtubule dynamics by Stu2p is essential for spindle orientation and metaphase chromosome alignment in yeast. Molecular Biology of the Cell **12**, 2870-2880.

Kost, B., Mathur, J. & Chua, N.H. (1999): Cytoskeleton in plant development. Current Opinion in Plant Biology **2**, 462-470.

Kropf, D.L., Bisgrove, S.R. & Hable, W.E. (1998): Cytoskeletal control of polar growth in plant cells. Current Opinion in Cell Biology **10**, 117-122.

Kull, F.J. & Endow, S.A. (2002): Kinesin: switch I & II and the motor mechanism. Journal of Cell Science **115**, 15-23.

Kuznetsov, S.A., Rodionov, V.I., Gelfand, V.I. & Rozenblat, V.A. (1981): Microtubule-Associated Protein Mapi - Purification and Evidence of Polymerizing Activity. Doklady Akademii Nauk Sssr **261**, 760-762.

Lan, W.J., Zhang, X., Kline-Smith, S.L., Rosasco, S.E., Barrett-Wilt, G.A., Shabanowitz, J., Walczak, C.E. & Stukenberg, P.T. (2004): Aurora B phosphorylates centromeric MCAK and regulates its localization and microtubule depolymerization activity. Current Biology **14**, 273-286.

Lancelle, S.A., Callaham, D.A. & Hepler, P.K. (1986): A Method for Rapid Freeze Fixation of Plant-Cells. Protoplasma **131**, 153-165.

Lawrence, C.J., Malmberg, R.L., Muszynski, M.G. & Dawe, R.K. (2002): Maximum likelihood methods reveal conservation of function among closely related kinesin families. Journal of Molecular Evolution **54**, 42-53.

Le Bot, N., Tsai, M.C., Andrews, R.K. & Ahringer, J. (2003): TAC-1, a regulator of microtubule length in the C-elegans embryo. Current Biology **13**, 1499-1505.

Ledizet, M. & Piperno, G. (1987): Identification of an Acetylation Site of Chlamydomonas Alpha-Tubulin. Proceedings of the National Academy of Sciences of the United States of America **84**, 5720-5724.

Lee, M.J., Gergely, F., Jeffers, K., Peak-Chew, S.Y. & Raff, J.W. (2001): Msps/XMAP215 interacts with the centrosomal protein D-TACC to regulate microtubule behaviour. Nature Cell Biology **3**, 643-649.

Lee, Y.R.J., Giang, H.M. & Liu, B. (2001): A novel plant kinesin-related protein specifically associates with the phragmoplast organelles. Plant Cell **13**, 2427-2439.

Lee, Y.R.J. & Liu, B. (2000): Identification of a phragmoplast-associated kinesin-related protein in higher plants. Current Biology **10**, 797-800.

Letunic, I., Goodstadt, L., Dickens, N.J., Doerks, T., Schultz, J., Mott, R., Ciccarelli, F., Copley, R.R., Ponting, C.P. & Bork, P. (2002): Recent improvements to the SMART domain-based sequence annotation resource. Nucleic Acids Research **30**, 242-244.

Lewis, S.A., Ivanov, I.E., Lee, G.H. & Cowan, N.J. (1989): Organization of Microtubules in Dendrites and Axons Is Determined by a Short Hydrophobic Zipper in Microtubule- Associated Proteins Map2 and Tau. Nature **342**, 498-505.

Lewis, S.A., Villasante, A., Sherline, P. & Cowan, N.J. (1986): Brain-Specific Expression of Map2 Detected Using a Cloned Cdna Probe. Journal of Cell Biology **102**, 2098-2105.

Lewis, S.A., Wang, D.S. & Cowan, N.J. (1988): Microtubule-Associated Protein Map2 Shares a Microtubule Binding Motif with Tau-Protein. Science **242**, 936-939.

Liu, B., Cyr, R.J. & Palevitz, B.A. (1996): A kinesin-like protein, KatAp, in the cells of arabidopsis and other plants. Plant Cell **8**, 119-132.

Liu, B. & Palevitz, B.A. (1996): Localization of a kinesin-like protein in generative cells of tobacco.

Protoplasma **195**, 78-89.

Lloyd, C. & Chan, J. (2002): Helical microtubule arrays and spiral growth. Plant Cell **14**, 2319-2324.

Lloyd, C., Chan, J. & Hussey, P.J. (2003): Microtubules & microtubule-associated proteins in The Plant Cytoskeleton in Cell Differentiation and Development Hussey, P.J. (Ed), Blackwell Publishing, 3-27

Lloyd, C. & Hussey, P. (2001): Microtubule-associated proteins in plants - Why we need a map. Nature Reviews Molecular Cell Biology **2**, 40-47.

Lodish, H., Berk, A., Zipursky, L.S, Matsudaira, P. Baltimore, D., Darnell, J.E., (2000): Molecular cell biology, 4th edition, Freeman & Company, 795-909

Lowe, J. & Amos, L.A. (1998): Crystal structure of the bacterial cell-division protein FtsZ. Nature **391**, 203-206.

Lu, B.W., Roegiers, F., Jan, L.Y. & Jan, Y.N. (2001): Adherens junctions inhibit asymmetric division in the Drosophila epithelium. Nature **409**, 522-525.

Luduena, R.F., Zimmermann, H.P. & Little, M. (1988): Identification of the Phosphorylated Beta-Tubulin Isotype in Differentiated Neuro-Blastoma Cells. Febs Letters **230**, 142-146.

Maiato, H., Sunkel, C.E. & Earnshaw, W.C. (2002): Role of CLASP1 in kinetochore association with the plus-ends of dynamic microtubules. Molecular Biology of the Cell **13**, 980.

Mandelkow & Mandelkow (1993): a/b-Tubulin in Guidebook to the cytoskeleton and motor proteins. Kreis, T. & Vale, R. (Ed), Oxford university press, 127-130

Maney, T., Hunter, A.W., Wagenbach, M. & Wordeman, L. (1998): Mitotic centromere-associated kinesin is important for anaphase chromosome segregation. Journal of Cell Biology **142**, 787-801.

Maney, T., Wagenbach, M. & Wordeman, L. (2001): Molecular dissection of the microtubule depolymerizing activity of mitotic centromere-associated kinesin. Journal of Biological Chemistry **276**, 34753-34758.

Marcus, A.I., Li, W., Ma, H. & Cyr, R.J. (2003): A kinesin mutant with an atypical bipolar spindle undergoes normal mitosis. Molecular Biology of the Cell **14**, 1717-1726.

Margolis, R.L. & Wilson, L. (1978): Opposite End Assembly and Disassembly of Microtubules at Steady-State Invitro. Cell **13**, 1-8.

Margolis, R.L. & Wilson, L. (1981): Microtubule Treadmills - Possible Molecular Machinery. Nature **293**, 705-711.

Mayer, U., Ruiz, R.A.T., Berleth, T., Misera, S. & Jurgens, G. (1991): Mutations Affecting Body Organization in the Arabidopsis Embryo. Nature **353**, 402-407.

McClinton, R.S., Chandler, J.S. & Callis, J. (2001): cDNA isolation, characterization, and protein intracellular localization of a katanin-like p60 subunit from Arabidopsis thaliana. Protoplasma **216**, 181-190.

McNally, F. (2003): Microtubule dynamics: New surprises from an old MAP. Current Biology **13**,

R597-R599.

McNally, F.J. (1999): Microtubule dynamics: Controlling split ends. Current Biology **9**, R274-R276.

McNally, K.P., Buster, D. & McNally, F.J. (2002): Katanin-mediated microtubule severing can be regulated by multiple mechanisms. Cell Motility and the Cytoskeleton **53**, 337-349.

Miller, R.K., Cheng, S.C. & Rose, M.D. (2000): Bim1p/Yeb1p mediates the Kar9p-dependent cortical attachment of cytoplasmic microtubules. Molecular Biology of the Cell **11**, 2949-2959.

Mineyuki, Y. & Gunning, B.E.S. (1990): A Role for Preprophase Bands of Microtubules in Maturation of New Cell-Walls, and a General Proposal on the Function of Preprophase Band Sites in Cell-Division in Higher-Plants. Journal of Cell Science **97**, 527-537.

Mitchison, T. & Kirschner, M. (1984): Dynamic Instability of Microtubule Growth. Nature **312**, 237-242.

Mitchison, T. & Kirschner, M. (1984): Microtubule Assembly Nucleated by Isolated Centrosomes. Nature **312**, 232-237.

Mitsui, H., Yamaguchishinozaki, K., Shinozaki, K., Nishikawa, K. & Takahashi, H. (1993): Identification of a Gene Family (Kat) Encoding Kinesin-Like Proteins in Arabidopsis-Thaliana and the Characterization of Secondary Structure of Kata. Molecular & General Genetics **238**, 362-368.

Monteiro, M.J. & Cleveland, D.W. (1988): Sequence of Chicken C-Beta-7 Tubulin Analysis of a Complete Set of Vertebrate Beta-Tubulin Isotypes. Journal of Molecular Biology **199**, 439-446.

Moore, R.C., Zhang, M., Cassimeris, L. & Cyr, R.J. (1997): In vitro assembled plant microtubules exhibit a high state of dynamic instability. Cell Motility and the Cytoskeleton **38**, 278-286.

Moores, C.A., Yu, M., Guo, J., Beraud, C., Sakowicz, R. & Milligan, R.A. (2002): A mechanism for microtubule depolymerization by Kinl kinesins. Molecular Cell **9**, 903-909.

Muller, S., Fuchs, E., Ovecka, M., Wysocka-Diller, J., Benfey, P.N. & Hauser, M.T. (2002): Two new loci, PLEIADE and HYADE, implicate organ-specific regulation of cytokinesis in Arabidopsis. Plant Physiology **130**, 312-324.

Muller, S., Smertenko, A., Wagner, V., Heinrich, M., Hussey, P.J. & Hauser, M.T. (2004): The plant microtubule-associated protein AtMAP65-3/PLE is essential for cytokinetic phragmoplast function. Current Biology **14**, 412-417.

Nakai, K. & Horton, P. (1999): PSORT: a program for detecting sorting signals in proteins and predicting their subcellular localization. Trends in Biochemical Sciences **24**, 34-35.

Nakamura, T., Nagao, K., Nakaseko, Y. & Yanagida, M. (2002): Cut1/separase C-terminus affects spindle pole body positioning in interphase of fission yeast: pointed nuclear formation. Genes to Cells **7**, 1113-1124.

Nakaseko, Y., Goshima, G., Morishita, J. & Yanagida, M. (2001): M phase-specific kinetochore proteins in fission yeast: Microtubule-associating Dis1 and Mtc1 display rapid separation and segregation during anaphase. Current Biology **11**, 537-549.

Nanninga, N. (2001): Cytokinesis in prokaryotes and eukaryotes: Common principles and different

solutions. Microbiology and Molecular Biology Reviews **65**, 319-+.

Nasmyth, K. (2002): Segregating sister genomes: The molecular biology of chromosome separation. Science **297**, 559-565.

Niederstrasser, H., Salehi-Had, H., Gan, E.C., Walczak, C. & Nogales, E. (2002): XKCM1 acts on a single protofilament and requires the C terminus of tubulin. Journal of Molecular Biology **316**, 817-828.

Nishihama, R., Soyano, T., Ishikawa, M., Araki, S., Tanaka, H., Asada, T., Irie, K., Ito, M., Terada, M., Banno, H., Yamazaki, Y. & Machida, Y. (2002): Expansion of the cell plate in plant cytokinesis requires a kinesin-like protein/MAPKKK complex. Cell **109**, 87-99.

Oakley, C.E. & Oakley, B.R. (1989): Identification of Gamma-Tubulin, a New Member of the Tubulin Superfamily Encoded by Mipa Gene of Aspergillus-Nidulans. Nature **338**, 662-664.

Ohi, R., Coughlin, M.L., Lane, W.S. & Mitchison, T.J. (2002): Simulation of XKCM1 activity by a novel component of the inner centromere. Molecular Biology of the Cell **13**, 936.

Ohi, R., Coughlin, M.L., Lane, W.S. & Mitchison, T.J. (2003): An inner centromere protein that stimulates the microtubule depolymerizing activity of a Kinl kinesin. Developmental Cell **5**, 309-321.

Ohkura, H., Adachi, Y., Kinoshita, N., Niwa, O., Toda, T. & Yanagida, M. (1988): Cold-Sensitive and Caffeine-Supersensitive Mutants of the Schizosaccharomyces-Pombe Dis Genes Implicated in Sister Chromatid Separation During Mitosis. Embo Journal **7**, 1465-1473.

Ohkura, H., Garcia, M.A. & Toda, T. (2001): Dis1/TOG universal microtubule adaptors - one MAP for all? Journal of Cell Science **114**, 3805-3812.

Oppenheimer, D.G., Pollock, M.A., Vacik, J., Szymanski, D.B., Ericson, B., Feldmann, K. & Marks, M.D. (1997): Essential role of a kinesin-like protein in Arabidopsis trichome morphogenesis. Proceedings of the National Academy of Sciences of the United States of America **94**, 6261-6266.

Otegui, M. & Staehelin, L.A. (2000): Cytokinesis in flowering plants: more than one way to divide a cell. Current Opinion in Plant Biology **3**, 493-502.

Ovechkina, Y., Wagenbach, M. & Wordeman, L. (2002): K-loop insertion restores microtubule depolymerizing activity of a "neckless" MCAK mutant. Journal of Cell Biology **159**, 557-562.

Ovechkina, Y.Y. & Wordeman, L.G. (2001): The role of the neck domain in the microtubule depolymerization activity of MCAK. Molecular Biology of the Cell **12**, 2405.

Pearson, C.G., Maddox, P.S., Zarzar, T.R., Salmon, E.D. & Bloom, K. (2003): Yeast kinetochores do not stabilize Stu2p-dependent spindle microtubule dynamics. Molecular Biology of the Cell **14**, 4181-4195.

Popov, A.V., Pozniakovsky, A., Arnal, I., Antony, C., Ashford, A.J., Kinoshita, K., Tournebize, R., Hyman, A.A. & Karsenti, E. (2000): XMAP215 regulates microtubule dynamics through two distinct domains. Molecular Biology of the Cell **11**, 1027.

Popov, A.V., Pozniakovsky, A., Arnal, I., Antony, C., Ashford, A.J., Kinoshita, K., Tournebize, R., Hyman, A.A. & Karsenti, E. (2001): XMAP215 regulates microtubule dynamics through two distinct domains. Embo Journal **20**, 397-410.

Popov, A.V., Severin, F. & Karsenti, E. (2002): XMAP215 is required for the microtubule-nucleating activity of centrosomes. Current Biology **12**, 1326-1330.

Porath, J., Carlsson, J., Olsson, I. & Belfrage, G. (1975): Metal Chelate Affinity Chromatography, a New Approach to Protein Fractionation. Nature **258**, 598-599.

Reddy, A.S., Day, I.S., (2001): Kinesins in the Arabidopsis genome: a comparative analysis among eukaryotes. BMC Genomics. **2**, 2.

Rehberg, M. & Graf, R. (2002): Dictyostelium EB1 is a genuine centrosomal component required for proper spindle formation. Molecular Biology of the Cell **13**, 2301-2310.

Reis, D., Roland, J.C. & Vian, B. (1985): Morphogenesis of Twisted Cell-Wall - Chronology Following an Osmotic Shock. Protoplasma **126**, 36-46.

Rieder, C.L. & Salmon, E.D. (1998): The vertebrate cell kinetochore and its roles during mitosis. Trends in Cell Biology **8**, 310-318.

Rogers, G.C., Rogers, S.L., Schwimmer, T.A., Stubbert, J., Walczak, C.E., Vale, R.D., Scholey, J.M. & Sharp, D.J. (2002): Identification and characterization of three Kin I family members in Drosophila: Evidence that mitosis in this system involves the coordinated action of functionally distinct classes of Kin I motors. Molecular Biology of the Cell **13**, 2390.

Rogers, S., Wells, R. & Rechsteiner, M. (1986): Amino-Acid-Sequences Common to Rapidly Degraded Proteins - the Pest Hypothesis. Science **234**, 364-368.

Rogers, S.L., Rogers, G.C., Sharp, D.J. & Vale, R.D. (2002): Drosophila EB1 is important for proper assembly, dynamics, and positioning of the mitotic spindle. Journal of Cell Biology **158**, 873-884.

Romney, S.J. & Gard, D.L. (2000): Mapping the microtubule binding sites of XMAP215. Molecular Biology of the Cell **11**, 1030.

Rosania, G.R., Merlie, J., Gray, N., Chang, Y.T., Schultz, P.G. & Heald, R. (1999): A cyclin-dependent kinase inhibitor inducing cancer cell differentiation: Biochemical identification using Xenopus egg extracts. Proceedings of the National Academy of Sciences of the United States of America **96**, 4797-4802.

Rusan, N.M., Fagerstrom, C.J., Yvon, A.M.C. & Wadsworth, P. (2001): Cell cycle-dependent changes in microtubule dynamics in living cells expressing green fluorescent protein-alpha tubulin. Molecular Biology of the Cell **12**, 971-980.

Salehi-Had, H., Niederstrasser, H., Walczak, C.E. & Nogales, E. (2000): XKCM1 depolymerization studies of tubulin polymers: Building a mechanistic model. Molecular Biology of the Cell **11**, 1856.

Salmon, E.D., Leslie, R.J., Saxton, W.M., Karow, M.L. & McIntosh, J.R. (1984): Spindle Microtubule Dynamics in Sea-Urchin Embryos - Analysis Using a Fluorescein-Labeled Tubulin and Measurements of Fluorescence Redistribution after Laser Photobleaching. Journal of Cell Biology **99**, 2165-2174.

Samuels, A.L., Giddings, T.H. & Staehelin, L.A. (1995): Cytokinesis in Tobacco by-2 and Root-Tip Cells - a New Model of Cell Plate Formation in Higher-Plants. Journal of Cell Biology **130**, 1345-1357.

Saxton, W.M., Stemple, D.L. & McIntosh, J.R. (1984): Microinjection of Colchicine Bound Tubulin into Tissue-Culture Cells - Colchicine Acts as a Substoichiometric Microtubule Poison Invivo. Journal of Cell Biology **99**, A38-A38.

Schatz, C.A., Santarella, R., Hoenger, A., Karsenti, E., Mattaj, I.W., Gruss, O.J. & Carazo-Salas, R.E. (2003): Importin alpha-regulated nucleation of microtubules by TPX2. Embo Journal **22**, 2060-2070.

Schiefelbein, J.W. & Somerville, C. (1990): Genetic-Control of Root Hair Development in Arabidopsis- Thaliana. Plant Cell **2**, 235-243.

Schneppenheim, R. & Rautenberg, P. (1987): A Luminescence Western-Blot with Enhanced Sensitivity for Antibodies to Human-Immunodeficiency-Virus. European Journal of Clinical Microbiology & Infectious Diseases **6**, 49-51.

Schultz, J., Milpetz, F., Bork, P. & Ponting, C.P. (1998): SMART, a simple modular architecture research tool: Identification of signaling domains. Proceedings of the National Academy of Sciences of the United States of America **95**, 5857-5864.

Schuyler, S.C., Liu, J.Y. & Pellman, D. (2003): The molecular function of Ase1p: evidence for a MAP-dependent midzone-specific spindle matrix. Journal of Cell Biology **160**, 517-528.

Schwartz, K., Richards, K. & Botstein, D. (1997): BIM1 encodes a microtubule-binding protein in yeast. Molecular Biology of the Cell **8**, 2677-2691.

Sedbrook, J.C., Ehrhardt, D.W., Fisher, S.E., Scheible, W.R. & Somerville, C.R. (2004): The Arabidopsis SKU6/SPIRAL1 gene encodes a plus end-localized microtubule-interacting protein involved in directional cell expansion. Plant Cell **16**, 1506-1520.

Segui-Simarro, J.M., Austin, J.R., White, E.A. & Staehelin, L.A. (2004): Electron tomographic analysis of somatic cell plate formation in meristematic cells of arabidopsis preserved by high-pressure freezing. Plant Cell **16**, 836-856.

Severin, F., Habermann, B., Huffaker, T. & Hyman, T. (2001): Stu2 promotes mitotic spindle elongation in anaphase. Journal of Cell Biology **153**, 435-442.

Shaw, S.L., Kamyar, R. & Ehrhardt, D.W. (2003): Sustained microtubule treadmilling in Arabidopsis cortical arrays. Science **300**, 1715-1718.

Shelansk.Ml (1973): Chemistry of Filaments and Tubules of Brain. Journal of Histochemistry & Cytochemistry **21**, 529-539.

Shipley, K., Hekmat-Nejad, M., Turner, J., Moores, C., Anderson, R., Milligan, R., Sakowicz, R. & Fletterick, R. (2004): Structure of a kinesin microtubule depolymerization machine. Embo Journal **23**, 1422-1432.

Shirasu-Hiza, M., Coughlin, P. & Mitchison, T. (2003): Identification of XMAP215 as a microtubule-destabilizing factor in Xenopus egg extract by biochemical purification. Journal of Cell Biology **161**, 349-358.

Skibbens, R.V., Skeen, V.P. & Salmon, E.D. (1993): Directional Instability of Kinetochore Motility During Chromosome Congression and Segregation in Mitotic Newt Lung- Cells - a Push-Pull

Mechanism. Journal of Cell Biology **122**, 859-875.

Skop, A.R., Liu, H.B., Yates, J., Meyer, B.J. & Heald, R. (2004): Dissection of the mammalian midbody proteome reveals conserved cytokinesis mechanisms. Science **305**, 61-66.

Smertenko, A., Saleh, N., Igarashi, H., Mori, H., Hauser-Hahn, I., Jiang, C.J., Sonobe, S., Lloyd, C.W. & Hussey, P.J. (2000): A new class of microtubule-associated proteins in plants. Nature Cell Biology **2**, 750-753.

Smertenko, A.P., Bozhkov, P.V., Filonova, L.H., von Arnold, S. & Hussey, P.J. (2003): Re-organisation of the cytoskeleton during developmental programmed cell death in Picea abies embryos. Plant Journal **33**, 813-824.

Smertenko, A.P., Chang, H.Y., Wagner, V., Kaloriti, D., Fenyk, S., Sonobe, S., Lloyd, C., Hauser, M.T. & Hussey, P.J. (2004): The Arabidopsis microtubule-associated protein AtMAP65-1: Molecular analysis of its microtubule bundling activity. Plant Cell **16**, 2035-2047.

Smirnova, E.A. & Bajer, A.S. (1994): Microtubule Converging Centers and Reorganization of the Interphase Cytoskeleton and the Mitotic Spindle in Higher-Plant Haemanthus. Cell Motility and the Cytoskeleton **27**, 219-233.

Smirnova, E.A., Reddy, A.S.N., Bowser, J. & Bajer, A.S. (1998): Minus end-directed kinesin-like motor protein, Kcbp, localizes to anaphase spindle poles in Haemanthus endosperm. Cell Motility and the Cytoskeleton **41**, 271-280.

Smith, L.G., Gerttula, S.M., Han, S.C. & Levy, J. (2001): TANGLED1: A microtubule binding protein required for the spatial control of cytokinesis in maize. Journal of Cell Biology **152**, 231-236.

Snustad, D.P., Haas, N.A., Kopczak, S.D. & Silflow, C.D. (1992): The Small Genome of Arabidopsis Contains at Least 9 Expressed Beta-Tubulin Genes. Plant Cell **4**, 549-556.

Sollner, R., Glasser, G., Wanner, G., Somerville, C.R., Jurgens, G. & Assaad, F.F. (2002): Cytokinesis-defective mutants of Arabidopsis. Plant Physiology **129**, 678-690.

Spencer, J.A., Eliazer, S., Ilaria, R.L., Richardson, J.A. & Olson, E.N. (2000): Regulation of microtubule dynamics and myogenic differentiation by MURF, a striated muscle RING-finger protein. Journal of Cell Biology **150**, 771-784.

Spittle, C., Charrasse, S., Larroque, C. & Cassimeris, L. (1997): Molecular dissection of the microtubule binding domains of TOGp. Molecular Biology of the Cell **8**, 292-292.

Spittle, C., Charrasse, S., Larroque, C. & Cassimeris, L. (2000): The interaction of TOGp with microtubules and tubulin. Journal of Biological Chemistry **275**, 20748-20753.

Spittle, C.S., Charrasse, S., Larroque, C. & Cassimeris, L. (1999): TOGp interaction with microtubules and tubulin. Molecular Biology of the Cell **10**, 1478.

Srayko, M., Quintin, S., Schwager, A. & Hyman, A.A. (2003): Caenorhabditis elegans TAC-1 and ZYG-9 form a complex that is essential for long astral and spindle microtubules. Current Biology **13**, 1506-1511.

Staehelin, L.A. & Driouich, A. (1997): Brefeldin A effects in plants - Are different Golgi responses caused by different sites of action? Plant Physiology **114**, 401-403.

Staehlin, L.A. & Hepler, P.K. (1996): Cytokinesis in higher plants. Cell **84**, 821-824.

Still, I.H., Hamilton, M., Vince, P., Wolfman, A. & Cowell, J.K. (1999): Cloning of TACC1, an embryonically expressed, potentially transforming coiled coil containing gene, from the 8p11 breast cancer amplicon. Oncogene **18**, 4032-4038.

Still, I.H., Vince, P. & Cowell, J.K. (1999): The third member of the transforming acidic coiled coil-containing gene family, TACC3, maps in 4p16, close to translocation breakpoints in multiple myeloma, and is upregulated in various cancer cell lines. Genomics **58**, 165-170.

Stoppin, V., Vantard, M., Schmit, A.C. & Lambert, A.M. (1994): Isolated Plant Nuclei Nucleate Microtubule Assembly - the Nuclear-Surface in Higher-Plants Has Centrosome-Like Activity. Plant Cell **6**, 1099-1106.

Stoppin-Mellet, V., Gaillard, J. & Vantard, M. (2002): Functional evidence for in vitro microtubule severing by the plant katanin homologue. Biochemical Journal **365**, 337-342.

Strompen, G., El Kasmi, F., Richter, S., Lukowitz, W., Assaad, F.F., Jurgens, G. & Mayer, U. (2002): The Arabidopsis HINKEL gene encodes a kinesin-related protein involved in cytokinesis and is expressed in a cell cycle- dependent manner. Current Biology **12**, 153-158.

Su, L.K., Burrell, M., Hill, D.E., Gyuris, J., Brent, R., Wiltshire, R., Trent, J., Vogelstein, B. & Kinzler, K.W. (1995): Apc Binds to the Novel Protein Eb1. Cancer Research **55**, 2972-2977.

Sugimoto, K., Himmelspach, R., Williamson, R.E. & Wasteneys, G.O. (2003): Mutation or drug-dependent microtubule disruption causes radial swelling without altering parallel cellulose microfibril deposition in Arabidopsis root cells. Plant Cell **15**, 1414-1429.

Sulkowski, E. (1985): Purification of Proteins by Imac. Trends in Biotechnology **3**, 1-7.

Sullivan, K.F. (1988): Structure and Utilization of Tubulin Isotypes. Annual Review of Cell Biology **4**, 687-716.

Swofford, D.L., (1991): PAUP, Phylogenetic Analysis Using Parsimony, Version 4.0b10 Computer program distributed by the Illinois Natural History Survey, Champaign, Illinois

Tamura, K., Nakatani, K., Mitsui, H., Ohashi, Y. & Takahashi, H. (1999): Characterization of katD, a kinesin-like protein gene specifically expressed in floral tissues of Arabidopsis thaliana. Gene **230**, 23-32.

Tanaka, T.U. (2002): Bi-orienting chromosomes on the mitotic spindle. Current Opinion in Cell Biology **14**, 365-371.

Tanaka, T.U., Rachidi, N., Janke, C., Pereira, G., Galova, M., Schiebel, E., Stark, M.J.R. & Nasmyth, K. (2002): Evidence that the Ipl1-Sli15 (Aurora knase-INCENP) complex by altering promotes chromosome bi-orientation kinetochore-spindle pole connections. Cell **108**, 317-329.

Terasaka, O. & Niitsu, T. (1990): Unequal Cell-Division and Chromatin Differentiation in Pollen Grain Cells .2. Microtubule Dynamics Associated with the Unequal Cell-Division. Botanical Magazine-Tokyo **103**, 133-142.

Thitamadee, S., Tuchihara, K. & Hashimoto, T. (2002): Microtubule basis for left-handed helical

growth in Arabidopsis. Nature **417**, 193-196.

Thormahlen, M., Marx, A., Sack, S. & Mandelkow, E. (1998): The coiled-coil helix in the neck of kinesin. Journal of Structural Biology **122**, 30-41.

Torresruiz, R.A. & Jurgens, G. (1994): Mutations in the Fass Gene Uncouple Pattern-Formation and Morphogenesis in Arabidopsis Development. Development **120**, 2967-2978.

Tournebize, R., Popov, A., Kinoshita, K., Ashford, A.J., Rybina, S., Pozniakovsky, A., Mayer, T.U., Walczak, C.E., Karsenti, E. & Hyman, A.A. (2000): Control of microtubule dynamics by the antagonistic activities of XMAP215 and XKCM1 in Xenopus egg extracts. Nature Cell Biology **2**, 13-19.

Traas, J., Bellini, C., Nacry, P., Kronenberger, J., Bouchez, D. & Caboche, M. (1995): Normal Differentiation Patterns in Plants Lacking Microtubular Preprophase Bands. Nature **375**, 676-677.

Tran, P.T., Walker, R.A. & Salmon, E.D. (1997): A metastable intermediate state of microtubule dynamic instability that differs significantly between plus and minus ends. Journal of Cell Biology **138**, 105-117.

Tuma, R.S., Beaudet, M.P., Jin, X.K., Jones, L.J., Cheung, C.Y., Yue, S. & Singer, V.L. (1999): Characterization of SYBR gold nucleic acid gel stain: A dye optimized for use with 300-nm ultraviolet transilluminators. Analytical Biochemistry **268**, 278-288.

Turner, J., Anderson, R., Guo, J., Beraud, C., Fletterick, R. & Sakowicz, R. (2001): Crystal structure of the mitotic spindle kinesin Eg5 reveals a novel conformation of the neck-linker. Journal of Biological Chemistry **276**, 25496-25502.

Twell, D., Park, S.K., Hawkins, T.J., Schubert, D., Schmidt, R., Smertenko, A. & Hussey, P.J. (2002): MOR1/GEM1 has an essential role in the plant-specific cytokinetic phragmoplast. Nature Cell Biology **4**, 711-714.

Twell, D., Park, S.K. & Lalanne, E. (1998): Asymmetric division and cell-fate determination in developing pollen. Trends in Plant Science **3**, 305-310.

Upadhyaya, M.K. & Nooden, L.D. (1977): Relationship between Induction of Swelling and Inhibition of Elongation in Corn Roots by Oryzalin. Plant Physiology **59**, 46-46.

Usui, T., Maekawa, H., Pereira, G. & Schiebel, E. (2003): The XMAP215 homologue Stu2 at yeast spindle pole bodies regulates microtubule dynamics and anchorage. Embo Journal **22**, 4779-4793.

Vale, R.D., Reese, T.S. & Sheetz, M.P. (1985): Identification of a Novel Force-Generating Protein, Kinesin, Involved in Microtubule-Based Motility. Cell **42**, 39-50.

Valiron, O., Caudron, N., Job, D., (2001): Microtubule dynamics. Cell Mol Life Sci. **58**, 2069-84.

van Breugel, M., Drechsel, D. & Hyman, A. (2003): Stu2p, the budding yeast member of the conserved Dis1/XMAP215 family of microtubule-associated proteins is a plus end-binding microtubule destabilizer. Journal of Cell Biology **161**, 359-369.

Vanderslice, R. & Hirsh, D. (1976): Temperature-Sensitive Zygote Defective-Mutants of Caenorhabditis-Elegans. Developmental Biology **49**, 236-249.

Vasquez, R.J., Gard, D. & Cassimeris, L. (1995): Promotion of Microtubule (Mt) Assembly by Xmap215 Is Regulated by Phosphorylation. Molecular Biology of the Cell **6**, 1486-1486.

Vasquez, R.J., Gard, D.L. & Cassimeris, L. (1999): Phosphorylation by CDK1 regulates XMAP215 function in vitro. Cell Motility and the Cytoskeleton **43**, 310-321.

Verma, D.P.S. (2001): Cytokinesis and building of the cell plate in plants. Annual Review of Plant Physiology and Plant Molecular Biology **52**, 751-784.

Verma, D.P.S. & Gu, X.J. (1996): Vesicle dynamics during cell-plate formation in plants. Trends in Plant Science **1**, 145-149.

Villasante, A., Wang, D., Dobner, P., Dolph, P., Lewis, S.A. & Cowan, N.J. (1986): 6 Mouse Alpha-Tubulin Messenger-Rnas Encode 5 Distinct Isotypes - Testis-Specific Expression of 2 Sister Genes. Molecular and Cellular Biology **6**, 2409-2419.

Voter, W.A. & Erickson, H.P. (1984): The Kinetics of Microtubule Assembly - Evidence for a 2-Stage Nucleation Mechanism. Journal of Biological Chemistry **259**, 430-438.

Wade, R.H. & Chretien, D. (1993): Cryoelectron Microscopy of Microtubules. Journal of Structural Biology **110**, 1-27.

Wade, R.H. & Hyman, A.A. (1997): Microtubule structure and dynamics. Current Opinion in Cell Biology **9**, 12-17.

Walczak, C.E. (2000): Microtubule dynamics and tubulin interacting proteins. Current Opinion in Cell Biology **12**, 52-56.

Walczak, C.E. (2003): The Kin I kinesins are microtubule end-stimulated ATPases. Molecular Cell **11**, 286-288.

Walczak, C.E., Desai, A. & Mitchison, T.J. (1997): Dissecting the function of kinetochore-bound XKCM1 in chromosome movement in vitro and in vivo. Molecular Biology of the Cell **8**, 724-724.

Walczak, C.E., Gan, E.C., Desai, A., Mitchison, T.J. & Kline-Smith, S.L. (2002): The microtubule-destabilizing kinesin XKCM1 is required for chromosome positioning during spindle assembly. Current Biology **12**, 1885-1889.

Walczak, C.E., Mitchison, T.J. & Desai, A. (1996): XKCM1: A Xenopus kinesin-related protein that regulates microtubule dynamics during mitotic spindle assembly. Cell **84**, 37-47.

Walker, R.A., Obrien, E.T., Pryer, N.K., Soboeiro, M.F., Voter, W.A., Erickson, H.P. & Salmon, E.D. (1988): Dynamic Instability of Individual Microtubules Analyzed by Video Light-Microscopy - Rate Constants and Transition Frequencies. Journal of Cell Biology **107**, 1437-1448.

Walther, A. & Wendland, J. (2003): Septation and cytokinesis in fungi. Fungal Genetics and Biology **40**, 187-196.

Wang, G.F., Kong, H.Z., Sun, Y.J., Zhang, X.H., Zhang, W., Altman, N., dePamphilis, C.W. & Ma, H. (2004): Genome-wide analysis of the cyclin family in Arabidopsis and comparative phylogenetic analysis of plant cyclin-like proteins. Plant Physiology **135**, 1084-1099.

Wang, P.J.J. & Huffaker, T.C. (1997): Stu2p: A microtubule-binding protein that is an essential

component of the yeast spindle pole body. Journal of Cell Biology **139**, 1271-1280.

Ward, R.D., Watts, N.R., Miller, M.W. & Sackett, D.L. (2000): HIV-1 Rev binds to tubulin, forming bilayered ring polymers and destabilizing microtubules. Molecular Biology of the Cell **11**, 1040.

Waring, M.J. (1965): Complex Formation between Ethidium Bromide and Nucleic Acids. Journal of Molecular Biology **13**, 269-&.

Waters, J.C. & Salmon, E.D. (1996): Cytoskeleton: A catastrophic kinesin. Current Biology **6**, 361-363.

Watts, N.R., Sackett, D.L., Ward, R.D., Miller, M.W., Wingfield, P.T., Stahl, S.S. & Steven, A.C. (2000): HIV-1 Rev depolymerizes microtubules to form stable bilayered rings. Journal of Cell Biology **150**, 349-360.

Webb, M., Jouannic, S., Foreman, J., Linstead, P. & Dolan, L. (2002): Cell specification in the Arabidopsis root epidermis requires the activity of ECTOPIC ROOT HAIR 3 - a katanin-p60 protein. Development **129**, 123-131.

Webb, M.C. & Gunning, B.E.S. (1990): Embryo Sac Development in Arabidopsis-Thaliana .1. Megasporogenesis, Including the Microtubular Cytoskeleton. Sexual Plant Reproduction **3**, 244-256.

West, R.R., Tenbarge, K.M. & Olmsted, J.B. (1991): A Model for Microtubule-Associated Protein-4 Structure - Domains Defined by Comparisons of Human, Mouse, and Bovine Sequences. Journal of Biological Chemistry **266**, 21886-21896.

Whittington, A.T., Vugrek, O., Wei, K.J., Hasenbein, N.G., Sugimoto, K., Rashbrooke, M.C. & Wasteneys, G.O. (2001): MOR1 is essential for organizing cortical microtubules in plants. Nature **411**, 610-613.

Wilde, A. & Zheng, Y.X. (1999): Stimulation of microtubule aster formation and spindle assembly by the small GTPase Ran. Science **284**, 1359-1362.

Wittmann, T., Hyman, A. & Desai, A. (2001): The spindle: a dynamic assembly of microtubules and motors. Nature Cell Biology **3**, E28-E34.

Woehlke, G., Ruby, A.K., Hart, C.L., Ly, B., HomBooher, N. & Vale, R.D. (1997): Microtubule interaction site of the kinesin motor. Cell **90**, 207-216.

Wolniak, S.M. & Larsen, P.M. (1995): The Timing of Protein-Kinase Activation Events in the Cascade That Regulates Mitotic Progression in Tradescantia Stamen Hair- Cells. Plant Cell **7**, 431-445.

Wood, W.B., Hecht, R., Carr, S., Vanderslice, R., Wolf, N. & Hirsh, D. (1980): Parental Effects and Phenotypic Characterization of Mutations That Affect Early Development in Caenorhabditis-Elegans. Developmental Biology **74**, 446-469.

Wordeman, L. & Mitchison, T.J. (1995): Identification and Partial Characterization of Mitotic Centromere-Associated Kinesin, a Kinesin-Related Protein That Associates with Centromeres During Mitosis. Journal of Cell Biology **128**, 95-105.

Wordeman, L., Wagenbach, M. & Maney, T. (1999): Mutations in the ATP-binding domain affect the

subcellular distribution of mitotic centromere-associated kinesin (MCAK). Cell Biology International **23**, 275-286.

Yasuhara, H., Muraoka, M., Shogaki, H., Mori, H. & Sonobe, S. (2002): TMBP200, a microtubule bundling polypeptide isolated from telophase tobacco BY-2 cells is a MOR1 homologue. Plant and Cell Physiology **43**, 595-603.

Yasuhara, H., Sonobe, S. & Shibaoka, H. (1993): Effects of Taxol on the Development of the Cell Plate and of the Phragmoplast in Tobacco by-2 Cells. Plant and Cell Physiology **34**, 21-29.

Yuan, M., Shaw, P.J., Warn, R.M. & Lloyd, C.W. (1994): Dynamic Reorientation of Cortical Microtubules, from Transverse to Longitudinal, in Living Plant-Cells. Proceedings of the National Academy of Sciences of the United States of America **91**, 6050-6053.

Yuen, C.Y.L., Pearlman, R.S., Silo-Suh, L., Hilson, P., Carroll, K.L. & Masson, P.H. (2003): WVD2 and WDL1 modulate helical organ growth and anisotropic cell expansion in Arabidopsis. Plant Physiology **131**, 493-506.

Zhai, Y., Kronebusch, P.J., Simon, P.M. & Borisy, G.G. (1996): Microtubule dynamics at the G(2)/M transition: Abrupt breakdown of cytoplasmic microtubules at nuclear envelope breakdown and implications for spindle morphogenesis. Journal of Cell Biology **135**, 201-214.